JIEGAO WANG

KINEMATIC ANALYSIS, DYNAMIC ANALYSIS AND STATIC BALANCING OF PLANAR AND SPATIAL PARALLEL MECHANISMS OR MANIPULATORS WITH REVOLUTE ACTUATORS

Thèse
présentée
à la Faculté des études supérieures
de l'Université Laval
pour l'obtention
du grade de Philosophiae Doctor (Ph.D.)

Département de génie mécanique
FACULTÉ DES SCIENCES ET DE GÉNIE
UNIVERSITÉ LAVAL
QUÉBEC

SEPTEMBER 1997

Short Abstract

The kinematic analysis, the dynamic analysis and the static balancing of planar and spatial parallel mechanisms or manipulators with revolute actuators are presented in this thesis.

First, the inverse kinematics of each mechanism is computed and a new general algorithm is proposed to locate the boundaries of the workspace of the mechanism. Two approaches are used to derive the velocity equations of the mechanisms. One of them is a new approach. The singularity loci is then determined using the velocity equations. The kinematic optimization of mechanisms with reduced degree of freedom is also discussed.

A new approach based on the principle of virtual work for the dynamic analysis of parallel mechanisms or manipulators is proposed in the thesis. The Newton-Euler approach is also used for the dynamic analysis of parallel mechanisms or manipulators. Each approach has its own advantages and is suitable for different usage.

Finally, the static balancing of parallel mechanisms or manipulators is studied in this thesis. Two approaches are used to derive the balancing conditions of the mechanisms.

Jiegao Wang

Clement M. Gosselin

Abstract

This thesis deals with the kinematic analysis, dynamic analysis and static balancing of planar and spatial parallel mechanisms or manipulators with revolute actuators.

The inverse kinematics of each mechanism is first computed and a new general algorithm is used to locate the boundaries of the workspace of the mechanism. Two approaches, namely, the *algebraic formulation* and the *vector formulation* are used to derive the velocity equations of the mechanisms. The singularity loci is then determined using the velocity equations. The approach of *vector formulation* is a new approach and leads to simpler expressions for the determination of the singularity loci . Kinematic optimization of mechanisms with reduced degrees of freedom is also discussed in the thesis. The generalized reduced gradient method of optimization is used to find the optimal solutions of the link parameters which enable the dependent Cartesian coordinates to follow an ideal trajectory as closely as possible when the independent Cartesian coordinates pass through some prescribed points.

A new approach for the dynamic analysis of parallel mechanisms or manipulators is proposed in the thesis. This approach is based on the principle of virtual work. As compared to the conventional approach of Newton-Euler, the new approach will lead to a faster algorithm for derivation of the generalized forces, which is useful for the control of a mechanism or manipulator. The Newton-Euler approach is also used for dynamic analysis of parallel mechanisms or manipulators. Since the constraint forces

between the links are computed in the latter approach, it is useful for the design and simulation of mechanisms or manipulators.

Finally, the static balancing of parallel mechanisms or manipulators is studied in this thesis. The conditions of static balancing of the parallel mechanisms or manipulators are derived using two approaches, namely, using counterweights and using springs. The two approaches each have their advantages and drawbacks and the approach to be used depends on the application of the balanced mechanism. Static balancing of parallel mechanisms or manipulators is useful since it leads to improvement of the control accuracy and energy efficiency of the mechanisms or manipulators.

Jiegao Wang

Clement M. Gosselin

Résumé

Cette thèse porte sur l'analyse cinématique et dynamique ainsi que sur l'équilibrage statique des mécanismes et manipulateurs parallèles plans et spatiaux avec actionneurs rotoïdes.

Le problème géométrique inverse de chaque mécanisme est d'abord résolu et un nouvel algorithme général est proposé pour la détermination des frontières de l'espace atteignable. Deux approches, soit la formulation *algébrique* et la formulation *vectorielle*, sont utilisées pour obtenir les équations de vitesse des mécanismes. Le lieu des configurations singulières est ensuite déterminé en utilisant les équations de vitesse. La formulation vectorielle est une nouvelle approche qui conduit à des expressions plus simples pour les lieux de singularité. L'optimisation cinématique de mécanismes à degré de liberté réduit est aussi traitée dans cette thèse. La méthode du gradient généralisé est utilisée afin de trouver des valeurs optimales des paramètres géométriques permettant aux coordonnées cartésiennes dépendantes de suivre une trajectoire prédéterminée en fonction des coordonnées cartésiennes dépendantes en certains points prescrits.

Une nouvelle approche pour l'analyse dynamique des mécanismes et manipulateurs parallèles est aussi proposée dans cette thèse. Cette approche est basée sur le principe du travail virtuel. En comparaison avec la formulation traditionnelle de Newton-Euler, la méthode proposée ici conduit à un algorithme plus rapide pour le calcul des efforts articulaires, ce qui est intéressant pour la commande. Les équations de Newton-Euler

sont également utilisées pour fin de comparaison. Cette dernière approche est aussi utile dans un contexte de design puisqu'elle permet de déterminer les efforts internes.

Finalement, l'équilibrage statique des mécanismes et manipulateurs parallèles est étudié dans cette thèse. Les conditions pour l'équilibrage statique de mécanismes et manipulateurs parallèles sont obtenues grâce à deux approches distinctes soit: l'utilisation de contrepoids et l'utilisation de ressorts. Chacune de ces approches a ses propres avantages et inconvénients et l'approche à privilégier dépend de l'application considérée. L'équilibrage statique des mécanismes ou manipulateurs est utile puisqu'il permet d'améliorer la qualité de la commande et l'efficacité énergétique.

Jiegao Wang

Clement M. Gosselin

Foreword

This thesis describes the most important aspects of my work in the Robotics Laboratory of the Department of Mechanical Engineering of Laval university, Québec, Canada.

Firstly, I would like to thank my supervisor Professor Clément M. Gosselin for his invaluable guidance, stimulating discussions and continuous encouragements in the whole research as well as the critical review of the manuscript and the translation of the abstract of the thesis into French.

Grateful thanks go to Professor Marc J. Richard for his prereview of my thesis and to Professor Li Cheng and Professor J. J. McPhee of the University of Waterloo for having accepted to examine my thesis and for their precious remarks.

Finally, I would like to express my gratitude to the colleagues in the Robotic Laboratory, namely Martin Jean, Boris Mayer St-Onge, Rémi Ricard and others, for their help in many aspects.

Contents

List of Tables

List of Figures

Chapter 1

Introduction

According to their geometric architecture, robot manipulators are classified as serial robot manipulators and parallel robot manipulators. Each type of robotic manipulator has its advantages and drawbacks and is suitable for different applications. Figure 1.1 represents simple planar two-degree-of-freedom serial and parallel manipulators. The serial manipulator (Figure 1.1(a)) consists of two moving links and two revolute joints. Two revolute actuators are respectively mounted at joint O and O_1 with joint variables θ_1 and θ_2. Point P is the position of the end-effector of the manipulator. The parallel manipulator represented in Figure 1.1(b) which will be studied in this thesis consists of two kinematic chains connecting the fixed base to the end-effector of the manipulator; the two kinematic chains are OO_2P and $O_1O_3O_4P$ respectively. Two revolute actuators are mounted at joints O and O_1 with joint variables θ_1 and θ_2, while joints O_2, O_3 and O_4 are passive revolute joints. Similarly, point P is the position of the end-effector of the manipulator.

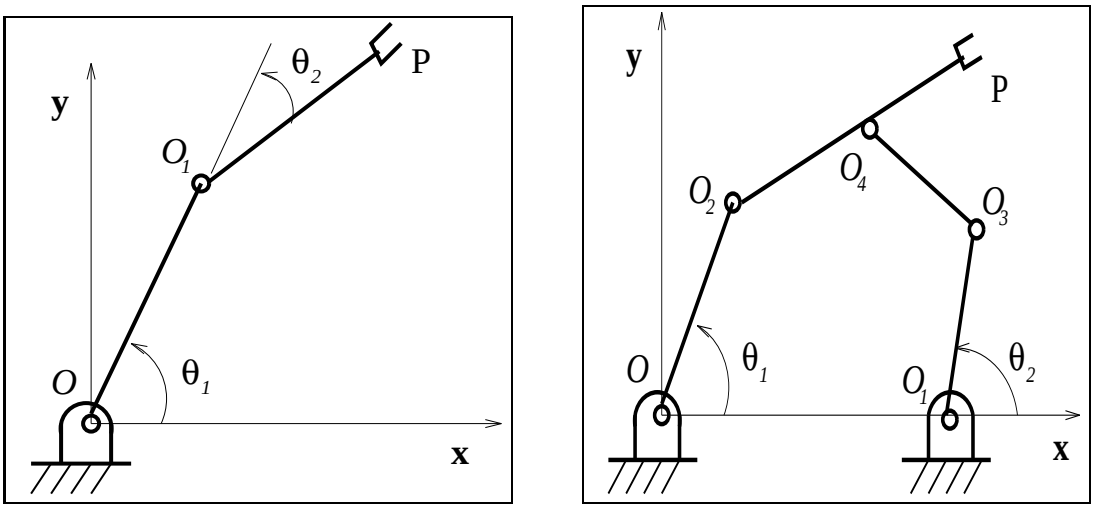

(a) Planar two-dof serial manipulator.

(b) Planar two-dof parallel manipulator.

Figure 1.1: Two different types of robotic manipulators.

In general, an n-degree-of-freedom parallel manipulator is one in which the end-effector is connected to the base with n distinct kinematic chains and in which one joint of each of these chains is actuated.

Comparing the two types of robot manipulators, one can realize that serial robot manipulators have a simpler structure, wider reachable area and relatively simpler kinematics. These advantages led to an extensive use of this type of manipulator in the industry, for instance, for assembling, welding, painting, etc. However, since the serial structure leads to low rigidity, this type of manipulator has smaller load capacity, lacks stiffness and cannot reach high dynamic performances. Therefore, they are not suitable for some applications where large load or high speed and accuracy are needed.

As opposed to serial robot manipulators, parallel robot manipulators consist of several kinematic chains connecting the fixed base to the end-effector, which leads to several advantages. For example, the weight of the manipulator is reduced and the rigidity of the manipulator is increased. Therefore, the manipulators have large load ability, good stiffness and high dynamic performances and are suitable for applications requiring large load ability or high speed and accuracy. However, complex parallel structures also lead to some drawbacks such as a smaller workspace and a complex mathematical model as compared to the serial robot manipulators. Two typical examples of

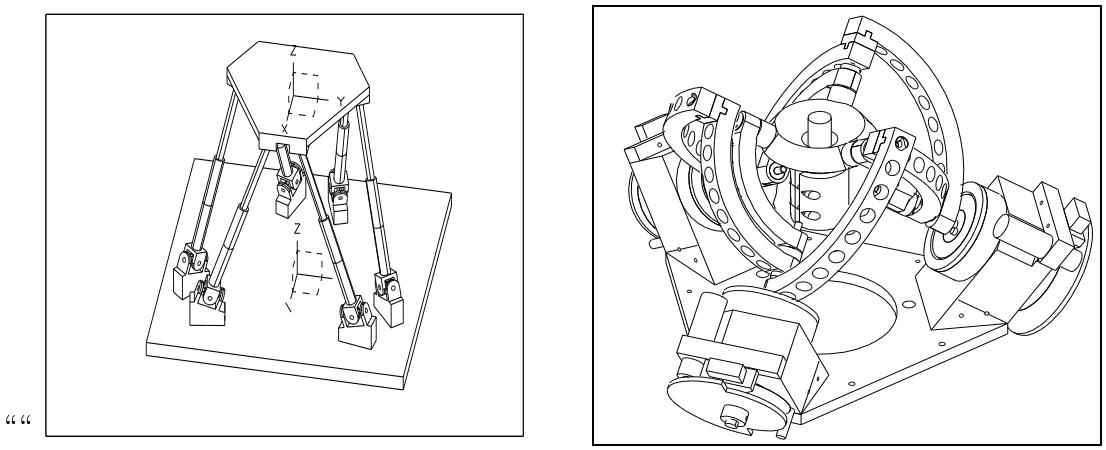

(a) Stewart platform. (b) Agile-eye.

Figure 1.2: Parallel mechanisms used for robot manipulators.

the application of parallel manipulators are the spatial six-degree-of-freedom parallel mechanism with prismatic actuators [48] (Gough-Stewart platform Figure 1.2(a)) and the spherical three-degree-of-freedom parallel mechanism with revolute actuators [17] (agile-eye Figure 1.2(b)). The former is used for flight simulators and the latter is used for the orientation of a camera at high speed. They respectively illustrate the cases of large load and high speed and accuracy.

Although parallel manipulators have received more and more attention over the last two decades (see for instance, [3], [4], [10], [11], [13], [14], [15] and [17], and many more), their applications have been limited to only a few areas so far. The complex mathematical models of parallel robot manipulators is the main factor to hinder their applications. Therefore, the development of efficient approaches for the kinematic and dynamic analysis is extremely important for the study and the application of the mechanisms.

It can be noticed in the literature that parallel mechanisms or manipulators with prismatic actuators have received more attention than those with revolute actuators. Indeed, parallel mechanisms or manipulators with prismatic actuators have a simpler architecture and kinematic model than those with revolute actuators. For example, the singularity loci of planar three-degree-of-freedom parallel manipulators with prismatic actuators is quadratic [47]. However, for the planar three-degree-of-freedom parallel

manipulator with revolute actuators, the curves representing the singularity loci in the Cartesian space are of a very high degree ([19] and [20]). However, as will be seen in the thesis, parallel mechanisms or manipulators with revolute actuators can be statically balanced. A statically balanced parallel manipulator could be easier to control and leads to higher energy efficiency. Additionally, since the architecture is similar, the approaches used in the kinematic and dynamic analysis of parallel mechanisms or manipulators with revolute actuators can be directly applied to parallel mechanisms or manipulators with prismatic actuators [58]. Therefore, in this thesis, only parallel mechanisms or manipulators with revolute actuators are discussed, which does not limit the generality of the study of parallel mechanisms or manipulators.

Depending on the applications, the parallel devices studied here may be called "mechanisms" or "manipulators"; both terms can be found in the literature. In general, the term "manipulator" is used in robotic applications while the more general term "mechanism" is used in all other applications. In this thesis, both terms will be used and will be considered equivalent since the present work is generic and is not application dependent.

In Chapter 2, the kinematic analysis of parallel mechanisms or manipulators is presented. Several important issues are addressed, namely, inverse kinematics and workspace analysis, the velocity equations and singularity loci and the kinematic optimization of mechanisms with reduced degrees of freedom.

The determination of the workspace of parallel manipulators has been studied by many authors, see for instance, [1], [2], [4], [11], [13], [37], [38], [40] and [65]. Most of the approaches proposed by these authors for the determination of the workspace mainly use analytical methods to find the explicit expressions of the boundary of the workspace. For some simple planar mechanisms or for the spatial six-dof (where "dof" stands for "degree of freedom") parallel mechanism with prismatic actuators [13], the boundaries of the workspace consist of low degree curves or surfaces. It is possible to find an explicit expression which will lead to a faster algorithm for locating the limits of the workspace. However, for some complex multi-degree-of-freedom spatial parallel mechanisms, especially, parallel mechanisms or manipulators with revolute actuators, it is very difficult or impossible to find explicit expressions of the boundary of the workspace since the curves or surfaces of the boundary are of a very high degree.

In Chapter 2, a new numerical algorithm for the determination of the workspace is proposed. The compact expressions corresponding to the workspace boundaries of parallel mechanisms or manipulators are first obtained from the analysis of the solution of the inverse kinematics. Then, a numerical procedure is used to locate the curve of the boundary of the workspace. Although this algorithm is much slower than those developed by the authors mentioned above, it is a general algorithm and it can be applied to any type of planar or spatial parallel manipulator.

Kinematic singularity is an important issue. When a mechanism or manipulator is in a singular configuration, the output link or the end-effector gains one or more degrees of freedom and the input links or the actuators lose their independence which means that the manipulator is uncontrollable. Such singular configurations must be avoided. Singularity loci consist of the sets of reachable end-effector poses corresponding to the singular configurations of the mechanism or manipulator. The singularity problem of parallel manipulators has been studied by some authors. The singularity of single-loop kinematic chains is analyzed in [24] and [50]. In [3], [30], [39] and [55] various criteria and classifications for the singularities of parallel mechanisms were analyzed and presented. However, these studies do not provide a systematic approach to determine the singularity loci.

Gosselin and Angeles in [16] used the Jacobian matrices of the input-output velocity equations of parallel manipulators to classify the different types of singularities. Three general types of singularities which can occur in parallel manipulators have been identified. This classification has been further refined in [66] where several sub-classes of singularities are defined. The approach presented in [16] allows the determination of singularity loci using velocity equations of manipulators and will therefore be used in the thesis. According to this singularity classification, the first type of singularity corresponds to the boundary of the workspace, which has been obtained using the new algorithm mentioned above and the third type of singularity can be avoided by proper arrangement of the architecture of the manipulator. Therefore, the second type of singularity loci is the major singularity whose loci must be determined using the Jacobian matrix of the velocity equations. In other words, the velocity equations are critical in the determination of the singularities of type two. Usually, the velocity equations are obtained through differentiation of the kinematic equations of manipulators. This

approach leads to a direct relationship between the joint and Cartesian velocities and will be referred to here as the *algebraic formulation*. It will be used for the derivation of the velocity equations. However, at the same time, a new approach for the derivation of the velocity equations of complex manipulators is introduced and will be referred to here as the *vector formulation*.

The new approach of derivation of the velocity equations consists in writing the velocity equations using components of angular velocities of the links to form the Cartesian velocity vector and relative velocities of some chosen points of the links to form the joint coordinate vector ([58], [60] and [61]). This leads to a redundant formulation, i.e., one in which the number of Cartesian or joint velocity components is larger than the degree of freedom of the mechanism. However, the Jacobian matrices obtained are rather simple and sparse and can be written in terms of the components of vectors associated with the geometry of the mechanism. Although the dimensions of the Jacobian matrices obtained with this method are larger than with the algebraic approach, the expression for the determinant — which is used for the determination of the singularity loci — is in general simpler, which leads to faster algorithms for the computation of the loci. On the other hand, for purposes of control of a mechanism, the algebraic approach leads to a more direct relationship between the joint and Cartesian velocities.

Finally, it is pointed out that the vector formulation characterizes the local behavior of the mechanism exactly as the algebraic formulation does and hence, singularity loci obtained with both approaches will lead to identical results.

For mechanisms with reduced degrees of freedom, such as planar two-dof as well as spatial four- and five-dof parallel mechanisms, since some Cartesian coordinates cannot be prescribed—they are dependent on the prescribed independent Cartesian coordinates—the kinematic optimization of the mechanisms is introduced in Chapter 2. The optimal synthesis of planar linkages has been addressed by many authors (for instance, [12], [32] and many others). The synthesis of multi-loop spatial mechanisms has also been studied in [44] using the Generalized Reduced Gradient method of optimization. However, the optimal synthesis of the trajectories of the dependent Cartesian coordinates of spatial parallel mechanisms or manipulators with reduced degrees of freedom has received less or no attention. The optimum design of these mechanisms is important for their practical applications. In Chapter 2, the optimization of planar

two-dof as well as spatial four- and five-dof parallel mechanisms is presented. The Generalized Reduced Gradient method of optimization is used.

In a context of design and control, the dynamic analysis of parallel manipulators is an important issue [5], [9], [43], [14], [17] and [34]. Indeed, it provides information on the internal constraint forces and moments on the links as well as on input forces or torques at the actuators for a specified trajectory.

The Newton-Euler equations of motion have been used by several authors for the dynamic analysis of spatial parallel manipulators, for instance, in [10], [14] and [49]. In this approach the links constituting the manipulator are isolated and the Newton-Euler equations are written for each link. Then, all interaction forces and moments between the links are obtained. In [36], the dynamic analysis of a three-degree-of-freedom parallel manipulator using a Lagrangian approach is presented. However, because of the complexity of the kinematic model of the spatial parallel manipulator, some assumptions have to be made to simplify the expressions of the kinetic energy and potential energy. Therefore, this approach is not general and efficient for the dynamic analysis of parallel mechanisms or manipulators.

In Chapter 3, the dynamic analysis of planar and spatial parallel mechanisms or manipulators with revolute actuators is performed. Two different approaches are used. The first approach is based on the principle of virtual work. This is a new approach which is applied to parallel manipulators for the first time [59]. In this approach the inertial forces and moments are determined using the linear and angular accelerations. Then, the equilibrium of the whole manipulator is considered and the principle of virtual work is applied to derive the input forces or torques. Since constraint forces and moments do not need to be computed, this approach leads to faster computational algorithms, which is an important advantage for the purposes of control of a manipulator. The other approach is based on the Newton-Euler formulation mentioned above. It is useful for the purposes of design. However, the computational algorithms are slower than with the new approach. Therefore, the two approaches have their own advantages and drawbacks and each of them is suitable for different applications.

The balancing of mechanisms has been an important research topic for several decades (see for instance [35] for a literature review). A balanced mechanism leads

to better dynamic characteristics and less vibrations caused by motion. Static and dynamic balancing of planar linkages have been studied extensively in the literature (see for instance [6], [23], [51], [52] and [64]). Mechanisms are said to be *force-balanced* when the total force applied by the mechanism on the fixed base is constant for any motion of the mechanism. In other words, a mechanism is force-balanced when its global center of mass remains fixed, for any arbitrary motion of the mechanism. This condition is very important in machinery since unbalanced forces on the base will lead to vibrations, wear and other undesirable side effects. For robotic manipulators or motion simulation devices, however, the forces on the base are usually not critical and designers are mostly concerned with the torques (or forces) which are required at the actuators to maintain the manipulator or mechanism in static equilibrium. Hence, in this context, manipulators or mechanisms are said to be *statically balanced*, when the weight of the links does not produce any torque (or force) at the actuators under static conditions, for any configuration of the manipulator or mechanism. This condition is also referred to as *gravity compensation*. Gravity-compensated serial manipulators have been designed in [26], [42], [53], [56] and [57] using counterweights, springs and sometimes cams and/or pulleys. A hybrid direct-drive gravity-compensated manipulator has also been developed in [31]. Moreover, a general approach for the equilibrium of planar linkages using springs has been presented in [53]. The balancing of spatial mechanisms has also been studied, for instance in [7] and [57].

However, the static balancing of spatial multi-degree-of-freedom parallel manipulators or mechanisms has received very little attention. Since spatial parallel manipulators find more and more applications in robotics and flight simulation, the static balancing of spatial parallel manipulators becomes an important issue. As mentioned above, a statically balanced parallel manipulator is one in which the actuators do not contribute to supporting the weight of the moving links, for all configurations. Hence, the actuators are used only to impart accelerations to the moving links, which leads to a reduction of the size and power of the actuators and results in the improvement of the accuracy of the control. In flight simulation, for instance, since the payload is very large (usually in the order of tons) and the motion of the platform of the mechanism is rather slow, the forces or torques exerted at the actuated joints are mainly due to the weight of the platform. Hence, if the mechanism is statically balanced, the actuating forces or torques will be greatly reduced, which will result in significant improvements

of the control and energy efficiency.

In Chapter 4, the static balancing of planar and spatial parallel mechanisms or manipulators with revolute joints is addressed. Two approaches of static balancing are presented, namely, *i*) static balancing using counterweights and *ii*) using springs ([21] and [62]). When the mechanism is balanced using counterweights, a mechanism with a fixed global center of mass is obtained. In other words, the static balancing is achieved in any direction of the Cartesian space of the mechanism. This property is useful for applications in which the mechanism is needed to be statically balanced in all directions (e.g. if the mechanism is to be installed in an arbitrary direction with respect to the gravity acceleration vector). However, for some parallel mechanisms, static balancing with counterweights is difficult to realize. For example, in flight simulators, since the mass of the platform is very large, the counterweights required would in general be too large to be practical. However, springs can be used in such instances. When springs — or other elastic elements — are used, the total potential energy of the manipulator — gravitational and elastic — can be kept constant and the weight of the whole manipulator can be balanced with a much smaller total mass than when using counterweights, as pointed out in [53]. However, a mechanism which is statically balanced using springs will be statically balanced for only one direction of the gravity vector, which may be unsuitable for some applications. Therefore, both methodologies are discussed in Chapter 4 since they each have their own merit.

Chapter 2

Kinematic analysis

Kinematic modeling is essential for the analysis and design of a parallel mechanism. Usually, the kinematic analysis consists of forward kinematics, inverse kinematics, determination of the workspace and singularity analysis. Unlike serial robotic manipulators, the forward kinematic analysis of parallel manipulators is more complex than its inverse kinematic analysis. For instance, for the spatial six-degree-of-freedom parallel manipulator with prismatic actuators (the Gough-Stewart platform) the inverse kinematic analysis is very simple while the forward kinematic analysis is extremely difficult and only numerical solutions can be obtained. Fortunately, the solution of the forward kinematics of a parallel manipulator is not necessary for its kinematic design. Moreover, the forward kinematic analysis of different types of parallel manipulators is often similar. Therefore, the forward kinematic analysis of parallel mechanisms is not discussed in this thesis.

The workspace of a manipulator is defined as the set of Cartesian poses (position and orientation) that the end-effector of the manipulator can reach. The workspace determines the volume or hyper-volume in which the manipulator can perform tasks. Therefore, the determination of the workspace is an important first step for the design of a manipulator. Moreover, inside the workspace of a manipulator there exist some positions and orientations in which the end-effector gains or loses one or more degrees of freedom and therefore the manipulator becomes uncontrollable. These positions and orientations are called singular configurations and they must be considered in the design of the manipulator. The singular configurations of parallel manipulators can be determined using the velocity equations [16]. The determination of the workspace and the singularity loci will be discussed here.

For mechanisms with reduced degrees of freedom, for instance, the planar two-degree-of-freedom and spatial four- and five-degree-of-freedom parallel mechanisms, only a subset of the three Cartesian coordinates x, y and ϕ (for planar parallel mechanisms) or of the six Cartesian coordinates x, y, z, ϕ, θ and ψ (for spatial parallel mechanism) are independent (where ϕ, θ and ψ are 3 Euler angles). If the manipulators' dependent coordinates are required to follow some desired trajectories as closely as possible when its independent coordinates pass exactly through the specified trajectories, there exists a kinematic optimization problem which can be solved to obtain a set of optimal linkage parameters. In this chapter, the optimization problem of planar two-degree-of-freedom and spatial four- and five-degree-of-freedom parallel mechanisms is presented in a separate section.

Therefore, the kinematic analysis presented here consists of the inverse kinematics and workspace analysis, the velocity equations and singularity loci as well as the kinematic optimization of mechanisms with reduced degrees of freedom. These topics will be addressed in the following sections.

2.1 Inverse kinematics and workspace

If $\mathbf{x}$ is the Cartesian coordinate vector and $\boldsymbol{\theta}$ is the actuated joint coordinate vector, the inverse kinematic problem can be stated as: given the position and orientation of

the platform $\mathbf{x}$, find the corresponding actuated joint variables $\boldsymbol{\theta}$. Since the trajectories are usually given in Cartesian space while the actuators are mounted at joints, the solution of the inverse kinematic problem is necessary for controlling a manipulator. In this section, the inverse kinematics of the planar two- and three-degree-of-freedom as well as spatial four-, five- and six-degree-of-freedom parallel mechanisms with revolute actuators is solved. It is the foundation for further analysis and design of the mechanisms.

Moreover, as mentioned above, the determination of the workspace of a manipulator is a basic requirement for its kinematic design. Based on the fact that the workspace of manipulators is related to the solution of the inverse kinematics, a new general numerical algorithm for the determination of the workspace is proposed. This algorithm is used to solve high degree nonlinear equations and to plot the resulting curves in a two-dimensional plane. In the algorithm, the bisection method is combined with Newton-Raphson's method to search for the roots of the equations. If it is assumed that a cross-section of the workspace in the $x-y$ plane is to be found, for given values of other independent Cartesian coordinates, the procedure can be described as follows:

Step 1: In the $x-y$ plane, divide the x axis and the y axis in m and n sections respectively. At the same time, compute the values of δ at points (x_i, y_j) $(i = 1, 2, ..., m$ and $j = 1, 2, ..., n)$, where δ is an expression arising from the solution of the inverse kinematic problem and which may be real (when the prescribed Cartesian coordinates are inside the workspace) or complex (when the prescribed Cartesian coordinates are outside the workspace). A typical example is the square root of an expression. Therefore, the boundary of the workspace can be obtained as the locus of points for which $\delta = 0$.

Step 2: Check the values of δ at points (x_i, y_j) and (x_i, y_{j+1}) $(j = 1, 2, ..., n)$ and if one of them is real while the other is not then it means that there is a root in this interval. Use Newton-Raphson's method to search for the root of equation $\delta = 0$ in the interval.

Step 3: Repeat step 2 m times, that is, let $i = 1, 2, ..., m$. Finally, all the points of the boundaries of the workspace of the manipulator are obtained.

Step 4: Plot these points in the $x-y$ plane.

This algorithm is much slower than the algorithm presented in [13]. However, it is more general and can be applied to any type of manipulator. This algorithm is used here to plot the boundaries of the workspace of the studied planar and spatial parallel mechanisms.

2.1.1 Planar parallel manipulators with revolute actuators

Planar two- and three-degree-of-freedom parallel manipulators are represented in Figures 2.1 and 2.2 respectively. All their joints are of the revolute type. The two-degree-of-freedom manipulator can be used to position a point on the plane and the Cartesian coordinates associated with this manipulator are the position coordinates of one point of the platform, noted (x, y) (Figure 2.1). The three-degree-of-freedom manipulator can be used to position and orient a body on the plane and hence, in this case the Cartesian coordinates are the position of one point of the platform, noted (x, y), and its orientation, given by angle ϕ (Figure 2.2). Vector $\boldsymbol{\theta}$ represents the actuated joint coordinates of the planar parallel manipulator and is defined as $\boldsymbol{\theta} = [\,\theta_1 \quad \theta_2 \quad \ldots \quad \theta_n\,]^T$, where n is the number of degrees of freedom of the manipulator studied. The only actuated joints are those which are directly connected to the fixed link (see for instance [16], [46] and [19]).

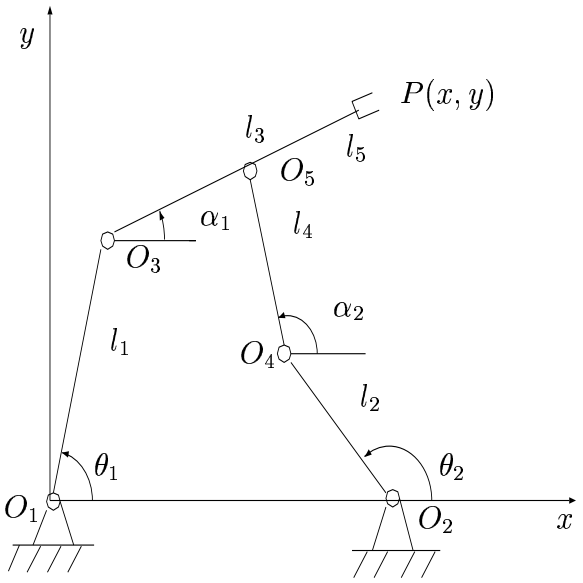

Figure 2.1: Planar two-degree-of-freedom parallel manipulator.

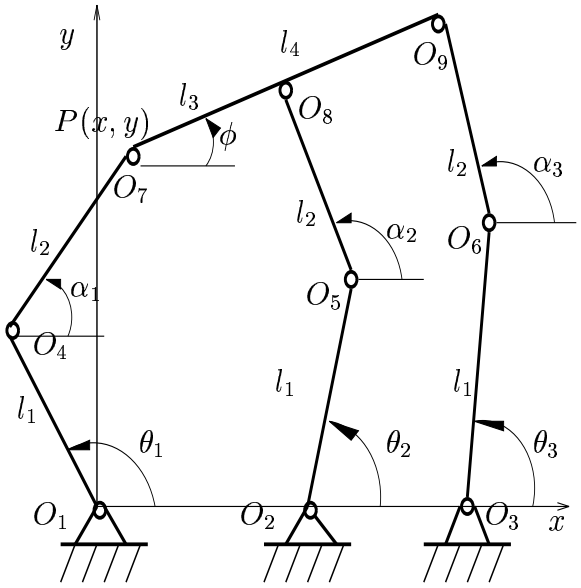

Figure 2.2: Planar three-degree-of-freedom parallel manipulator.

2.1.1.1 Planar two-degree-of-freedom manipulator

I) Inverse kinematics

This manipulator, illustrated in Figure 2.1, has four movable links and five revolute joints (identified as O_1 to O_5). The two links whose length are l_1 and l_2 are the input links and the joints O_1 and O_2 are the only actuated joints. The lengths of the other two links are noted l_3 and l_4 respectively. Moreover, l_5 is the distance from joint O_5 to point $P(x, y)$. Point $P(x, y)$ is the point to be positioned by the manipulator. The origin of the fixed Cartesian coordinate system is located on joint O_1. Moreover, (x_{o1}, y_{o1}) and (x_{o2}, y_{o2}) are the coordinates of points O_1 and O_2 respectively, and one has $x_{o1} = y_{o1} = y_{o2} = 0$.

From the geometry of the linkage one can write

$$(x_{2i} - l_{i+2}\cos\alpha_i)^2 + (y_{2i} - l_{i+2}\sin\alpha_i)^2 = l_i^2, \quad i = 1, 2 \tag{2.1}$$

where the intermediate variables x_{2i} and y_{2i} $(i = 1, 2)$ are defined as

$$x_{21} = x - x_{o1} \tag{2.2}$$

$$y_{21} = y - y_{o1} \tag{2.3}$$

$$x_{22} = x - l_5\cos\alpha_1 - x_{o2} \tag{2.4}$$

$$y_{22} = y - l_5\sin\alpha_1 - y_{o2} \tag{2.5}$$

and where angles α_1 and α_2 represent respectively the orientation of the links of length l_3 and l_4 with respect to the fixed link.

From eq.(2.1), one obtains

$$\sin\alpha_i = \frac{b_i c_i + K_i a_i \sqrt{\delta_i}}{a_i^2 + b_i^2}, \quad i = 1, 2 \tag{2.6}$$

$$\cos\alpha_i = \frac{a_i c_i - K_i b_i \sqrt{\delta_i}}{a_i^2 + b_i^2}, \quad i = 1, 2 \tag{2.7}$$

where

$$a_i = x_{2i}, \quad i = 1, 2 \tag{2.8}$$

$$b_i = y_{2i}, \quad i = 1, 2 \tag{2.9}$$

$$c_i = \frac{l_{i+2}^2 - l_i^2 + x_{2i}^2 + y_{2i}^2}{2 l_{i+2}}, \quad i = 1, 2 \tag{2.10}$$

$$\delta_i = a_i^2 + b_i^2 - c_i^2, \quad i = 1, 2 \tag{2.11}$$

$$K_i = \pm 1, \quad i = 1, 2$$

where K_i is the ith branch index, which can be used to distinguish the four branches of the inverse kinematic problem. Finally, the solution of the inverse kinematic problem for this manipulator can be obtained as

$$\theta_i = \text{atan2}[(y_{2i} - l_{i+2}\sin\alpha_i), (x_{2i} - l_{i+2}\cos\alpha_i)], \quad i = 1, 2 \tag{2.12}$$

where $\theta_i (i = 1, 2)$ are defined as the angles between the link of length l_i and the x axis of the fixed Cartesian frame and atan2 is the inverse tangent function which uses 2 arguments and returns a unique value.

II) Determination of the workspace

Considering eqs.(2.6), (2.7), it is clear that whether or not angle α_i is real depends on δ_i. If $\delta_i < 0$, α_i is not real; if $\delta_i > 0$, α_i can be real; and if δ_i=0, α_i has a unique real solution. Because α_i is related to the solution of the inverse kinematics of the manipulator, in fact it means that when $\delta_i = 0$ the inverse kinematic problem has fewer solutions. Recalling the properties of the first type of singularity of parallel manipulators [16], it follows that the workspace boundaries of the planar parallel manipulators consist of the set of configurations which satisfy the following equation in the Cartesian space of the manipulator.

$$\delta = \sqrt{\delta_1}\sqrt{\delta_2} = 0 \tag{2.13}$$

The problem of determining the boundaries of the workspace of parallel manipulators is equivalent to solving equation (2.13). Since the latter equation is highly nonlinear, it is usually impossible to obtain analytical solutions. Therefore, the numerical method mentioned in a preceding section can be used to solve the equation and plot the workspace limits in a two-dimensional plane.

A numerical example is now given to illustrate the application of the algorithm for plotting the boundaries of the workspace.

For this manipulator, let $l_1 = 0.8$, $l_2 = 1.0$, $l_3 = 1.5$, $l_4 = 0.8$, $l_5 = 0.6$, $x_{o1} = 0.0$, $y_{o1} = 0.0$, $x_{o2} = 2.0$ and $y_{02} = 0.0$.

Figure 2.3 show two different workspaces with two different values of the branch index K_1, namely, the workspace of the manipulator is different with $K_1 = 1$ and $K_1 = -1$. This is because angle α_2 is a function of angle α_1. In other words, there are two different workspaces for this manipulator, depending on the value of K_1.

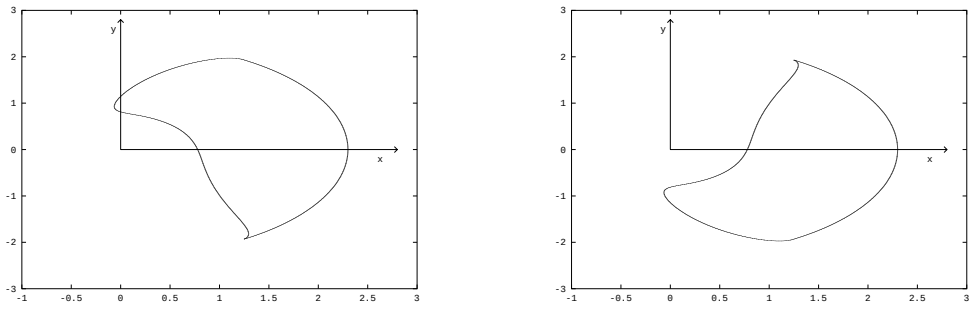

(a) Workspace 1 of the two-dof manipulator with $K_1 = +1$.

(b) Workspace 2 of the two-dof manipulator with $K_1 = -1$.

Figure 2.3: Workspace of the two-dof manipulator

2.1.1.2 Planar three-degree-of-freedom manipulator

I) Inverse kinematics

A planar three-degree-of-freedom manipulator consists of seven movable links and nine revolute joints (identified as O_1 to O_9), as indicated in Figure 2.2. Such an architecture has been studied in [15]. The moving link with three revolute joints is considered

as the platform of the manipulator. The three links connected to the base are the input links and the three joints O_1, O_2 and O_3 are the actuated joints. Joints O_1 and O_7 are respectively the origin of the fixed Cartesian coordinate frame and the point to be positioned by the end effector. It is assumed here that the three input links have the same length l_1 and that the other three links which connect the input links to the platform have a length l_2.

From the geometry of the linkage, one can write

$$(x_{2i} - l_2 \cos\alpha_i)^2 + (y_{2i} - l_2 \sin\alpha_i)^2 = l_1^2, \quad i = 1,2,3 \tag{2.14}$$

where α_i is defined as the angle between the ith link of length l_2 and the x axis of the fixed Cartesian frame; l_3 and l_4 are as indicated on Figure 2.2 and where (x_{oi}, y_{oi}), i=1,2,3 are the coordinates of point O_i, with $x_{o1} = y_{o1} = y_{o2} = y_{o3} = 0$, and

$$x_{21} = x - x_{01} \tag{2.15}$$

$$y_{21} = y - y_{01} \tag{2.16}$$

$$x_{22} = x + l_3 \cos\phi - x_{02} \tag{2.17}$$

$$y_{22} = y + l_3 \sin\phi - y_{02} \tag{2.18}$$

$$x_{23} = x + l_4 \cos\phi - x_{03} \tag{2.19}$$

$$y_{23} = y + l_4 \sin\phi - y_{03} \tag{2.20}$$

From eq. (2.14) one obtains

$$\sin\alpha_i = \frac{b_i c_i + K_i a_i \sqrt{\delta_i}}{a_i^2 + b_i^2}, \quad i = 1,2,3 \tag{2.21}$$

$$\cos\alpha_i = \frac{a_i c_i - K_i b_i \sqrt{\delta_i}}{a_i^2 + b_i^2}, \quad i = 1,2,3 \tag{2.22}$$

where

$$a_i = x_{2i}, \quad i = 1,2,3 \tag{2.23}$$

$$b_i = y_{2i}, \quad i = 1,2,3 \tag{2.24}$$

$$c_i = \frac{l_2^2 - l_1^2 + x_{2i}^2 + y_{2i}^2}{2l_2}, \quad i = 1,2,3 \tag{2.25}$$

$$\delta_i = a_i^2 + b_i^2 - c_i^2, \quad i = 1,2,3 \tag{2.26}$$

$$K_i = \pm 1, \quad i = 1,2,3$$

where K_i is defined as the ith branch index [14], which can be used to distinguish the eight branches of the inverse kinematic problem.

Finally, the solution of the inverse kinematic problem for this manipulator is obtained as

$$\theta_i \quad = \quad \text{atan2}[(y_{2i} - l_2 \sin\alpha_i), (x_{2i} - l_2 \cos\alpha_i)], \quad i = 1, 2, 3 \tag{2.27}$$

where $\theta_i (i = 1, 2, 3)$ is defined as the angle between the ith link of length l_1 and the x axis of the fixed Cartesian frame.

II) Determination of the workspace

The workspace boundaries of the planar three-degree-of-freedom parallel manipulator consist of the set of configurations which satisfy the following equation in the Cartesian space of the manipulator.

$$\delta = \sqrt{\delta_1}\sqrt{\delta_2}\sqrt{\delta_3} = 0 \tag{2.28}$$

Similarly to the previous case, in order to obtain the boundaries of the workspace of this type of parallel manipulator, the algorithm presented in the first section of this chapter is used to solve eq.(2.28).

A numerical example is now presented in order to illustrate the determination of the workspace.

For this manipulator, let $l_1 = 1.2$, $l_2 = 1.5$, $l_3 = 0.7$, $l_4 = 1.6$, $x_{o1} = 0.0$, $y_{o1} = 0.0$, $x_{o2} = 1.0$, $y_{o2} = 0.0$, $x_{o3} = 2.4$, $y_{o3} = 0.0$ and $\phi = \pi/12$.

The resulting workspace is represented in Figure 2.4.

2.1.1.3 Branches of parallel manipulators

In planar or spatial mechanisms with multiple chains, branches usually exist. Different branches may have different kinematic characteristics. Sometimes, it is impossible for a given mechanism to assume several branches without being disassembled. Hence, it is important to be able to distinguish the different branches and to know their kinematic characteristics in order to choose a configuration which is best suitable for the manipulator to be designed.

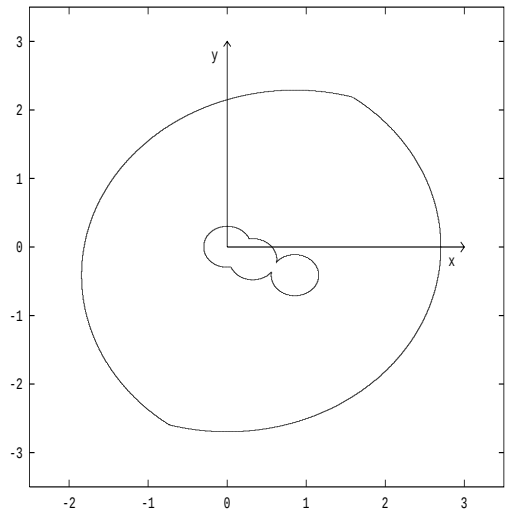

Figure 2.4: Workspace of the three-dof manipulator.

From eqs.(2.6) and (2.7) and from eqs.(2.21) and (2.22), it is clear that angles α_i ($i = 1, 2$ for the two-degree-of-freedom manipulator and $i = 1, 2, 3$ for the three-degree-of-freedom manipulator) have two different solutions which depend on the value of K_i. Therefore the inverse kinematics of the manipulators have different sets of solutions and K_i is the ith branch index of the manipulator. It represents the two different configurations of the ith leg of the manipulator. Hence, the three-degree-of-freedom manipulator has eight different branches caused by the different configurations of its three legs and, similarly, the two-degree-of-freedom manipulator has four different branches.

2.1.2 Spatial parallel manipulators with revolute actuators

Spatial four-, five- and six-degree-of-freedom parallel mechanisms are respectively represented in Figures 2.5, 2.6 and 2.7.

A fixed reference frame $O - xyz$ is attached to the base of the manipulator and a moving coordinate frame $O' - x'y'z'$ is attached to the platform. Moreover, the points of attachment of the actuated legs to the base are noted O_i and the points of attachment of all legs to the platform are noted P_i, with $i = 1, \ldots, n$ where n is equal to 5, 6 and 6 respectively, for each of the manipulators studied here. Point $O = O_n$ is located at

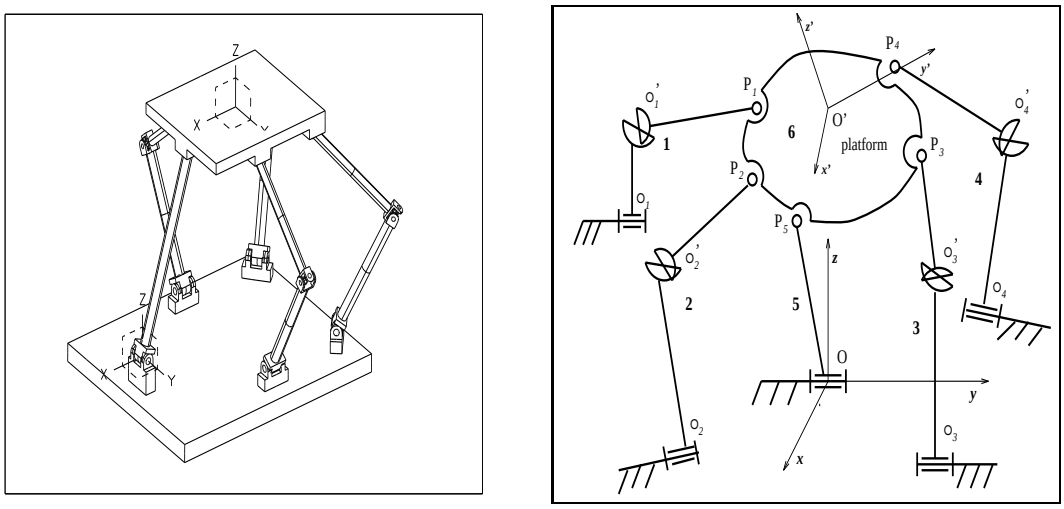

(a) CAD model

(b) Schematic representation

Figure 2.5: Spatial four-degree-of-freedom parallel manipulator with revolute actuators.

the center of the joint connecting the nth leg to the base.

The Cartesian coordinates of the platform are given by the position of point O' with respect to the fixed frame, noted $\mathbf{p} = [\, x \quad y \quad z \,]^T$ and the orientation of the platform (orientation of frame $O' - x'y'z'$ with respect to the fixed frame), represented by three Euler angles ϕ, θ and ψ or by the matrix $\mathbf{Q}$.

If the coordinates of point P_i in the moving reference frame are noted (a_i, b_i, c_i) and if the coordinates of point O_i in the fixed frame are noted (x_{io}, y_{io}, z_{io}), then one has

$$\mathbf{p}_i = \begin{bmatrix} x_i \\ y_i \\ z_i \end{bmatrix}, \quad \mathbf{p}_i^{'} = \begin{bmatrix} a_i \\ b_i \\ c_i \end{bmatrix}, \quad \text{for } i = 1, \ldots, n, \quad \mathbf{p} = \begin{bmatrix} x \\ y \\ z \end{bmatrix} \tag{2.29}$$

where $\mathbf{p}_i$ is the position vector of point P_i expressed in the fixed coordinate frame — and whose coordinates are defined as (x_i, y_i, z_i) —, $\mathbf{p}_i^{'}$ is the position vector of point P_i expressed in the moving coordinate frame, and $\mathbf{p}$ is the position vector of point O' expressed in the fixed frame as defined above. One can then write

$$\mathbf{p}_i = \mathbf{p} + \mathbf{Q}\mathbf{p}_i^{'}, \quad i = 1, \ldots, n \tag{2.30}$$

where $\mathbf{Q}$ is the rotation matrix corresponding to the orientation of the platform of the manipulator with respect to the base coordinate frame. This rotation matrix can be

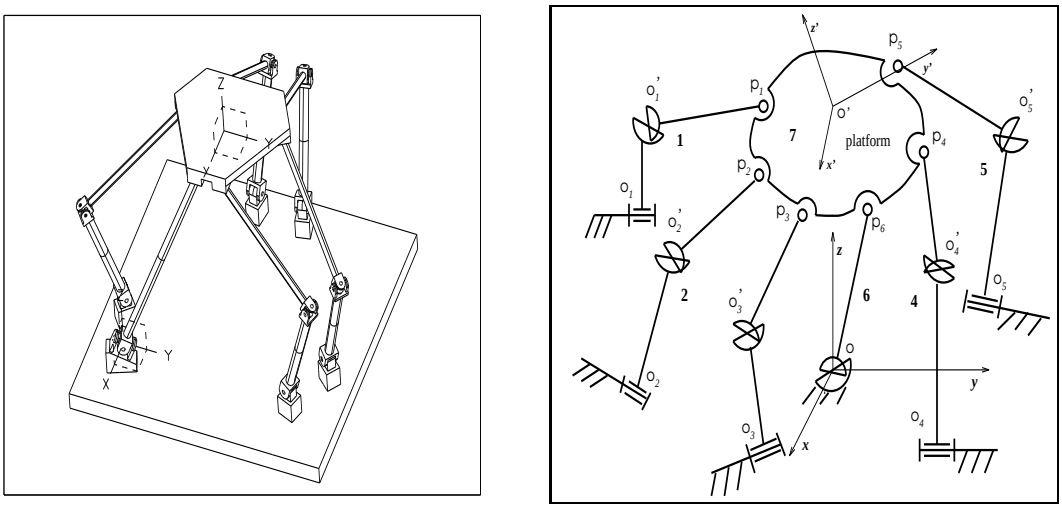

(a) CAD model (b) Schematic representation

Figure 2.6: Spatial five-dof parallel manipulator with revolute actuators.

written as a function of the three Euler angles defined above. With the Euler angle convention used in the present work, this matrix is written as

$$\mathbf{Q} = \begin{bmatrix} c_\phi c_\theta c_\psi - s_\phi s_\psi & -c_\phi c_\theta s_\psi - s_\phi c_\psi & c_\phi s_\theta \\ s_\phi c_\theta c_\psi + c_\phi s_\psi & -s_\phi c_\theta s_\psi + c_\phi c_\psi & s_\phi s_\theta \\ -s_\theta c_\psi & s_\theta s_\psi & c_\theta \end{bmatrix} \tag{2.31}$$

where s_x denotes the sine of angle x while c_x denotes the cosine of angle x.

2.1.2.1 Spatial four-degree-of-freedom parallel manipulator with revolute actuators

I) Inverse kinematics

As represented in figure 2.5, this type of manipulator consists of five kinematic chains, numbered from 1 to 5, connecting the fixed base to a moving platform. Four of these kinematic chains have the same topology. The kinematic chains associated with these four legs consist — from base to platform — of a fixed actuated revolute joint, a moving link, a Hooke joint, a second moving link and a spherical joint attached to the platform. The fifth chain connecting the base to the platform is not actuated and has an architecture which differs from the other chains. It consists of a revolute joint attached to the base, a moving link and a spherical joint attached to the platform. This

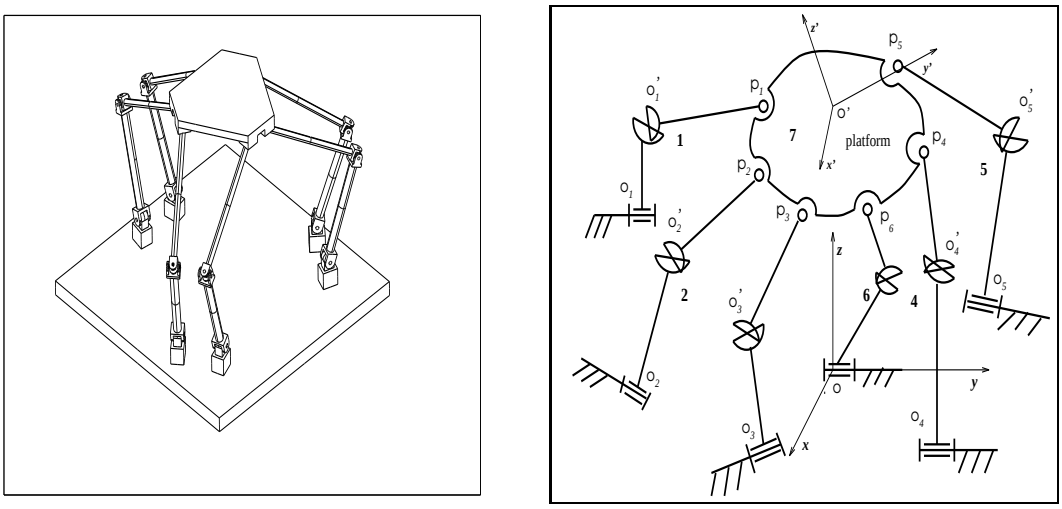

(a) CAD model

(b) Schematic representation

Figure 2.7: Spatial six-dof parallel manipulator with revolute actuators.

last leg is used to constrain the motion of the platform to only four degrees of freedom. It is pointed out, however, that the manipulator could also be built using only four legs, i.e., by removing one of the four identical legs and actuating the first joint of the special leg. Both arrangements lead to similar kinematic equations.

Since the platform of the manipulator has four degrees of freedom, only four out of the six Cartesian coordinates of the platform are independent. In the present study, the independent Cartesian coordinates have been chosen as (x, y, z, ϕ) since it is assumed that the manipulator will be used to position a point in space while specifying a rotation about one axis. The two remaining coordinates, i.e., Euler angles θ and ψ can be determined using the constraints associated with the special 5th leg. Although this choice of coordinates is arbitrary, it can be easily justified by the applications. Moreover, the analysis reported here can easily be repeated with a different choice of coordinates, which would lead to very similar results.

Hence, the four independent coordinates (x, y, z, ϕ) are first specified and the remaining Cartesian coordinates describing the pose of the platform are then determined using the kinematic constraints associated with the special leg. This constitutes the first step of the solution of the inverse kinematic problem. Hence, eq.(2.30) is first

written for chain 5, i.e.,

$$\mathbf{p}_5 - \mathbf{p} = \mathbf{Q}\mathbf{p}_5' \tag{2.32}$$

Taking the square of the norm of both sides of eq.(2.32), one then obtains

$$(x_5 - x)^2 + (y_5 - y)^2 + (z_5 - z)^2 = a_5^2 + b_5^2 + c_5^2 \tag{2.33}$$

Since the unactuated leg is mounted on a passive fixed revolute joint (Figure 2.5), point P_5 is constrained to move on a circle and hence, the coordinates of this point can be written as

$$x_5 = l_5 \sin\alpha, \quad y_5 = 0, \quad z_5 = l_5 \cos\alpha \tag{2.34}$$

where α is the angle defined by link OP_5 with respect to the Z axis of the fixed coordinate frame, as illustrated in Figure 2.8, and l_5 is the length of link OP_5 of the fifth kinematic chain. It is noted that the fixed coordinate frame is defined such that the axis of the fixed revolute joint is along the Y axis of the fixed frame and point O is located such that point P_5 is constrained to move in the XZ plane.

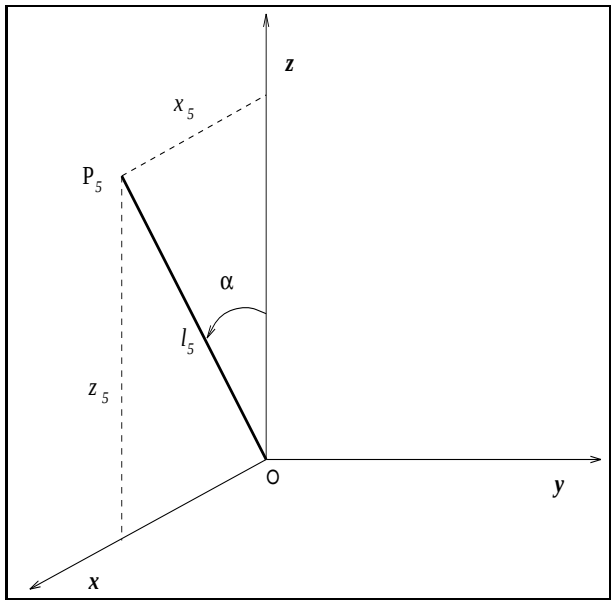

Figure 2.8: Geometry of the fifth leg of the four-dof mechanism.

Upon substitution of eq.(2.34) into eq.(2.33) and further simplification, one then obtains

$$A_{41}\cos\alpha + B_{41}\sin\alpha = C_{41} \tag{2.35}$$

where

$$A_{41} = z \tag{2.36}$$

$$B_{41} = x \tag{2.37}$$

$$C_{41} = \frac{x^2 + y^2 + z^2 + l_5^2 - a_5^2 - b_5^2 - c_5^2}{2l_5} \tag{2.38}$$

The solution of eq.(2.35) then leads to

$$\sin\alpha = \frac{B_{41}C_{41} + K_1 A_{41}\sqrt{\Delta_{41}}}{A_{41}^2 + B_{41}^2} \tag{2.39}$$

$$\cos\alpha = \frac{A_{41}C_{41} - K_1 B_{41}\sqrt{\Delta_{41}}}{A_{41}^2 + B_{41}^2} \tag{2.40}$$

where $K_1 = \pm 1$ is the branch index associated with the fifth kinematic chain of the manipulator and where

$$\Delta_{41} = A_{41}^2 + B_{41}^2 - C_{41}^2 \tag{2.41}$$

Once angle α is obtained, eq.(2.32) can be used to compute the dependent Euler angles ψ and θ. Indeed, multiplying the second component of the latter equation by $\cos\phi$ and subtracting from the first component times $\sin\phi$, one obtains

$$A_{42}\cos\psi + B_{42}\sin\psi = C_{42} \tag{2.42}$$

where

$$A_{42} = b_5 \tag{2.43}$$

$$B_{42} = a_5 \tag{2.44}$$

$$C_{42} = -y\cos\phi - (l_5\sin\alpha - x)\sin\phi \tag{2.45}$$

which leads to

$$\sin\psi = \frac{B_{42}C_{42} + K_2 A_{42}\sqrt{\Delta_{42}}}{A_{42}^2 + B_{42}^2} \tag{2.46}$$

$$\cos\psi = \frac{A_{42}C_{42} - K_2 B_{42}\sqrt{\Delta_{42}}}{A_{42}^2 + B_{42}^2} \tag{2.47}$$

where $K_2 = \pm 1$ is another branch index associated with the orientation of the platform and where

$$\Delta_{42} = A_{42}^2 + B_{42}^2 - C_{42}^2 \tag{2.48}$$

Moreover, the last two component of eq.(2.32) can be rewritten as

$$\mathbf{A}\mathbf{t}_\theta = \mathbf{b} \tag{2.49}$$

where

$$\mathbf{A} = \begin{bmatrix} a_5 \sin\phi\cos\psi - b_5 \sin\phi\sin\psi & c_5 \sin\phi \\ c_5 & b_5 \sin\psi - a_5 \cos\psi \end{bmatrix}$$
$$\mathbf{t}_\theta = \begin{bmatrix} \cos\theta \\ \sin\theta \end{bmatrix}, \quad \mathbf{b} = \begin{bmatrix} -y - a_5 \cos\phi\sin\psi - b_5 \cos\phi\cos\psi \\ l_5 \cos\alpha - z \end{bmatrix}$$

Hence, once angles ϕ and ψ are known, angle θ can be determined by solving eq.(2.49) for $\mathbf{t}_\theta$.

Having obtained the Euler angles, the pose of the platform (its position and orientation) is completely known. The rest of the inverse kinematic procedure therefore consists in computing the actuated coordinates for a given Cartesian pose of the platform. This problem is rather straightforward.

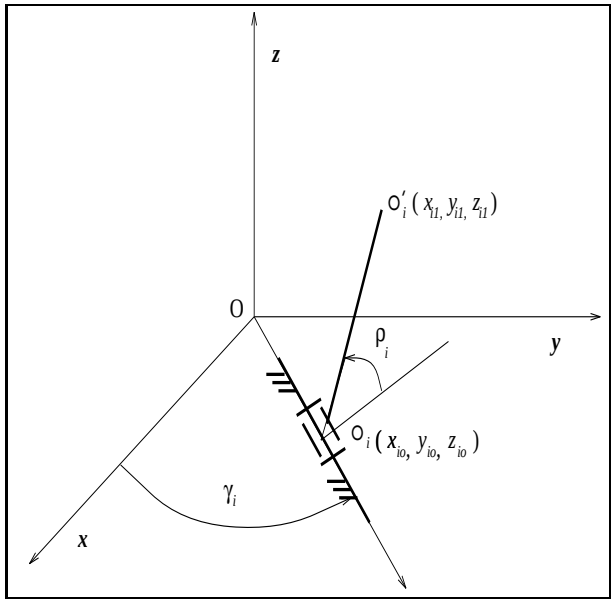

Figure 2.9: Configuration of the ith actuated joint of the four-dof manipulator with revolute actuators.

Figure 2.9 represents the configuration of the ith actuated joint of the manipulator with revolute actuators. Point O_i' is defined as the center of the Hooke joint connecting the two moving links of the ith actuated leg. Moreover, the Cartesian coordinates of point O_i' expressed in the fixed coordinate frame are noted (x_{i1}, y_{i1}, z_{i1}). Since the axis

of the fixed revolute joint of the ith actuated leg is assumed to be parallel to the xy plane of the fixed coordinate frame (Figure 2.9), one can write

$$x_{i1} = x_{io} - l_{i1}\sin\gamma_i\cos\rho_i, \quad i = 1,\ldots,4 \tag{2.50}$$

$$y_{i1} = y_{io} + l_{i1}\cos\gamma_i\cos\rho_i, \quad i = 1,\ldots,4 \tag{2.51}$$

$$z_{i1} = z_{io} + l_{i1}\sin\rho_i, \quad i = 1,\ldots,4 \tag{2.52}$$

where γ_i is the angle between the positive direction of the x axis of the base coordinate frame and the axis of the ith actuated joint while ρ_i is the joint variable — rotation angle around the fixed revolute joint — associated with the ith actuated leg. Moreover, l_{i1} is the length of the first link of the ith actuated leg. From the geometry of the mechanism, one can write

$$(x_{i1} - x_i)^2 + (y_{i1} - y_i)^2 + (z_{i1} - z_i)^2 = l_{i2}^2, \quad i = 1,\ldots,4 \tag{2.53}$$

where x_i, y_i, z_i have been previously defined as the coordinates of point P_i and l_{i2} is the length of the second link of the ith actuated leg.

Substituting eqs.(2.50), (2.51) and (2.52) into equation (2.53), one obtains

$$R_i\cos\rho_i + S_i\sin\rho_i = T_i, \quad i = 1,\ldots,4 \tag{2.54}$$

where

$$\begin{aligned} R_i &= (y_i - y_{io})\cos\gamma_i - (x_i - x_{io})\sin\gamma_i \\ S_i &= z_i - z_{io} \\ T_i &= \frac{(x_i - x_{io})^2 + (y_i - y_{io})^2 + (z_i - z_{io})^2 + l_{i1}^2 - l_{i2}^2}{2l_{i1}} \end{aligned}$$

which leads directly to

$$\sin\rho_i = \frac{S_iT_i + K_{i3}R_i\sqrt{V_i}}{R_i^2 + S_i^2}, \quad i = 1,\ldots,4 \tag{2.55}$$

$$\cos\rho_i = \frac{R_iT_i - K_{i3}S_i\sqrt{V_i}}{R_i^2 + S_i^2}, \quad i = 1,\ldots,4 \tag{2.56}$$

where $K_{i3} = \pm 1$ is the branch index of the manipulator associated with the configuration of the ith leg and

$$V_i = R_i^2 + S_i^2 - T_i^2, \quad i = 1,\ldots,4 \tag{2.57}$$

The solution of the inverse kinematic problem is then completed by performing

$$\rho_i = \text{atan2}[\sin\rho_i, \cos\rho_i], \quad i = 1, \ldots, 4 \tag{2.58}$$

Since two solutions are obtained for each of the ρ_i's, it is clear that the inverse kinematic problem of this manipulator leads to 64 solutions.

II) Determination of the workspace

Similarly to what was done for planar parallel mechanisms, the first type of singularity will be obtained by finding the boundaries of the Cartesian workspace of the manipulator. Hence, the locus of the limit of the workspace is given by the following equation

$$\Delta_4 = \left(\prod_{i=1}^{2}\sqrt{\Delta_{4i}}\right)\left(\prod_{i=1}^{4}\sqrt{V_i}\right) = 0 \tag{2.59}$$

where Δ_{41}, Δ_{42} and V_i are respectively defined in eqs.(2.42), (2.48) and (2.57) and the same algorithm is used here to determine the curves corresponding to this locus.

An example is now given to illustrate the determination of the workspace of this type of mechanism. The parameters used in this example are given as

$$x_{o1} = -1.5,\ y_{o1} = 1.5,\ x_{o2} = -3.0,\ y_{o2} = 1.5,\ x_{o3} = -3.0,\ y_{o3} = -1.5$$

$$x_{o4} = -1.5,\ y_{o4} = -1.5,\ x_{o5} = 0.0,\ y_{o5} = 0.0,\ z_{oi} = 0.0 (i = 1, \ldots, 5)$$

$$a_1 = 0.2,\ b_1 = 0.6,\ c_1 = -0.4,\ a_2 = -0.6,\ b_2 = 0.6,\ c_2 = -0.4$$

$$a_3 = -0.6,\ b_3 = -0.6,\ c_3 = -0.4,\ a_4 = 0.2,\ b_4 = -0.6,\ c_4 = -0.4$$

$$a_5 = 0.6,\ b_5 = 0.0,\ c_5 = 0.0$$

$$\gamma_1 = \frac{\pi}{4},\ \gamma_2 = \frac{\pi}{4},\ \gamma_3 = \frac{3\pi}{4},\ \gamma_4 = \frac{3\pi}{4}$$

$$l_5 = 1.0,\ l_{i1} = 2.0,\ l_{i2} = 3.0 (i = 1, \ldots, 4)$$

and the Cartesian coordinates being imposed are respectively

$$\phi = \frac{\pi}{10},\ y = 0.0 \text{ and } \phi = \frac{\pi}{10},\ x = -1.25$$

with $K_1 = K_2 = K_{i3} = -1,\ i = 1, \ldots, 4$.

Figure 2.10 shows two sections of the workspace for this example.

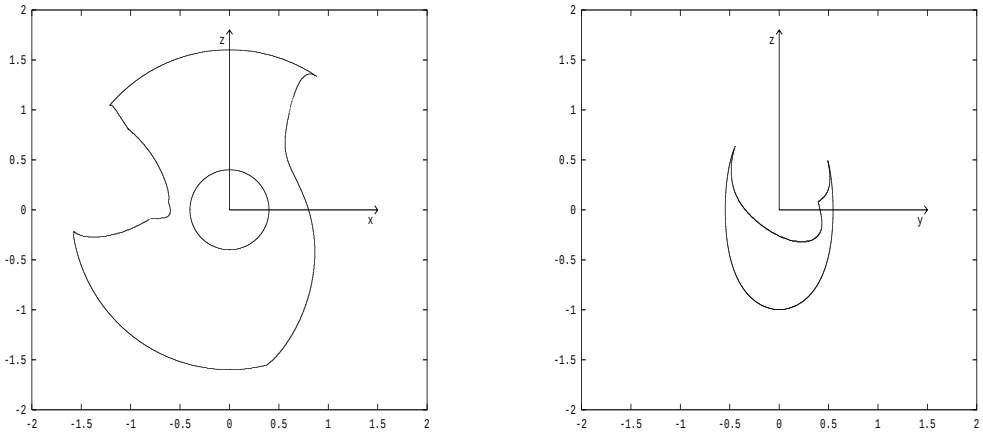

(a) A section of the workspace (over x and z).

(b) A section of the workspace (over y and z).

Figure 2.10: Example of the workspace of the four-dof mechanism

2.1.2.2 Spatial five-degree-of-freedom parallel manipulator with revolute actuators

I) Inverse kinematics

As represented in Figure 2.6, the spatial five-degree-of-freedom parallel manipulator mechanism consists of six kinematic chains, numbered from 1 to 6, connecting the fixed base to a moving platform. Five of these kinematic chains have the same topology. The kinematic chains associated with these five legs consist — from base to platform — of a fixed actuated revolute joint, a moving link, a Hooke joint, a second moving link and a spherical joint attached to the platform (Figure 2.6). The sixth chain connecting the base to the platform is not actuated and has an architecture which differs from the other chains. It consists of a Hooke joint attached to the base, a moving link and a spherical joint attached to the platform. This last leg is used to constrain the motion of the platform to only five degrees of freedom. Similarly to the case of the four-dof mechanism, this mechanism could also be built using only five legs, i.e., by removing one of the five identical legs and actuating the first joint of the special leg. Both arrangements lead to similar kinematic equations.

Since the platform of the mechanism has five degrees of freedom, only five of the

six Cartesian coordinates of the platform are independent. In the present study, the independent Cartesian coordinates have been chosen as (x, y, z, ϕ, θ) since it is assumed that the mechanism will be used to position a point in space while specifying two independent rotations. The remaining coordinate, i.e., Euler angle ψ can be determined using the constraints associated with the special 6th leg. Similarly to the four-degree-of-freedom parallel mechanism, although this choice of coordinates is arbitrary, it can be justified by the applications to be considered, i.e., the position and orientation of axisymmetric bodies, and the analysis reported here can easily be repeated with a different choice of coordinates, which would lead to very similar results.

Hence, the five independent coordinates (x, y, z, ϕ, θ) are first specified and the remaining Cartesian coordinate describing the pose of the platform is then determined using the kinematic constraints associated with the special leg. Hence, eq.(2.30) is first written for chain 6, i.e.,

$$\mathbf{p}_6 = \mathbf{p} + \mathbf{Q}\mathbf{p}_6^{'} \tag{2.60}$$

or, in terms of the components,

$$\begin{aligned} x_6 &= x + a_6(\cos\phi\cos\theta\cos\psi - \sin\phi\sin\psi) + b_6(-\cos\phi\cos\theta\sin\psi - \sin\phi\cos\psi) \\ &\quad + c_6\cos\phi\sin\theta \qquad (2.61) \\ y_6 &= y + a_6(\sin\phi\cos\theta\cos\psi + \cos\phi\sin\psi) + b_6(-\sin\phi\cos\theta\sin\psi + \cos\phi\cos\psi) \\ &\quad + c_6\sin\phi\sin\theta \qquad (2.62) \\ z_6 &= z + a_6(-\sin\theta\cos\psi) + b_6\sin\theta\sin\psi + c_6\cos\theta \qquad (2.63) \end{aligned}$$

Moreover, from the geometry of the special leg, one can write

$$x_6^2 + y_6^2 + z_6^2 = l_6^2 \tag{2.64}$$

where l_6 is the length of the special leg.

Squaring both sides of equations (2.61), (2.62) and (2.63) and adding, one then obtains

$$A\cos\psi + B\sin\psi = C \tag{2.65}$$

where

$$A = 2b_6 y\cos\phi + a_6 x\cos(\phi - \theta) + a_6 x\cos(\phi + \theta) - 2b_6 x\sin\phi + a_6 y\sin(\phi - \theta)$$

$$-2a_6 z\sin\theta + a_6 y\sin(\phi+\theta) \tag{2.66}$$

$$\begin{aligned} B &= 2a_6 y\cos\phi - b_6 x\cos(\phi-\theta) - b_6 x\cos(\phi+\theta) - 2a_6 x\sin\phi - b_6 y\sin(\phi-\theta) \\ &\quad +2b_6 z\sin\theta - b_6 y\sin(\phi+\theta) \end{aligned} \tag{2.67}$$

$$\begin{aligned} C &= l_6^2 - (a_6^2 + b_6^2 + c_6^2 + x^2 + y^2 + z^2 + c_6 y\cos(\phi-\theta) + 2c_6 z\cos\theta - c_6 y\cos(\phi+\theta) \\ &\quad -c_6 x\sin(\phi-\theta) + c_6 x\sin(\phi+\theta)) \end{aligned} \tag{2.68}$$

The solution of eq.(2.65) then leads to

$$\sin\psi = \frac{BC + K_6 A\sqrt{\Delta}}{A^2+B^2} \tag{2.69}$$

$$\cos\psi = \frac{AC - K_6 B\sqrt{\Delta}}{A^2+B^2} \tag{2.70}$$

where $K_6 = \pm 1$ is the branch index associated with the sixth kinematic chain of the mechanism and where

$$\Delta = A^2 + B^2 - C^2 \tag{2.71}$$

Having obtained the last Euler angle, the pose of the platform (its position and orientation) is completely known. The rest of the inverse kinematic procedure therefore consists in computing the actuated coordinates for a given Cartesian pose of the platform. It is identical to what is encountered in the four-degree-of-freedom parallel mechanism and the procedure is not repeated here.

Since two solutions are obtained for each of the ρ_i's, it is clear that the inverse kinematic problem of this mechanism leads to 64 solutions, which can be distinguished using branch indices K_1 to K_6.

II) Determination of the workspace

Similarly, for this mechanism the locus of the limit of the workspace, namely, the first type of singularity locus, are given by the following equation

$$\delta = \sqrt{\Delta}\prod_{i=1}^{5}\sqrt{V_i} = 0 \tag{2.72}$$

where V_i is defined in eq.(2.57) and Δ is defined in eq.(2.71).

An example is now given to illustrate the determination of the workspace of this type of mechanism. The parameters used in this example are given as

$$x_{o1} = 2.0,\ y_{o1} = 1.5,\ x_{o2} = -1.0,\ y_{o2} = 1.5,\ x_{o3} = -2.0,\ y_{o3} = 0.0,$$
$$x_{o4} = -1.0,\ y_{o4} = -1.5,\ x_{o5} = 2.0,\ y_{o5} = -1.5,\ x_{o6} = 0.0,\ y_{o6} = 0.0,$$
$$z_{oi} = 0.0 (i = 1, \ldots, 6),$$
$$a_1 = 0.8,\ b_1 = 0.6,\ c_1 = -0.4,\ a_2 = -0.4,\ b_2 = 0.6,\ c_2 = -0.4$$
$$a_3 = -0.8,\ b_3 = 0.0,\ c_3 = -0.4,\ a_4 = -0.4,\ b_4 = -0.6,\ c_4 = -0.4,$$
$$a_5 = 0.8,\ b_5 = -0.6,\ c_5 = -0.4,\ a_6 = 0.1,\ b_6 = 0.2,\ c_6 = -0.6$$
$$\gamma_1 = \tfrac{3\pi}{4},\ \gamma_2 = \tfrac{5\pi}{4},\ \gamma_3 = \tfrac{3\pi}{2},\ \gamma_4 = \tfrac{7\pi}{4},\ \gamma_5 = \tfrac{9\pi}{4},$$
$$l_6 = 1.0,\ l_{i1} = 3.0,\ l_{i2} = 3.0, (i = 1, \ldots, 5)$$

and the three fixed Cartesian coordinates are respectively given by

$$\phi = \frac{\pi}{6}, \quad \theta = \frac{\pi}{3}, \quad y = 0$$
$$\phi = \frac{\pi}{6}, \quad \theta = \frac{\pi}{3}, \quad x = 1.0$$
$$K_i = 1,\ i = 1, \ldots, 6$$

Figure 2.11 shows two sections of the workspace for the above example.

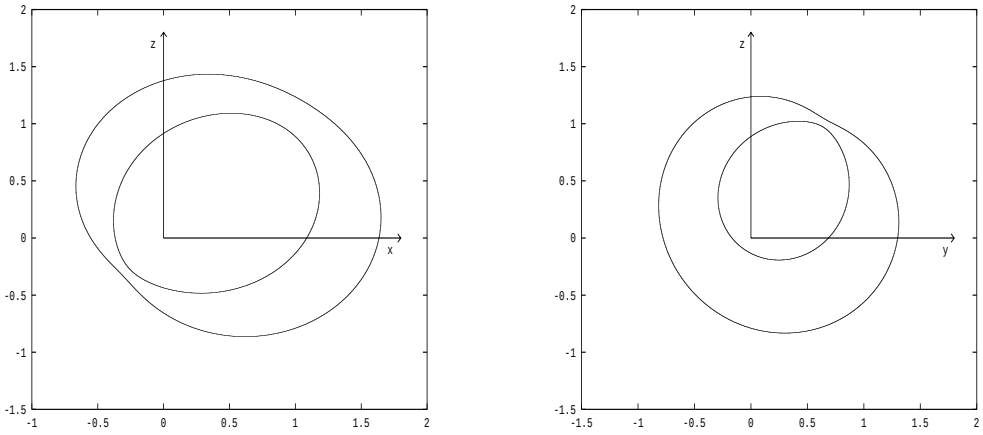

(a) A section of the workspace (over x and z).

(b) A section of the workspace (over y and z).

Figure 2.11: Example of the workspace of the five-dof mechanism.

2.1.2.3 Spatial six-degree-of-freedom parallel manipulator with revolute actuators

As represented in Figure 2.7, spatial six-degree-of-freedom parallel manipulator consists of six identical legs connecting the base to the platform. Each of these legs consists of an actuated revolute joint attached to the base, a first moving link, a passive Hooke joint, a second moving link and a passive spherical joint attached to the platform. A parallel manipulator of this type was described in [8].

The procedure for the computation of the inverse kinematics therefore consists in computing the actuated joint coordinates for a given Cartesian pose of the platform. It is exactly identical to the procedure of the last part of the computation of the inverse kinematics of the four- and five-degree-of-freedom parallel mechanisms and is not repeated here.

Similarly, for this mechanism the locus of the limit of the workspace is given by the following equation

$$\delta = \prod_{i=1}^{6} \sqrt{V_i} = 0 \tag{2.73}$$

where V_i is defined in eq.(2.57).

However, it is pointed out here that for this mechanism there exists an algorithm to find the analytical description of the boundary of the workspace [13].

An example is now given to illustrate the determination of the workspace of this type of mechanism. The parameters used in this example are given as

$$x_{o1} = -1.0,\ y_{o1} = 1.5,\ x_{o2} = -3.0,\ y_{o2} = 1.5,\ x_{o3} = -4.0,\ y_{o3} = 0.0,$$
$$x_{o4} = -3.0,\ y_{o4} = -1.5,\ x_{o5} = -1.0,\ y_{o5} = -1.5,\ x_{o6} = 0.0,\ y_{o6} = 0.0,$$
$$z_{oi} = 0.0 (i = 1, \ldots, 6),$$
$$a_1 = 0.8,\ b_1 = 0.6,\ c_1 = -0.4,\ a_2 = -0.4,\ b_2 = 0.6,\ c_2 = -0.4$$
$$a_3 = -0.8,\ b_3 = 0.0,\ c_3 = -0.4,\ a_4 = -0.4,\ b_4 = -0.6,\ c_4 = -0.4,$$
$$a_5 = 0.8,\ b_5 = -0.6,\ c_5 = -0.4,\ a_6 = 0.8,\ b_6 = -0.6,\ c_6 = -0.4$$
$$\gamma_1 = \tfrac{3\pi}{4},\ \gamma_2 = \tfrac{5\pi}{4},\ \gamma_3 = \tfrac{3\pi}{2},\ \gamma_4 = \tfrac{7\pi}{4},\ \gamma_5 = \tfrac{9\pi}{4},\ \gamma_6 = \tfrac{\pi}{2},$$
$$l_{i1} = 2.0,\ l_{i2} = 2.0,\ (i = 1, \ldots, 6)$$

and the four fixed Cartesian coordinates are respectively given by

$$\phi = \frac{\pi}{3}, \quad \theta = \frac{\pi}{6}, \quad \psi = \frac{\pi}{3}, \quad y = 0.0$$

$$\phi = \frac{\pi}{6}, \quad \theta = \frac{\pi}{3}, \quad \psi = \frac{\pi}{3}, \quad x = -2.0$$

$$K_i = -1, \; i = 1, \ldots, 6$$

Figure 2.12 shows two sections of the workspace for this example.

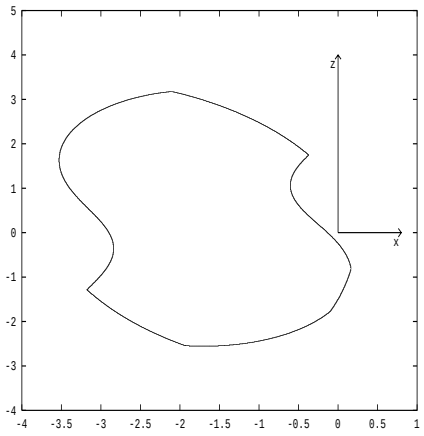

(a) A section of the workspace (over x and z).

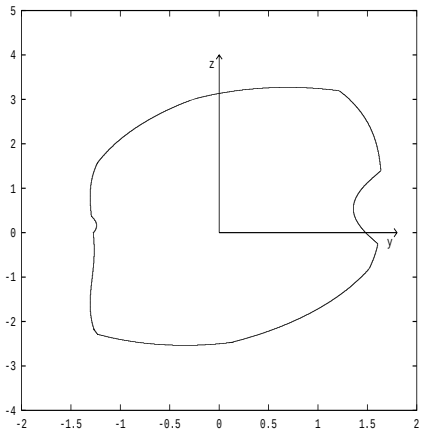

(b) A section of the workspace (over y and z).

Figure 2.12: Example of the workspace of the six-dof mechanism.

2.2 Velocity equations and singularity loci

The velocity equations of manipulators are important for their kinematic analysis. Indeed, since the velocity equations represent the linear mapping between the actuated joint velocities and the Cartesian velocities, they characterize the kinematic accuracy of a manipulator and they allow the determination of the singularities. Here, two different methods will be used to derive the velocity equations of the manipulators studied. Each of these methods has its own advantages and drawbacks, as will be shown below.

Moreover, the determination of the singular configurations of mechanisms is an issue of the utmost importance, since when the singularities occur, the end-effector of the manipulator gains or loses one or more degree(s) of freedom and therefore becomes uncontrollable. Hence, such configurations must be avoided.

In [16], three general types of singularities which can occur in parallel manipulators have been identified. Moreover, in [66], this classification has been further refined and several types of singularities have been defined according to their physical interpretation. However, the mathematical description of these types of singularities is more difficult to obtain and hence, the classification proposed in [16] will be used here. Indeed, the mathematical expressions allowing the identification of these singularities is readily available.

In what follows, vector $\boldsymbol{\theta}$ is used to denote the actuated joint coordinates of the manipulator, representing the vector of kinematic input. Moreover, vector $\mathbf{x}$ denotes the Cartesian coordinates of the manipulator gripper, representing the kinematic output. The velocity equations of the manipulator can be written as

$$\mathbf{A}\dot{\mathbf{x}} + \mathbf{B}\dot{\boldsymbol{\theta}} = \mathbf{0} \tag{2.74}$$

where

$$\dot{\boldsymbol{\theta}} = [\,\dot{\theta}_1 \quad \dot{\theta}_2 \quad \ldots \quad \dot{\theta}_n\,]^T$$
$$\dot{\mathbf{x}} = [\,\dot{x}_1 \quad \dot{x}_2 \quad \ldots \quad \dot{x}_n\,]^T$$

and where $\mathbf{A}$ and $\mathbf{B}$ are square matrices of dimension n, called Jacobian matrices, with n representing the number of degrees of freedom of the manipulator.

Referring to eq.(2.74), Gosselin and Angeles [16] have defined three types of singularities which can occur in parallel manipulators.

I) The first type of singularity occurs when $\det(\mathbf{B}) = 0$. In such a situation, the gripper of the manipulator loses one or more degrees of freedom and lies in a deadpoint position. In other words, the gripper can resist one or more forces or moments without exerting any torque or force at the actuated joints. These configurations correspond to a set of points defining the outer and internal boundaries of the workspace of the manipulator. They have been studied in the previous section of this chapter.

II) The second type of singularity occurs when $\det(\mathbf{A}) = 0$. As opposed to the first one, the gripper of the manipulator gains one or more degrees of freedom, namely, it cannot resist the forces or moments from one or more directions even when all actuated joints are locked. The actuated joints are at a deadpoint. This kind of singularity corresponds to a set of points within the workspace of the manipulator.

III) The third kind of singularity occurs when the positioning equations degenerate. This type of singularity is also referred to as an architecture singularity [6]. Only when the parameters of a manipulator satisfy certain special conditions can this kind of singularity occur. It corresponds to a set of configurations where a finite motion of the gripper of the manipulator is possible even if the actuated joints are locked (referred to as self-motion in [27], [28] and [29]) or where a finite motion of the actuated joints produces no motion of the gripper.

The singularity classification method presented above is applicable to any parallel manipulator. In this Chapter, it is used to analyze the second type of singularity of the manipulators introduced earlier in order to find Cartesian loci associated with this type of singularity. For the first type of singularity, the loci can be obtained by computing the boundary of the workspace of the manipulator, which has been completed in the previous section and will not be discussed any further here. The second type of singularity loci will be found from the expressions of the determinant of the Jacobian matrices of the mechanisms, as will be shown in the following. Furthermore, it is assumed that the third type of singularity is avoided by a proper choice of the kinematic parameters.

In [47], the singularity loci of planar three-degree-of-freedom parallel manipulators with prismatic actuators have been obtained. Because of the prismatic actuators, the mathematical expressions obtained were very simple and the loci were shown to correspond to quadratic forms. However, for manipulators with revolute actuators, expressions are much more complex as will be shown next and the simple approach used in the latter reference cannot be applied directly. Similarly, for spatial six-degree-of-freedom parallel manipulators with prismatic joints, an expression for the singularity loci has been obtained in [41]. It was shown, in the latter reference, that for a given orientation of the platform, the loci were surfaces of degree 3. However, this approach cannot be directly applied to manipulators with revolute actuators, since the joint coordinates and the Cartesian coordinates both appear in the Jacobian matix.

2.2.1 Planar parallel manipulators

The velocity equations of planar two- and three-degree-of-freedom parallel mechanisms or manipulators will first be derived, and then used to determine the singularity loci of type II.

Let $\mathbf{a}_i$ be the two-dimensional position vector connecting the ith joint O_i to one of its neighboring joints, as indicated in Figures 2.13 and 2.16 (except $\mathbf{a}_3$ and $\mathbf{a}_5$ on Figure 2.13, which connect O_3 and O_5 to P and a_8 in Figure 2.16, which connects O_7 to O_9), and let ω_i be the angular velocity of the ith link. From these definitions, it is possible to obtain the velocity equations, as will now be illustrated.

2.2.1.1 Two-degree-of-freedom manipulator

Using the closed loop of the two-degree-of-freedom manipulator $O_1O_3O_5O_4O_2$, one can write

$$\omega_1\mathbf{E}\mathbf{a}_1 + \omega_3\mathbf{E}(\mathbf{a}_3 - \mathbf{a}_5) = \omega_2\mathbf{E}\mathbf{a}_2 + \omega_4\mathbf{E}\mathbf{a}_4 \tag{2.75}$$

where

$$\mathbf{E} = \begin{bmatrix} 0 & -1 \\ 1 & 0 \end{bmatrix}$$

is a 2×2 operator rotating an arbitrary two-dimensional vector counterclockwise

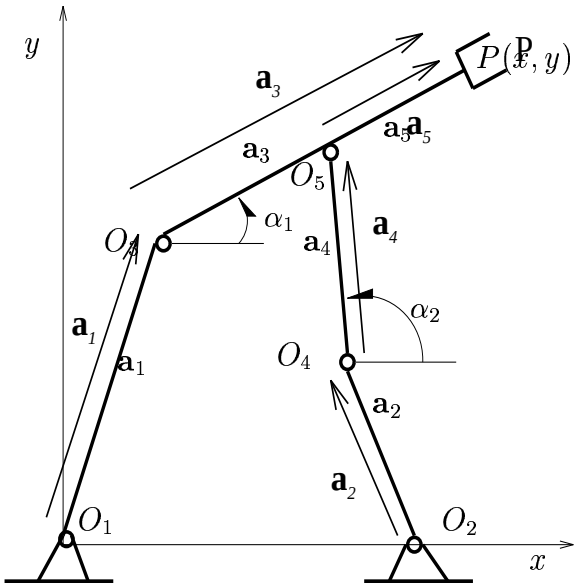

Figure 2.13: Loop vectors associated with the two-degree-of-freedom manipulator.

through an angle of 90^o [45]. Using eq.(2.75) as the velocity equation of the manipulator is equivalent to using the angular velocity of links of length l_3 and l_4 to represent its Cartesian velocity instead of using the velocity of one of the points on the platform.

Then, from eq.(2.75), one obtains

$$\mathbf{A}^*\mathbf{w}_O + \mathbf{B}^*\mathbf{w}_I = \mathbf{0} \tag{2.76}$$

where

$$\begin{aligned}
\mathbf{A}^* &= [\,(\mathbf{a}_3 - \mathbf{a}_5) \quad -\mathbf{a}_4\,] \\
\mathbf{B}^* &= [\,\mathbf{a}_1 \quad -\mathbf{a}_2\,] \\
\mathbf{w}_O &= \begin{bmatrix} \omega_3 \\ \omega_4 \end{bmatrix} \\
\mathbf{w}_I &= \begin{bmatrix} \omega_1 \\ \omega_2 \end{bmatrix}
\end{aligned}$$

Equation (2.76) can be used as the velocity equation of the two-degree-of-freedom manipulator since for this manipulator, we can use the angular velocities of links 3 and 4 as the output vector. From eq.(2.76), $\mathbf{A}^*$ is then written as

$$\mathbf{A}^* = \begin{bmatrix} (l_3 - l_5)\cos\alpha_1 & -l_4\cos\alpha_2 \\ (l_3 - l_5)\sin\alpha_1 & -l_4\sin\alpha_2 \end{bmatrix} \tag{2.77}$$

From eq.(2.77), one then obtains

$$\det(\mathbf{A}^*) = l_3 l_4 \sin(\alpha_1 - \alpha_2) \tag{2.78}$$

From eq.(2.78), it is clear that when $\alpha_1 = \alpha_2 + n\pi, n = 0, \pm 1, \pm 2, ...$, then $\det(\mathbf{A}^*) = 0$. In other words, if the two vectors $\mathbf{a}_3$ and $\mathbf{a}_4$ are aligned, the manipulator is in a configuration which corresponds to the second type of singularity. The polynomial formulation of the singularity loci for this type of mechanism is given in Appendix A. It leads to a curve of degree 6.

The determination of the singularity loci of the manipulators consists in finding the roots of equation $\det(\mathbf{A}^*) = 0$. This can be accomplished using the expressions of eqs.(2.78) directly. The detailed expressions associated with the equation are given in Appendix B.

The above equations can be solved using a numerical procedure in order to determine the singularity loci for each of the branches and to represent them graphically. This results in the singularity locus according to each branch of the manipulator within its workspace. The singularity loci of all the branches of the manipulator can also be superimposed on the workspace.

With the same parameters used in the example on the determination of the workspace of the manipulator, one can obtain the singularity loci over the workspace in each branch, as shown in Figures 2.14 and 2.15.

The manipulators in Figures 2.14(b) and 2.14(d) are shown in a singular configuration while they are represented in a nonsingular configuration in Figures 2.14(a) and 2.14(c). The singularity loci of all branches in the two workspaces of the manipulator are shown in Figures 2.15(a) and 2.15(b), respectively.

2.2.1.2 Three-degree-of-freedom manipulator

From Figure 2.16, it is clear that this manipulator contains two independent closed loops: for instance $O_1O_4O_7O_8O_5O_2$ and $O_1O_4O_7O_8O_9O_6O_3$. Therefore, by using the loop constraints, one can write the following velocity equations:

$$\omega_1 \mathbf{E}\mathbf{a}_1 + \omega_4 \mathbf{E}\mathbf{a}_4 + \omega_7 \mathbf{E}\mathbf{a}_7 = \omega_2 \mathbf{E}\mathbf{a}_2 + \omega_5 \mathbf{E}\mathbf{a}_5 \tag{2.79}$$

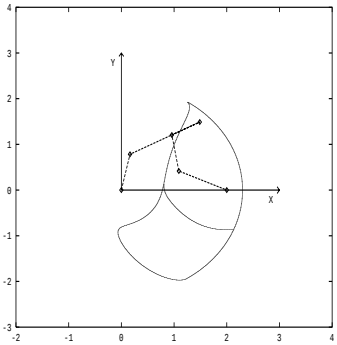

(a) Branch **1**: $K_1 = -1, K_2 = -1$.

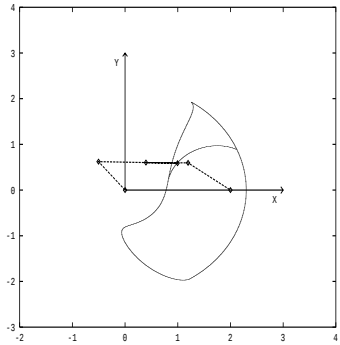

(b) Branch **2**: $K_1 = -1, K_2 = +1$.

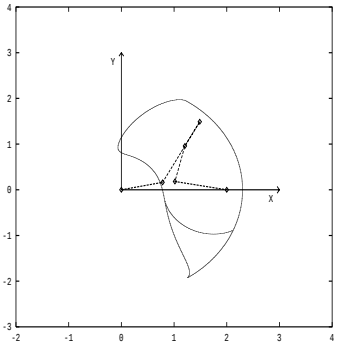

(c) Branch **3**: $K_1 = +1, K_2 = -1$.

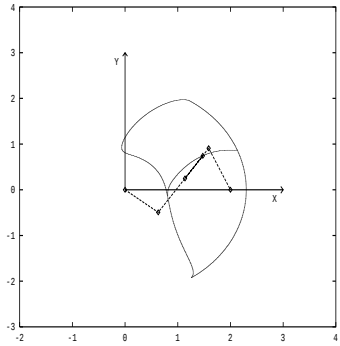

(d) Branch **4**: $K_1 = +1, K_2 = +1$.

Figure 2.14: Singularity locus and workspace of the two-dof manipulator.

$$\omega_1 \mathbf{E}\mathbf{a}_1 + \omega_4 \mathbf{E}\mathbf{a}_4 + \omega_7 \mathbf{E}\mathbf{a}_8 = \omega_3 \mathbf{E}\mathbf{a}_3 + \omega_6 \mathbf{E}\mathbf{a}_6 \tag{2.80}$$

From eqs.(2.79) and (2.80), one obtains

$$\mathbf{A}^* \mathbf{w}_O + \mathbf{B}^* \mathbf{w}_I = \mathbf{0} \tag{2.81}$$

where

$$\mathbf{A}^* = \begin{bmatrix} \mathbf{a}_4 & -\mathbf{a}_5 & \mathbf{0} & \mathbf{a}_7 \\ \mathbf{a}_4 & \mathbf{0} & -\mathbf{a}_6 & \mathbf{a}_8 \end{bmatrix}$$

$$\mathbf{B}^* = \begin{bmatrix} \mathbf{a}_1 & -\mathbf{a}_2 & \mathbf{0} \\ \mathbf{a}_1 & \mathbf{0} & -\mathbf{a}_3 \end{bmatrix}$$

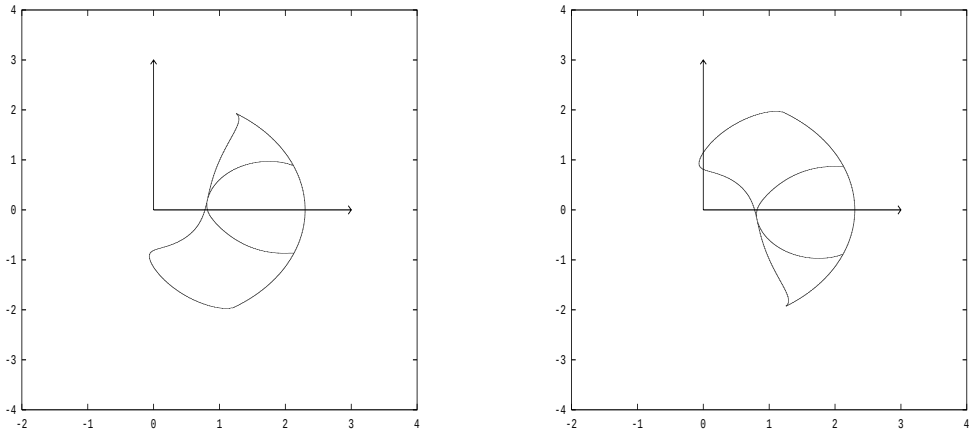

(a) Singularity locus of workspace 1. (b) Singularity locus of workspace 2.

Figure 2.15: Singularity locus and workspace of the two-dof manipulator.

$$\begin{aligned} \mathbf{w}_O &= \begin{bmatrix} \omega_4 & \omega_5 & \omega_6 & \omega_7 \end{bmatrix}^T \\ \mathbf{w}_I &= \begin{bmatrix} \omega_1 & \omega_2 & \omega_3 \end{bmatrix}^T \end{aligned}$$

Equation (2.81) can be used as the velocity equation of the three-degree-of-freedom manipulator, where the angular velocities of the input links are used as the joint velocities and the angular velocities of the other moving links are used as the Cartesian velocities.

Comparing eqs.(2.81) and (2.74), it is possible to use the angular velocities of links 4, 5, 6 and 7 as output velocities, and hence, to write

$$\mathbf{w}_I = \dot{\boldsymbol{\theta}} \tag{2.82}$$

$$\mathbf{w}_O = \dot{\mathbf{x}} \tag{2.83}$$

Therefore, considering eqs. (2.82), (2.83) and (2.81) together, it can be concluded that if $\det(\mathbf{A}^*) = 0$, then the manipulator is in a singular configuration corresponding to the second type of singularity. In other words, matrices $\mathbf{A}^*$ and $\mathbf{A}$ are equivalent for the purpose of determining the second type of singularity of the manipulator. In a singular configuration, since the nullspace of $\mathbf{A}^*$ is not empty, there exist nonzero vectors $\mathbf{w}_O$ which will be mapped into the origin by $\mathbf{A}^*$.

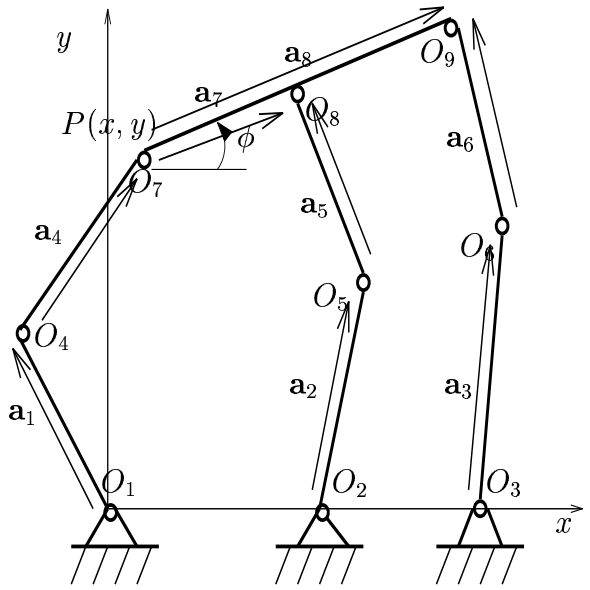

Figure 2.16: Loop vectors associated with the three-degree-of-freedom manipulator.

It can be easily shown that when the three vectors $\mathbf{a}_4$, $\mathbf{a}_5$ and $\mathbf{a}_6$ are parallel to one another or intersect at a common point $Q(x_q, y_q)$, as represented in Figure 2.17, then $\det(\mathbf{A}^*) = 0$, namely, the second type of singularity of the manipulator occurs. This result has been obtained in [25].

Matrix $\mathbf{A}^*$ can be written as

$$\mathbf{A}^* = \begin{bmatrix} l_2\cos\alpha_1 & -l_2\cos\alpha_2 & 0 & l_3\cos\phi \\ l_2\sin\alpha_1 & -l_2\sin\alpha_2 & 0 & l_3\sin\phi \\ l_2\cos\alpha_1 & 0 & -l_2\cos\alpha_3 & l_4\cos\phi \\ l_2\sin\alpha_1 & 0 & -l_2\sin\alpha_3 & l_4\sin\phi \end{bmatrix} \tag{2.84}$$

where the notation for the link lengths refers to Figure 2.2.

From eq.(2.84), one has

$$\begin{aligned} \det(\mathbf{A}^*) \;=\; & l_2^3\sin\phi(l_4\cos\alpha_1\sin\alpha_2\cos\alpha_3 \\ & -l_4\sin\alpha_1\cos\alpha_2\cos\alpha_3 \\ & -l_3\cos\alpha_1\cos\alpha_2\sin\alpha_3 \\ & +l_3\sin\alpha_1\cos\alpha_2\cos\alpha_3) \\ & +l_2^3\cos\phi(l_4\sin\alpha_1\cos\alpha_2\sin\alpha_3 \\ & -l_4\cos\alpha_1\sin\alpha_2\sin\alpha_3 \end{aligned}$$

$$-l_3 \sin\alpha_1 \sin\alpha_2 \cos\alpha_3$$
$$+l_3 \cos\alpha_1 \sin\alpha_2 \sin\alpha_3) \qquad (2.85)$$

and two cases may arise.

a) If $\mathbf{a}_4$, $\mathbf{a}_5$ and $\mathbf{a}_6$ are parallel to one another, then

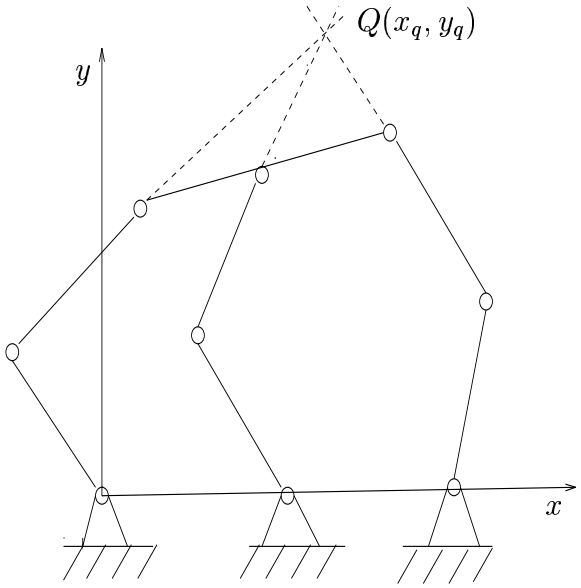

Figure 2.17: Three-degree-of-freedom manipulator in a configuration corresponding to the second type of singularity.

$$\alpha_2 = \alpha_1 + m_1\pi, \quad m_1 = 0, \pm1, \pm2, ... \qquad (2.86)$$
$$\alpha_3 = \alpha_1 + m_2\pi, \quad m_2 = 0, \pm1, \pm2, ... \qquad (2.87)$$

The substitution of eqs.(2.86) and (2.87) into eq.(2.85), leads to

$$\det(\mathbf{A}^*) = 0$$

b) If the three vectors $\mathbf{a}_4$, $\mathbf{a}_5$ and $\mathbf{a}_6$ intersect at a common point $Q(x_q, y_q)$ (as represented in Figure 2.17), then one can write

$$\tan\alpha_1 x_q - y_q + (y_{21} - x_{21}\tan\alpha_1) = 0 \qquad (2.88)$$
$$\tan\alpha_2 x_q - y_q + (y_{22} - x_{22}\tan\alpha_2) = 0 \qquad (2.89)$$
$$\tan\alpha_3 x_q - y_q + (y_{23} - x_{23}\tan\alpha_3) = 0 \qquad (2.90)$$

where α_1, α_2 and $\alpha_3 \neq \pi/2 + m\pi$, $m = 0, \pm 1, \pm 2, ...$

Eqs.(2.88)–(2.90) constitute a linear system of 3 equations in two unknowns x_q, y_q. Hence, the following condition is required to obtain a real solution for x_q and y_q:

$$\det(\mathbf{H}) = 0 \tag{2.91}$$

where $\mathbf{H}$ is a matrix defined as

$$\mathbf{H} = \begin{bmatrix} \tan\alpha_1 & -1 & (y_{21} - x_{21}\tan\alpha_1) \\ \tan\alpha_2 & -1 & (y_{22} - x_{22}\tan\alpha_2) \\ \tan\alpha_3 & -1 & (y_{23} - x_{23}\tan\alpha_3) \end{bmatrix}$$

The substitution of eqs.(2.15)–(2.20) into eq.(2.91) leads to

$$\det(\mathbf{H}) = \det(\mathbf{A}^*)\cos\alpha_1\cos\alpha_2\cos\alpha_3 = 0 \tag{2.92}$$

Since $\cos\alpha_1\cos\alpha_2\cos\alpha_3 \neq 0$, from (2.88)–(2.90), one finally obtains

$$\det(\mathbf{A}^*) = 0$$

Therefore, in the formulation derived above, matrices $\mathbf{A}^*$ can be used to investigate the singularities of both manipulators.

Similarly to the previous case, the polynomial formulation of the singularity loci for this type of mechanism is also found in Appendix A and the detailed expressions associated with the equation are given in Appendix B. A polynomial of degree 64 is obtained in this case.

For this manipulator, let $l_1 = 1.2$, $l_2 = 1.5$, $l_3 = 0.7$, $l_4 = 1.6$, $x_{o1} = 0.0$, $y_{o1} = 0.0$, $x_{o2} = 1.0$, $y_{o2} = 0.0$, $x_{o3} = 2.4$, $y_{o3} = 0.0$ and $\phi = \pi/12$.

The singularity loci of the eight branches of the manipulator are shown on Figures 2.18 and 2.19, where the outer and internal solid curves are the boundaries of the workspace of the manipulator—they are also the locus of the first type of singularity of the manipulator—and where the curves within the workspace are the locus of the second type of singularity of the manipulator.

The branch configurations of the three-degree-of-freedom manipulator are shown on each graph. Figures 2.18(b), 2.18(c) and 2.19(d) show the manipulator in a configuration corresponding to a singularity of type II while on the other graphs, the manipulator is represented in a nonsingular configuration.

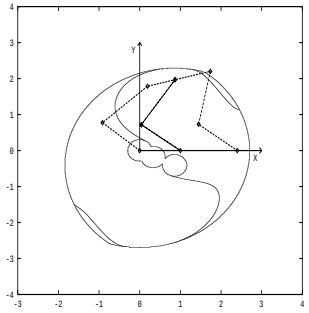

(a) Branch **1**: $K_1 = -1, K_2 = -1, K_3 = -1$.

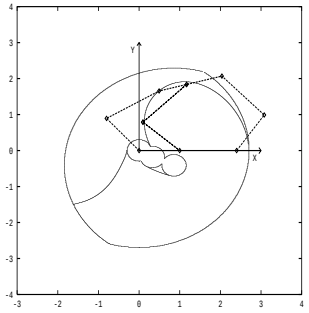

(b) Branch **2**: $K_1 = -1, K_2 = -1, K_3 = +1$.

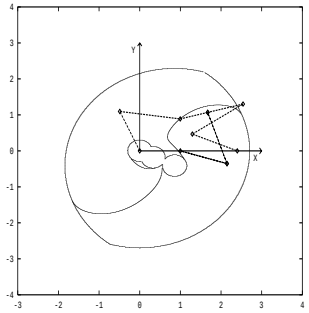

(c) Branch **3**: $K_1 = -1, K_2 = +1, K_3 = -1$.

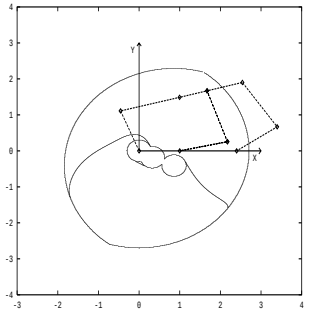

(d) Branch **4**: $K_1 = -1, K_2 = +1, K_3 = +1$.

Figure 2.18: Singularity locus and workspace of the three-dof manipulator with branches 1–4.

2.2.2 Spatial parallel manipulators

In this subsection, the velocity equations of the spatial four-, five- and six-degree-of-freedom parallel mechanisms or manipulators are first derived using two approaches, namely, the algebraic and vector formulation.

The first approach presented for the derivation of the velocity equations consists in a direct differentiation of the kinematic equations derived above. It is the most popular approach used for the derivation of the velocity equations of parallel manipulators [16].

The second approach, as mentioned in the introduction, is a new approach. In fact,

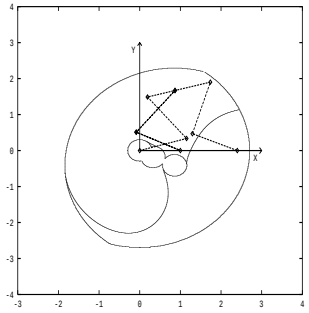

(a) Branch **5**: $K_1 = +1, K_2 = -1, K_3 = -1$.

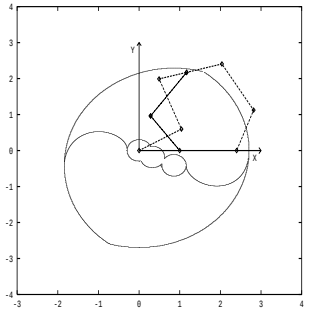

(b) Branch **6**: $K_1 = +1, K_2 = -1, K_3 = +1$.

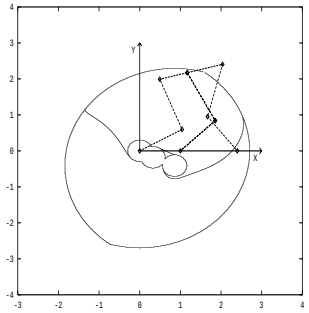

(c) Branch **5**: $K_1 = +1, K_2 = +1, K_3 = -1$.

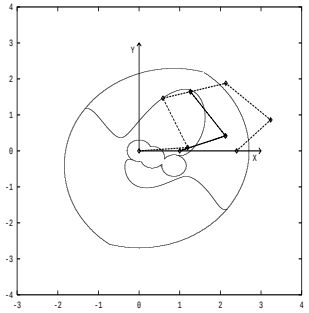

(d) Branch **6**: $K_1 = +1, K_2 = +1, K_3 = +1$.

Figure 2.19: Singularity locus and workspace of the three-dof manipulator with branches 5–8.

it is the extension of the approach used above for the planar parallel mechanisms to complex spatial parallel mechanisms.

2.2.2.1 Spatial four-degree-of-freedom parallel manipulators with revolute actuators

I) Algebraic formulation

Differentiating eq.(2.54) with respect to time, one obtains

$$l_{i1}(S_i \cos \rho_i - R_i \sin \rho_i)\dot{\rho}_i$$

$$
\begin{aligned}
&= (x_i - x_{io} - l_{i1}\sin\gamma_i\cos\rho_i)\dot{x}_i \\
&+(y_i - y_{io} + l_{i1}\cos\gamma_i\sin\rho_i)\dot{y}_i \\
&+(z_i - z_{io} + l_{i1}\sin\rho_i)\dot{z}_i, \quad i = 1,\ldots,4
\end{aligned} \tag{2.93}
$$

where $\dot{x}_i, \dot{y}_i$ and $\dot{z}_i$ can be obtained by the differentiation of eq.(2.30) with respect to time, namely

$$\dot{x}_i = \dot{x} + C^i_{x\phi}\dot{\phi} + C^i_{x\theta}\dot{\theta} + C^i_{x\psi}\dot{\psi}, \quad i = 1,\ldots,4 \tag{2.94}$$

$$\dot{y}_i = \dot{y} + C^i_{y\phi}\dot{\phi} + C^i_{y\theta}\dot{\theta} + C^i_{y\psi}\dot{\psi}, \quad i = 1,\ldots,4 \tag{2.95}$$

$$\dot{z}_i = \dot{z} + C^i_{z\phi}\dot{\phi} + C^i_{z\theta}\dot{\theta} + C^i_{z\psi}\dot{\psi}, \quad i = 1,\ldots,4 \tag{2.96}$$

where one has, for $i = 1$ to 4,

$$
\begin{aligned}
C^i_{x\phi} &= a_i(-\sin\phi\cos\theta\cos\psi - \cos\phi\sin\psi) + b_i(\sin\phi\cos\theta\sin\psi - \cos\phi\cos\psi) \\
&\quad +c_i(-\sin\phi\sin\theta) \\
C^i_{x\theta} &= a_i(-\cos\phi\sin\theta\cos\psi) + b_i(\cos\phi\sin\theta\sin\psi) + c_i\cos\phi\cos\theta \\
C^i_{x\psi} &= a_i(-\cos\phi\cos\theta\sin\psi - \sin\phi\cos\psi) + b_i(-\cos\phi\cos\theta\cos\psi + \sin\phi\sin\psi) \\
C^i_{y\phi} &= a_i(\cos\phi\cos\theta\cos\psi - \sin\phi\sin\psi) + b_i(-\cos\phi\cos\theta\sin\psi - \sin\phi\cos\psi) \\
&\quad +c_i\cos\phi\sin\theta \\
C^i_{y\theta} &= a_i(-\sin\phi\sin\theta\cos\psi) + b_i(\sin\phi\sin\theta\sin\psi) + c_i\sin\phi\cos\theta \\
C^i_{y\psi} &= a_i(-\sin\phi\cos\theta\sin\psi + \cos\phi\cos\psi) + b_i(-\sin\phi\cos\theta\cos\psi - \cos\phi\sin\psi) \\
C^i_{z\phi} &= 0 \\
C^i_{z\theta} &= a_i(-\cos\theta\cos\psi) + b_i\cos\theta\sin\psi - c_5\sin\theta \\
C^i_{z\psi} &= a_i(\sin\theta\sin\psi) + b_i\sin\theta\cos\psi
\end{aligned}
$$

Substituting eqs.(2.94)–(2.96) into eq.(2.93) then leads to

$$\mathbf{B}_r\dot{\boldsymbol{\rho}} = \mathbf{K}_r\dot{\mathbf{t}} \tag{2.97}$$

where vectors $\dot{\mathbf{t}}$ and $\dot{\boldsymbol{\rho}}$ are defined as

$$
\begin{aligned}
\dot{\mathbf{t}} &= [\,\dot{x} \quad \dot{y} \quad \dot{z} \quad \dot{\phi} \quad \dot{\theta} \quad \dot{\psi}\,]^T \\
\dot{\boldsymbol{\rho}} &= [\,\dot{\rho}_1 \quad \dot{\rho}_2 \quad \dot{\rho}_3 \quad \dot{\rho}_4\,]^T
\end{aligned}
$$

Moreover, matrices $\mathbf{B}_r$ and $\mathbf{K}_r$ can be written as $\mathbf{B}_r = \text{diag}[b_1^r\ b_2^r\ b_3^r\ b_4^r]$ and

$$\mathbf{K}_r = \begin{bmatrix} k_{11}^r & k_{12}^r & k_{13}^r & k_{14}^r & k_{15}^r & k_{16}^r \\ k_{21}^r & k_{22}^r & k_{23}^r & k_{24}^r & k_{25}^r & k_{26}^r \\ k_{31}^r & k_{32}^r & k_{33}^r & k_{34}^r & k_{35}^r & k_{36}^r \\ k_{41}^r & k_{42}^r & k_{43}^r & k_{44}^r & k_{45}^r & k_{46}^r \end{bmatrix} \tag{2.98}$$

with, for $i = 1, \ldots, 4$,

$$\begin{aligned}
b_i^r &= l_{i1}(S_i \cos\rho_i - R_i \sin\rho_i), \quad i = 1, \ldots, 4 \\
k_{i1}^r &= x_i - x_{io} + l_{i1} \sin\gamma_i \cos\rho_i \\
k_{i2}^r &= y_i - y_{io} - l_{i1} \cos\gamma_i \sin\rho_i \\
k_{i3}^r &= z_i - z_{io} - l_{i1} \sin\rho_i \\
k_{i4}^r &= C_{x\phi}^i (x_i - x_{io} + l_{i1} \sin\gamma_i \cos\rho_i) \\
&\quad + C_{y\phi}^i (y_i - y_{io} - l_{i1} \cos\gamma_i \sin\rho_i) \\
&\quad + C_{z\phi}^i (z_i - z_{io} - l_{i1} \sin\rho_i) \\
k_{i5}^r &= C_{x\theta}^i (x_i - x_{io} + l_{i1} \sin\gamma_i \cos\rho_i) \\
&\quad + C_{y\theta}^i (y_i - y_{io} - l_{i1} \cos\gamma_i \sin\rho_i) \\
&\quad + C_{z\theta}^i (z_i - z_{io} - l_{i1} \sin\rho_i) \\
k_{i6}^r &= C_{x\psi}^i (x_i - x_{io} + l_{i1} \sin\gamma_i \cos\rho_i) \\
&\quad + C_{y\psi}^i (y_i - y_{io} - l_{i1} \cos\gamma_i \sin\rho_i) \\
&\quad + C_{z\psi}^i (z_i - z_{io} - l_{i1} \sin\rho_i)
\end{aligned}$$

Then, from the geometry of the 5th leg of the manipulator, i.e., from eq.(2.32), one can write

$$x_5^2 + z_5^2 = l_5^2, \quad \text{and} \quad y_5 = 0 \tag{2.99}$$

Differentiating eqs.(2.99), one then obtains

$$x_5 \dot{x_5} + z_5 \dot{z_5} = 0, \quad \text{and} \quad \dot{y_5} = 0 \tag{2.100}$$

where $\dot{x_5}, \dot{y_5}, \dot{z_5}$ can be obtained by the differentiation of eqs.(2.32), i.e.,

$$\dot{x_5} = \dot{x} + C_{x\phi}^5 \dot{\phi} + C_{x\theta}^5 \dot{\theta} + C_{x\psi}^5 \dot{\psi} \tag{2.101}$$

$$\dot{y_5} = \dot{y} + C_{y\phi}^5 \dot{\phi} + C_{y\theta}^5 \dot{\theta} + C_{y\psi}^5 \dot{\psi} \tag{2.102}$$

$$\dot{z_5} = \dot{z} + C_{z\phi}^5 \dot{\phi} + C_{z\theta}^5 \dot{\theta} + C_{z\psi}^5 \dot{\psi} \tag{2.103}$$

Substituting eqs.(2.101)–(2.103) into eqs.(2.100) then leads to an expression of the dependent Cartesian velocities as a function of the independent velocities which can be written as

$$\dot{\mathbf{t}} = \mathbf{J}_r \dot{\mathbf{x}} \tag{2.104}$$

where $\dot{\mathbf{x}} = [\, \dot{x}\, \dot{y}\, \dot{z}\, \dot{\phi}\,]^T$ and

$$\mathbf{J}_r = \begin{bmatrix} 1 & 0 & 0 & 0 \\ 0 & 1 & 0 & 0 \\ 0 & 0 & 1 & 0 \\ 0 & 0 & 0 & 1 \\ j^r_{51} & j^r_{52} & j^r_{53} & j^r_{54} \\ j^r_{61} & j^r_{62} & j^r_{63} & j^r_{64} \end{bmatrix} \tag{2.105}$$

where

$$\begin{aligned}
j^r_{51} &= x_5 C^5_{y\psi}/U, \qquad j^r_{61} = -x_5 C^5_{y\theta}/U \\
j^r_{52} &= -(x_5 C^5_{x\psi} + z_5 C^5_{z\psi})/U, \qquad j^r_{62} = C^5_{y\theta}/U \\
j^r_{53} &= z_5 C^5_{y\psi}/U, \qquad j^r_{63} = -z_5 C^5_{y\theta}/U \\
j^r_{54} &= [(x_5 C^5_{x\phi} + z_5 C^5_{z\phi}) C^5_{y\psi} - C^5_{y\phi}(x_5 C^5_{x\psi} + z_5 C^5_{z\psi})]/U \\
j^r_{64} &= [(x_5 C^5_{x\theta} + z_5 C^5_{z\theta} C^5_{y\phi} - (x_5 C^5_{x\phi} + z_5 C^5_{z\phi}) C^5_{y\theta})]/U
\end{aligned}$$

with $U = (x_5 C^5_{x\theta} + z_5 C^5_{z\theta}) C^5_{y\psi} - C^5_{y\theta}(x_5 C^5_{x\psi} + z_5 C^5_{z\psi})$. Eq.(2.104) represents the kinematic velocity constraints associated with the special unactuated kinematic chain — the fifth leg — connecting the base to the platform.

Finally, substituting eq.(2.104) into eq.(2.97), one obtains the velocity equations of the four-degree-of-freedom manipulator with revolute actuators, i.e.,

$$\mathbf{B}_r \dot{\boldsymbol{\rho}} = \mathbf{A}_r \dot{\mathbf{x}} \tag{2.106}$$

where $\mathbf{A}_r$ is a 4 by 4 matrix which is defined as $\mathbf{A}_r = \mathbf{K}_r \mathbf{J}_r$.

II) Vector formulation

Considering the quantities defined in Figure 2.20, one can write the velocity equations associated with the closed loop $O_i O_i' P_i P_5 O$, for $i = 1, \ldots, 4$, as

$$\boldsymbol{\omega}_{i1} \times \mathbf{l}_{i1} + \boldsymbol{\omega}_{i2} \times \mathbf{l}_{i2} + \boldsymbol{\omega} \times \mathbf{v}_i = \boldsymbol{\omega}_5 \times \mathbf{p}_5, \quad i = 1, \ldots, 4 \tag{2.107}$$

where $\boldsymbol{\omega}_{ij}$ $(i = 1, \ldots, 4$ and $j = 1, 2)$ is the vector of the angular velocity of the jth link of the ith leg, while $\mathbf{l}_{i1}$ $(i = 1, \ldots, 4)$ is the vector connecting point O_i to point O_i' and $\mathbf{l}_{i2}$ $(i = 1, \ldots, 4)$ is the vector connecting point O_i' to point P_i. Eq.(2.107) can be

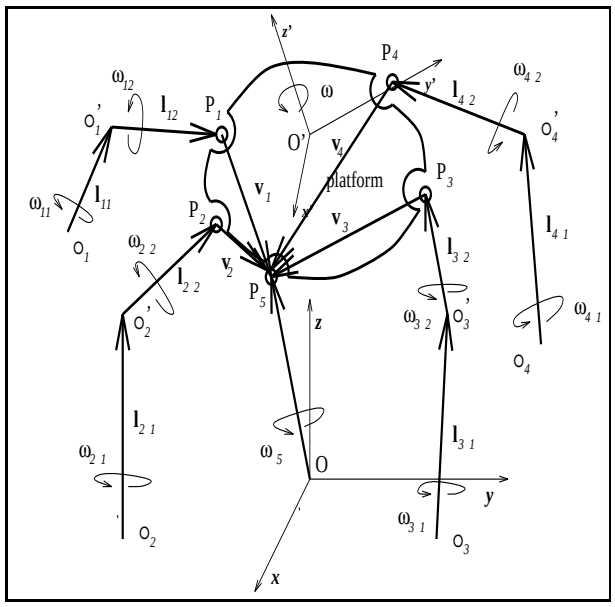

Figure 2.20: Position and velocity vectors associated with the spatial four-degree-of-freedom parallel manipulator with revolute actuators.

rewritten as

$$-\mathbf{L}_{i1}\mathbf{e}_i\dot{\rho}_i = \mathbf{L}_{i2}\boldsymbol{\omega}_{i2} + \mathbf{V}_i\boldsymbol{\omega} + \mathbf{C}\omega_c, \quad i = 1, \ldots, 4 \tag{2.108}$$

where the cross products appearing in eq.(2.107) have been written in matrix form and where ω_c is the only nonvanishing component of vector $\boldsymbol{\omega}_5$, i.e., the latter vector can be written as

$$\boldsymbol{\omega}_5 = [\, 0 \quad \omega_c \quad 0 \,]^T \tag{2.109}$$

and where vector $\boldsymbol{\omega}_{i1}$ has been written as

$$\boldsymbol{\omega}_{i1} = \dot{\rho}_i\mathbf{e}_i, \quad i = 1, \ldots, 4 \tag{2.110}$$

with $\mathbf{e}_i$ the unit vector associated with the direction of the axis of the actuator. The matrices used above are defined as

$$\begin{aligned} \mathbf{V}_i &= [\mathbf{1}] \times \mathbf{v}_i, \quad i = 1, \ldots, 4 \\ \mathbf{C} &= [p_{5z}\ 0\ p_{5x}]^T \\ \mathbf{L}_{i1} &= [\mathbf{1}] \times \mathbf{l}_{i1}, \quad i = 1, \ldots, 4 \\ \mathbf{L}_{i2} &= [\mathbf{1}] \times \mathbf{l}_{i2}, \quad i = 1, \ldots, 4 \end{aligned} \tag{2.111}$$

where $\mathbf{1}$ stands for the 3×3 identity matrix. Vectors $\mathbf{l}_{i2}(i = 1, \ldots, 4)$ are easily written

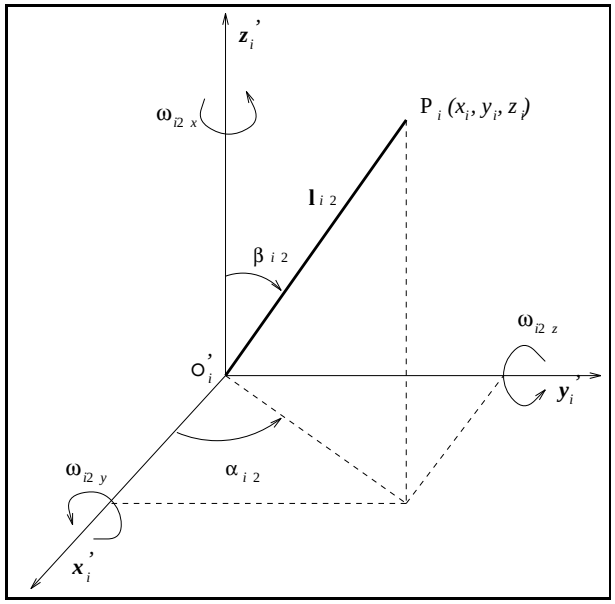

Figure 2.21: Vector $\mathbf{l}_{i2}$ represented in spherical coordinates.

using spherical coordinates, as shown in Figure 2.21. Hence, one has

$$\boldsymbol{\omega}_{i2} = \mathbf{G}_i \boldsymbol{\omega}_{i2s}, \quad i = 1, \ldots, 4 \tag{2.112}$$

where

$$\mathbf{G}_i = \begin{bmatrix} 0 & -\sin\alpha_i \\ 0 & \cos\alpha_i \\ 1 & 0 \end{bmatrix} \tag{2.113}$$
$$\boldsymbol{\omega}_{i2s} = [\dot{\alpha}_{i2} \ \dot{\beta}_{i2}]^T$$

Substituting eqs.(2.112) into eq.(2.108) and using eq.(2.110), one obtains the velocity equations of the manipulator as

$$\mathbf{B}_{rv}\dot{\boldsymbol{\rho}} = \mathbf{J}_{rv}\mathbf{w} \tag{2.114}$$

where $\mathbf{B}_{rv}$ is a 12×4 matrix defined as

$$\mathbf{B}_{rv} = \begin{bmatrix} -\mathbf{L}_{11}\mathbf{e}_1 & \mathbf{0} & \mathbf{0} & \mathbf{0} \\ \mathbf{0} & -\mathbf{L}_{21}\mathbf{e}_2 & \mathbf{0} & \mathbf{0} \\ \mathbf{0} & \mathbf{0} & -\mathbf{L}_{31}\mathbf{e}_3 & \mathbf{0} \\ \mathbf{0} & \mathbf{0} & \mathbf{0} & -\mathbf{L}_{41}\mathbf{e}_4 \end{bmatrix} \tag{2.115}$$

where $\mathbf{0}$ denotes a zero 3-dimensional column vector, with $\dot{\boldsymbol{\rho}}$ the joint velocity vector defined as $\dot{\boldsymbol{\rho}} = [\,\dot{\rho}_1 \quad \dot{\rho}_2 \quad \dot{\rho}_3 \quad \dot{\rho}_4\,]^T$, with vector $\mathbf{w}$ a 12-dimensional vector defined as

$$\mathbf{w} = [\,\boldsymbol{\omega}_{1s}^T \quad \boldsymbol{\omega}_{2s}^T \quad \boldsymbol{\omega}_{3s}^T \quad \boldsymbol{\omega}_{4s}^T \quad \boldsymbol{\omega}^T \quad \omega_c\,]^T \tag{2.116}$$

and with $\mathbf{J}_{rv}$ a 12×12 matrix defined as

$$\mathbf{J}_{rv} = \begin{bmatrix} \mathbf{S}_1 & \mathbf{0} & \mathbf{0} & \mathbf{0} & \mathbf{V}_1 & \mathbf{C} \\ \mathbf{0} & \mathbf{S}_2 & \mathbf{0} & \mathbf{0} & \mathbf{V}_2 & \mathbf{C} \\ \mathbf{0} & \mathbf{0} & \mathbf{S}_3 & \mathbf{0} & \mathbf{V}_3 & \mathbf{C} \\ \mathbf{0} & \mathbf{0} & \mathbf{0} & \mathbf{S}_4 & \mathbf{V}_4 & \mathbf{C} \end{bmatrix} \tag{2.117}$$

where $\mathbf{0}$ denotes a 3×2 zero matrix and where

$$\mathbf{S}_i = \mathbf{L}_{i2}\mathbf{G}_i, \quad i = 1, \ldots, 4 \tag{2.118}$$

III) Determination of the singularity loci

The determination of the second type of singularity loci consists in finding the roots of the following equations, i.e.,

$$\det(\mathbf{A}_r) = 0 \quad \text{or} \quad \det(\mathbf{J}_{rv}) = 0 \tag{2.119}$$

It can be noticed that the procedure to obtain matrix $\mathbf{A}_r$ using the algebraic approach is much more complicated than the one followed to obtain matrix $\mathbf{J}_{rv}$ using the vector method, which means that the expressions of the elements of matrix $\mathbf{A}_r$ will be much more complex than the expressions of the elements of matrix $\mathbf{J}_{rv}$. However, the former matrix is of dimension 4×4 while the latter is of dimension 12×12 and the expression of the determinant of a larger matrix will be much more complicated than for a smaller matrix. On the other hand, matrix $\mathbf{J}_{rv}$ is rather sparse and it is therefore easy to reduce the expression of its determinant to the expression of the determinant of a 4×4 matrix. The procedure for this simplification is given in Appendix C. Hence, globally, the use of the matrices obtained with the vector method will provide simpler expressions which will therefore lead to faster algorithms.

The loci of the singularities of the second type are determined using

$$\det(\mathbf{J}_r) = D_o \det(\mathbf{J}) = 0 \tag{2.120}$$

where

$$\begin{aligned} D_o &= (l_{12y}\sin\alpha_1 + l_{12x}\cos\alpha_1)(l_{22y}\sin\alpha_2 + l_{22x}\cos\alpha_2) \\ &\quad (l_{32y}\sin\alpha_3 + l_{32x}\cos\alpha_3)(l_{42y}\sin\alpha_{42} + l_{4x}\cos\alpha_4) \end{aligned}$$

$$\mathbf{J} = \begin{bmatrix} (\mathbf{l}_{12}\times\mathbf{v}_1)^T & (\mathbf{p}_5\times\mathbf{l}_{12})^T\mathbf{u} \\ (\mathbf{l}_{22}\times\mathbf{v}_2)^T & (\mathbf{p}_5\times\mathbf{l}_{22})^T\mathbf{u} \\ (\mathbf{l}_{32}\times\mathbf{v}_3)^T & (\mathbf{p}_5\times\mathbf{l}_{32})^T\mathbf{u} \\ (\mathbf{l}_{42}\times\mathbf{v}_4)^T & (\mathbf{p}_5\times\mathbf{l}_{42})^T\mathbf{u} \end{bmatrix}$$

where $\mathbf{u} = [0\ 1\ 0]^T$.

From the above equations, it is clear, by inspection, that $D_o \neq 0$. Therefore, eq.(2.120) reduces to

$$\det(\mathbf{J}) = 0 \tag{2.121}$$

where $\mathbf{J}$ is a 4×4 matrix and hence, the determination of the singularity loci is greatly simplified.

IV) Example

All the examples presented below have been produced using the two sets of velocity equations described above (obtained with the algebraic method and with the vector method). Both approaches have given identical results and the vector method has led to faster computation times.

Since the manipulator has four degrees of freedom, its workspace is four-dimensional. In order to be able to visualize the results, a computer program has been written in which it is possible to fix two of the Cartesian coordinates and to obtain a two-dimensional section of the workspace associated with the two other coordinates and on which the limits of the workspace and the singularity loci can be plotted.

Using the parameters used in the example of determination of the workspace of the mechanism, one can obtain the singularity locus over the workspace in two sections, as represented in Figures 2.22.

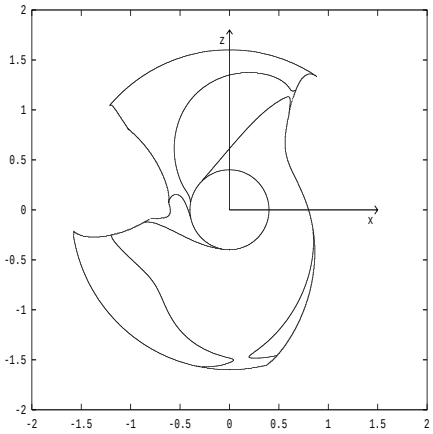

(a) A section of the singularity loci (over x and z) for the manipulator and with $K_{41} = 1, K_{42} = 1, V_i = 1 (i = 1, \ldots, 4)$.

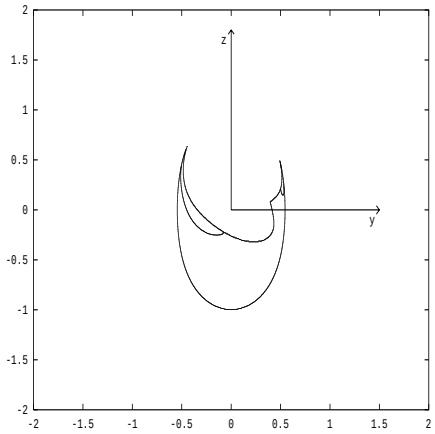

(b) A section of the singularity loci (over y and z) for the manipulator and with $K_{41} = 1, K_{42} = 1, V_i = 1 (i = 1, \ldots, 4)$.

Figure 2.22: Singularity locus and workspace of the four-dof manipulator.

2.2.2.2 Spatial five-degree-of-freedom parallel manipulators with revolute actuators

I) Algebraic formulation

Since the identical actuated legs of the four-, five- and six-degree-of-freedom mechanisms have the same architecture, one can directly use eq.(2.54) for the derivation of the velocity equations of the mechanism.

Differentiating eq.(2.54) with respect to time, one obtains eqs.(2.93)–(2.96) with the same coefficients, except that i ranges now from 1 to 5.

One then obtains an equation identical to eq.(2.97) but with

$$\begin{aligned} \dot{\rho} &= [\, \dot{\rho}_1 \quad \dot{\rho}_2 \quad \dot{\rho}_3 \quad \dot{\rho}_4 \quad \dot{\rho}_5 \,]^T \\ \mathbf{B}_r &= \mathrm{diag}\,[\, b_1^r \quad b_2^r \quad b_3^r \quad b_4^r \quad b_5^r \,] \end{aligned}$$

and

$$\mathbf{K}_r = \begin{bmatrix} k^r_{11} & k^r_{12} & k^r_{13} & k^r_{14} & k^r_{15} & k^r_{16} \\ k^r_{21} & k^r_{22} & k^r_{23} & k^r_{24} & k^r_{25} & k^r_{26} \\ k^r_{31} & k^r_{32} & k^r_{33} & k^r_{34} & k^r_{35} & k^r_{36} \\ k^r_{41} & k^r_{42} & k^r_{43} & k^r_{44} & k^r_{45} & k^r_{46} \\ k^r_{51} & k^r_{52} & k^r_{53} & k^r_{54} & k^r_{55} & k^r_{56} \end{bmatrix} \tag{2.122}$$

where the k^r_{ij} are defined after eq.(2.98) but should now be taken for $i = 1, \ldots, 5$.

Now, in order to include the constraint associated with the special sixth leg eq.(2.64) is differentiated with respect to time, which leads to

$$x_6\dot{x}_6 + y_6\dot{y}_6 + z_6\dot{z}_6 = 0 \tag{2.123}$$

Setting $i = 6$ in eqs.(2.94)–(2.96)—which is justified since the sixth leg is now considered—and substituting the latter equations in eq.(2.123), one obtains

$$\dot{\mathbf{t}} = \mathbf{J}_r\dot{\mathbf{x}} \tag{2.124}$$

with

$$\dot{\mathbf{x}} = [\, \dot{x} \quad \dot{y} \quad \dot{z} \quad \dot{\phi} \quad \dot{\theta}\,]^T$$

and

$$\mathbf{J}_r = \begin{bmatrix} 1 & 0 & 0 & 0 & 0 \\ 0 & 1 & 0 & 0 & 0 \\ 0 & 0 & 1 & 0 & 0 \\ 0 & 0 & 0 & 1 & 0 \\ 0 & 0 & 0 & 0 & 1 \\ j^r_{61} & j^r_{62} & j^r_{63} & j^r_{64} & j^r_{65} \end{bmatrix} \tag{2.125}$$

and

$$\begin{aligned} j^r_{61} &= \frac{-x_6}{x_6C^6_{x\psi} + y_6C^6_{y\psi} + z_6C^6_{z\psi}} \\ j^r_{62} &= \frac{-y_6}{x_6C^6_{x\psi} + y_6C^6_{y\psi} + z_6C^6_{z\psi}} \\ j^r_{63} &= \frac{-z_6}{x_6C^6_{x\psi} + y_6C^6_{y\psi} + z_6C^6_{z\psi}} \\ j^r_{64} &= \frac{-x_6C^6_{x\phi} - y_6C^6_{y\phi} - z_6C^6_{z\phi}}{x_6C^6_{x\psi} + y_6C^6_{y\psi} + z_6C^6_{z\psi}} \\ j^r_{65} &= \frac{-x_6C^6_{x\theta} - y_6C^6_{y\theta} - z_6C^6_{z\theta}}{x_6C^6_{x\psi} + y_6C^6_{y\psi} + z_6C^6_{z\psi}} \end{aligned}$$

Eq.(2.124) represents the kinematic velocity constraints associated with the special unactuated kinematic chain — the sixth leg — connecting the base to the platform.

Finally, substituting eq.(2.124) into eq.(2.97) written for the five-degree-of-freedom mechanism one obtains the velocity equations of this mechanism, i.e.,

$$\mathbf{B}_r \dot{\boldsymbol{\rho}} = \mathbf{A}_r \dot{\mathbf{x}} \tag{2.126}$$

where $\mathbf{A}_r$ is a 5 by 5 matrix which is defined as

$$\mathbf{A}_r = \mathbf{K}_r \mathbf{J}_r$$

II) Vector formulation

Considering the quantities defined in Figure 2.23, one can write the velocity equations associated with the closed loop $O_i O_i' P_i P_6 O$, for $i = 1, \ldots, 5$, as

$$\boldsymbol{\omega}_{i1} \times \mathbf{l}_{i1} + \boldsymbol{\omega}_{i2} \times \mathbf{l}_{i2} + \boldsymbol{\omega} \times \mathbf{v}_i = \boldsymbol{\omega}_6 \times \mathbf{p}_6, \quad i = 1, \ldots, 5 \tag{2.127}$$

where $\boldsymbol{\omega}_{ij}$ ($i = 1, \ldots, 5$ and $j = 1, 2$) is the angular velocity vector of the jth link of the ith leg, while $\mathbf{l}_{i1}$ ($i = 1, \ldots, 5$) is the position vector from point O_i to point O_i' and $\mathbf{l}_{i2}$ ($i = 1, \ldots, 5$) is the position vector from point O_i' to point P_i.

Eq.(2.127) can be rewritten as

$$-\mathbf{l}_{i1} \times \boldsymbol{\omega}_{i1} = \mathbf{l}_{i2} \times \boldsymbol{\omega}_{i2} + \mathbf{v}_i \times \boldsymbol{\omega} - \mathbf{p}_6 \times \boldsymbol{\omega}_6, \quad i = 1, \ldots, 5 \tag{2.128}$$

Moreover, the cross products appearing in eq.(2.128) can be written in matrix form, which leads to

$$-\mathbf{L}_{i1} \mathbf{e}_i \dot{\rho}_i = \mathbf{L}_{i2} \boldsymbol{\omega}_{i2} + \mathbf{V}_i \boldsymbol{\omega} - \mathbf{P}_6 \boldsymbol{\omega}_6, \quad i = 1, \ldots, 5 \tag{2.129}$$

where vector $\boldsymbol{\omega}_{i1}$ has been written as

$$\boldsymbol{\omega}_{i1} = \dot{\rho}_i \mathbf{e}_i, \quad i = 1, \ldots, 5 \tag{2.130}$$

where $\mathbf{e}_i$ is the unit vector associated with the direction of the axis of the ith actuator. Moreover, the matrices used above are defined as

$$\begin{aligned}
\mathbf{L}_{i1} &= [\mathbf{1}] \times \mathbf{l}_{i1}, \quad i = 1, \ldots, 5 \\
\mathbf{L}_{i2} &= [\mathbf{1}] \times \mathbf{l}_{i2}, \quad i = 1, \ldots, 5 \\
\mathbf{V}_i &= [\mathbf{1}] \times \mathbf{v}_i, \quad i = 1, \ldots, 5 \\
\mathbf{P}_6 &= [\mathbf{1}] \times \mathbf{p}_6 = \begin{bmatrix} 0 & -z_i & y_i \\ z_i & 0 & -x_i \\ -y_i & x_i & 0 \end{bmatrix}
\end{aligned}$$

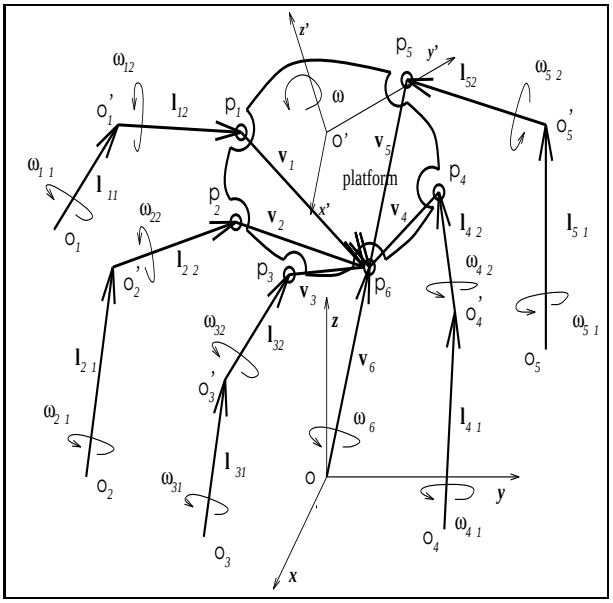

Figure 2.23: Position and velocity vectors associated with the spatial five-degree-of-freedom parallel mechanism with revolute actuators.

where l_{i1x}, l_{i1y} and l_{i1z} are the components of vector $\mathbf{l}_{i1}$ and l_{i2x}, l_{i2y} and l_{i2z} are the components of vector $\mathbf{l}_{i2}$.

One can represent vectors $\mathbf{l}_{i2}(i = 1, \ldots, 5)$ and vector $\mathbf{p}_6$ using spherical coordinates, as shown in Figure2.21. Hence, one has

$$\boldsymbol{\omega}_{i2} = \mathbf{G}_i \boldsymbol{\omega}_{is}, \quad i = 1, \ldots, 5 \tag{2.131}$$

and

$$\boldsymbol{\omega}_6 = \mathbf{G}_6 \boldsymbol{\omega}_{6s} \tag{2.132}$$

where $\mathbf{G}_i$ is defined in eq.(2.113) (now for i=1,...,6) and

$$\boldsymbol{\omega}_{is} = \begin{bmatrix} \dot{\alpha}_i \\ \dot{\beta}_i \end{bmatrix}, \quad i = 1, \ldots, 6 \tag{2.133}$$

Substituting eqs.(2.131) and eq.(2.132) into eq.(2.129), one obtains

$$-\mathbf{L}_{i1}\mathbf{e}_i\dot{\rho}_i = \mathbf{T}_i\boldsymbol{\omega}_{is} + \mathbf{V}_i\boldsymbol{\omega} - \mathbf{S}_6\boldsymbol{\omega}_{6s}, \quad i = 1, \ldots, 5 \tag{2.134}$$

where

$$\mathbf{T}_i = \mathbf{L}_{i2}\mathbf{G}_i, \quad i = 1, \ldots, 5 \tag{2.135}$$

and $\mathbf{V}_i$ and $\mathbf{S}_i$ are as previously defined.

Finally, the velocity equations of the five-degree-of-freedom mechanism with revolute actuators is obtained from eq.(2.134) as

$$\mathbf{B}_{rv}\dot{\boldsymbol{\rho}} = \mathbf{J}_{rv}\mathbf{w} \tag{2.136}$$

where $\mathbf{B}_{rv}$ is a 15×5 matrix defined as

$$\mathbf{B}_{rv} = \begin{bmatrix} -\mathbf{L}_{11}\mathbf{e}_1 & \mathbf{0} & \mathbf{0} & \mathbf{0} & \mathbf{0} \\ \mathbf{0} & -\mathbf{L}_{21}\mathbf{e}_2 & \mathbf{0} & \mathbf{0} & \mathbf{0} \\ \mathbf{0} & \mathbf{0} & -\mathbf{L}_{31}\mathbf{e}_3 & \mathbf{0} & \mathbf{0} \\ \mathbf{0} & \mathbf{0} & \mathbf{0} & -\mathbf{L}_{41}\mathbf{e}_4 & \mathbf{0} \\ \mathbf{0} & \mathbf{0} & \mathbf{0} & \mathbf{0} & -\mathbf{L}_{51}\mathbf{e}_5 \end{bmatrix} \tag{2.137}$$

where $\mathbf{0}$ denotes a 3-dimensional zero column vector, and $\dot{\boldsymbol{\rho}}$ is the joint velocity vector previously defined.

Moreover, vector $\mathbf{w}$ is a 15-dimensional vector defined as

$$\mathbf{w} = [\,\boldsymbol{\omega}_{1s}^T \quad \boldsymbol{\omega}_{2s}^T \quad \boldsymbol{\omega}_{3s}^T \quad \boldsymbol{\omega}_{4s}^T \quad \boldsymbol{\omega}_{5s}^T \quad \boldsymbol{\omega}^T \quad \boldsymbol{\omega}_{6s}^T\,]^T \tag{2.138}$$

and matrix $\mathbf{J}_{rv}$ a 15×15 matrix defined as

$$\mathbf{J}_{rv} = \begin{bmatrix} \mathbf{T}_1 & \mathbf{0} & \mathbf{0} & \mathbf{0} & \mathbf{0} & \mathbf{V}_1 & -\mathbf{S}_6 \\ \mathbf{0} & \mathbf{T}_2 & \mathbf{0} & \mathbf{0} & \mathbf{0} & \mathbf{V}_2 & -\mathbf{S}_6 \\ \mathbf{0} & \mathbf{0} & \mathbf{T}_3 & \mathbf{0} & \mathbf{0} & \mathbf{V}_3 & -\mathbf{S}_6 \\ \mathbf{0} & \mathbf{0} & \mathbf{0} & \mathbf{T}_4 & \mathbf{0} & \mathbf{V}_4 & -\mathbf{S}_6 \\ \mathbf{0} & \mathbf{0} & \mathbf{0} & \mathbf{0} & \mathbf{T}_5 & \mathbf{V}_5 & -\mathbf{S}_6 \end{bmatrix} \tag{2.139}$$

where $\mathbf{0}$ denotes a 3×2 zero matrix.

III) Determination of the singularity loci

The determination of the second type of singularity loci consists in finding the roots of the following equations, i.e.,

$$\det(\mathbf{A}_r) = 0 \tag{2.140}$$

or

$$\det(\mathbf{J}_{rv}) = 0 \tag{2.141}$$

Since matrix $\mathbf{J}_{rv}$ is rather sparse, it is therefore easy to reduce the expression of its determinant to the expression of the determinant of a 5×5 matrix. Hence, the use of the matrix obtained with the vector method will lead to faster algorithms.

$$\det(\mathbf{J}_{rv}) = D_o \det(\mathbf{J}) = 0 \tag{2.142}$$

where

$$D_o = \prod_{i=1}^{5} \mathbf{l}_{i2}^T \mathbf{d}_i \tag{2.143}$$

with vector $\mathbf{d}_i$ defined as

$$\mathbf{d}_i = [\cos\alpha_i \quad \sin\alpha_i \quad 0]^T, \quad i = 1, \ldots, 6 \tag{2.144}$$

and where matrix $\mathbf{J}$ can be written as

$$\mathbf{J} = \begin{bmatrix} (\mathbf{l}_{12} \times \mathbf{v}_1)^T & (\mathbf{p}_6 \times \mathbf{l}_{12})^T \mathbf{u} & \mathbf{l}_{12}^T \mathbf{h} \\ (\mathbf{l}_{22} \times \mathbf{v}_2)^T & (\mathbf{p}_6 \times \mathbf{l}_{22})^T \mathbf{u} & \mathbf{l}_{22}^T \mathbf{h} \\ (\mathbf{l}_{32} \times \mathbf{v}_3)^T & (\mathbf{p}_6 \times \mathbf{l}_{32})^T \mathbf{u} & \mathbf{l}_{32}^T \mathbf{h} \\ (\mathbf{l}_{42} \times \mathbf{v}_4)^T & (\mathbf{p}_6 \times \mathbf{l}_{42})^T \mathbf{u} & \mathbf{l}_{42}^T \mathbf{h} \\ (\mathbf{l}_{52} \times \mathbf{v}_5)^T & (\mathbf{p}_6 \times \mathbf{l}_{52})^T \mathbf{u} & \mathbf{l}_{52}^T \mathbf{h} \end{bmatrix} \tag{2.145}$$

where

$$\mathbf{h} = \mathbf{u}\mathbf{p}_6^T \mathbf{d}_6 - \mathbf{d}_6 \mathbf{p}_6^T \mathbf{u} \tag{2.146}$$

with

$$\mathbf{u} = [0 \quad 0 \quad 1]^T \tag{2.147}$$

From the above equations, it is clear, by inspection, that $D_o \neq 0$. Therefore, eqs.(2.140) and (2.141) can be reduced to

$$\det(\mathbf{J}) = 0 \tag{2.148}$$

where $\mathbf{J}$ is a 5×5 matrix and hence, the determination of the singularity loci is greatly simplified.

IV) Example

Two examples are given to illustrate the results. Since the mechanisms have five degrees of freedom, their workspace is five-dimensional. In order to be able to visualize the results, three of the Cartesian coordinates are fixed and one then obtains a two-dimensional section of the workspace associated with the other two coordinates on which the limits of the workspace and the singularity loci can be plotted.

Using the same parameters as the ones used in the example on the determination of the workspace of the mechanism, one can obtain the singularity locus over the workspace in two sections, as represented in Figures 2.24.

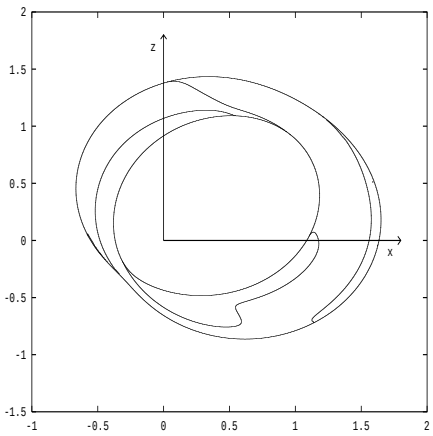

(a) a section of the workspace (over x and z) with $K_i = 1, (i = 1, \ldots, 6)$.

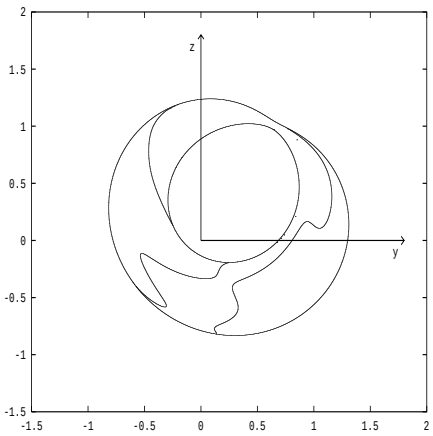

(b) a section of the workspace (over y and z) with $K_i = 1, (i = 1, \ldots, 6)$.

Figure 2.24: Singularity locus and workspace of the five-dof manipulator.

2.2.2.3 Spatial six-degree-of-freedom parallel manipulators with revolute actuators

I) Algebraic formulation

Similarly to the previous cases, differentiating eq.(2.54) with respect to time, one obtains

$$\begin{aligned} l_{i1}(S_i \cos\rho_i - R_i \sin\rho_i)\dot{\rho}_i &= (x_i - x_{io} + l_{i1}\sin\gamma_i \cos\rho_i)\dot{x}_i + (y_i - y_{io} - l_{i1}\cos\gamma_i \sin\rho_i)\dot{y}_i \\ &\quad + (z_i - z_{io} - l_{i1}\sin\rho_i)\dot{z}_i, \quad i = 1, \ldots, 6 \end{aligned} \tag{2.149}$$

Substituting eqs.(2.94)–(2.96) into eq.(2.149), one obtains the velocity equations of the six-degree-of-freedom mechanism with revolute actuators, i.e.,

$$\mathbf{B}_r \dot{\boldsymbol{\rho}} = \mathbf{K}_r \dot{\mathbf{t}} \tag{2.150}$$

where vector $\dot{\mathbf{t}}$ has been defined above and where $\dot{\boldsymbol{\rho}} = [\, \dot{\rho}_1 \quad \dot{\rho}_2 \quad \dot{\rho}_3 \quad \dot{\rho}_4 \quad \dot{\rho}_5 \quad \dot{\rho}_6 \,]^T$ and matrices $\mathbf{B}_r$ and $\mathbf{K}_r$ can be written as

$$\mathbf{B}_r = \mathrm{diag}\,[\, b_1^r \quad b_2^r \quad b_3^r \quad b_4^r \quad b_5^r \quad b_6^r \,] \tag{2.151}$$

and

$$\mathbf{K}_r = \begin{bmatrix} k_{11}^r & k_{12}^r & k_{13}^r & k_{14}^r & k_{15}^r & k_{16}^r \\ k_{21}^r & k_{22}^r & k_{23}^r & k_{24}^r & k_{25}^r & k_{26}^r \\ k_{31}^r & k_{32}^r & k_{33}^r & k_{34}^r & k_{35}^r & k_{36}^r \\ k_{41}^r & k_{42}^r & k_{43}^r & k_{44}^r & k_{45}^r & k_{46}^r \\ k_{51}^r & k_{52}^r & k_{53}^r & k_{54}^r & k_{55}^r & k_{56}^r \\ k_{61}^r & k_{62}^r & k_{63}^r & k_{64}^r & k_{65}^r & k_{66}^r \end{bmatrix} \tag{2.152}$$

where the k_{ij} are defined after eq.(2.98) but should now be taken for $i = 1, \ldots, 6$.

Since no constraining kinematic chains are introduced in this manipulator, the velocity equations are rather simple.

II) Vector formulation

Similarly, considering the quantities defined in Figure 2.25, one can write the velocity equations associated with the closed loop $O_i O_i' P_i P_6 O_6$, for $i = 1, \ldots, 5$, as

$$\boldsymbol{\omega}_{i1} \times \mathbf{l}_{i1} + \boldsymbol{\omega}_{i2} \times \mathbf{l}_{i2} + \boldsymbol{\omega} \times \mathbf{v}_i = \boldsymbol{\omega}_{61} \times \mathbf{l}_{61} + \boldsymbol{\omega}_{62} \times \mathbf{l}_{62}, \quad i = 1, \ldots, 5 \tag{2.153}$$

where $\boldsymbol{\omega}_{ij}$ ($i = 1, \ldots, 6$ and $j = 1, 2$) is the angular velocity vector of the jth link of the ith leg, while $\mathbf{l}_{i1}$ ($i = 1, \ldots, 6$) is the position vector from point O_i to point O_i' and $\mathbf{l}_{i2}$ ($i = 1, \ldots, 6$) is the position vector from point O_i' to point P_i.

Eq.(2.149) can be rewritten as

$$-\mathbf{l}_{i1} \times \boldsymbol{\omega}_{i1} - \mathbf{l}_{61} \times \boldsymbol{\omega}_{61} = \mathbf{l}_{i2} \times \boldsymbol{\omega}_{i2} + \mathbf{v}_i \times \boldsymbol{\omega} - \mathbf{l}_{62} \times \boldsymbol{\omega}_{62}, \quad i = 1, \ldots, 5 \tag{2.154}$$

The cross products appearing in eq.(2.154) can be written in matrix form

$$-\mathbf{L}_{i1}\mathbf{e}_i\dot{\rho}_i - \mathbf{L}_{61}\mathbf{e}_6\dot{\rho}_6 = \mathbf{L}_{i2}\boldsymbol{\omega}_{i2} + \mathbf{V}_i\boldsymbol{\omega} - \mathbf{L}_{62}\boldsymbol{\omega}_{62}, \quad i = 1, \ldots, 5 \tag{2.155}$$

where vector $\boldsymbol{\omega}_{i1}$ has been written as

$$\boldsymbol{\omega}_{i1} = \dot{\rho}_i \mathbf{e}_i, \quad i = 1, \ldots, 6 \tag{2.156}$$

where $\mathbf{e}_i$ is the unit vector associated with the direction of the axis of the ith actuator. Moreover, the matrices used above are defined after eq.(2.112), but now for $i = 1, \ldots, 6$, where l_{i1x}, l_{i1y} and l_{i1z} are the components of vector $\mathbf{l}_{i1}$ and l_{i2x}, l_{i2y} and l_{i2z} are the components of vector $\mathbf{l}_{i2}$, and where matrices $\mathbf{V}_i$ has also been defined after eq.(2.111).

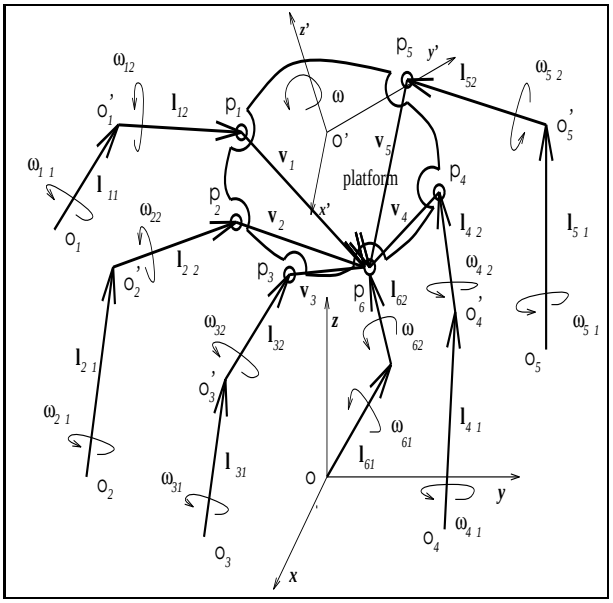

Figure 2.25: Position and velocity vectors associated with the spatial six-degree-of-freedom parallel mechanism with revolute actuators.

One can represent vectors $\mathbf{l}_{i2}(i = 1, \ldots, 6)$ and vector $\mathbf{p}_6$ using spherical coordinates, as represented in Figure2.21. Hence, one has

$$\boldsymbol{\omega}_{i2} = \mathbf{G}_i \boldsymbol{\omega}_{is}, \quad i = 1, \ldots, 6 \tag{2.157}$$

where $\mathbf{G}_i$ was defined in eq.(2.113) and $\boldsymbol{\omega}_{is} = [\, \dot{\alpha}_i \quad \dot{\beta}_i \,]^T, i = 1, \ldots, 6.$

Substituting eqs.(2.156) and eq.(2.157) into eq.(2.155), one obtains

$$-\mathbf{L}_{i1}\mathbf{e}_i\dot{\rho}_i - \mathbf{L}_{61}\mathbf{e}_6\dot{\rho}_6 = \mathbf{T}_i\boldsymbol{\omega}_{is} + \mathbf{V}_i\boldsymbol{\omega} - \mathbf{T}_6\boldsymbol{\omega}_{6s}, \quad i = 1, \ldots, 5 \tag{2.158}$$

where

$$\mathbf{T}_i = \mathbf{L}_{i2}\mathbf{G}_i, \quad i = 1, \ldots, 6 \tag{2.159}$$

and $\mathbf{V}_i$ and $\mathbf{S}_i$ are as previously defined.

Finally, the velocity equations of the mechanism are obtained from eq.(2.158) as

$$\mathbf{B}_{rv}\dot{\boldsymbol{\rho}} = \mathbf{J}_{rv}\mathbf{w} \tag{2.160}$$

where $\mathbf{B}_{rv}$ is a 15×6 matrix defined as

$$\mathbf{B}_{rv} = \begin{bmatrix} -\mathbf{L}_{11}\mathbf{e}_1 & \mathbf{0} & \mathbf{0} & \mathbf{0} & \mathbf{0} & -\mathbf{L}_{61}\mathbf{e}_6 \\ \mathbf{0} & -\mathbf{L}_{21}\mathbf{e}_2 & \mathbf{0} & \mathbf{0} & \mathbf{0} & -\mathbf{L}_{61}\mathbf{e}_6 \\ \mathbf{0} & \mathbf{0} & -\mathbf{L}_{31}\mathbf{e}_3 & \mathbf{0} & \mathbf{0} & -\mathbf{L}_{61}\mathbf{e}_6 \\ \mathbf{0} & \mathbf{0} & \mathbf{0} & -\mathbf{L}_{41}\mathbf{e}_4 & \mathbf{0} & -\mathbf{L}_{61}\mathbf{e}_6 \\ \mathbf{0} & \mathbf{0} & \mathbf{0} & \mathbf{0} & -\mathbf{L}_{51}\mathbf{e}_5 & -\mathbf{L}_{61}\mathbf{e}_6 \end{bmatrix} \tag{2.161}$$

where $\mathbf{0}$ denotes a 3-dimensional zero column vector, and $\dot{\boldsymbol{\rho}}$ is the joint velocity vector previously defined.

Moreover, vector $\mathbf{w}$ is a 15-dimensional vector defined as

$$\mathbf{w} = [\,\boldsymbol{\omega}_{1s}^T \quad \boldsymbol{\omega}_{2s}^T \quad \boldsymbol{\omega}_{3s}^T \quad \boldsymbol{\omega}_{4s}^T \quad \boldsymbol{\omega}_{5s}^T \quad \boldsymbol{\omega}^T \quad \boldsymbol{\omega}_{6s}^T\,]^T \tag{2.162}$$

and matrix $\mathbf{J}_{rv}$ a 15×15 matrix defined as

$$\mathbf{J}_{rv} = \begin{bmatrix} \mathbf{T}_1 & \mathbf{0} & \mathbf{0} & \mathbf{0} & \mathbf{0} & \mathbf{V}_1 & -\mathbf{T}_6 \\ \mathbf{0} & \mathbf{T}_2 & \mathbf{0} & \mathbf{0} & \mathbf{0} & \mathbf{V}_2 & -\mathbf{T}_6 \\ \mathbf{0} & \mathbf{0} & \mathbf{T}_3 & \mathbf{0} & \mathbf{0} & \mathbf{V}_3 & -\mathbf{T}_6 \\ \mathbf{0} & \mathbf{0} & \mathbf{0} & \mathbf{T}_4 & \mathbf{0} & \mathbf{V}_4 & -\mathbf{T}_6 \\ \mathbf{0} & \mathbf{0} & \mathbf{0} & \mathbf{0} & \mathbf{T}_5 & \mathbf{V}_5 & -\mathbf{T}_6 \end{bmatrix} \tag{2.163}$$

where $\mathbf{0}$ denotes a 3×2 zero matrix.

III) Determination of the singularity loci

Again, the determination of the second type of singularity loci consists in finding the roots of the following equations, i.e.,

$$\det(\mathbf{A}_r) = 0 \tag{2.164}$$

or

$$\det(\mathbf{J}_{rv}) = 0 \tag{2.165}$$

Matrix $\mathbf{J}_{rv}$ is rather sparse and it is therefore easy to reduce the expression of its determinant to the expression of the determinant of a 5×5 matrix. Hence, globally, the use of the matrices obtained with the vector method will provide simpler expressions which will therefore lead to faster algorithms.

$$\det(\mathbf{J}_{rv}) = D_o \det(\mathbf{J}) = 0 \tag{2.166}$$

where

$$D_o = \prod_{i=1}^{6} \mathbf{l}_{i2}^T \mathbf{d}_i \tag{2.167}$$

with vector $\mathbf{l}_{i2}$ defined above, with vector $\mathbf{d}_i$ defined in eq.(2.144) and where matrix $\mathbf{J}$ can be written as

$$\mathbf{J} = \begin{bmatrix} (\mathbf{l}_{12} \times \mathbf{v}_1)^T & (\mathbf{L}_{62} \times \mathbf{l}_{12})^T \mathbf{u} & \mathbf{l}_{12}^T \mathbf{h} \\ (\mathbf{l}_{22} \times \mathbf{v}_2)^T & (\mathbf{L}_{62} \times \mathbf{l}_{22})^T \mathbf{u} & \mathbf{l}_{22}^T \mathbf{h} \\ (\mathbf{l}_{32} \times \mathbf{v}_3)^T & (\mathbf{L}_{62} \times \mathbf{l}_{32})^T \mathbf{u} & \mathbf{l}_{32}^T \mathbf{h} \\ (\mathbf{l}_{42} \times \mathbf{v}_4)^T & (\mathbf{L}_{62} \times \mathbf{l}_{42})^T \mathbf{u} & \mathbf{l}_{42}^T \mathbf{h} \\ (\mathbf{l}_{52} \times \mathbf{v}_5)^T & (\mathbf{L}_{62} \times \mathbf{l}_{52})^T \mathbf{u} & \mathbf{l}_{52}^T \mathbf{h} \end{bmatrix} \tag{2.168}$$

where $\mathbf{h}$ and $\mathbf{u}$ are defined respectively in eqs.(2.146) and (2.147).

From the above equations, it is clear, by inspection, that $D_o \neq 0$. Therefore, eqs.(2.164) and (2.165) can be reduced to

$$\det(\mathbf{J}) = 0 \tag{2.169}$$

where $\mathbf{J}$ is a 5×5 matrix and hence, the determination of the singularity loci is greatly simplified.

IV) Example

Similarly to the other cases, in order to illustrate the results, two examples are presented below. Since the mechanism has six degrees of freedom, its workspace is six-dimensional. In order to be able to visualize the results, one has to fix four of the Cartesian coordinates and then obtain a two-dimensional section of the workspace associated with the other two coordinates on which the limits of the workspace and the singularity loci can be plotted.

Using the same parameters as the ones used in the example on the determination of the workspace of the mechanism, one can obtain the singularity locus over the workspace in two sections, as represented in Figures 2.26.

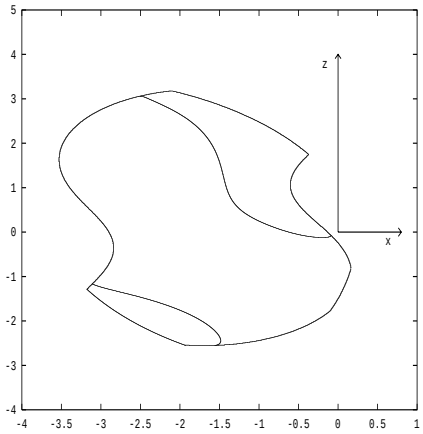

(a) A section of the workspace (over x and z) with $K_i = 1, (i = 1, \ldots, 6)$.

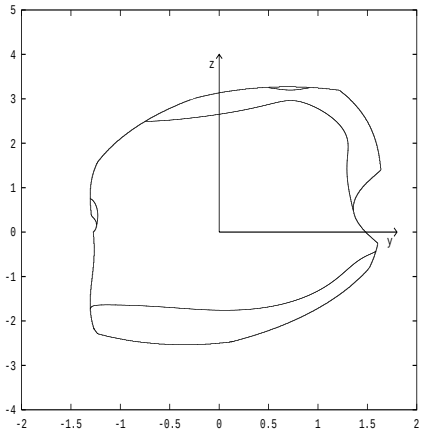

(b) A section of the workspace (over y and z) with $K_i = 1, (i = 1, \ldots, 6)$.

Figure 2.26: Singularity locus and workspace of the six-dof manipulator.

2.3 Kinematic optimization of mechanisms with reduced degrees of freedom

In this section, the optimization of planar two-degree-of-freedom as well as spatial four- and five-degree-of-freedom parallel manipulators is addressed. The objective is to synthesize manipulators in which the uncontrollable dependent Cartesian coordinates will follow certain trajectories which are functions of the independent Cartesian coordinates and which are prescribed by design. This may be suitable in certain applications where the dependent Cartesian coordinates would be required to follow prescribed — and fixed — trajectories. The dependent Cartesian coordinates are first expressed as functions of the relative linkage parameter of the manipulator using the kinematic equations. The objective functions are formed using the least square method. The limits of the workspace of the manipulators are used as the constraints in the optimization in order to ensure that all specified trajectory points are in the Cartesian space and located inside the workspace of the optimized manipulators.

2.3.1 Planar two-degree-of-freedom manipulator

Referring to Figure 2.1, it is clear that the orientation of the end-effector of the two-degree-of-freedom planar mechanism is only related to the two links of the first leg. Hence, in order to simplify the study, it is assumed that the mechanism studied consists of two moving links and two revolute joints, as illustrated in Figure 2.27, and the lengths of the two links of the second leg can be arbitrarily chosen to meet the kinematic requirements of the resulting mechanism.

Two reference coordinate frames are defined. Coordinate frame $O-\mathbf{x}-\mathbf{y}$ is attached to the base and its origin O lies at the center of the joint connecting the first moving link and the base. Coordinate frame $O' - \mathbf{x}' - \mathbf{y}'$ is fixed to the second moving link and its origin O' is coincident with point P where the end-effector of the manipulator is assumed to be positioned. Point P_1 denotes the center point of the joint connecting the two moving links.

Let l_1 denote the length of the first moving link, (a, b) the coordinates of point P_1 in the moving reference frame $O' - \mathbf{x}' - \mathbf{y}'$ and (x, y) the coordinates of point P in the fixed reference frame $O - \mathbf{x} - \mathbf{y}$. From the geometry of the manipulator, one can write

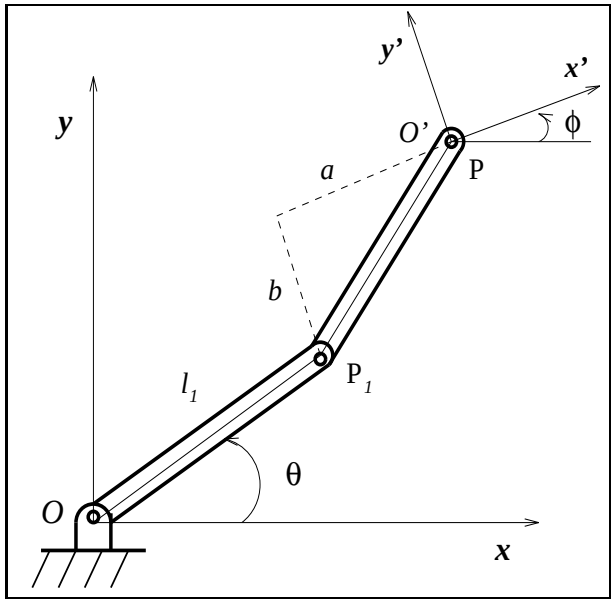

Figure 2.27: First leg of the planar two-degree-of-freedom parallel manipulator.

the following vector equation

$$\mathbf{p}_1 = \mathbf{p} + \mathbf{Q}\mathbf{r} \tag{2.170}$$

where

$$\mathbf{r} = [\, a \quad b \,]^T \tag{2.171}$$

$\mathbf{Q}$ is the orientation matrix of the moving frame with respect to the fixed frame, which is written as

$$\mathbf{Q} = \begin{bmatrix} \cos\phi & -\sin\phi \\ \sin\phi & \cos\phi \end{bmatrix} \tag{2.172}$$

where ϕ is the angle between coordinate axes $\mathbf{x}'$ and $\mathbf{x}$.

If one chooses any two coordinates of the three Cartesian coordinates x, y and ϕ, for instance x and y, as the independent coordinates of the manipulator, the dependent angle ϕ can be computed from equation (2.170).

From equation (2.170) one can write

$$l_1 \cos\theta = x + (a\cos\phi - b\sin\phi) \tag{2.173}$$

$$l_1 \sin\theta = y + (a\sin\phi + b\cos\phi) \tag{2.174}$$

Squaring both sides of equations (2.173) and (2.174) and then adding leads to

$$A\cos\phi + B\sin\phi = C \tag{2.175}$$

where

$$A = 2(ax + by) \tag{2.176}$$

$$B = 2(ay - bx) \tag{2.177}$$

$$C = x^2 + y^2 + a^2 + b^2 - l_1^2 \tag{2.178}$$

From equation (2.175) one obtains

$$\sin\phi = \frac{BC + KA\sqrt{\Delta}}{A^2 + B^2} \tag{2.179}$$

$$\cos\phi = \frac{AC + KB\sqrt{\Delta}}{A^2 + B^2} \tag{2.180}$$

where

$$\Delta = A^2 + B^2 - C^2 \tag{2.181}$$

$$K = \pm 1$$

Variables Δ and K are two important factors in the optimization of the manipulator. Δ is the discriminant of equation (2.175). A value of Δ larger than zero means that point $P(x, y)$ is located inside the workspace of the manipulator. K is the branch index of the manipulator, its two values determine the two possible configurations of the manipulator.

From eq.(2.175), it is clear that when x and y are given, angle ϕ is only related to linkage parameters l_1, a and b. Therefore, these three linkage parameters are chosen as optimization variables.

Assuming that the two-degree-of-freedom manipulator is used to position n points of the plane from $P(x_1, y_1)$ to $P(x_n, y_n)$ while the orientation of the end-effector of the manipulator corresponding to these points is required to be as close as possible to prescribed values noted $\bar{\phi}_1$ to $\bar{\phi}_n$, one can formulate the optimization problem as follows

Minimize:

$$\mathrm{F}(\mathbf{x}) \tag{2.182}$$

Subject to:

$$g_i(\mathbf{x}) \geq 0, \quad i = 1, \ldots, n \tag{2.183}$$

where

$$\begin{aligned} \mathbf{x} &= [\, u_1 \quad u_2 \quad u_3 \,]^T && (2.184)\\ &= [\, l_1 \quad a \quad b \,]^T && (2.185)\\ \mathrm{F}(\mathbf{x}) &= \frac{1}{2}\mathbf{e}^T\mathbf{W}\mathbf{e} && (2.186)\\ g_i(\mathbf{x}) &= \Delta_i, \quad i = 1, \ldots, n && (2.187) \end{aligned}$$

where $\mathbf{W}$ is a $2n$ by $2n$ weighting matrix and $\mathbf{e}$ is a $2n$ dimensional error vector, written as

$$\mathbf{e} = \begin{bmatrix} \sin\phi_1 - \sin\overline{\phi}_1 \\ \cos\phi_1 - \cos\overline{\phi}_1 \\ \cdots \\ \cdots \\ \sin\phi_n - \sin\overline{\phi}_n \\ \cos\phi_n - \cos\overline{\phi}_n \end{bmatrix} \tag{2.188}$$

where $\sin\phi_i$, $\cos\phi_i$ and Δ_i $(i = 1, 2, ..., n)$ are computed according to eqs.(2.179), (2.180) and (2.181) respectively.

The generalized reduced gradient method is used here [63]. This method is an extension of the reduced gradient method which is used to solve equality-constrained optimization problems, where one adds one slack variable to each inequality constraint thereby transforming the inequality-constrained optimization problem into an equality-constrained one.

This method is efficient for both objective and constraint functions which are highly nonlinear. In the method, a search direction is found such that any active constraints remain precisely active for some small move in this direction. If a move is made, because of nonlinearity, some currently active constraint does not remain precisely satisfied, Newton's method is used to return to the constraint boundary.

An algorithm written in FORTRAN language by Wang and Xie [63] is directly applied for the optimization. The expressions of the partial derivatives of the objective and constraint functions are needed. They can be obtained as follows:

Assuming $\mathbf{W} = [\mathbf{1}], [\mathbf{1}]$ denoting a $2n$ by $2n$ identity matrix, differentiating equation (2.186) with respect to $\mathbf{x}$ one then has

$$\frac{\partial \mathrm{F}(\mathbf{x})}{\partial \mathbf{x}} = (\frac{\partial \mathbf{e}}{\partial \mathbf{x}})^T \mathbf{e} \tag{2.189}$$

From equation (2.188) one can obtain

$$\frac{\partial \mathbf{e}}{\partial \mathbf{x}} = \begin{bmatrix} \cos\phi_1 (\frac{\partial \phi_1}{\partial \mathbf{x}})^T \\ -\sin\phi_1 (\frac{\partial \phi_1}{\partial \mathbf{x}})^T \\ \cdots \\ \cdots \\ \cos\phi_n (\frac{\partial \phi_n}{\partial \mathbf{x}})^T \\ -\sin\phi_n (\frac{\partial \phi_n}{\partial \mathbf{x}})^T \end{bmatrix} \tag{2.190}$$

where $\frac{\partial \phi_i}{\partial \mathbf{x}}$ can be obtained from equation (2.175)

$$\frac{\partial \phi_i}{\partial \mathbf{x}} = (\frac{\partial C_i}{\partial \mathbf{x}} - \frac{\partial A_i}{\partial \mathbf{x}} \cos\phi_i - \frac{\partial B_i}{\partial \mathbf{x}} \sin\phi_i)/(B_i \cos\phi_i - A_i \sin\phi_i), \quad i = 1, 2, ..., n \tag{2.191}$$

where $\frac{\partial C_i}{\partial \mathbf{x}}$, $\frac{\partial A_i}{\partial \mathbf{x}}$ and $\frac{\partial B_i}{\partial \mathbf{x}}$ can be easily obtained from equations (2.176)–(2.178) as

$$\frac{\partial C_i}{\partial \mathbf{x}} = \begin{bmatrix} -2u_1 \\ 2u_2 \\ 2u_3 \end{bmatrix}, \quad \frac{\partial A_i}{\partial \mathbf{x}} = \begin{bmatrix} 0 \\ 2x_i \\ 2y_i \end{bmatrix}, \quad \frac{\partial B_i}{\partial \mathbf{x}} = \begin{bmatrix} 0 \\ 2y_i \\ -2x_i \end{bmatrix} \tag{2.192}$$

	P_1	P_2	P_3	P_4	P_5	P_6	P_7	P_8	P_9	P_{10}
x	1.5	1.8	2.1	2.4	2.7	3.0	3.3	3.6	3.9	4.2
y	0.5	0.8	1.1	1.4	1.7	2.0	2.3	2.6	2.9	3.2
$\overline{\phi}$	150	140	130	120	110	100	90	80	70	60

Table 2.1: Data set for the two-dof parallel manipulator, lengths are in meters and angles in degrees, $K = -1$.

The partial derivatives of the constraint functions can be obtained by differentiating equation (2.181) with respect to $\mathbf{x}$, i.e.,

$$\frac{\partial g_i(\mathbf{X})}{\partial \mathbf{x}} = \frac{\partial \Delta_i}{\partial \mathbf{x}} = 2A_i \frac{\partial A_i}{\partial \mathbf{x}} + 2B_i \frac{\partial B_i}{\partial \mathbf{x}} + 2C_i \frac{\partial C_i}{\partial \mathbf{x}} \tag{2.193}$$

Prescribing 10 points of the X–Y plane, $P_1, P_2, ..., P_{10}$, as well as a set of orientation angles corresponding to each of these points and noted $\overline{\phi}_1, \overline{\phi}_2, ..., \overline{\phi}_{10}$, it is desired to find the most suitable three linkage parameters l_1, a and b so that when the end-effector of the manipulator passes through points P_i $(i = 1, 2, ..., 10)$ its orientation angles ϕ_i $(i = 1, 2, ..., 10)$ are as close as possible to the specified values $\overline{\phi}_i$ $(i = 1, 2, ..., 10)$. An example data set is given in Table 2.1.

Using the program GRGM (Generalized Reduced Gradient Method) [63] one obtains the following results for the optimization

$$l_1 = 3.39,\ a = -2.09,\ b = 0.004$$

and

$$\phi = [\,153.00 \quad 137.32 \quad 126.53 \quad 117.47 \quad 109.11 \quad 100.91 \quad 92.47 \quad 83.31 \quad 72.58 \quad 57.54\,]^T \tag{2.194}$$

The square of the sum of the errors gives

$$err = \sum_{i=1}^{10} (\phi_i - \overline{\phi}_i)^2 = 2.0\text{E} - 02 \tag{2.195}$$

The corresponding error curve is shown in Figure 2.28. This example illustrates that when the end-effector of the two-dof manipulator passes through a set of prescribed points, it is possible that its orientation angles can be close to the desired values by an optimal choice of the linkage parameters.

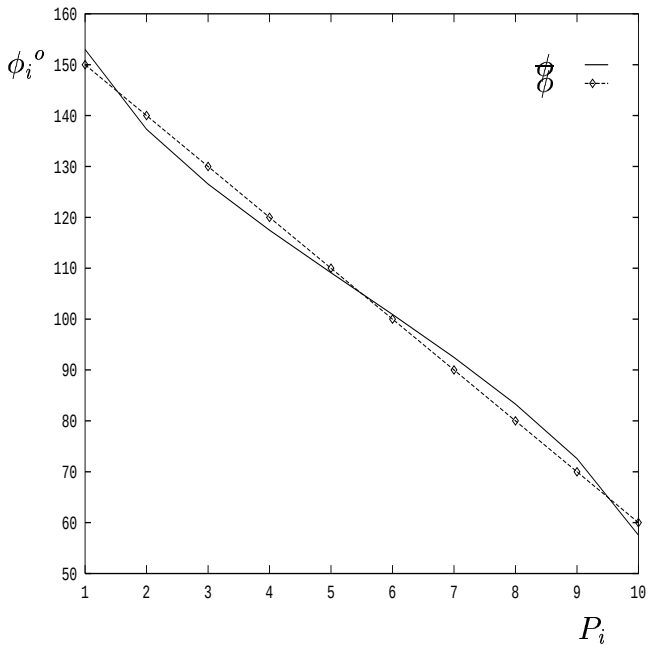

Figure 2.28: Example of optimization synthesis of the two-dof mechanism.

2.3.2 Spatial four-degree-of-freedom manipulator

Similarly, the optimization problem for the four-degree-of-freedom manipulator can be stated as:

Specifying a set of points $P_i(x_i, y_i, z_i, \psi_i) i = 1, \ldots, n$ in the four dimensional space and the corresponding sets of Euler angles $\overline{\theta}_i$ and $\overline{\psi}_i$, determine a set of optimal parameters l_5, a_5, b_5 and c_5 of the manipulator, for which, when the manipulator passes through points P_i, the two dependent Euler angles θ_i and ψ_i are as close as possible to their prescribed value $\overline{\theta}_i$ and $\overline{\psi}_i$.

It can be formulated as

Minimize:

$$F(\mathbf{x})$$

subject to:

$$\mathbf{g}_i(\mathbf{x}) \geq 0, \quad i = 1, \ldots, n$$

where $F(\mathbf{x})$ is the objective function and $\mathbf{g}_i$ is the constraint function.

$$F(\mathbf{x}) = \frac{1}{2}\mathbf{e}_1^T \mathbf{W}_1 \mathbf{e}_1 + \frac{1}{2}\mathbf{e}_2^T \mathbf{W}_2 \mathbf{e}_2 \tag{2.196}$$

$$\begin{aligned} \mathbf{x} &= [\, u_1 \quad u_2 \quad u_3 \quad u_4 \,]^T \\ &= [\, l_5 \quad a_5 \quad b_5 \quad c_5 \,]^T \end{aligned} \tag{2.197}$$

where $\mathbf{W}_1$ and $\mathbf{W}_2$ are two weighting matrices, and

$$\mathbf{e}_1 = \begin{bmatrix} \sin\theta_1 - \sin\overline{\theta}_1 \\ \cos\theta_1 - \cos\overline{\theta}_1 \\ \cdots \\ \cdots \\ \sin\theta_n - \sin\overline{\theta}_n \\ \cos\theta - \cos\overline{\theta}_n \end{bmatrix}, \quad \mathbf{e}_2 = \begin{bmatrix} \sin\psi_1 - \sin\overline{\psi}_1 \\ \cos\psi_1 - \cos\overline{\psi}_1 \\ \cdots \\ \cdots \\ \sin\psi_n - \sin\overline{\psi}_n \\ \cos\psi_n - \cos\overline{\psi}_n \end{bmatrix} \tag{2.198}$$

The constraint function is written as

$$\mathbf{g}_i = [\, g_{1i} \quad g_{2i} \quad g_{3i} \quad g_{4i} \quad g_{5i} \quad g_{6i} \,], \quad i = 1, \ldots, n \tag{2.199}$$

where

$$g_{1i}(\mathbf{x}) = \Delta_{41}^i \tag{2.200}$$

$$g_{2i}(\mathbf{x}) = \Delta_{42}^i \tag{2.201}$$

$$g_{(j+2)i}(\mathbf{x}) = V_j^i \tag{2.202}$$

$$\begin{aligned} i &= 1, ..., n \\ j &= 1, ..., 4 \end{aligned}$$

where $g_{(j+2)i}(\mathbf{x})$ are the constraints associated with the jth actuated leg while Δ_{41}, Δ_{42} and V_j have been defined in eqs.(2.41), (2.48) and (2.57) respectively.

The generalized reduced gradient method is used for the optimization problem. The expressions of the partial derivatives of the objective and constraint functions are written as follows

Assuming $\mathbf{W}_1 = \mathbf{W}_2 = [\mathbf{1}]$, with $[\mathbf{1}]$ the identity matrix,

$$\frac{\partial \mathrm{F}(\mathbf{x})}{\partial \mathbf{x}} = (\frac{\partial \mathbf{e}_1}{\partial \mathbf{x}})^T \mathbf{e}_1 + (\frac{\partial \mathbf{e}_2}{\partial \mathbf{x}})^T \mathbf{e}_2 \tag{2.203}$$

Differentiating equations (2.198) with respect to the optimization variables $\mathbf{x}$, one

then obtains

$$\frac{\partial \mathbf{e}_1}{\partial \mathbf{x}} = \begin{bmatrix} \cos\theta_1(\frac{\partial\theta_1}{\partial \mathbf{x}})^T \\ -\sin\theta_1(\frac{\partial\theta_1}{\partial \mathbf{x}})^T \\ \cdots \\ \cdots \\ \cos\theta_n(\frac{\partial\theta_n}{\partial \mathbf{x}})^T \\ -\sin\theta_n(\frac{\partial\theta_n}{\partial \mathbf{x}})^T \end{bmatrix}, \quad \frac{\partial \mathbf{e}_2}{\partial \mathbf{x}} = \begin{bmatrix} \cos\psi_1(\frac{\partial\psi_1}{\partial \mathbf{x}})^T \\ -\sin\psi_1(\frac{\partial\psi_1}{\partial \mathbf{x}})^T \\ \cdots \\ \cdots \\ \cos\psi_n(\frac{\partial\psi_n}{\partial \mathbf{x}})^T \\ -\sin\psi_n(\frac{\partial\psi_n}{\partial \mathbf{x}})^T \end{bmatrix} \tag{2.204}$$

where $\frac{\partial\psi_i}{\partial \mathbf{x}}$ and $\frac{\partial\theta_i}{\partial \mathbf{x}}$ $(i = 1, 2, ..., n)$ can be obtained by differentiating equations (2.42) and (2.49) respectively, i.e.,

$$\frac{\partial\psi_i}{\partial \mathbf{x}} = (\frac{\partial C^i_{42}}{\partial \mathbf{x}} - \frac{\partial A^i_{42}}{\partial \mathbf{x}}\cos\psi_i - \frac{\partial B^i_{42}}{\partial \mathbf{x}}\sin\psi_i)/(B^i_{42}\cos\psi_i - A^i_{42}\sin\psi_i), \quad i = 1, \ldots, n \tag{2.205}$$

$$\frac{\partial\theta_i}{\partial \mathbf{x}} = (\frac{\partial \mathbf{b}}{\partial \mathbf{x}} - \frac{\partial \mathbf{A}}{\partial \mathbf{x}})/(\mathbf{A}\frac{\partial \mathbf{t}_{\theta_i}}{\partial\theta}) \quad i = 1, \ldots, n \tag{2.206}$$

and $\frac{\partial A^i_{42}}{\partial \mathbf{x}}$, $\frac{\partial B^i_{42}}{\partial \mathbf{x}}$ and $\frac{\partial C^i_{42}}{\partial \mathbf{x}}$ can be easily obtained by differentiating equations (2.43)–(2.45) as

$$\frac{\partial A^i_{42}}{\partial \mathbf{x}} = \begin{bmatrix} 0 \\ 0 \\ 1 \\ 0 \end{bmatrix}, \quad \frac{\partial B^i_{42}}{\partial \mathbf{x}} = \begin{bmatrix} 0 \\ 1 \\ 0 \\ 0 \end{bmatrix}, \quad \frac{\partial C^i_{42}}{\partial \mathbf{x}} = \begin{bmatrix} -\sin\phi_i(\sin\alpha_i + u_1\cos\alpha_i\frac{\partial\alpha_i}{\partial \mathbf{u}_1}) \\ -u_1\sin\phi_i\cos\alpha_i\frac{\partial\alpha_i}{\partial \mathbf{u}_2} \\ -u_1\sin\phi_i\cos\alpha_i\frac{\partial\alpha_i}{\partial \mathbf{u}_3} \\ -u_1\sin\phi_i\cos\alpha_i\frac{\partial\alpha_i}{\partial \mathbf{u}_4} \end{bmatrix} \tag{2.207}$$

Differentiating equation (2.35) with respect to $\mathbf{x}$, one has

$$\frac{\partial\alpha_i}{\partial \mathbf{x}} = (\frac{\partial C^i_{41}}{\partial \mathbf{x}} - \frac{\partial A^i_{41}}{\partial \mathbf{x}}\cos\alpha_i - \frac{\partial B^i_{41}}{\partial \mathbf{x}}\sin\alpha_i)/(B^i_{42}\cos\alpha_i - A^i_{41}\sin\alpha_i), \quad i = 1, 2, ..., n \tag{2.208}$$

and similarly, by differentiating eqs.(2.36)–(2.38), one then obtains

$$\frac{\partial A^i_{41}}{\partial \mathbf{x}} = \mathbf{0}, \quad \frac{\partial B^i_{41}}{\partial \mathbf{x}} = \mathbf{0}, \quad \frac{\partial C^i_{41}}{\partial \mathbf{x}} = \begin{bmatrix} 2u_1 \\ -2u_2 \\ -2u_3 \\ -2u_4 \end{bmatrix} \tag{2.209}$$

The partial derivatives of the constraint functions can then be obtained as follows

$$\begin{aligned} \frac{\partial g_{1i}}{\partial \mathbf{x}} &= 2\frac{\partial A^i_{41}}{\partial \mathbf{x}} + 2\frac{\partial B^i_{41}}{\partial \mathbf{x}} - 2\frac{\partial C^i_{41}}{\partial \mathbf{x}} \\ \frac{\partial g_{2i}}{\partial \mathbf{x}} &= 2\frac{\partial A^i_{42}}{\partial \mathbf{x}} + 2\frac{\partial B^i_{42}}{\partial \mathbf{x}} - 2\frac{\partial C^i_{42}}{\partial \mathbf{x}} \end{aligned}$$

and

$$\frac{\partial g(j+2)_i(\mathbf{x})}{\partial \mathbf{x}} = 2\frac{\partial R_i}{\partial \mathbf{x}} + 2\frac{\partial S_i}{\partial \mathbf{x}} - 2\frac{\partial T_i}{\partial \mathbf{x}} \tag{2.210}$$

where

$$\begin{aligned}
\frac{\partial R_i}{\partial \mathbf{x}} &= \frac{\partial y_i}{\partial \mathbf{x}} \\
\frac{\partial R_i}{\partial \mathbf{x}} &= \frac{\partial z_i}{\partial \mathbf{x}} \\
\frac{\partial T_i}{\partial \mathbf{x}} &= \frac{2(x_i - x_{io})\frac{\partial x_i}{\partial \mathbf{x}} + 2(y_i - y_{io})\frac{\partial y_i}{\partial \mathbf{x}} + 2(z_i - z_{io})\frac{\partial z_i}{\partial \mathbf{x}}}{2l_{i1}}
\end{aligned}$$

where x_i, y_i and z_i are the three components of vector $\mathbf{p}_i$, namely

$$\frac{\partial \mathbf{p}_i}{\partial \mathbf{x}} = \begin{bmatrix} \frac{\partial x_i}{\partial \mathbf{x}} \\ \frac{\partial y_i}{\partial \mathbf{x}} \\ \frac{\partial z_i}{\partial \mathbf{x}} \end{bmatrix} \tag{2.211}$$

The same optimization program GRGM used for the optimization of the two-dof mechanism is used here. A numerical example illustrating the application of the above procedure to the four-degree-of-freedom manipulator is now presented.

Given 10 points, $P_1, P_2, ..., P_{10}$, for which the four independent Cartesian coordinates are prescribed as well as two sets of dependent orientation angles associated to these points, $\overline{\theta}_1, \overline{\theta}_2, ..., \overline{\theta}_{10}$ and $\overline{\psi}_1, \overline{\psi}_2, ..., \overline{\psi}_{10}$, find the most suitable four linkage parameters l_5, a_5, b_5 and c_5 so that when the end-effector of the manipulator passes through points P_i $(i = 1, 2, ..., 10)$ its two sets of dependent orientation angles $\theta_1, \theta_2, ..., \theta_{10}$ and $\psi_1, \psi_2, ..., \psi_{10}$ are as close as possible to the specified values $\overline{\theta}_1, \overline{\theta}_2, ..., \overline{\theta}_{10}$ and $\overline{\psi}_1, \overline{\psi}_2, ..., \overline{\psi}_{10}$.

The parameters used in this example are given as

$$x_{o1} = -1.5,\ y_{o1} = 1.5,\ x_{o2} = -3.0,\ y_{o2} = 1.5,\ x_{o3} = -3.0,\ y_{o3} = -1.5$$

$$x_{o4} = -1.5,\ y_{o4} = -1.5,\ x_{o5} = 0.0,\ y_{o5} = 0.0,\ z_{oi} = 0.0 (i = 1, \ldots, 5)$$

$$a_1 = 0.2,\ b_1 = 0.6,\ c_1 = -0.4,\ a_2 = -0.6,\ b_2 = 0.6,\ c_2 = -0.4$$

$$a_3 = -0.6,\ b_3 = -0.6,\ c_3 = -0.4,\ a_4 = 0.2,\ b_4 = -0.6,\ c_4 = -0.4$$

$$\gamma_1 = \frac{\pi}{4},\ \gamma_2 = \frac{\pi}{4},\ \gamma_3 = \frac{3\pi}{4},\ \gamma_4 = \frac{3\pi}{4}$$

$$l_{i1} = 4.0,\ l_{i2} = 4.0 (i = 1, \ldots, 4)$$

	P_1	P_2	P_3	P_4	P_5	P_6	P_7	P_8	P_9	P_{10}
x_i	-1.45	-1.4	-1.35	-1.3	-1.25	-1.2	-1.15	-1.1	-1.05	-1.0
y_i	0.1	0.1	0.1	0.1	0.1	0.1	0.1	0.1	0.1	0.1
z_i	0.8	0.8	0.8	0.8	0.8	0.8	0.8	0.8	0.8	0.8
ϕ_i	5	5	5	5	5	5	5	5	5	5
$\overline{\theta}_i$	5	10	15	20	25	30	35	40	45	50
$\overline{\psi}_i$	5	5	5	5	5	5	5	5	5	5

Table 2.2: Data set for the 4-dof parallel manipulator, lengths are in meters and angles in degrees, $K_1 = -1$ and $K_2 = 1$.

The specified Cartesian poses are represented in Table 2.2.

The results of the optimization are

$$l_5 = 2.614,\ a_5 = -1.044,\ b_5 = 0.108,\ c_5 = -0.959$$

which leads to

$$\boldsymbol{\theta} = [7.676\ 11.312\ 15.150\ 19.221\ 23.563\ 28.228\ 33.284\ 38.834\ 45.043\ 52.211]^T$$

$$\boldsymbol{\psi} = [5.806\ 5.572\ 5.351\ 5.145\ 4.961\ 4.804\ 4.683\ 4.610\ 4.604\ 4.696]^T$$

The least square sum of the error gives

$$err = \sum_{i=1}^{10}[(\theta_i - \overline{\theta}_i)^2 + (\psi_i - \overline{\psi}_i)^2] = 7.774\text{E} - 03 \tag{2.212}$$

The error curves are shown in Figure 2.29.

It can be seen from the example that by an optimal choice of the parameters of the special leg, the two dependent Cartesian coordinates assume the desired values when the independent Cartesian coordinates pass through the prescribed trajectories.

2.3.3 Spatial five-degree-of-freedom manipulators

The optimization problem of the five-degree-of-freedom manipulator can be stated as:

Specifying a set of points $P_i(x_i, y_i, z_i, \psi_i, \theta_i)$ $i = 1, \ldots, n$ in the five-dimensional space and the corresponding set of Euler angles $\overline{\psi}_i$, find the four optimal parameters

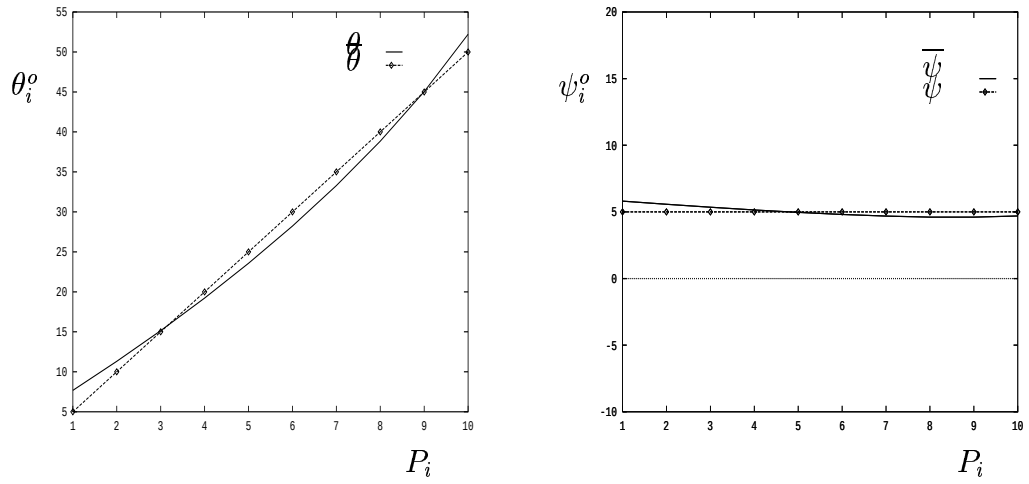

(a) First dependent Euler angle θ (b) Second dependent Euler angle ψ

Figure 2.29: Example of optimal synthesis of the spatial four-dof manipulator.

of the manipulator l_6, a_6, b_6 and c_6, for which, when the manipulator passes through points P_i, the dependent Euler angle ψ_i is as close as possible to its prescribed value $\overline{\psi}_i$.

This can be expressed mathematically as

Minimize:

$$F(\mathbf{x})$$

subject to:

$$\mathbf{g}_i(\mathbf{x}) \geq 0, \quad i = 1, 2, ..., n$$

where n is the number of prescribed Cartesian points.

$$F(\mathbf{x}) = \frac{1}{2}\mathbf{e}^T\mathbf{W}\mathbf{e} \tag{2.213}$$

$$\mathbf{x} = [\, x_1 \quad x_2 \quad x_3 \quad x_4 \,]^T$$

$$= [\, l_6 \quad a_6 \quad b_6 \quad c_6 \,]^T \tag{2.214}$$

where $\mathbf{W}$ is a n by n weighting matrix and

$$\mathbf{e} = \begin{bmatrix} \sin\psi_1 - \sin\overline{\psi}_1 \\ \cos\psi_1 - \cos\overline{\psi}_1 \\ \cdots \\ \cdots \\ \sin\psi_n - \sin\overline{\psi}_n \\ \cos\psi - \cos\overline{\psi}_n \end{bmatrix} \tag{2.215}$$

The constraint function is

$$\mathbf{g}_i = [\, g_{1i} \quad g_{2i} \quad g_{3i} \quad g_{4i} \quad g_{5i} \quad g_{6i} \,] \tag{2.216}$$

where

$$g_{1i}(\mathbf{x}) = \Delta^i \tag{2.217}$$

$$g_{(j+1)i}(\mathbf{x}) = V_j^i \tag{2.218}$$

$$i = 1, ..., n$$

$$j = 1, ..., 5$$

and where $g_{(j+1)i}(\mathbf{x})$ are the constraints associated with the jth actuated leg, moreover, Δ and V_j have been defined in eqs.(2.57) and (2.66) respectively.

Similarly to the previous case, we assume $\mathbf{W} = [\mathbf{1}]$, with $[\mathbf{1}]$ an identity matrix.

One can write

$$\frac{\partial \mathrm{F}(\mathbf{x})}{\partial \mathbf{x}} = (\frac{\partial \mathbf{e}}{\partial \mathbf{x}})^T \mathbf{e} \tag{2.219}$$

Differentiating equations (2.215) with respect to $\mathbf{x}$, one then obtains

$$\frac{\partial \mathbf{e}}{\partial \mathbf{x}} = \begin{bmatrix} \cos\psi(\frac{\partial\psi}{\partial\mathbf{x}})^T \\ -\sin\psi(\frac{\partial\psi}{\partial\mathbf{x}})^T \\ \cdots \\ \cdots \\ \cos\psi(\frac{\partial\psi}{\partial\mathbf{x}})^T \\ -\sin\psi(\frac{\partial\psi}{\partial\mathbf{x}})^T \end{bmatrix} \tag{2.220}$$

where $\frac{\partial\psi_i}{\partial\mathbf{x}}$ $(i = 1, 2, ..., n)$ can be obtained by differentiating equation (2.65)

$$\frac{\partial\psi_i}{\partial\mathbf{x}} = (\frac{\partial C^i}{\partial\mathbf{x}} - \frac{\partial A^i}{\partial\mathbf{x}}\cos\psi_i - \frac{\partial B^i}{\partial\mathbf{x}}\sin\psi_i)/(B^i\cos\psi_i - A^i\sin\psi_i), \quad i = 1, \ldots, n \tag{2.221}$$

where $\frac{\partial A^i}{\partial \mathbf{x}}$, $\frac{\partial B^i}{\partial \mathbf{x}}$ and $\frac{\partial C^i}{\partial \mathbf{x}}$ can be easily obtained from equations (2.66)–(2.68) as

$$\frac{\partial A^i}{\partial \mathbf{x}} = \begin{bmatrix} 0 \\ 2(x_i \cos\phi_i \cos\theta_i + y_i \sin\phi_i \cos\theta_i - z_i \sin\theta_i) \\ 2(y_i \cos\phi_i - x_i \sin\phi_i) \\ 0 \end{bmatrix} \tag{2.222}$$

$$\frac{\partial B^i}{\partial \mathbf{x}} = \begin{bmatrix} 0 \\ 2(y_i \cos\phi_i - x_i \sin\phi_i) \\ 2(x_i \cos\phi_i \cos\theta_i + y_i \sin\phi_i \cos\theta_i - \sin\theta_i) \\ 0 \end{bmatrix} \tag{2.223}$$

$$\frac{\partial C^i}{\partial \mathbf{x}} = \begin{bmatrix} 2u_1 \\ -2u_2 \\ -2u_3 \\ -2(u_4 - x_i \cos\phi_i \sin\theta_i + y_i \sin\phi_i \sin\theta_i + z_i \cos\theta_i \end{bmatrix} \tag{2.224}$$

The partial derivatives of the constraint functions can be respectively obtained as follows

$$\frac{\partial g_{1i}}{\partial \mathbf{x}} = 2\frac{\partial A^i}{\partial \mathbf{x}} + 2\frac{\partial B^i}{\partial \mathbf{x}} - 2\frac{\partial C^i}{\partial \mathbf{x}}$$

and

$$\frac{\partial g_{(j+1)i}(\mathbf{x})}{\partial \mathbf{x}} = 2\frac{\partial R_i}{\partial \mathbf{x}} + 2\frac{\partial S_i}{\partial \mathbf{x}} - 2\frac{\partial T_i}{\partial \mathbf{x}} \tag{2.225}$$

where

$$\begin{aligned} \frac{\partial R_i}{\partial \mathbf{x}} &= \frac{\partial y_i}{\partial \mathbf{x}} \\ \frac{\partial R_i}{\partial \mathbf{x}} &= \frac{\partial z_i}{\partial \mathbf{x}} \\ \frac{\partial T_i}{\partial \mathbf{x}} &= \frac{2(x_i - x_{io})\frac{\partial x_i}{\partial \mathbf{x}} + 2(y_i - y_{io})\frac{\partial y_i}{\partial \mathbf{x}} + 2(z_i - z_{io})\frac{\partial z_i}{\partial \mathbf{x}}}{2l_{i1}} \end{aligned}$$

similarly, where x_i, y_i and z_i are the three components of vector $\mathbf{p}_i$, i.e.,

$$\frac{\partial \mathbf{p}_i}{\partial \mathbf{x}} = \begin{bmatrix} \frac{\partial x_i}{\partial \mathbf{x}} \\ \frac{\partial y_i}{\partial \mathbf{x}} \\ \frac{\partial z_i}{\partial \mathbf{x}} \end{bmatrix} \tag{2.226}$$

Again, the same numerical algorithm is used for the optimization.

Given 10 points $P_1, P_2, ..., P_{10}$, for which the five independent Cartesian coordinates are prescribed as well as the dependent angle associated to these points, find the most

	P_1	P_2	P_3	P_4	P_5	P_6	P_7	P_8	P_9	P_{10}
x_i	-1.0	-1.1	-1.2	-1.3	-1.4	-1.5	-1.6	-1.7	-1.8	-1.9
y_i	0.1	0.1	0.1	0.1	0.1	0.1	0.1	0.1	0.1	0.1
z_i	0.6	0.7	0.8	0.9	1.0	1.1	1.2	1.3	1.4	1.5
ϕ_i	5	5	5	5	5	5	5	5	5	5
θ_i	5	5	5	5	5	5	5	5	5	5
$\overline{\psi}_i$	55	50	45	40	35	30	25	20	15	10

Table 2.3: Data set for the 5-dof parallel manipulator, lengths are in meters and angles in degrees, $K_1 = -1$.

suitable four linkage parameters l_5, a_5, b_5 and c_5 so that when the end-effector of the manipulator passes through points P_i $(i = 1, 2, ..., 10)$ its dependent orientation angles $\psi_1, \psi_2, ..., \psi_{10}$ are as close as possible to the prescribed values $\overline{\psi}_1, \overline{\psi}_2, ..., \overline{\psi}_{10}$.

The parameters used in this example are given as

$$x_{o1} = 2.0,\ y_{o1} = 1.5,\ x_{o2} = -1.0,\ y_{o2} = 1.5,\ x_{o3} = -2.0,\ y_{o3} = 0.0,$$
$$x_{o4} = -1.0,\ y_{o4} = -1.5,\ x_{o5} = 2.0,\ y_{o5} = -1.5,\ x_{o6} = 0.0,\ y_{o6} = 0.0,$$
$$z_{oi} = 0.0 (i = 1, \ldots, 6),$$
$$a_1 = 0.8,\ b_1 = 0.6,\ c_1 = -0.4,\ a_2 = -0.4,\ b_2 = 0.6,\ c_2 = -0.4$$
$$a_3 = -0.8,\ b_3 = 0.0,\ c_3 = -0.4,\ a_4 = -0.4,\ b_4 = -0.6,\ c_4 = -0.4,$$
$$\gamma_1 = \tfrac{3\pi}{4},\ \gamma_2 = \tfrac{5\pi}{4},\ \gamma_3 = \tfrac{3\pi}{2},\ \gamma_4 = \tfrac{7\pi}{4},\ \gamma_5 = \tfrac{9\pi}{4},$$
$$l_{i1} = 4.0,\ l_{i2} = 4.0,\ (i = 1, \ldots, 5)$$

The specified Cartesian poses are represented in Table 2.3.

The results of the optimization are

$$l_6 = 2.278,\ a_6 = 0.285,\ b_6 = 0.876,\ c_6 = -1.854$$

which leads to

$$\boldsymbol{\psi} = [55.219\ 50.131\ 45.031\ 39.961\ 34.930\ 29.934\ 24.957\ 19.980\ 14.982\ 9.937]^T$$

with $K = -1$. The least square sum of the error gives

$$err = \sum_{i=1}^{10}[(\psi_i - \overline{\psi}_i)^2] = 2.554\text{E} - 05 \tag{2.227}$$

The error curve is shown in Figure 2.30.

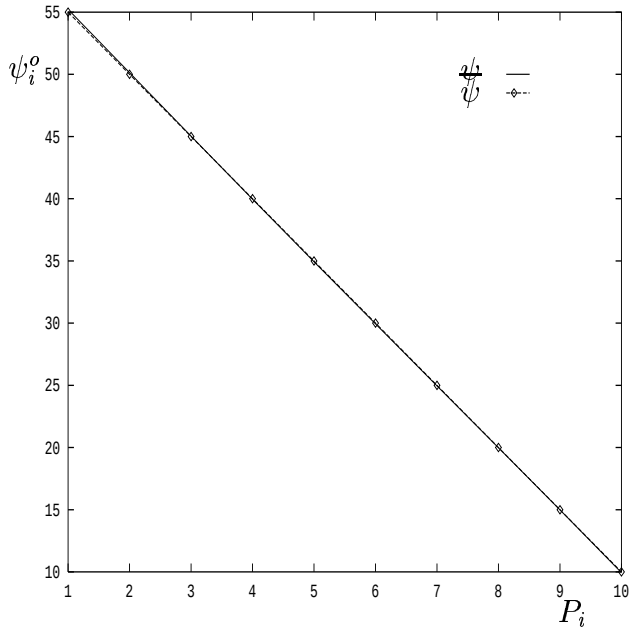

Figure 2.30: Example of optimal synthesis of spatial five-dof manipulator.

Similarly, one can realize from the example that by an optimal choice of the parameters of the special leg, the dependent Cartesian coordinates can be close to the desired values when the five independent Cartesian coordinates pass through the prescribed trajectories.

Moreover, it can be noticed from the examples that the results obtained for the five-degree-of-freedom manipulator are better than those obtained for the four-degree-of-freedom manipulator. This is because the five-degree-of-freedom manipulator has more degrees of freedom and it is therefore easier to adapt to the prescribed poses.

2.4 Conclusion

The kinematic analysis of planar and spatial parallel mechanisms has been addressed in this chapter. The inverse kinematics of these mechanisms has been solved and their workspace has been determined using a simple novel algorithm. This general numerical algorithm can be applied to the determination of the workspace of any type of planar and spatial parallel mechanism.

The velocity equations of the mechanisms have then been derived using two approaches, namely, the algebraic and the vector formulation. The latter approach is a new approach which can lead to simple expressions of the determinants of the Jacobian matrices of the mechanisms. The singularity loci of the mechanisms have been determined by the two approaches, both approaches leading to identical results. The algorithm for the determination of the singularity loci using the latter approach is however, much faster than the former one.

The kinematic optimization of mechanisms with reduced degrees of freedom has also been discussed. The generalized reduced gradient method has been used for the optimization and led to a fast converge. The dependent Cartesian coordinates of the mechanisms can follow desired trajectories as closely as possible when the independent Cartesian coordinates pass through the prescribed points using the optimization procedure presented in this chapter. This property is important for the practical applications of mechanisms with reduced degrees of freedom.

Chapter 3

Dynamic analysis

The dynamic analysis of planar and spatial parallel manipulators is presented in this chapter. A new approach based on the principle of virtual work is first used to derive the generalized input forces of the manipulators. This approach is efficient and suitable for the control of manipulators. Then, the conventional approach used for dynamic analysis of parallel mechanisms or manipulators, namely, the Newton–Euler equations, is also applied to derive the generalized input forces of the manipulators. Since the constraint forces between the links are computed, this approach leads to a slower algorithm compared to the approach based on the principle of virtual work; however, it is useful for the simulation and design of the manipulators. Finally, the corresponding algorithms are compared and numerical examples are given in order to illustrate the results.

3.1 Approach using the principle of virtual work

The approach based on the principle of virtual work consists in expressing the inertial force and moment acting on the links of the manipulator and then considering the manipulator to be in "static" equilibrium. The virtual displacement of each link caused by the virtual displacement of each actuated joint is computed. Finally, the principle of virtual work is applied to obtain the actuator forces or torques.

3.1.1 Planar parallel manipulators with revolute actuators

In chapter 2, the inverse kinematics of the planar two- and three-degree-of-freedom mechanisms is computed and the orientations of the all moving links of the two mechanisms have been determined. Therefore, the determination of the position and orientation of the moving links is not mentioned here for reason of simplicity. The procedure for deriving the generalized forces or torques using this approach, therefore, will consist of the following steps: velocity analysis, acceleration analysis, computation of the inertial forces and moments, determination of the virtual displacements and determination of generalized input forces or torques.

3.1.1.1 Two-degree-of-freedom manipulator

I) Velocity analysis

From the two kinematic chains of the mechanism (see Figure 2.13), one can write

$$\boldsymbol{\omega}_1 \times \mathbf{a}_1 + \boldsymbol{\omega}_3 \times \mathbf{a}_3 = \dot{\mathbf{p}} \tag{3.1}$$

$$\boldsymbol{\omega}_2 \times \mathbf{a}_2 + \boldsymbol{\omega}_4 \times \mathbf{a}_4 = \dot{\mathbf{p}} - \boldsymbol{\omega}_3 \times \mathbf{a}_5 \tag{3.2}$$

where $\boldsymbol{\omega}_i\,(i = 1, \ldots, 4)$ and $\mathbf{a}_i\,(i = 1, \ldots, 5)$ are respectively the vector of the angular velocity and position vector of the ith moving link, vector $\dot{\mathbf{p}}$ is the given Cartesian velocity vector of the end-effector, i.e.,

$$\dot{\mathbf{p}} = \begin{bmatrix} \dot{x} \\ \dot{y} \end{bmatrix} \tag{3.3}$$

Eqs.(3.1) and (3.2) can be rewritten in matrix form as

$$\mathbf{A}_1\boldsymbol{\eta}_1 = \mathbf{b}_1 \tag{3.4}$$

$$\mathbf{A}_2\boldsymbol{\eta}_2 = \mathbf{b}_2 \tag{3.5}$$

where

$$\boldsymbol{\eta}_1 = \begin{bmatrix}\omega_1\\ \omega_3\end{bmatrix}, \quad \mathbf{A}_1 = \begin{bmatrix}-l_1\sin\theta_1 & -l_3\sin\alpha_1\\ l_1\cos\theta_1 & l_3\cos\alpha_1\end{bmatrix}, \quad \mathbf{b}_1 = \dot{\mathbf{p}} = \begin{bmatrix}\dot{x}\\ \dot{y}\end{bmatrix}$$

$$\boldsymbol{\eta}_2 = \begin{bmatrix}\omega_2\\ \omega_4\end{bmatrix}, \quad \mathbf{A}_2 = \begin{bmatrix}-l_2\sin\theta_2 & -l_4\sin\alpha_2\\ l_2\cos\theta_2 & l_4\cos\alpha_2\end{bmatrix}$$

$$\mathbf{b}_2 = \dot{\mathbf{p}} - \boldsymbol{\omega}_3 \times \mathbf{a}_5 = \begin{bmatrix}\dot{x} + \omega_3 l_5\sin\alpha_1\\ \dot{y} - \omega_3 l_5\cos\alpha_1\end{bmatrix}$$

where all quantities in the above equations are as defined in Chapter 2.

The solution of eqs.(3.4) and (3.5) respectively leads to

$$\boldsymbol{\eta}_1 = \mathbf{A}_1^{-1}\mathbf{b}_1 \tag{3.6}$$

$$\boldsymbol{\eta}_2 = \mathbf{A}_2^{-1}\mathbf{b}_2 \tag{3.7}$$

II) Acceleration analysis

Differentiating eqs.(3.1) and (3.2), one then obtains

$$\dot{\boldsymbol{\omega}}_1 \times \mathbf{a}_1 + \dot{\boldsymbol{\omega}}_3 \times \mathbf{a}_3 = \mathbf{e}_1 \tag{3.8}$$

$$\dot{\boldsymbol{\omega}}_2 \times \mathbf{a}_2 + \dot{\boldsymbol{\omega}}_4 \times \mathbf{a}_4 = \mathbf{e}_2 \tag{3.9}$$

where $\ddot{\mathbf{p}}$ is the given acceleration vector of the end-effector, and

$$\begin{aligned}\mathbf{e}_1 &= \ddot{\mathbf{p}} - \boldsymbol{\omega}_1 \times (\boldsymbol{\omega}_1 \times \mathbf{a}_1) - \boldsymbol{\omega}_3 \times (\boldsymbol{\omega}_3 \times \mathbf{a}_3)\\ \mathbf{e}_2 &= \ddot{\mathbf{p}} - \dot{\boldsymbol{\omega}}_3 \times \mathbf{a}_5 - \boldsymbol{\omega}_3 \times (\boldsymbol{\omega}_3 \times \mathbf{a}_5)\\ &\quad -\boldsymbol{\omega}_2 \times (\boldsymbol{\omega}_2 \times \mathbf{a}_2) - \boldsymbol{\omega}_4 \times (\boldsymbol{\omega}_4 \times \mathbf{a}_4)\end{aligned} \tag{3.10}$$

Similarly, eqs.(3.8) and (3.9) can be rewritten as

$$\mathbf{A}_1\dot{\boldsymbol{\eta}}_1 = \mathbf{e}_1 \tag{3.11}$$

$$\mathbf{A}_2\dot{\boldsymbol{\eta}}_2 = \mathbf{e}_2 \tag{3.12}$$

where

$$\dot{\boldsymbol{\eta}}_1 = \begin{bmatrix} \dot{\omega}_1 \\ \dot{\omega}_3 \end{bmatrix}, \quad \dot{\boldsymbol{\eta}}_2 = \begin{bmatrix} \dot{\omega}_2 \\ \dot{\omega}_4 \end{bmatrix} \tag{3.13}$$

From eqs.(3.11) and (3.12), one can obtain

$$\dot{\boldsymbol{\eta}}_1 = \mathbf{A}_1^{-1}\mathbf{e}_1 \tag{3.14}$$

$$\dot{\boldsymbol{\eta}}_2 = \mathbf{A}_2^{-1}\mathbf{e}_2 \tag{3.15}$$

III) Computation of the forces and torques acting on the center of mass of each link

The force acting on the center of mass of each link consists of two parts: the inertial force and the gravity force. The moment acting on each link is the inertial moment.

In order to compute inertial forces, one must first determine the linear acceleration of the center of mass of each link.

One can write

$$\mathbf{a}_i = \dot{\boldsymbol{\omega}}_i \times \mathbf{Q}_i\mathbf{r}_i + \boldsymbol{\omega}_i \times (\boldsymbol{\omega}_i \times \mathbf{Q}_i\mathbf{r}_i), \quad i = 1, 2 \tag{3.16}$$

$$\begin{aligned} \mathbf{a}_j = {} & \dot{\boldsymbol{\omega}}_j \times \mathbf{Q}_j\mathbf{l}_{j-2} + \boldsymbol{\omega}_j \times (\boldsymbol{\omega}_j \times \mathbf{Q}_j\mathbf{l}_{j-2}) \\ & + \dot{\boldsymbol{\omega}}_j \times \mathbf{Q}_j\mathbf{r}_j + \boldsymbol{\omega}_j \times (\boldsymbol{\omega}_j \times \mathbf{Q}_j\mathbf{r}_j), \quad j = 3, 4 \end{aligned} \tag{3.17}$$

where $\mathbf{Q}_i$ and $\mathbf{l}_i$ are respectively the orientation matrix of the ith link and the position vector of the length of the link while $\mathbf{r}_i$ is the position vector from the center of mass of the ith link to the center of the revolute joint connecting the current link to the former link, and

$$\mathbf{Q}_i = \begin{bmatrix} \cos\alpha_i & -\sin\alpha_i \\ \sin\alpha_i & \cos\alpha_i \end{bmatrix}, \quad \mathbf{l}_i = \begin{bmatrix} 0 \\ l_i \end{bmatrix}, \quad \mathbf{r}_i = \begin{bmatrix} 0 \\ r_i \end{bmatrix} \tag{3.18}$$

Then, the force and moment acting on the center of mass of each link can be directly computed as follows

$$\mathbf{f}_i = -m_i\mathbf{a}_i + \mathbf{w}_i, \quad i = 1, \ldots, 4 \tag{3.19}$$

$$\mathbf{m}_i = -\frac{\mathrm{d}}{\mathrm{dt}}(\mathbf{Q}_i\mathbf{I}_i\mathbf{Q}_i^T\boldsymbol{\omega}_i), \quad i = 1, \ldots, 4 \tag{3.20}$$

where $\mathbf{f}_i$ and $\mathbf{m}_i$ denote the inertial force and moment acting on the ith link. Moreover, $\mathbf{I}_i$ and $\mathbf{w}_i$ denote the moment of inertia and gravity vector of the ith link.

VI) Computation of the virtual displacements of the links

The computation of the virtual displacements of the links is the most important step for the determination of the generalized input forces. For this mechanism, one directly uses the velocity equations obtained in Chapter 2. From eq.(2.76) one has

$$\mathbf{w}_O = -\mathbf{A}^{*-1}\mathbf{B}^*\mathbf{w}_I \tag{3.21}$$

where $\mathbf{A}^{*-1}$ is the inverse matrix of matrix $\mathbf{A}^*$.

Now, let $\delta\theta_i$ be the virtual angular displacement of the ith leg corresponding to angles θ_i $(i = 1, 2)$ and $\delta\omega_{j+2}$ be the virtual angular displacement corresponding to angles α_j $(j = 1, 2)$.

From eq.(3.21) one can obtain

$$\delta\mathbf{w}_O^i = -\mathbf{A}^{*-1}\mathbf{B}^*\delta\mathbf{w}_I^i, \quad i = 1, 2 \tag{3.22}$$

where

$$\delta\mathbf{w}_O^i = \begin{bmatrix} \delta\omega_3^i \\ \delta\omega_4^i \end{bmatrix}, \quad \delta\mathbf{w}_I^1 = \begin{bmatrix} 1 \\ 0 \end{bmatrix}, \quad \delta\mathbf{w}_I^2 = \begin{bmatrix} 0 \\ 1 \end{bmatrix} \tag{3.23}$$

Having obtained the virtual angular displacements of each of the links of the manipulator, the virtual linear displacements of the center of mass of each link can be computed as follows

$$\boldsymbol{\delta}_i = \delta\boldsymbol{\omega}_i \times \mathbf{Q}_i\mathbf{r}_i, \quad i = 1, 2 \tag{3.24}$$

$$\boldsymbol{\delta}_j = \delta\boldsymbol{\omega}_j \times \mathbf{Q}_j\mathbf{l}_{j-2} + \delta\boldsymbol{\omega}_j \times \mathbf{Q}_j\mathbf{r}_j, \quad j = 3, 4 \tag{3.25}$$

where $\boldsymbol{\delta}_i (i = 1, 2)$ and $\boldsymbol{\delta}_j (j = 3, 4)$ are respectively the virtual linear displacement of the center of mass of the 1,2nd and 3,4th links.

V) Computation of the actuator force/torque

Finally, the principle of virtual work can be applied to compute the actuating torques

$$\tau_i = \sum_{j=1}^{4} (\mathbf{f}_j\boldsymbol{\delta}_j^i + \mathbf{m}_j\delta\boldsymbol{\omega}_j^i), \; i = 1, 2$$

where τ_i is the actuating force or torque at the ith actuated joint.

3.1.1.2 Three-degree-of-freedom manipulator

I) velocity analysis

From the three kinematic closed loops of the mechanism (see Figure 2.16), one can write

$$\boldsymbol{\omega}_1 \times \mathbf{a}_1 + \boldsymbol{\omega}_4 \times \mathbf{a}_4 = \dot{\mathbf{p}} \tag{3.26}$$

$$\boldsymbol{\omega}_2 \times \mathbf{a}_2 + \boldsymbol{\omega}_5 \times \mathbf{a}_5 = \dot{\mathbf{p}} + \boldsymbol{\omega}_7 \times \mathbf{a}_7 \tag{3.27}$$

$$\boldsymbol{\omega}_3 \times \mathbf{a}_3 + \boldsymbol{\omega}_6 \times \mathbf{a}_6 = \dot{\mathbf{p}} + \boldsymbol{\omega}_7 \times \mathbf{a}_8 \tag{3.28}$$

where $\boldsymbol{\omega}_i$, $i = 1, \ldots, 6$ is the vector of the angular velocity of the ith link while $\dot{\mathbf{p}}$ and $\boldsymbol{\omega}_7$ are respectively the vectors of the linear and angular velocity of the end-effector, i.e.,

$$\dot{\mathbf{p}} = \begin{bmatrix} \dot{x} \\ \dot{y} \end{bmatrix} \tag{3.29}$$

Rewriting eqs.(3.26)–(3.28) in matrix form, one has

$$\mathbf{A}_1 \boldsymbol{\eta}_1 = \mathbf{b}_1 \tag{3.30}$$

$$\mathbf{A}_2 \boldsymbol{\eta}_2 = \mathbf{b}_2 \tag{3.31}$$

$$\mathbf{A}_3 \boldsymbol{\eta}_3 = \mathbf{b}_3 \tag{3.32}$$

where

$$\boldsymbol{\eta}_1 = \begin{bmatrix} \omega_1 \\ \omega_3 \end{bmatrix}, \quad \mathbf{A}_1 = \begin{bmatrix} -l_1 \sin\theta_1 & -l_3 \sin\alpha_1 \\ l_1 \cos\theta_1 & l_3 \cos\alpha_1 \end{bmatrix}, \quad \mathbf{b}_1 = \dot{\mathbf{p}} = \begin{bmatrix} \dot{x} \\ \dot{y} \end{bmatrix}$$

$$\boldsymbol{\eta}_2 = \begin{bmatrix} \omega_2 \\ \omega_5 \end{bmatrix}, \quad \mathbf{A}_2 = \begin{bmatrix} -l_2 \sin\theta_2 & -l_5 \sin\alpha_2 \\ l_2 \cos\theta_2 & l_5 \cos\alpha_2 \end{bmatrix}, \quad \mathbf{b}_2 = \dot{\mathbf{p}} - \boldsymbol{\omega}_7 \times \mathbf{a}_7 = \begin{bmatrix} \dot{x} + \omega_7 l_7 \sin\phi \\ \dot{y} - \omega_7 l_7 \cos\phi \end{bmatrix}$$

$$\boldsymbol{\eta}_3 = \begin{bmatrix} \omega_3 \\ \omega_6 \end{bmatrix}, \quad \mathbf{A}_3 = \begin{bmatrix} -l_3 \sin\theta_3 & -l_6 \sin\alpha_3 \\ l_3 \cos\theta_3 & l_6 \cos\alpha_3 \end{bmatrix}, \quad \mathbf{b}_3 = \dot{\mathbf{p}} - \boldsymbol{\omega}_7 \times \mathbf{a}_8 = \begin{bmatrix} \dot{x} + \omega_7 l_8 \sin\phi \\ \dot{y} - \omega_3 l_8 \cos\phi \end{bmatrix}$$

where all quantities in the above equations are as defined in Chapter 2.

The solution of eqs.(3.30)–(3.32) respectively leads to

$$\boldsymbol{\eta}_1 = \mathbf{A}_1^{-1} \mathbf{b}_1 \tag{3.33}$$

$$\boldsymbol{\eta}_2 = \mathbf{A}_2^{-1} \mathbf{b}_2 \tag{3.34}$$

$$\boldsymbol{\eta}_3 = \mathbf{A}_3^{-1} \mathbf{b}_3 \tag{3.35}$$

II) Acceleration analysis

Differentiating eqs.(3.26) to (3.28), one then obtains

$$\dot{\boldsymbol{\omega}}_1 \times \mathbf{a}_1 + \dot{\boldsymbol{\omega}}_4 \times \mathbf{a}_4 = \mathbf{e}_1 \tag{3.36}$$

$$\dot{\boldsymbol{\omega}}_2 \times \mathbf{a}_2 + \dot{\boldsymbol{\omega}}_5 \times \mathbf{a}_5 = \mathbf{e}_2 \tag{3.37}$$

$$\dot{\boldsymbol{\omega}}_3 \times \mathbf{a}_3 + \dot{\boldsymbol{\omega}}_6 \times \mathbf{a}_6 = \mathbf{e}_3 \tag{3.38}$$

where $\ddot{\mathbf{p}}$ is the given acceleration vector of the end-effector, and

$$\begin{aligned}
\mathbf{e}_1 &= \ddot{\mathbf{p}} - \boldsymbol{\omega}_1 \times (\boldsymbol{\omega}_1 \times \mathbf{a}_1) - \boldsymbol{\omega}_4 \times (\boldsymbol{\omega}_4 \times \mathbf{a}_4) \\
\mathbf{e}_2 &= \ddot{\mathbf{p}} + \dot{\boldsymbol{\omega}}_7 \times \mathbf{a}_7 - \boldsymbol{\omega}_7 \times (\boldsymbol{\omega}_7 \times \mathbf{a}_7) - \boldsymbol{\omega}_2 \times (\boldsymbol{\omega}_2 \times \mathbf{a}_2) - \boldsymbol{\omega}_5 \times (\boldsymbol{\omega}_5 \times \mathbf{a}_5) \\
\mathbf{e}_3 &= \ddot{\mathbf{p}} + \dot{\boldsymbol{\omega}}_7 \times \mathbf{a}_8 - \boldsymbol{\omega}_7 \times (\boldsymbol{\omega}_7 \times \mathbf{a}_8) - \boldsymbol{\omega}_3 \times (\boldsymbol{\omega}_3 \times \mathbf{a}_3) - \boldsymbol{\omega}_6 \times (\boldsymbol{\omega}_6 \times \mathbf{a}_6)
\end{aligned}$$

Eqs.(3.36) to (3.38) can be rewritten as

$$\mathbf{A}_1 \dot{\boldsymbol{\eta}}_1 = \mathbf{e}_1 \tag{3.39}$$

$$\mathbf{A}_2 \dot{\boldsymbol{\eta}}_2 = \mathbf{e}_2 \tag{3.40}$$

$$\mathbf{A}_3 \dot{\boldsymbol{\eta}}_3 = \mathbf{e}_3 \tag{3.41}$$

where

$$\dot{\boldsymbol{\eta}}_1 = \begin{bmatrix} \dot{\omega}_1 \\ \dot{\omega}_4 \end{bmatrix}, \quad \dot{\boldsymbol{\eta}}_2 = \begin{bmatrix} \dot{\omega}_2 \\ \dot{\omega}_5 \end{bmatrix}, \quad \dot{\boldsymbol{\eta}}_3 = \begin{bmatrix} \dot{\omega}_3 \\ \dot{\omega}_6 \end{bmatrix} \tag{3.42}$$

From eqs.(3.39) and (3.41), one can finally obtain

$$\dot{\boldsymbol{\eta}}_1 = \mathbf{A}_1^{-1} \mathbf{e}_1 \tag{3.43}$$

$$\dot{\boldsymbol{\eta}}_2 = \mathbf{A}_2^{-1} \mathbf{e}_2 \tag{3.44}$$

$$\dot{\boldsymbol{\eta}}_3 = \mathbf{A}_3^{-1} \mathbf{e}_3 \tag{3.45}$$

III) Computation of the forces and torques acting on the center of mass of each link

One can write

$$\mathbf{a}_i = \dot{\boldsymbol{\omega}}_i \times \mathbf{Q}_i \mathbf{r}_i + \boldsymbol{\omega}_i \times (\boldsymbol{\omega}_i \times \mathbf{Q}_i \mathbf{r}_i), \quad i = 1, 2, 3 \tag{3.46}$$

$$\begin{aligned}
\mathbf{a}_j &= \dot{\boldsymbol{\omega}}_j \times \mathbf{Q}_i \mathbf{l}_{j-3} + \boldsymbol{\omega}_j \times (\boldsymbol{\omega}_j \times \mathbf{Q}_i \mathbf{l}_{j-3}) \\
&\quad + \dot{\boldsymbol{\omega}}_j \times \mathbf{Q}_j \mathbf{r}_j + \boldsymbol{\omega}_j \times (\boldsymbol{\omega}_j \times \mathbf{Q}_j \mathbf{r}_j), \quad j = 4, 5, 6
\end{aligned} \tag{3.47}$$

$$\mathbf{a}_7 = \ddot{\mathbf{p}} + \dot{\boldsymbol{\omega}}_7 \times \mathbf{Q}\mathbf{r}_7 + \boldsymbol{\omega}_7 \times (\boldsymbol{\omega}_7 \times \mathbf{Q}\mathbf{r}_7) \tag{3.48}$$

where $\mathbf{Q}$ is the orientation matrix of the 7th link, $\mathbf{Q}_i$ and $\mathbf{l}_i$ are respectively the orientation matrix of the ith link and the position vector of the length of the link while $\mathbf{r}_i$ is the position vector from the center of mass of ith link to the center of the revolute joint connecting the current link to the former link, and

$$\begin{aligned}
\mathbf{Q} &= \begin{bmatrix} \cos\phi & -\sin\phi \\ \sin\phi & \cos\phi \end{bmatrix}, \quad \mathbf{Q}_i = \begin{bmatrix} \cos\theta_i & -\sin\theta_i \\ \sin\theta_i & \cos\theta_i \end{bmatrix}, \quad i = 1,2,3 \\
\mathbf{Q}_i &= \begin{bmatrix} \cos\alpha_i & -\sin\alpha_i \\ \sin\alpha_i & \cos\alpha_i \end{bmatrix}, \quad i = 4,5,6 \quad \mathbf{l}_i = \begin{bmatrix} 0 \\ l_i \end{bmatrix}, \quad i = 1,\ldots,7 \\
\mathbf{r}_i &= \begin{bmatrix} 0 \\ r_i \end{bmatrix}, \quad i = 1,\ldots,7
\end{aligned}$$

The force and moment acting on the center of mass of each link can be directly computed as follows

$$\mathbf{f}_i = -m_i\mathbf{a}_i + \mathbf{w}_i, \quad i = 1,\ldots,7 \tag{3.49}$$

$$\mathbf{m}_i = -\frac{\mathrm{d}}{\mathrm{dt}}(\mathbf{Q}_i\mathbf{I}_i\mathbf{Q}_i^T\boldsymbol{\omega}_i), \quad i = 1,\ldots,7 \tag{3.50}$$

where $\mathbf{f}_i$ and $\mathbf{m}_i$ denote the inertial force and moment acting on the ith link and $\mathbf{I}_i$ is the inertial matrix of the link.

VI) Computation of the virtual displacements of the links

For this mechanism, one directly uses the velocity equations obtained in Chapter 2. Form eq.(2.81) one has

$$\mathbf{w}_O = -\mathbf{A}^{*-1}\mathbf{B}^*\mathbf{w}_I \tag{3.51}$$

where $\mathbf{A}^{*-1}$ is the inverse matrix of matrix $\mathbf{A}^*$.

Similarly to the previous case, let $\delta\theta_i$ be the virtual angular displacement of the ith leg corresponding to angles θ_i $(i = 1,2,3)$ and $\delta\omega_{j+3}$ be the virtual angular displacements of the jth leg corresponding to angles α_j $(j = 1,2,3)$, $\delta\omega_7$ be the virtual angular displacement of the end-effector and δx and δy be the virtual linear displacements of the end-effector along axes x and y.

From eq.(3.51) one can obtain

$$\delta\mathbf{w}_O^i = -\mathbf{A}^{*-1}\mathbf{B}^*\delta\mathbf{w}_I^i, \quad i = 1,\ldots,3 \tag{3.52}$$

where

$$\begin{aligned}\delta\mathbf{w}_O^i &= [\,\delta\omega_4^i \quad \delta\omega_5^i \quad \delta\omega_6^i \quad \delta\omega_7^i\,]^T \\ \delta\mathbf{w}_I^1 &= \begin{bmatrix}1\\0\\0\end{bmatrix}, \quad \delta\mathbf{w}_I^2 = \begin{bmatrix}0\\1\\0\end{bmatrix}, \quad \delta\mathbf{w}_I^3 = \begin{bmatrix}0\\0\\1\end{bmatrix}\end{aligned}$$

Having obtained the virtual angular displacements of each of the links of the manipulator, the virtual linear displacements of the center of mass of each link can be computed as follows

$$\boldsymbol{\delta}_i = \delta\boldsymbol{\omega}_i \times \mathbf{Q}_i\mathbf{r}_i, \quad i = 1,2,3 \tag{3.53}$$

$$\begin{aligned}\boldsymbol{\delta}_j &= \delta\boldsymbol{\omega}_j \times \mathbf{Q}_j\mathbf{l}_{j-3} \\ &\quad +\delta\boldsymbol{\omega}_j \times \mathbf{Q}_j\mathbf{r}_j, \quad j = 4,5,6\end{aligned} \tag{3.54}$$

$$\boldsymbol{\delta}_7 = \delta\mathbf{p} + \delta\boldsymbol{\omega}_7 \times \mathbf{Q}\mathbf{r}_7 \tag{3.55}$$

where $\boldsymbol{\delta}_i (i = 1,2,3)$ and $\boldsymbol{\delta}_j (j = 4,5,6)$ are respectively the virtual linear displacement of the center of mass of the 1,2,3rd and 4,5,6th link, $\boldsymbol{\delta}_7$ is the virtual linear displacement of the center of mass of the 7th link, $\delta\mathbf{p}$ is the vector of virtual displacement of the end-effector, i.e.,

$$\delta\mathbf{p} = \begin{bmatrix}\delta x\\ \delta y\end{bmatrix} \tag{3.56}$$

VI) Computation of the actuator force/torque

Finally, by application of the principle of virtual work one can obtain the actuating torques

$$\tau_i = \sum_{j=1}^{7}(\mathbf{f}_j\boldsymbol{\delta}_j^i + \mathbf{m}_j\delta\boldsymbol{\omega}_j^i),\ i = 1,2,3$$

where τ_i is the actuating force or torque at the ith actuated joint.

3.1.2 Spatial parallel manipulators with revolute actuators

In this subsection, the computation of the kinematics, velocity and acceleration analyses are first performed. Then, the principle of virtual work is applied to derive the generalized forces of three types of spatial parallel manipulators. For the spatial four-

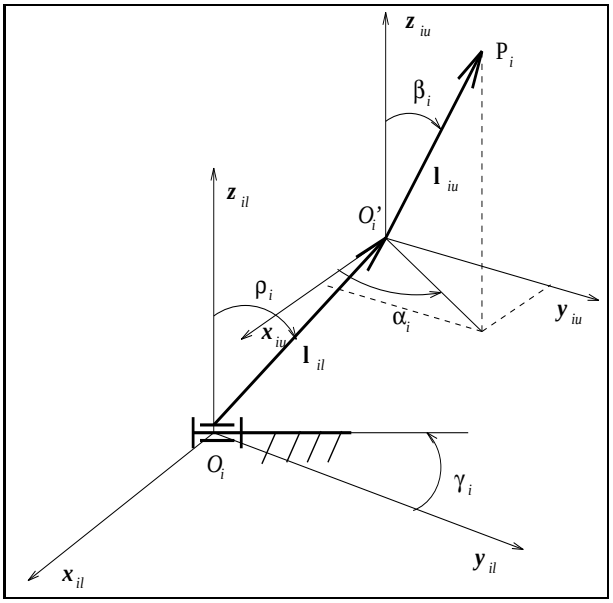

Figure 3.1: Vectors $\mathbf{l}_{iu}$ and $\mathbf{l}_{il}$ represented in spherical coordinates.

and five-degree-of-freedom parallel manipulators, the algorithms for the computation of the dependent Cartesian coordinates from the independent Cartesian coordinates presented in Chapter 2 will be used directly and are therefore not repeated here.

3.1.2.1 Four-degree-of-freedom manipulator

I) Inverse kinematics

For the four-dof mechanism, once angles θ and ψ have been determined, the six Cartesian coordinates of the platform are available and one can directly compute the position of point P_i.

One can write

$$\mathbf{p}_i = \mathbf{Q}_{iu}\mathbf{l}_{iu} + \mathbf{Q}_{il}\mathbf{l}_{il} + \mathbf{p}_{io}, \quad i = 1, \ldots, 4 \tag{3.57}$$

where $\mathbf{Q}_{iu}$ and $\mathbf{Q}_{il}$ are respectively the rotation matrices describing the orientation of the upper and lower links of the ith leg with respect to the base coordinate frame. Moreover, $\mathbf{l}_{iu}$ and $\mathbf{l}_{il}$ are the vectors from O_i' to P_i and from O_i to O_i' expressed in their

local frames, respectively, as represented in Figure 3.1. One has,

$$\begin{aligned}
\mathbf{Q}_{iu} &= \begin{bmatrix} \cos\alpha_i\cos\beta_i & -\sin\alpha_i & \cos\alpha_i\sin\beta_i \\ \sin\alpha_i\cos\beta_i & \cos\alpha_i & \sin\alpha_i\sin\beta_i \\ -\sin\beta_i & 0 & \cos\beta_i \end{bmatrix}, \quad i = 1,\ldots,4 \\
\mathbf{Q}_{il} &= \begin{bmatrix} \cos\gamma_i\cos\rho_i & -\sin\gamma_i & \cos\gamma_i\sin\rho_i \\ \sin\gamma_i\cos\rho_i & \cos\gamma_i & \sin\gamma_i\sin\rho_i \\ -\sin\rho_i & 0 & \cos\rho_i \end{bmatrix}, \quad i = 1,\ldots,4 \\
\mathbf{p}_i &= \begin{bmatrix} x_i \\ y_i \\ z_i \end{bmatrix}, \quad \mathbf{l}_{iu} = \begin{bmatrix} 0 \\ 0 \\ l_{i2} \end{bmatrix}, \quad \mathbf{l}_{il} = \begin{bmatrix} 0 \\ 0 \\ l_{i1} \end{bmatrix}, \quad \mathbf{p}_{io} = \begin{bmatrix} x_{io} \\ y_{io} \\ z_{io} \end{bmatrix}, \quad i = 1,\ldots,4
\end{aligned}$$

where angles α_i, β_i, γ_i and ρ_i are as defined in Figure 3.1. Equation (3.57) consists of three scalar equations with three unknowns ρ_i, α_i and β_i, and can be rewritten as

$$l_{i2}\cos\alpha_i\sin\beta_i = x_i - l_{i1}\cos\gamma_i\sin\rho_i - x_{io} \tag{3.58}$$

$$l_{i2}\sin\alpha_i\sin\beta_i = y_i - l_{i1}\sin\gamma_i\sin\rho_i - y_{io} \tag{3.59}$$

$$l_{i2}\cos\beta_i = z_i - l_{i1}\cos\rho_i - z_{io} \tag{3.60}$$

From eqs.(3.58)–(3.60), one can obtain

$$R_i\cos\rho_i + S_i\sin\rho_i = T_i, \quad i = 1,\ldots,4 \tag{3.61}$$

where

$$\begin{aligned}
R_i &= z_i - z_{io} \\
S_i &= (y_i - y_{io})\sin\gamma_i + (x_i - x_{io})\cos\gamma_i \\
T_i &= \frac{(x_i - x_{io})^2 + (y_i - y_{io})^2 + (z_i - z_{io})^2 + l_{i1}^2 - l_{i2}^2}{2l_{i1}} \\
V_i &= R_i^2 + S_i^2 - T_i^2 \\
i &= 1,\ldots,4
\end{aligned}$$

which leads directly to

$$\sin\rho_i = \frac{S_iT_i + K_{i3}R_i\sqrt{V_i}}{R_i^2 + S_i^2}, \quad i = 1,\ldots,4 \tag{3.62}$$

$$\cos\rho_i = \frac{R_iT_i - K_{i3}S_i\sqrt{V_i}}{R_i^2 + S_i^2}, \quad i = 1,\ldots,4 \tag{3.63}$$

with $K_{i3} = \pm 1$ the branch index of the manipulator associated with the configuration of the ith leg. Finally, one has

$$\cos\beta_i = (z_i - l_{i1}\cos\rho_i - z_{io})/l_{i2} \tag{3.64}$$

$$\sin\beta_i = \sqrt{1-\cos^2\beta_i}, \quad (0 \le \beta_i \le \pi) \tag{3.65}$$

$$\cos\alpha_i = (x_i - l_{i1}\cos\gamma_i\sin\rho_i - x_{io})/(l_{i2}\sin\beta_i) \tag{3.66}$$

$$\sin\alpha_i = (y_i - l_{i1}\sin\gamma_i\sin\rho_i - y_{io})/(l_{i2}\sin\beta_i) \tag{3.67}$$

and the three variables ρ_i, α_i and β_i allow one to completely determine the position and orientation of the two links in the ith leg.

II) Velocity analysis

The linear and angular velocities of all moving links will be computed from the given independent Cartesian velocities of the platform $\dot{x}, \dot{y}, \dot{z}$ and ω_x, where the angular velocity of the platform is defined as $\boldsymbol{\omega} = [\omega_x, \omega_y, \omega_z]^T$.

First, the two dependent components of the angular velocity, ω_y and ω_z, need to be determined using a special kinematic chain.

One can write the linear velocity of point P_5 as

$$\dot{\mathbf{p}}_5 = \dot{\mathbf{p}} + \boldsymbol{\omega} \times \mathbf{Q}\mathbf{p}_5^{'} \tag{3.68}$$

where

$$\dot{\mathbf{p}}_5 = \begin{bmatrix} l_5\dot{\alpha}\cos\alpha \\ 0 \\ -l_5\dot{\alpha}\sin\alpha \end{bmatrix}, \quad \dot{\mathbf{p}} = \begin{bmatrix} \dot{x} \\ \dot{y} \\ \dot{z} \end{bmatrix}, \quad \boldsymbol{\omega} = \begin{bmatrix} \omega_x \\ \omega_y \\ \omega_z \end{bmatrix}, \quad \mathbf{p}_5^{'} = \begin{bmatrix} a_5 \\ b_5 \\ c_5 \end{bmatrix} \tag{3.69}$$

Equation (3.68) can be rewritten in matrix form as

$$\mathbf{A}\boldsymbol{\eta} = \mathbf{b} \tag{3.70}$$

where

$$\mathbf{A} = \begin{bmatrix} l_5\cos\alpha & c_5^{'} & -b_5^{'} \\ 0 & 0 & a_5^{'} \\ -l_5\sin\alpha & -c_5^{'} & 0 \end{bmatrix}, \quad \boldsymbol{\eta} = \begin{bmatrix} \dot{\alpha} \\ \omega_y \\ \omega_z \end{bmatrix}, \quad \mathbf{b} = \begin{bmatrix} \dot{x} \\ \dot{y} + c_5^{'}\omega_x \\ \dot{z} - b_5^{'}\omega_x \end{bmatrix} \tag{3.71}$$

and $[a_5^{'}, b_5^{'}, c_5^{'}]^T = \mathbf{Q}\mathbf{p}_5^{'}$ and eq.(3.70) is easily solved for vector $\boldsymbol{\eta}$.

Having obtained the six Cartesian velocity components $\dot{x}, \dot{y}, \dot{z}, \omega_x, \omega_y$ and ω_z, the linear velocity of the center of joint P_i connecting each leg to the platform can be computed as follows

$$\dot{\mathbf{p}}_i = \dot{\mathbf{p}} + \boldsymbol{\omega} \times \mathbf{Q}\mathbf{p}_i^{'}, \quad i = 1, \ldots, 4 \tag{3.72}$$

Moreover, $\dot{\mathbf{p}}_i$ can be expressed using the angular velocities of the ith leg, i.e.,

$$\dot{\mathbf{p}}_i = \boldsymbol{\omega}_{iu} \times \mathbf{Q}_{iu}\mathbf{l}_{iu} + \boldsymbol{\omega}_{il} \times \mathbf{Q}_{il}\mathbf{l}_{il}, \quad i = 1, \ldots, 4 \tag{3.73}$$

where $\boldsymbol{\omega}_{iu}$ and $\boldsymbol{\omega}_{il}$ are the angular velocities of upper and lower links of the ith leg, i.e.,

$$\dot{\mathbf{p}}_i = \begin{bmatrix} \dot{x}_i \\ \dot{y}_i \\ \dot{z}_i \end{bmatrix}, \quad \boldsymbol{\omega}_{iu} = \begin{bmatrix} -\dot{\beta}_i \sin\alpha_i \\ \dot{\beta}_i \cos\alpha_i \\ \dot{\alpha}_i \end{bmatrix}, \quad \boldsymbol{\omega}_{il} = \begin{bmatrix} -\dot{\rho}_i \sin\gamma_i \\ \dot{\rho}_i \cos\gamma_i \\ 0 \end{bmatrix} \tag{3.74}$$

Equation (3.73) can be rewritten in matrix form as

$$\mathbf{C}_{ir}\boldsymbol{\lambda}_{ir} = \dot{\mathbf{p}}_i, \quad i = 1, \ldots, 4 \tag{3.75}$$

where

$$\begin{aligned} \mathbf{C}_{ir} &= \begin{bmatrix} l_{i1}\cos\gamma_i\cos\rho_i & -l_{i2}\sin\alpha_i\sin\beta_i & l_{i2}\cos\alpha_i\cos\beta_i \\ -l_{i1}\sin\gamma_i\cos\rho_i & -l_{i2}\cos\alpha_i\sin\beta_i & -l_{i2}\sin\alpha_i\cos\beta_i \\ -l_{i1}\sin\rho_i & 0 & -l_{i2}\sin\beta_i \end{bmatrix} \\ \boldsymbol{\lambda}_{ir} &= [\,\dot{\rho}_i \quad \dot{\alpha}_i \quad \dot{\beta}_i\,]^T \end{aligned} \tag{3.76}$$

Solving eq.(3.75), one readily obtains $\dot{\rho}_i$, $\dot{\alpha}_i$ and $\dot{\beta}_i$. Once these three quantities are known, the velocities of the links are easily determined.

III) Acceleration analysis

The linear and angular accelerations of each of the moving bodies will now be determined from the given Cartesian accelerations of the platform, i.e., $\ddot{x}, \ddot{y}, \ddot{z}$ and $\dot{\omega}_x$.

First, the two dependent acceleration components $\dot{\omega}_y$ and $\dot{\omega}_z$ must be determined.This can be achieved by using the kinematic geometry of the fifth leg.

Differentiating eq.(3.68) with respect to time, one obtains the expression of the linear acceleration of point P_5 as follows:

$$\ddot{\mathbf{p}}_5 = \ddot{\mathbf{p}} + \dot{\boldsymbol{\omega}} \times \mathbf{Q}\mathbf{p}_5^{'} + \boldsymbol{\omega} \times (\boldsymbol{\omega} \times \mathbf{Q}\mathbf{p}_5^{'}) \tag{3.77}$$

where

$$\ddot{\mathbf{p}}_5 = \begin{bmatrix} l_5\ddot{\alpha}\cos\alpha - l_5\dot{\alpha}^2\sin\alpha \\ 0 \\ -l_5\ddot{\alpha}\sin\alpha - l_5\dot{\alpha}^2\cos\alpha \end{bmatrix}, \quad \ddot{\mathbf{p}} = \begin{bmatrix} \ddot{x} \\ \ddot{y} \\ \ddot{z} \end{bmatrix}, \quad \dot{\boldsymbol{\omega}} = \begin{bmatrix} \dot{\omega}_x \\ \dot{\omega}_y \\ \dot{\omega}_z \end{bmatrix} \tag{3.78}$$

Since the velocity analysis has already been performed, eq.(3.77) consists of three scalar equations which contain only three unknowns: $\ddot{\alpha}, \dot{\omega}_y$ and $\dot{\omega}_z$. Therefore, it is easy to solve for these unknowns.

Equation (3.77) is rewritten in matrix form as

$$\mathbf{A}\dot{\boldsymbol{\eta}} = \mathbf{e} \tag{3.79}$$

where

$$\dot{\boldsymbol{\eta}} = \begin{bmatrix} \ddot{\alpha} \\ \dot{\omega}_y \\ \dot{\omega}_z \end{bmatrix}, \quad \mathbf{e} = \begin{bmatrix} \ddot{x} + l_5\sin\alpha\dot{\alpha}^2 + a_x \\ \ddot{y} + c_5'\dot{\omega}_x + a_y \\ \ddot{z} + l_5\cos\alpha\dot{\alpha}^2 + a_z \end{bmatrix} \tag{3.80}$$

where matrix $\mathbf{A}$ has been previously defined and where $[a_x\, a_y\, a_z]^T = \boldsymbol{\omega} \times (\boldsymbol{\omega} \times \mathbf{QP}_5')$.

Equation (3.79) is readily solved for $\dot{\boldsymbol{\eta}}$, which leads to the desired acceleration components. All the Cartesian accelerations of the platform are then known, and the linear and angular accelerations of each of the leg bodies can then be determined.

The linear and angular accelerations of the two links of each of the legs can be obtained from the linear accelerations of points P_i which have been computed from the six Cartesian acceleration components.

Differentiating eq.(3.73) with respect to time, one obtains

$$\begin{aligned} \ddot{\mathbf{p}}_i &= \dot{\boldsymbol{\omega}}_{iu} \times \mathbf{Q}_{iu}\mathbf{l}_{iu} + \boldsymbol{\omega}_{iu} \times (\boldsymbol{\omega}_{iu} \times \mathbf{Q}_{iu}\mathbf{l}_{iu}) \\ &\quad + \dot{\boldsymbol{\omega}}_{il} \times \mathbf{Q}_{il}\mathbf{l}_{il} + \boldsymbol{\omega}_{il} \times (\boldsymbol{\omega}_{il} \times \mathbf{Q}_{il}\mathbf{l}_{il}), \quad i = 1, \ldots, 4 \end{aligned} \tag{3.81}$$

where

$$\ddot{\mathbf{p}}_i = \begin{bmatrix} \ddot{x}_i \\ \ddot{y}_i \\ \ddot{z}_i \end{bmatrix}, \quad \dot{\boldsymbol{\omega}}_{iu} = \begin{bmatrix} -\ddot{\beta}_i\sin\alpha_i - \dot{\alpha}_i\dot{\beta}_i\cos\alpha_i \\ \ddot{\beta}_i\cos\alpha_i - \dot{\alpha}_i\dot{\beta}_i\sin\alpha_i \\ \ddot{\alpha}_i \end{bmatrix}, \quad \dot{\boldsymbol{\omega}}_{il} = \begin{bmatrix} -\ddot{\rho}_i\sin\gamma_i \\ \ddot{\rho}_i\cos\gamma_i \\ 0 \end{bmatrix} \tag{3.82}$$

Equation (3.81) can then be rewritten in matrix form as

$$\mathbf{C}_{ir}\dot{\boldsymbol{\lambda}}_{ir} = \mathbf{s}_i, \quad i = 1, \ldots, 4 \tag{3.83}$$

where $\mathbf{C}_{ir}$ is given in eq.(3.76) and where

$$\ddot{\boldsymbol{\lambda}}_{ir} = [\, \ddot{\rho}_i \quad \ddot{\alpha}_i \quad \ddot{\beta}_i \,]^T \tag{3.84}$$

$$\mathbf{s}_i = [\, s_x \quad s_y \quad s_z \,]^T \tag{3.85}$$

where

$$\begin{aligned}
s_x &= l_2(-(\dot{\alpha}_i\dot{\beta}_i \cos\beta_i \sin\alpha_i) + \cos\alpha_i(-\dot{\alpha}_i^2 - \dot{\beta}_i^2 \cos\alpha_i^2)\sin\beta_i \\
&\quad -\dot{\beta}_i^2 \cos\alpha_i \sin\alpha_i^2 \sin\beta_i) - \dot{\rho}_i^2 l_1 \cos\gamma_i \sin\rho_i \\
s_y &= l_2(\dot{\alpha}_i\dot{\beta}_i \cos\alpha_i \cos\beta_i - \dot{\beta}_i^2 \cos\alpha_i^2 \sin\alpha_i \sin\beta_i \\
&\quad + \sin\alpha_i(-\dot{\alpha}_i^2 - \dot{\beta}_i^2 \sin\alpha_i^2)\sin\beta_i) - \dot{\rho}_i^2 l_1 \sin\gamma_i \sin\rho_i \\
s_z &= -(\dot{\beta}_i^2 l_2 \cos\beta_i) - \dot{\rho}_i^2 l_1 \cos\rho_i
\end{aligned}$$

The solution of eq.(3.83) for $\ddot{\boldsymbol{\lambda}}_{ir}$ will then allow the determination of the linear and angular accelerations of the moving bodies of each of the legs.

VI) Computation of the inertial forces and torques acting on the center of mass of each link

In order to compute inertial forces, one must first determine the linear acceleration of the center of mass of each link.

One can write

$$\mathbf{a}_{iu} = \ddot{\mathbf{p}}_i + \dot{\boldsymbol{\omega}}_{iu} \times \mathbf{Q}_{iu}\mathbf{r}_{iu} + \boldsymbol{\omega}_{iu} \times (\boldsymbol{\omega}_{iu} \times \mathbf{Q}_{iu}\mathbf{r}_{iu}), \quad i = 1, \ldots, 4 \tag{3.86}$$

$$\mathbf{a}_{il} = \dot{\boldsymbol{\omega}}_{il} \times \mathbf{Q}_{il}\mathbf{r}_{il} + \boldsymbol{\omega}_{il} \times (\boldsymbol{\omega}_{il} \times \mathbf{Q}_{il}\mathbf{r}_{il}), \quad i = 1, \ldots, 4 \tag{3.87}$$

where $\mathbf{a}_{iu}$ and $\mathbf{a}_{il}$ are the linear accelerations of the center of mass of the upper and lower links of the ith leg, vectors $\mathbf{r}_{iu}$ and $\mathbf{r}_{il}$ are the position vectors of the center of mass of the upper and lower link of the ith leg and are expressed in the leg's reference frame, while $\mathbf{w}_{iu}$ and $\mathbf{w}_{il}$ are the weight vectors, and

$$\mathbf{r}_{iu} = \begin{bmatrix} 0 \\ 0 \\ r_{iu} \end{bmatrix}, \quad \mathbf{r}_{il} = \begin{bmatrix} 0 \\ 0 \\ r_{il} \end{bmatrix}, \quad \mathbf{w}_{iu} = \begin{bmatrix} 0 \\ 0 \\ -m_{iu}g \end{bmatrix}, \quad \mathbf{w}_{il} = \begin{bmatrix} 0 \\ 0 \\ -m_{il}g \end{bmatrix} \tag{3.88}$$

where g is the gravitational acceleration.

The linear acceleration of the center of mass of the 5th leg and the platform can be computed as follows

$$\mathbf{a}_5 = \dot{\boldsymbol{\omega}}_5 \times \mathbf{Q}_5\mathbf{r}_5 + \boldsymbol{\omega}_5 \times (\boldsymbol{\omega}_5 \times \mathbf{Q}_5\mathbf{r}_5) \tag{3.89}$$

$$\mathbf{a}_p = \ddot{\mathbf{p}} + \dot{\boldsymbol{\omega}} \times \mathbf{Q}\mathbf{r}_p + \boldsymbol{\omega} \times (\boldsymbol{\omega} \times \mathbf{Q}\mathbf{r}_p) \tag{3.90}$$

where $\mathbf{a}_5$ is the linear acceleration of the center of mass of the 5th leg, $\mathbf{Q}_5$ is the orientation matrix of coordinate frame $O - x_5y_5z_5$ with respect to the fixed coordinate frame $O - xyz$, $\boldsymbol{\omega}_5$ is the angular velocity of the 5th leg, $\dot{\boldsymbol{\omega}}_5$ is its angular acceleration, $\mathbf{r}_5$ is the vector connecting point O to the center of mass of the 5th leg noted C_5, i.e.,

$$\mathbf{Q}_5 = \begin{bmatrix} \cos\alpha & 0 & \sin\alpha \\ 0 & 1 & 0 \\ -\sin\alpha & 0 & \cos\alpha \end{bmatrix}, \quad \boldsymbol{\omega}_5 = \begin{bmatrix} 0 \\ \dot{\alpha} \\ 0 \end{bmatrix}, \quad \dot{\boldsymbol{\omega}}_5 = \begin{bmatrix} 0 \\ \ddot{\alpha} \\ 0 \end{bmatrix}, \quad \mathbf{r}_5 = \begin{bmatrix} 0 \\ 0 \\ r_5 \end{bmatrix} \tag{3.91}$$

and $\mathbf{a}_p$ is the linear acceleration of the platform, and where $\mathbf{r}_p$ is the vector connecting point $O^{'}$ to the center of mass of the platform, namely, $\mathbf{r}_p = [\, x_p \quad y_p \quad z_p \,]^T$.

Then, the force and moment acting on the center of mass of each link can be directly computed as follows

$$\mathbf{f}_{iu} = -m_{iu}\mathbf{a}_{iu} + \mathbf{w}_{iu}, \quad i = 1, \ldots, 4 \tag{3.92}$$

$$\mathbf{f}_{il} = -m_{il}\mathbf{a}_{il} + \mathbf{w}_{il}, \quad i = 1, \ldots, 4 \tag{3.93}$$

$$\mathbf{m}_{iu} = -\frac{\mathrm{d}}{\mathrm{dt}}(\mathbf{Q}_{iu}\mathbf{I}_{iu}\mathbf{Q}_{iu}^T\boldsymbol{\omega}_{iu}), \quad i = 1, \ldots, 4 \tag{3.94}$$

$$\mathbf{m}_{il} = -\frac{\mathrm{d}}{\mathrm{dt}}(\mathbf{Q}_{il}\mathbf{I}_{il}\mathbf{Q}_{il}^T\boldsymbol{\omega}_{il}), \quad i = 1, \ldots, 4 \tag{3.95}$$

where $\mathbf{f}_{iu}, \mathbf{m}_{iu}, \mathbf{f}_{il}$ and $\mathbf{m}_{il}$ denote the force acting on the upper link, the moment acting on the upper link, the force acting on the lower link and the moment acting on the lower link of the ith leg, $\mathbf{I}_{iu}$ and $\mathbf{I}_{iu}$ are respectively the inertia tensor of the upper and lower links with respect to their center of mass.

Finally, one has

$$\mathbf{f}_5 = -m_5\mathbf{a}_5 + \mathbf{w}_5 \tag{3.96}$$

$$\mathbf{f}_p = -m_p\mathbf{a}_p + \mathbf{w}_p \tag{3.97}$$

$$\mathbf{m}_5 = -\frac{\mathrm{d}}{\mathrm{dt}}(\mathbf{Q}_5\mathbf{I}_5\mathbf{Q}_5^T\boldsymbol{\omega}_5) \tag{3.98}$$

$$\mathbf{m}_p = -\frac{\mathrm{d}}{\mathrm{dt}}(\mathbf{Q}\mathbf{I}_p\mathbf{Q}^T\boldsymbol{\omega}_p) \tag{3.99}$$

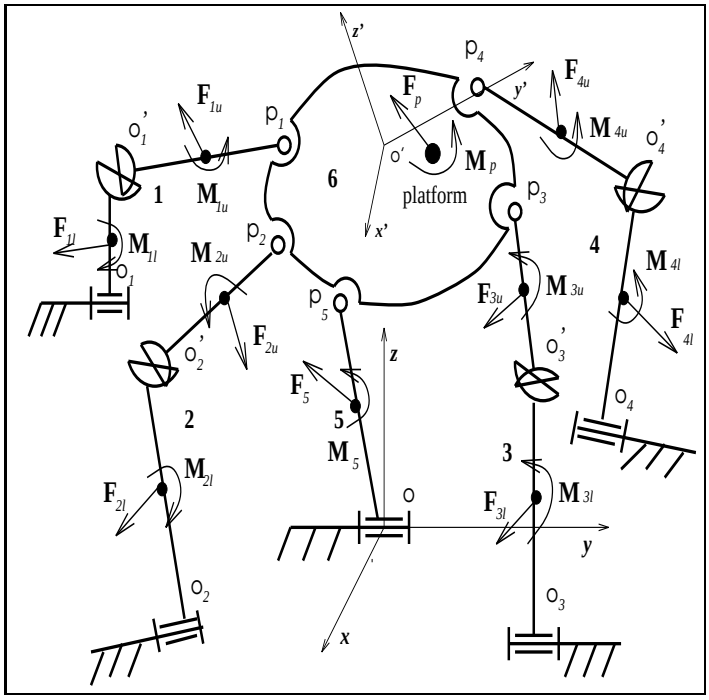

Figure 3.2: Body forces acting on the links of the manipulator with revolute actuators.

where $\mathbf{f}_5$ and $\mathbf{m}_5$ denote the force and moment acting on 5th leg while $\mathbf{f}_p$ and $\mathbf{m}_p$ denote the force and moment acting on the platform, $\mathbf{I}_5$ and $\mathbf{I}_p$ are the inertia tensor of the 5th leg and the platform with respect to their center of mass.

The forces and moments acting on the center of mass of each link of this type of manipulator are represented schematically in Figure 3.2.

V) Computation of the virtual displacements of the links

The virtual linear displacements of the center of mass and the virtual angular displacements of each link will be obtained from the given joint virtual displacements of the manipulator. This is the most important step for the determination of the generalized input forces by this approach.

From the kinematic geometry of the 5th leg, one can write

$$x_5^2 + z_5^2 = l_5^2 \tag{3.100}$$

$$y_5 = 0 \tag{3.101}$$

Differentiating eqs.(3.100) and (3.101), one obtains

$$x_5\dot{x}_5 + z_5\dot{z}_5 = 0 \tag{3.102}$$

$$\dot{y}_5 \;=\; 0 \tag{3.103}$$

Letting $\dot{\mathbf{p}}_5 = [\,\dot{x}_5 \quad \dot{y}_5 \quad \dot{z}_5\,]^T$ and substituting eq.(3.68) into eqs.(3.102) and (3.103), one obtains

$$\dot{\mathbf{t}} = \mathbf{J}_r\dot{\mathbf{x}}, \quad \text{or} \quad \delta\mathbf{t} = \mathbf{J}_r\delta\mathbf{x} \tag{3.104}$$

where $\delta\mathbf{t} = [\,\delta x \quad \delta y \quad \delta z \quad \delta\omega_x \quad \delta\omega_y \quad \delta\omega_z\,]^T$, and

$$\delta\mathbf{x} = \begin{bmatrix} \delta x \\ \delta y \\ \delta z \\ \delta\omega_x \end{bmatrix}, \quad \mathbf{J}_r = \begin{bmatrix} 1 & 0 & 0 & 0 \\ 0 & 1 & 0 & 0 \\ 0 & 0 & 1 & 0 \\ 0 & 0 & 0 & 1 \\ \frac{-x_5}{c_5'x_5 - a_5'z_5} & \frac{-b_5'x_5}{c_5'x_5 - a_5'z_5} & \frac{-z_5}{c_5'x_5 - a_5'z_5} & \frac{b_5'c_5'x_5 + b_5'z_5}{c_5'x_5 - a_5'z_5} \\ 0 & -1 & 0 & c_5' \end{bmatrix} \tag{3.105}$$

Differentiating eq.(3.61), one obtains

$$\begin{aligned} l_{i1}(S_i\cos\rho_i - R_i\sin\rho_i)\delta\rho_i \;=\; & (x_i - x_{io} - l_{i1}\sin\gamma_i\cos\rho_i)\delta x_i \\ & +(y_i - y_{io} + l_{i1}\cos\gamma_i\sin\rho_i)\delta y_i \\ & +(z_i - z_{io} + l_{i1}\sin\rho_i)\delta z_i, \quad i = 1,\ldots,4 \end{aligned} \tag{3.106}$$

Substituting eq.(3.72) into eq.(3.106), one obtains

$$\mathbf{B}_r\delta\boldsymbol{\rho} = \mathbf{K}_r\delta\mathbf{t} \tag{3.107}$$

where $\delta\boldsymbol{\rho} = [\,\delta\rho_1 \quad \delta\rho_2 \quad \delta\rho_3 \quad \delta\rho_4\,]^T$, and

$$\mathbf{B}_r \;=\; \text{diag}\,[\,b_1 \quad b_2 \quad b_3 \quad b_4\,]$$

$$\mathbf{K}_r \;=\; \begin{bmatrix} l_{12x} & l_{12y} & l_{12z} & (b_1'l_{12z} - c_1'l_{12y}) & (c_1'l_{12x} - a_1'l_{12z}) & (a_1'l_{12y} - b_1'l_{12x}) \\ l_{22x} & l_{22y} & l_{22z} & (b_2'l_{22z} - c_2'l_{22y}) & (c_2'l_{22x} - a_2'l_{22z}) & (a_2'l_{22y} - b_2'l_{22x}) \\ l_{32x} & l_{32y} & l_{32z} & (b_3'l_{32z} - c_3'l_{32y}) & (c_3'l_{32x} - a_3'l_{32z}) & (a_3'l_{32y} - b_3'l_{32x}) \\ l_{42x} & l_{42y} & l_{42z} & (b_4'l_{42z} - c_4'l_{42y}) & (c_4'l_{42x} - a_4'l_{42z}) & (a_4'l_{42y} - b_4'l_{42x}) \end{bmatrix}$$

where

$$\begin{aligned} b_i \;&=\; l_{i1}(S_i\cos\rho_i - R_i\sin\rho_i), \quad i = 1,\ldots,4 \\ l_{i2x} \;&=\; x_i - x_{io} - l_{i1}\sin\gamma_i\cos\rho_i, \quad i = 1,\ldots,4 \\ l_{i2y} \;&=\; y_i - y_{io} + l_{i1}\cos\gamma_i\sin\rho_i, \quad i = 1,\ldots,4 \\ l_{i2z} \;&=\; z_i - z_{io} + l_{i1}\sin\rho_i, \quad i = 1,\ldots,4 \end{aligned}$$

Substituting eq.(3.104) into eq.(3.107) one finally obtains

$$\mathbf{B}_r \delta\boldsymbol{\rho} = \mathbf{A}_r \delta\mathbf{x} \tag{3.108}$$

where

$$\mathbf{A}_r = \mathbf{K}_r \mathbf{J}_r \tag{3.109}$$

From eq.(3.108), one can obtain

$$\delta\mathbf{x}^i = \mathbf{A}_r^{-1}\mathbf{B}_r \delta\boldsymbol{\rho}^i, \quad i = 1, \ldots, 4 \tag{3.110}$$

From eqs.(3.70) and (3.75), one can obtain

$$\delta\boldsymbol{\eta}^i = \mathbf{A}^{-1}\delta\mathbf{b}^i, \quad i = 1, \ldots, 4 \tag{3.111}$$

and

$$\delta\boldsymbol{\lambda}_{jr}^i = \mathbf{C}_{jr}^{-1}\delta\mathbf{p}_j^i, \quad i, j = 1, \ldots, 4 \tag{3.112}$$

where $\mathbf{C}_{jr}^{-1}$ is the inverse of matrix $\mathbf{C}_{jr}$ which was previously obtained, and

$$\delta\boldsymbol{\lambda}_{jr}^i = [\, \delta\rho_j^i \quad \delta\alpha_j^i \quad \delta\beta_j^i \,], \quad i, j = 1, \ldots, 4 \tag{3.113}$$

and finally, the linear virtual displacements are given as

$$\begin{aligned}
\boldsymbol{\delta}_{ju}^i &= \delta\boldsymbol{\omega}_5{}^i \times \mathbf{r}_5^i + \delta\boldsymbol{\omega}^i \times (\mathbf{r}_j - \mathbf{r}_5) + \delta\boldsymbol{\omega}_j{}^i \times \mathbf{Q}_j \mathbf{r}_{ju}, \quad i, j = 1, \ldots, 4 \\
\boldsymbol{\delta}_{jl}^i &= \delta\boldsymbol{\omega}_j{}^i \times \mathbf{Q}_j \mathbf{r}_{j1}, \quad i, j = 1, \ldots, 4 \\
\boldsymbol{\delta}_5^i &= \delta\boldsymbol{\omega}_5{}^i \times \mathbf{Q}_5 \mathbf{r}_5, \quad i = 1, \ldots, 4 \\
\boldsymbol{\delta}_p^i &= \delta\mathbf{p}^i + + \delta\boldsymbol{\omega}^i \times \mathbf{Q}\mathbf{r}_p, \quad i = 1, \ldots, 4
\end{aligned}$$

where all quantities are as previously defined.

IV) Computation of the actuator force/torque

The principle of virtual work can then be applied and leads to

$$\begin{aligned}
\tau_i &= \mathbf{f}_5 \boldsymbol{\delta}_5^i + \mathbf{m}_5 \delta\boldsymbol{\omega}_5^i + \mathbf{f}_p \boldsymbol{\delta}_p^i + \mathbf{m}_p \delta\boldsymbol{\omega}^i \\
&\quad + \sum_{j=1}^{4} [\mathbf{f}_{ju} \boldsymbol{\delta}_{ju}^i + \mathbf{f}_{jl} \boldsymbol{\delta}_{jl}^i + \mathbf{m}_{ju} \delta\boldsymbol{\omega}_{ju}^i + \mathbf{m}_{jl} \delta\boldsymbol{\omega}_{jl}^i], \quad i = 1, \ldots, 4
\end{aligned}$$

where τ_i is the actuating force or torque at the ith actuated joint.

3.1.2.2 Five-degree-of-freedom manipulator

I) Inverse kinematics

Since the computation of the dependent Cartesian coordinate ψ from the specified independent Cartesian coordinates x, y, z, ϕ, θ has been completed in Chapter 2, the only task related to the inverse kinematics which must still be reformed is to obtain the position and orientation of the links of the manipulator from the known pose of the platform. However, this procedure is exactly identical to what has been done in the computation of the inverse kinematics of the spatial four-dof parallel manipulator since the architecture of the actuated legs is the same for the two types of mechanisms. Hence, it is not repeated here.

II) Velocity analysis

In this section, the linear and angular velocities of all moving links will be computed from the given independent Cartesian velocities of the platform $\dot{x}$, $\dot{y}$, $\dot{z}$, ω_x and ω_y, where the angular velocity of the platform is defined as $\boldsymbol{\omega} = [\omega_x, \omega_y, \omega_z]^T$.

First, the dependent component of the angular velocity, ω_z, needs to be determined using the special kinematic chain.

One can write the linear velocities of point P_6 as

$$\dot{\mathbf{p}}_6 = \dot{\mathbf{p}} + \boldsymbol{\omega} \times \mathbf{Q}\mathbf{p}_6^{'} \tag{3.114}$$

where

$$\dot{\mathbf{p}}_6 = \begin{bmatrix} l_6(\dot{\beta}_6 \cos\beta_6 \cos\alpha_6 - \dot{\alpha}_6 \sin\beta_6 \sin\alpha_6) \\ l_6(\dot{\beta}_6 \cos\beta_6 \sin\alpha_6 - l_6\dot{\alpha}_6 \sin\beta_6 \cos\alpha_6) \\ -l_6\dot{\beta}_6 \sin\beta_6 \end{bmatrix}$$

$$\dot{\mathbf{p}} = \begin{bmatrix} \dot{x} \\ \dot{y} \\ \dot{z} \end{bmatrix}, \quad \dot{\mathbf{p}}_6 = \begin{bmatrix} \dot{x}_6 \\ \dot{y}_6 \\ \dot{z}_6 \end{bmatrix}, \quad \boldsymbol{\omega} = \begin{bmatrix} \omega_x \\ \omega_y \\ \omega_z \end{bmatrix}, \quad \mathbf{p}_6^{'} = \begin{bmatrix} a_6 \\ b_6 \\ c_6 \end{bmatrix}$$

Equation (3.114) can be rewritten in matrix form

$$\mathbf{A}\boldsymbol{\eta} = \mathbf{b} \tag{3.115}$$

where

$$\mathbf{A} = \begin{bmatrix} b_6' & -l_6\dot{\alpha}_6 \sin\alpha_6 \sin\beta_6 & l_6\dot{\beta}_6 \cos\alpha_6 \cos\beta_6 \\ -b_6' & l_6\dot{\alpha}_6 \cos\alpha_6 \sin\beta_6 & -l_6\dot{\beta}_6 \sin\alpha_6 \cos\beta_6 \\ 0 & 0 & l_6\dot{\beta}_6 \sin\beta_6(\sin\alpha_6 - \cos\alpha_6) \end{bmatrix}$$

$$\boldsymbol{\eta} = \begin{bmatrix} \omega_z \\ \dot{\alpha}_6 \\ \dot{\beta}_6 \end{bmatrix}, \quad \mathbf{b} = \begin{bmatrix} -c_6'\omega_y \\ c_6'\omega_x \\ a_6'\omega_y - b_6'\omega_x \end{bmatrix}$$

and $[a_6', b_6', c_6'] = \mathbf{Q}\mathbf{p}_6'$ and eq.(3.115) is easily solved for vector $\boldsymbol{\eta}$.

Having obtained the six Cartesian velocity components $\dot{x}, \dot{y}, \dot{z}, \omega_x, \omega_y$ and ω_z, the linear velocities of the center of joints P_i connecting each leg to the platform can be computed as follows

$$\dot{\mathbf{p}}_i = \dot{\mathbf{p}} + \boldsymbol{\omega} \times \mathbf{Q}\mathbf{p}_i', \quad i = 1, \ldots, 5 \tag{3.116}$$

The rest of the procedure is to determine the velocities of the other bodies from the linear velocity of points P_i. This is identical to what was presented in the previous subsection on the velocity analysis of the spatial four-dof parallel mechanism.

III) Acceleration analysis

The linear and angular accelerations of each of the moving bodies will now be determined from the given Cartesian accelerations of the platform, i.e., $\ddot{x}, \ddot{y}, \ddot{z}$, $\dot{\omega}_x$ and $\dot{\omega}_y$.

First, the dependent acceleration component $\dot{\omega}_z$ must be determined. This can be achieved by using the kinematic geometry of the special leg.

Differentiating eq.(3.114) with respect to time and letting $i = 6$, one obtains the expression of the linear acceleration of point P_6 as follows:

$$\ddot{\mathbf{p}}_6 = \ddot{\mathbf{p}} + \dot{\boldsymbol{\omega}} \times \mathbf{Q}\mathbf{P}_6' + \boldsymbol{\omega} \times (\boldsymbol{\omega} \times \mathbf{Q}\mathbf{P}_6') \tag{3.117}$$

where

$$\ddot{\mathbf{p}}_6 = \begin{bmatrix} \ddot{x}_6 \\ \ddot{y}_6 \\ \ddot{z}_6 \end{bmatrix}, \quad \ddot{\mathbf{p}} = \begin{bmatrix} \ddot{x} \\ \ddot{y} \\ \ddot{z} \end{bmatrix}, \quad \dot{\boldsymbol{\omega}} = \begin{bmatrix} \dot{\omega}_x \\ \dot{\omega}_y \\ \dot{\omega}_z \end{bmatrix} \tag{3.118}$$

where

$$\ddot{x}_6 = l_6(\ddot{\beta}_6 \cos\beta_6 \cos\alpha_6 - \ddot{\alpha}_6 \sin\beta_6 \sin\alpha_6 - \dot{\beta}_6^2 \sin\beta_6 \cos\alpha_6$$

$$
\begin{aligned}
& -\dot{\alpha}_6^2 \sin\beta_6 \cos\alpha_6 - \dot{\alpha}_6\dot{\beta}_6 \cos\beta_6 \sin\alpha_6 - \dot{\alpha}_6\dot{\beta}_6 \cos\beta_6 \sin\alpha_6) \\
\ddot{y}_6 &= l_6(\ddot{\beta}_6 \cos\beta_6 \sin\alpha_6 \ddot{\alpha}_6 \sin\beta_6 \cos\alpha_6 - \dot{\beta}_6^2 \sin\beta_6 \sin\alpha_6 \\
& -\dot{\alpha}_6^2 \sin\beta_6 \sin\alpha_6 + \dot{\alpha}_6\dot{\beta}_6 \cos\beta_6 \cos\alpha_6 + dot\beta_6\dot{\alpha}_6 \cos\beta_6 \cos\alpha_6) \\
\ddot{z}_6 &= -l_6(\ddot{\beta}_6 \sin\beta_6 + \dot{\beta}_6^2 \cos\beta_6)
\end{aligned}
$$

Since the velocity analysis has already been performed, eq.(3.117) consists of three scalar equations which contain only three unknowns: $\ddot{\alpha}, \dot{\omega}_y$ and $\dot{\omega}_z$. Therefore, it is easy to solve for these unknowns.

Equation (3.117) is rewritten in matrix form as

$$\mathbf{A}\dot{\boldsymbol{\eta}} = \mathbf{e} \tag{3.119}$$

where $\dot{\boldsymbol{\eta}} = [\,\ddot{\alpha}_6 \quad \dot{\beta}_6 \quad \dot{\omega}_z\,]^T$ and $\mathbf{e} = [\,e_x \quad e_y \quad e_z\,]^T$, and

$$
\begin{aligned}
e_x &= \dot{x} + l_6(-\dot{\beta}_6^2 \sin\beta_6 \cos\alpha_6 - \dot{\alpha}_6^2 \sin\beta_6 \cos\alpha_6 \\
& -\dot{\alpha}_6\dot{\beta}_6 \cos\beta_6 \sin\alpha_6 - \dot{\alpha}_6\dot{\beta}_6 \cos\beta_6 \sin\alpha_6) + a_x \\
e_y &= \ddot{y} + l_6(-\dot{\beta}_6^2 \sin\beta_6 \sin\alpha_6 - \dot{\alpha}_6^2 \sin\beta_6 \sin\alpha_6 \\
& +\dot{\alpha}_6\dot{\beta}_6 \cos\beta_6 \cos\alpha_6 + dot\beta_6\dot{\alpha}_6 \cos\beta_6 \cos\alpha_6) + a_y \\
e_z &= \ddot{z} - l_6(\dot{\beta}_6^2 \cos\beta_6) + a_z
\end{aligned}
$$

and matrix $\mathbf{A}$ was previously defined and where $[a_x\, a_y\, a_z]^T = \boldsymbol{\omega} \times (\boldsymbol{\omega} \times \mathbf{QP}_6')$.

Equation (3.119) is readily solved for $\dot{\boldsymbol{\eta}}$, which leads to the desired acceleration components. All the Cartesian accelerations of the platform are then known, and the linear and angular accelerations of each of the leg bodies of the two types of manipulators can then be determined.

The rest of the procedure is to obtain the linear and angular accelerations of the two links of each of the legs from the linear accelerations of points P_i and can be found in the acceleration analysis of the spatial four-dof parallel mechanism.

VI) Computation of the inertial forces and torques acting on the center of mass of each link

Because of the similarity of the architectures of the five-dof and four-dof mechanisms, only the formulas for the computation of the inertial forces and torques of the

special 6th leg are different and the others can be found in the previous subsection on the four-dof mechanism.

The linear acceleration of the center of mass of the 6th leg and the platform can be computed as follows

$$\mathbf{a}_6 = \dot{\boldsymbol{\omega}}_6 \times \mathbf{Q}_6\mathbf{r}_6 + \boldsymbol{\omega}_6 \times (\boldsymbol{\omega}_6 \times \mathbf{Q}_6\mathbf{r}_6) \tag{3.120}$$

$$\mathbf{a}_p = \ddot{\mathbf{p}} + \dot{\boldsymbol{\omega}} \times \mathbf{Q}\mathbf{r}_p + \boldsymbol{\omega} \times (\boldsymbol{\omega} \times \mathbf{Q}\mathbf{r}_p) \tag{3.121}$$

where $\mathbf{a}_6$ and $\mathbf{a}_p$ are respectively the linear accelerations of the center of mass of the 6th leg and the platform, and where $\boldsymbol{\omega}_6$ is the angular velocity of the 6th leg, $\dot{\boldsymbol{\omega}}_6$ is its angular acceleration and where $\mathbf{r}_6$ is the vector connecting point O to the center of mass of the 6th leg noted C_6, and where

$$\mathbf{Q}_6 = \begin{bmatrix} \cos\alpha_6\cos\beta_6 & -\sin\alpha_6 & \cos\alpha_6\sin\beta_6 \\ \sin\alpha_6\cos\beta_6 & \cos\alpha_6 & \sin\alpha_6\sin\beta_6 \\ -\sin\beta_6 & 0 & \cos\beta_6 \end{bmatrix}, \quad \mathbf{r}_6 = \begin{bmatrix} 0 \\ 0 \\ r_6 \end{bmatrix} \tag{3.122}$$

$$\boldsymbol{\omega}_6 = \begin{bmatrix} -\dot{\beta}_6\sin\alpha_6 \\ \dot{\beta}_6\cos\alpha_6 \\ \dot{\alpha}_6 \end{bmatrix}, \quad \dot{\boldsymbol{\omega}}_6 = \begin{bmatrix} -\ddot{\beta}_6\sin\alpha_6 - \dot{\beta}_6\dot{\alpha}_6\cos\alpha_6 \\ \ddot{\beta}_6\cos\alpha_6 - \dot{\beta}_6\dot{\alpha}_6\sin\alpha_6 \\ \ddot{\alpha}_6 \end{bmatrix} \tag{3.123}$$

The force and moment acting on the center of mass of the link of the 6th leg can be directly computed as follows

$$\mathbf{f}_6 = -m_6\mathbf{a}_6 + \mathbf{w}_6 \tag{3.124}$$

$$\mathbf{f}_p = -m_p\mathbf{a}_p + \mathbf{w}_p \tag{3.125}$$

$$\mathbf{m}_6 = -\frac{\mathrm{d}}{\mathrm{dt}}(\mathbf{Q}_6\mathbf{I}_6\mathbf{Q}_6^T\boldsymbol{\omega}_6) \tag{3.126}$$

$$\mathbf{m}_p = -\frac{\mathrm{d}}{\mathrm{dt}}(\mathbf{Q}\mathbf{I}_p\mathbf{Q}^T\boldsymbol{\omega}_p) \tag{3.127}$$

where $\mathbf{f}_6$ and $\mathbf{m}_6$ denote the force and moment acting on the 6th leg while $\mathbf{f}_p$ and $\mathbf{m}_p$ denote the force and moment acting on the platform, $\mathbf{I}_6$ and $\mathbf{I}_p$ are the inertia tensors of the 6th leg and the platform with respect to their center of mass.

The forces and moments acting on the center of mass of each link of this type of manipulator are represented in Figure 3.3.

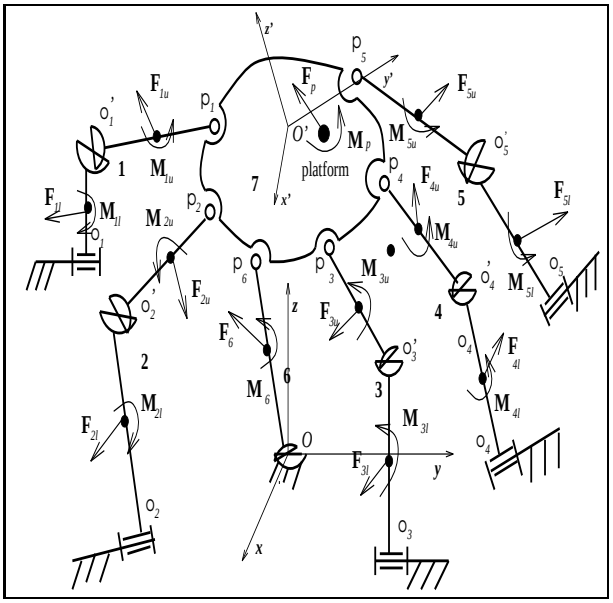

Figure 3.3: Body forces acting on the links of the manipulator with revolute actuators.

V) Computation of the virtual displacements of the links

In this section, the virtual linear displacement of the center of mass and the virtual angular displacement of each link are obtained from the given joint virtual displacement of the manipulator. It is the crucial step for determining the generalized input force by this approach.

From the kinematic geometry of the 6th leg, one can write

$$x_6^2 + y_6^2 + z_6^2 \;=\; l_6^2 \tag{3.128}$$

Differentiating eq.(3.128), one has

$$x_6\dot{x}_6 + y_6\dot{y}_6 + z_6\dot{z}_6 \;=\; 0 \tag{3.129}$$

Letting $\dot{\mathbf{p}}_6 = [\,\dot{x}_6 \quad \dot{y}_6 \quad \dot{z}_6\,]^T$ and substituting eq.(3.114) into eqs.(3.129), one obtains

$$\dot{\mathbf{t}} = \mathbf{J}_r\dot{\mathbf{x}}, \quad \text{or} \quad \delta\mathbf{t} = \mathbf{J}_r\delta\mathbf{x} \tag{3.130}$$

where $\delta\mathbf{t}$ is as previous defined, and

$$\delta\mathbf{x} = \begin{bmatrix} \delta x \\ \delta y \\ \delta z \\ \delta\omega_x \\ \delta\omega_y \end{bmatrix}, \quad \mathbf{J}_r = \begin{bmatrix} 1 & 0 & 0 & 0 & 0 \\ 0 & 1 & 0 & 0 & 0 \\ 0 & 0 & 1 & 0 & 0 \\ 0 & 0 & 0 & 1 & 0 \\ 0 & 0 & 0 & 0 & 1 \\ \frac{x_6}{b_6'x_6+a_6'y_6} & \frac{y_6}{b_6'x_6+a_6'y_6} & \frac{z_6}{b_6'x_6+a_6'y_6} & \frac{b_6'z_6+c_6'y_6}{b_6'x_6+a_6'y_6} & \frac{c_6'x_6+a_6'z_6}{b_6'x_6+a_6'y_6} \end{bmatrix} \tag{3.131}$$

Differentiating eq.(3.61), one obtains

$$\begin{aligned} l_{i1}(S_i\cos\rho_i - R_i\sin\rho_i)\delta\rho_i &= (x_i - x_{io} - l_{i1}\sin\gamma_i\cos\rho_i)\delta x_i \\ &\quad +(y_i - y_{io} + l_{i1}\cos\gamma_i\sin\rho_i)\delta y_i \\ &\quad +(z_i - z_{io} + l_{i1}\sin\rho_i)\delta z_i, \quad i = 1,\ldots,5 \end{aligned} \tag{3.132}$$

Substituting eq.(3.72) into eq.(3.132), one obtains

$$\mathbf{B}_r\delta\boldsymbol{\rho} = \mathbf{K}_r\delta\mathbf{t} \tag{3.133}$$

where

$$\begin{aligned} \mathbf{B}_r &= \mathrm{diag}\,[\,b_1 \quad b_2 \quad b_3 \quad b_4 \quad b_5\,] \\ \mathbf{K}_r &= \begin{bmatrix} l_{12x} & l_{12y} & l_{12z} & (b_1'l_{12z} - c_1'l_{12y}) & (c_1'l_{12x} - a_1'l_{12z}) & (a_1'l_{12y} - b_1'l_{12x}) \\ l_{22x} & l_{22y} & l_{22z} & (b_2'l_{22z} - c_2'l_{22y}) & (c_2'l_{22x} - a_2'l_{22z}) & (a_2'l_{22y} - b_2'l_{22x}) \\ l_{32x} & l_{32y} & l_{32z} & (b_3'l_{32z} - c_3'l_{32y}) & (c_3'l_{32x} - a_3'l_{32z}) & (a_3'l_{32y} - b_3'l_{32x}) \\ l_{42x} & l_{42y} & l_{42z} & (b_4'l_{42z} - c_4'l_{42y}) & (c_4'l_{42x} - a_4'l_{42z}) & (a_4'l_{42y} - b_4'l_{42x}) \\ l_{52x} & l_{52y} & l_{52z} & (b_5'l_{52z} - c_5'l_{52y}) & (c_5'l_{52x} - a_5'l_{52z}) & (a_5'l_{52y} - b_5'l_{52x}) \end{bmatrix} \end{aligned}$$

where

$$\begin{aligned} b_i &= l_{i1}(S_i\cos\rho_i - R_i\sin\rho_i) \\ l_{i2x} &= x_i - x_{io} - l_{i1}\sin\gamma_i\cos\rho_i \\ l_{i2y} &= y_i - y_{io} + l_{i1}\cos\gamma_i\sin\rho_i \\ l_{i2z} &= z_i - z_{io} + l_{i1}\sin\rho_i \\ i &= 1,\ldots,5 \end{aligned}$$

Substituting eq.(3.130) into eq.(3.133) one finally obtains

$$\mathbf{B}_r\delta\boldsymbol{\rho} = \mathbf{A}_r\delta\mathbf{x} \tag{3.134}$$

where

$$\mathbf{A}_r = \mathbf{K}_r \mathbf{J}_r \tag{3.135}$$

Similarly, one can obtain

$$\delta \mathbf{x}^i = \mathbf{A}_r^{-1} \mathbf{B}_r \delta \boldsymbol{\rho}^i \tag{3.136}$$

where $\delta \mathbf{x}^i$ and $\delta \boldsymbol{\rho}^i$ are as previously defined.

Then, one can obtain

$$\delta \boldsymbol{\eta}^i = \mathbf{A}^{-1} \delta \mathbf{b}^i \tag{3.137}$$

and

$$\delta \boldsymbol{\lambda}_{jr}^i = \mathbf{C}_{jr}^{-1} \delta \mathbf{p}_j^i, \quad j = 1, \ldots, 5 \tag{3.138}$$

where

$$\delta \boldsymbol{\lambda}_{jr}^i = [\, \delta \rho_j^i \quad \delta \alpha_j^i \quad \delta \beta_j^i \,], \quad j = 1, \ldots, 5 \tag{3.139}$$

and finally, the linear virtual displacements are given as

$$\begin{aligned}
\boldsymbol{\delta}_{ju}^i &= \delta \boldsymbol{\omega}_6{}^i \times \mathbf{r}_6^i + \delta \boldsymbol{\omega}^i \times (\mathbf{r}_j - \mathbf{r}_6) + \delta \boldsymbol{\omega}_j{}^i \times \mathbf{Q}_j \mathbf{r}_{ju}, \quad i, j = 1, \ldots, 5 \\
\boldsymbol{\delta}_{jl}^i &= \delta \boldsymbol{\omega}_j{}^i \times \mathbf{Q}_j \mathbf{r}_{j1}, \quad i, j = 1, \ldots, 5 \\
\boldsymbol{\delta}_6^i &= \delta \boldsymbol{\omega}_6{}^i \times \mathbf{Q}_6 \mathbf{r}_6, \quad i = 1, \ldots, 5 \\
\boldsymbol{\delta}_p^i &= \delta \mathbf{p}^i + + \delta \boldsymbol{\omega}^i \times \mathbf{Q} \mathbf{r}_p, \quad i = 1, \ldots, 5
\end{aligned}$$

where all quantities are as as previously defined.

IV) Computation of the actuator force/torque

The principle of virtual work can then be applied and leads to

$$\begin{aligned}
\tau_i &= \mathbf{f}_6 \boldsymbol{\delta}_6^i + \mathbf{m}_6 \delta \boldsymbol{\omega}_6^i + \mathbf{f}_p \boldsymbol{\delta}_p^i + \mathbf{m}_p \delta \boldsymbol{\omega}^i \\
&\quad + \sum_{j=1}^{5} [\mathbf{f}_{ju} \boldsymbol{\delta}_{ju}^i + \mathbf{f}_{jl} \boldsymbol{\delta}_{jl}^i + \mathbf{m}_{ju} \delta \boldsymbol{\omega}_{ju}^i + \mathbf{m}_{jl} \delta \boldsymbol{\omega}_{jl}^i], \quad i = 1, \ldots, 5
\end{aligned}$$

where τ_i is the actuating force or torque at the ith actuated joint.

3.1.2.3 Six-degree-of-freedom manipulator

Since the architectures of the six- and five-degree-of-freedom manipulators are very similar, the procedure for the computation of the inverse kinematics, the velocity analysis, the acceleration analysis and the computation of the inertial forces or moments

for the six-degree-of-freedom manipulator can be directly obtained from the analysis of the five-degree-of-freedom manipulator. Therefore, for the 6-dof manipulator it is only needed to describe the final two steps, namely, the computation of the virtual displacements of the links and the determination of the generalized forces/torques.

V) Computation of the virtual displacements of the links

The virtual linear displacement of the center of mass and the virtual angular displacement of each link are computed from the given joint virtual displacement of the manipulator.

Differentiating eq.(3.61), one obtains

$$\begin{aligned} l_{i1}(S_i\cos\rho_i - R_i\sin\rho_i)\delta\rho_i &= (x_i - x_{io} - l_{i1}\sin\gamma_i\cos\rho_i)\delta x_i \\ &\quad +(y_i - y_{io} + l_{i1}\cos\gamma_i\sin\rho_i)\delta y_i \\ &\quad +(z_i - z_{io} + l_{i1}\sin\rho_i)\delta z_i, \quad i = 1,\ldots,6 \end{aligned} \tag{3.140}$$

Substituting eq.(3.72) into eq.(3.140), one obtains

$$\mathbf{B}_r\delta\boldsymbol{\rho} = \mathbf{A}_r\delta\mathbf{x} \tag{3.141}$$

where

$$\begin{aligned} \delta\mathbf{x} &= [\,\delta x \quad \delta y \quad \delta z \quad \delta\omega_x \quad \delta\omega_y \quad \delta\omega_z\,] \\ \mathbf{B}_r &= \mathrm{diag}\,[\,b_1 \quad b_2 \quad b_3 \quad b_4 \quad b_5 \quad b_6\,] \\ \mathbf{A}_r &= \begin{bmatrix} l_{12x} & l_{12y} & l_{12z} & (b_1'l_{12z} - c_1'l_{12y}) & (c_1'l_{12x} - a_1'l_{12z}) & (a_1'l_{12y} - b_1'l_{12x}) \\ l_{22x} & l_{22y} & l_{22z} & (b_2'l_{22z} - c_2'l_{22y}) & (c_2'l_{22x} - a_2'l_{22z}) & (a_2'l_{22y} - b_2'l_{22x}) \\ l_{32x} & l_{32y} & l_{32z} & (b_3'l_{32z} - c_3'l_{32y}) & (c_3'l_{32x} - a_3'l_{32z}) & (a_3'l_{32y} - b_3'l_{32x}) \\ l_{42x} & l_{42y} & l_{42z} & (b_4'l_{42z} - c_4'l_{42y}) & (c_4'l_{42x} - a_4'l_{42z}) & (a_4'l_{42y} - b_4'l_{42x}) \\ l_{52x} & l_{52y} & l_{52z} & (b_5'l_{52z} - c_5'l_{52y}) & (c_5'l_{52x} - a_5'l_{52z}) & (a_5'l_{52y} - b_5'l_{52x}) \\ l_{62x} & l_{62y} & l_{62z} & (b_6'l_{62z} - c_6'l_{62y}) & (c_6'l_{62x} - a_6'l_{62z}) & (a_6'l_{62y} - b_6'l_{62x}) \end{bmatrix} \end{aligned}$$

where

$$\begin{aligned} b_i &= l_{i1}(S_i\cos\rho_i - R_i\sin\rho_i) \\ l_{i2x} &= x_i - x_{io} - l_{i1}\sin\gamma_i\cos\rho_i \\ l_{i2y} &= y_i - y_{io} + l_{i1}\cos\gamma_i\sin\rho_i \\ l_{i2z} &= z_i - z_{io} + l_{i1}\sin\rho_i \\ i &= 1,\ldots,6 \end{aligned}$$

Then, one can obtain

$$\delta \mathbf{x}^i = \mathbf{A}_r^{-1} \mathbf{B}_r \delta \boldsymbol{\rho}^i \tag{3.142}$$

where $\delta \mathbf{x}^i$ and $\delta \boldsymbol{\rho}^i$ are as previously defined.

Then, one can also obtain

$$\delta \boldsymbol{\eta}^i = \mathbf{A}^{-1} \delta \mathbf{b}^i \tag{3.143}$$

and

$$\delta \boldsymbol{\lambda}_{jr}^i = \mathbf{C}_{jr}^{-1} \delta \mathbf{p}_j^i, \quad j = 1, \ldots, 6 \tag{3.144}$$

where

$$\delta \boldsymbol{\lambda}_{jr}^i = [\, \delta \rho_j^i \quad \delta \alpha_j^i \quad \delta \beta_j^i \,], \quad j = 1, \ldots, 6 \tag{3.145}$$

and finally, the linear virtual displacements are given as

$$\begin{aligned}
\boldsymbol{\delta}_{ju}^i &= \delta \boldsymbol{\omega}_{jl}{}^i \times \mathbf{Q}_{jl} \mathbf{l}_{jl}^i + \delta \boldsymbol{\omega}_{ju}{}^i \times \mathbf{Q}_{ju} \mathbf{r}_{ju}, \quad i, j = 1, \ldots, 6 \\
\boldsymbol{\delta}_{jl}^i &= \delta \boldsymbol{\omega}_{jl}{}^i \times \mathbf{Q}_{jl} \mathbf{r}_{jl}, \quad i, j = 1, \ldots, 6 \\
\boldsymbol{\delta}_p^i &= \delta \mathbf{p}^i + + \delta \boldsymbol{\omega}^i \times \mathbf{Q} \mathbf{r}_p, \quad i = 1, \ldots, 6
\end{aligned}$$

where all the quantities are as previously defined.

IV) Computation of the actuator force/torque

The principle of virtual work can then be applied and leads to

$$\begin{aligned}
\tau_i &= \mathbf{f}_p \boldsymbol{\delta}_p^i + \mathbf{m}_p \delta \boldsymbol{\omega}^i \\
&\quad + \sum_{j=1}^{6} [\mathbf{f}_{ju} \boldsymbol{\delta}_{ju}^i + \mathbf{f}_{jl} \boldsymbol{\delta}_{jl}^i + \mathbf{m}_{ju} \delta \boldsymbol{\omega}_{ju}^i + \mathbf{m}_{jl} \delta \boldsymbol{\omega}_{jl}^i], \quad i = 1, \ldots, 6
\end{aligned}$$

where τ_i is the actuating force or torque at the ith actuated joint.

3.2 Newton-Euler formulation

In order to verify the results obtained using the approach presented in the previous section, a second approach based on the Newton–Euler formulation is now developed. Each link of the manipulator is considered individually and constraint forces between the links are computed. Although this approach leads to a slower computational algorithm than the approach based on the principle of virtual work, the internal constraint

forces between the links are computed here, which may be useful for design and simulation of a mechanism or manipulator. Therefore, this approach is suitable for the design of the mechanism. This approach has been used by other authors for the dynamic analysis of 6-dof parallel mechanisms (see for instance [14] and [22]).

3.2.1 Planar parallel manipulators with revolute actuators

Since the application of the Newton-Euler formulas to solve the dynamic problem of planar mechanisms is rather straightforward, the detailed procedure for the dynamic analysis of planar two- and three-degree-of-freedom manipulators is not given here. However, in order to verify the results obtained with the approach based on the principle of virtual work, two computation programs corresponding to the two approaches have been written for the two types of planar parallel mechanisms. Finally, an example is given for each manipulator and it can be verified from the examples that the two approaches lead to identical results.

3.2.1.1 Two-degree-of-freedom manipulator

An example for the planar two-degree-of-freedom manipulator with revolute actuators is now given to illustrate the results. It is assumed that the end-effector of the manipulator follows a simple trajectory involving vertical motion along the direction of the **y** axis. The trajectory is described in detail below. The force and torque needed to produce the specified motion are obtained by the approach based on the principle of virtual work and the Newton-Euler formulation. The two approaches lead to identical results and the approach based on the principle of virtual work leads to a faster algorithm.

The parameters used in this example are

$$x_{o1} = 0.0,\ y_{o1} = 0.0,\ x_{o2} = 2.0, y_{o2} = 0.0$$

$$l_1 = 0.8,\ l_2 = 1.0,\ l_3 = 1.5,\ l_4 = 0.8,\ l_5 = 0.6$$

$$r_1 = 0.3,\ r_2 = 0.4,\ r_3 = 0.75,\ r_4 = 0.4$$

$$m_1 = 0.1,\ m_2 = 0.1,\ m_3 = 1.0,\ m_4 = 0.1$$

$$\mathbf{I}_1 = \mathbf{I}_2 = \mathbf{I}_4 = \begin{bmatrix} 0 & 0 & 0 \\ 0 & 0.1/16 & 0 \\ 0 & 0 & 0.1/16 \end{bmatrix}, \quad \mathbf{I}_3 = \begin{bmatrix} 0 & 0 & 0 \\ 0 & 0.06 & 0 \\ 0 & 0 & 0.06 \end{bmatrix}$$

The specified trajectory is

$$x = 1.7, \quad y = 1.0 + 0.2 \sin 3t, \tag{3.146}$$

with $K_1 = -1$, $K_2 = 1$, the masses are given in tons, the lengths in meters and the angles in radians.

The generalized input forces obtained for the two actuated joints are represented in Figure 3.4.

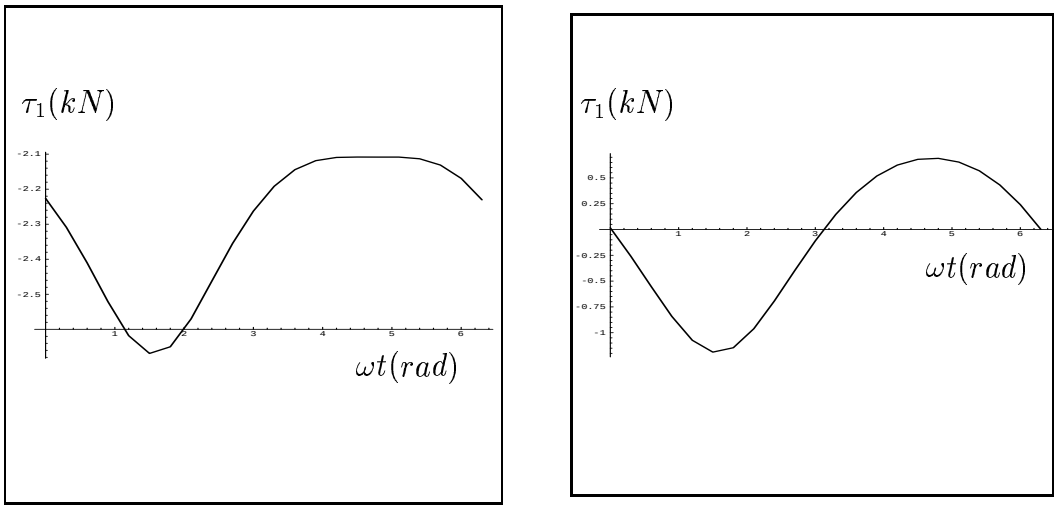

(a) Torque at the actuated joint 1.

(b) Torque at the actuated joint 2.

Figure 3.4: Generalized actuator force in the planar two-dof mechanism

3.2.1.2 Three-degree-of-freedom manipulator

Similarly, an example for the planar three-degree-of-freedom manipulator with revolute actuators is now given to illustrate the results. It is assumed that the end-effector of the manipulator follows a simple trajectory involving vertical motion along the direction of the **y** axis with the orientation angle ϕ fixed. The trajectory is described in detail below. The force and torque needed to produce the specified motion are obtained by the two approaches.

The parameters used in this example are

$$x_{o1} = 0.0,\ y_{o1} = 0.0,\ x_{o2} = 1.0, y_{o2} = 0.0,\ x_{o2} = 2.4, y_{o2} = 0.0$$

$$l_{il} = 1.2,\ l_{iu} = 1.5\,(i = 1, 2, 3),\ l_3 = 0.7,\ l_4 = 1.6$$

$$r_{il} = 0.3,\ r_{iu} = 0.4\,(i = 1, 2, 3),\ r_3 = 0.75,\ r_4 = 0.4$$

$$m_{il} = 0.1,\ m_{iu} = 0.1\,(i = 1, 2, 3),\ m_3 = 1.0,\ m_4 = 0.1$$

$$\mathbf{I}_{il} = \mathbf{I}_{iu} = \begin{bmatrix} 0 & 0 & 0 \\ 0 & 0.1/16 & 0 \\ 0 & 0 & 0.1/16 \end{bmatrix}, \quad i = 1, 2, 3 \quad \mathbf{I}_p = \begin{bmatrix} 0 & 0 & 0 \\ 0 & 0.06 & 0 \\ 0 & 0 & 0.06 \end{bmatrix}$$

The specified trajectory is

$$x = 1.2, \quad y = 1.5 + 0.2 \sin 3t,\ \phi = \frac{\pi}{6}; \tag{3.147}$$

with $K_1 = -1$, $K_2 = 1$, $K_3 = 1$, the masses are given in tons, the lengths in meters and the angles in radians.

The generalized input forces obtained for the three actuated joints are represented in Figures 3.5 and 3.6.

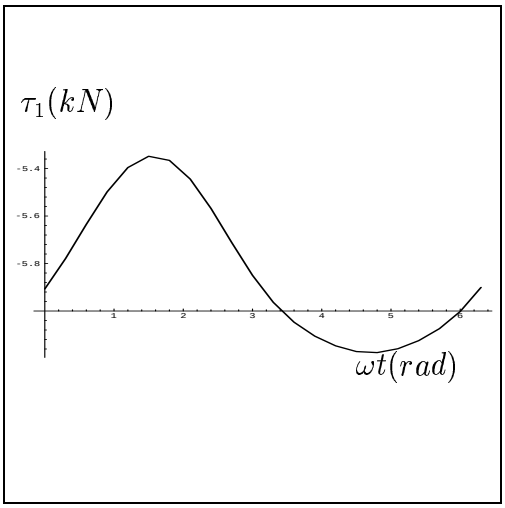

(a) Torque at the actuated joint 1.

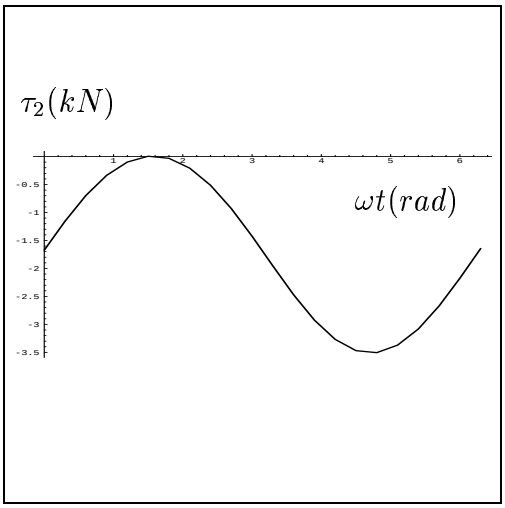

(b) Torque at the actuated joint 2.

Figure 3.5: Generalized force in the planar three-dof mechanism at the actuated joints 1 and 2.

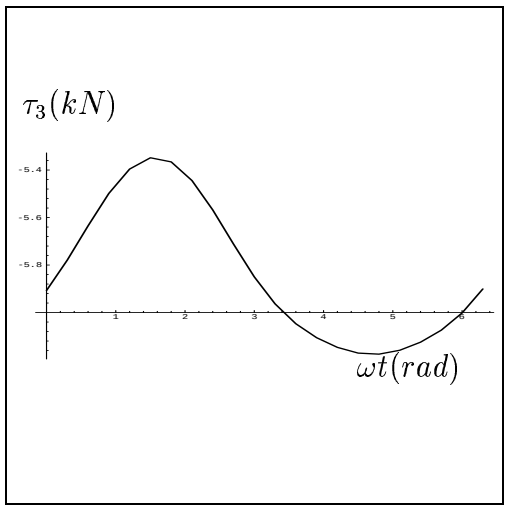

Figure 3.6: Generalized force in the planar three-dof mechanism at the actuated joint 3.

3.2.2 Spatial parallel manipulators with revolute actuators

As mentioned in the introduction and in the previous subsection, the dynamic analysis of spatial parallel manipulators using the Newton-Euler formulation has been studied by many authors, for example, the dynamic analysis of spatial six-degree-of-freedom parallel manipulators using the latter approach [10] and [14]. Therefore, similarly to the planar parallel manipulators, the procedure for the dynamic analysis of the spatial six-degree-of-freedom parallel manipulator using the Newton-Euler formulation is not discussed here and only an example is given to verify the results obtained with the approach based on the principle of virtual work. However, for the spatial parallel manipulators with reduced degree of freedom, namely, the spatial four- and five-degree-of-freedom parallel manipulators, since their architectures differ from the spatial six-degree-of-freedom parallel manipulator, the procedures for the dynamic analysis using the Newton-Euler formulation is different and will be described below.

3.2.2.1 Four-degree-of-freedom manipulator

The constraint forces between the 5th leg and the platform and the associated coordinate frame are represented in Figure 3.7. Here it is assumed that $\mathbf{g}_5$ and $\mathbf{f}_5$ are normal

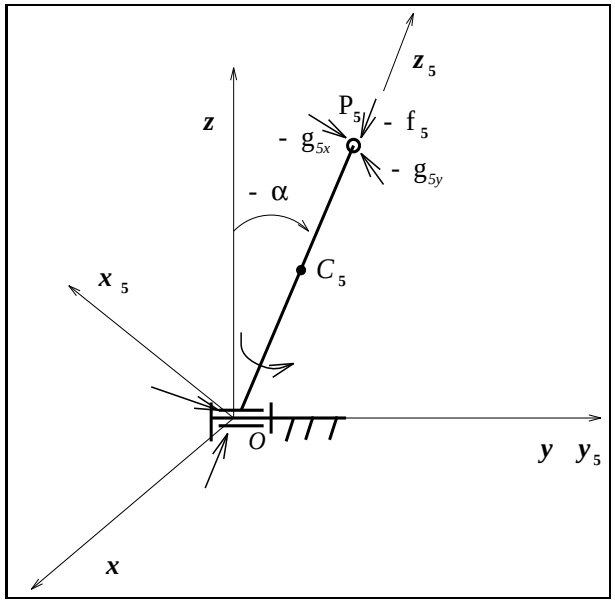

Figure 3.7: The constraint forces between the fifth leg and the platform.

to and along the direction of the 5th leg OP_5, namely

$$\mathbf{g}_5 = \begin{bmatrix} g_{5x} \\ g_{5y} \\ 0 \end{bmatrix}, \quad \mathbf{f}_5 = \begin{bmatrix} 0 \\ 0 \\ f_5 \end{bmatrix} \tag{3.148}$$

Moreover, the linear acceleration of the center of mass of the 5th leg can be obtained as follows

$$\mathbf{a}_5 = \dot{\boldsymbol{\omega}}_5 \times \mathbf{Q}_5\mathbf{r}_5 + \boldsymbol{\omega}_5 \times (\boldsymbol{\omega}_5 \times \mathbf{Q}_5\mathbf{r}_5) \tag{3.149}$$

where $\mathbf{Q}_5$, $\boldsymbol{\omega}_5$, $\dot{\boldsymbol{\omega}}_5$ and $\mathbf{r}_5$ are as previously defined.

Considering axis y, one obtains one element g_{5x} of the force $\mathbf{g}_5$ by the application of the Euler equation around this axis. This Euler equation can be written as

$$-\mathbf{Q}_5[(\mathbf{g}_5 + \mathbf{f}_5) \times \mathbf{l}_5] + \mathbf{w}_5 \times \mathbf{Q}_5\mathbf{r}_5 = m_5\mathbf{a}_5 \times \mathbf{Q}_5\mathbf{r}_5 + \frac{\mathrm{d}}{\mathrm{dt}}(\mathbf{Q}_5\mathbf{I}_5\mathbf{Q}_5^T\boldsymbol{\omega}_5) \tag{3.150}$$

where $\mathbf{l}_5 = [0, 0, l_5]^T$ is the vector connecting point O to P_5 and $\mathbf{w}_5 = [0,\ 0,\ -m_5 g]^T$ is the weight of the 5th leg, where g is the gravitational acceleration and $\mathbf{I}_5$ is the inertia tensor of the 5th leg with respect to its center of mass.

Substituting eq.(3.91) into eq.(3.150) and extracting the second component, one then obtains

$$g_{5x} = [m_5 g r_5 \sin\alpha - (I_{5y} + m_5 r_5^2)\ddot{\alpha}]/l_5 \tag{3.151}$$

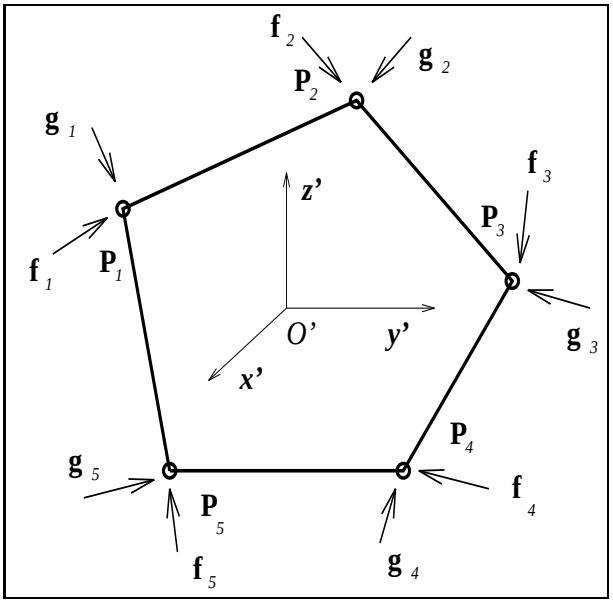

Figure 3.8: The constraint forces on the platform.

where I_{5y} is the moment of the inertia of the 5th leg about the $\mathbf{y}$ axis with respect to its center of mass.

It is then assumed that forces $\mathbf{g}_i (i = 1, 2, 3, 4)$—their determination will be discussed below—and g_{5x} are known, and therefore forces $\mathbf{f}_i (i = 1, \ldots, 5)$ and g_{5y} can be determined by the application of the Newton–Euler equations to the platform of the manipulator in the coordinate system of the platform. Figure 3.8 shows the platform of the manipulator and the forces acting on it. Forces g_{ix}, g_{iy} $(i = 1, \ldots, 4)$ and g_{5x} are obtained from the ith $(i = 1, \ldots, 4)$ and 5th leg respectively as will be shown below. The remaining unknown action forces are only six elements, i.e., f_i $(i = 1, \ldots, 5)$ and g_{5y}. Hence, these unknown forces can be obtained by the application of Newton–Euler equations to the platform of the manipulator, i.e.,

$$\mathbf{Q}_5(\mathbf{g}_5 + \mathbf{f}_5) + \mathbf{Q}_i \sum_{i=1}^{4} (\mathbf{f}_i + \mathbf{g}_i) = m_p \mathbf{a}_{O'} \tag{3.152}$$

$$\mathbf{Q}_5(\mathbf{g}_5 + \mathbf{f}_5) \times \mathbf{Q}\mathbf{p}_5^{'} + [\mathbf{Q}_i \sum_{i=1}^{4} (\mathbf{f}_i + \mathbf{g}_i)] \times \mathbf{Q}\mathbf{p}_i^{'} = \frac{\mathrm{d}}{\mathrm{dt}} (\mathbf{Q}\mathbf{I}_p\mathbf{Q}^T\boldsymbol{\omega}) \tag{3.153}$$

where $\mathbf{a}_{O'}$ is the acceleration of point $O^{'}$ and where it is assumed that the center of mass of the platform lies in $O^{'}$ and $\mathbf{I}_p$ is the inertia tensor of the platform body expressed in

the local frame, and

$$\mathbf{f}_i = \begin{bmatrix} 0 \\ 0 \\ f_i \end{bmatrix}, \quad \mathbf{a}_{O'} = \begin{bmatrix} \ddot{x} \\ \ddot{y} \\ \ddot{z} \end{bmatrix} \tag{3.154}$$

with $i = 1, \ldots, 5$.

Equations (3.152) and (3.153) consist of six scalar equations and six unknowns, which can be written as

$$\mathbf{d}_f = \mathbf{C}_f \mathbf{f} \tag{3.155}$$

where

$$\begin{aligned} \mathbf{f} &= [\, f_1 \quad f_2 \quad f_3 \quad f_4 \quad f_5 \quad g_{5y} \,]^T \\ \mathbf{d}_f &= [\, d_{fx} \quad d_{fy} \quad d_{fz} \quad d_{mx} \quad d_{my} \quad d_{mz} \,]^T \\ \mathbf{C}_f &= \begin{bmatrix} c_f^{11} & c_f^{12} & c_f^{13} & c_f^{14} & c_f^{15} & c_f^{16} \\ c_f^{21} & c_f^{22} & c_f^{23} & c_f^{24} & c_f^{25} & c_f^{26} \\ c_f^{31} & c_f^{32} & c_f^{33} & c_f^{34} & c_f^{35} & c_f^{36} \\ c_f^{41} & c_f^{42} & c_f^{43} & c_f^{44} & c_f^{45} & c_f^{46} \\ c_f^{51} & c_f^{52} & c_f^{53} & c_f^{54} & c_f^{55} & c_f^{56} \\ c_f^{61} & c_f^{62} & c_f^{63} & c_f^{64} & c_f^{65} & c_f^{66} \end{bmatrix} \end{aligned}$$

where the elements of vector $\mathbf{d}_f$ and matrix $\mathbf{C}_f$ are obtained from eqs.(3.152) and (3.153). Equation (3.155) is readily solved for vector $\mathbf{f}$. The determination of the forces $\mathbf{g}_i (i = 1, \ldots, 4)$ mentioned above is now discussed. Moreover, the detailed expressions associated with the elements of the matrix $\mathbf{C}_f$ and vector $\mathbf{d}_f$ are given in Appendix D.

Figure 3.9 represents the forces acting on the two links of each leg. First, considering the upper link, by the application of the Euler equation with respect to point O_i', one can obtain force $\mathbf{g}_i$. One has

$$-\mathbf{Q}_{iu}[(\mathbf{g}_i + \mathbf{f}_i) \times \mathbf{l}_{iu}] - (m_{iu}\mathbf{a}_{iu} - \mathbf{w}_{iu}) \times \mathbf{Q}_{iu}\mathbf{r}_{iu} = \mathbf{f}_{iu} + \mathbf{m}_{iu}, \quad i = 1, \ldots, 4 \tag{3.156}$$

where $\mathbf{g}_i$ is a force vector normal to the axis of the second moving link and $\mathbf{a}_{iu}$ is the linear acceleration of the center of mass of the upper link of the ith leg. They are expressed in the fixed coordinate system. Vectors $\mathbf{r}_{iu}$ and $\mathbf{w}_{iu}$ have been previously defined, and

$$\mathbf{g}_i = \begin{bmatrix} g_{ix} \\ g_{iy} \\ 0 \end{bmatrix}, \quad \mathbf{f}_i = \begin{bmatrix} 0 \\ 0 \\ f_i \end{bmatrix} \tag{3.157}$$

and

$$\begin{aligned}
\mathbf{a}_{iu} &= \ddot{\mathbf{p}}_i + \dot{\boldsymbol{\omega}}_{iu} \times (\mathbf{Q}_{iu}\mathbf{r}_{iu}) + \boldsymbol{\omega}_{iu} \times (\boldsymbol{\omega}_{iu} \times (\mathbf{Q}_{iu}\mathbf{r}_{iu})) \\
\mathbf{a}_{il} &= \dot{\boldsymbol{\omega}}_i \times \mathbf{r}_{il} + \boldsymbol{\omega}_i \times (\boldsymbol{\omega}_i \times \mathbf{r}_{il}) \\
\mathbf{f}_{iu} &= m_{iu}\mathbf{a}_{iu} \times \mathbf{Q}_i(\boldsymbol{\rho}_i - \mathbf{r}_{iu}) = \begin{bmatrix} F_{iux} \\ F_{iuy} \\ F_{iuz} \end{bmatrix} \\
\mathbf{f}_{il} &= m_{il}\mathbf{a}_{il} \times \mathbf{Q}_i\mathbf{r}_{il} = \begin{bmatrix} F_{ilx} \\ F_{ily} \\ F_{ilz} \end{bmatrix} \\
\mathbf{m}_{iu} &= \frac{\mathrm{d}}{\mathrm{dt}}(\mathbf{Q}_{iu}\mathbf{I}_{iu}\mathbf{Q}_{iu}^T\boldsymbol{\omega}_{iu}) = \begin{bmatrix} M_{iux} \\ M_{iuy} \\ M_{iuz} \end{bmatrix} \\
\mathbf{m}_{il} &= \frac{\mathrm{d}}{\mathrm{dt}}(\mathbf{Q}_{il}\mathbf{I}_{il}\mathbf{Q}_{il}^T\boldsymbol{\omega}_{il}) = \begin{bmatrix} M_{ilx} \\ M_{ily} \\ M_{ilz} \end{bmatrix}
\end{aligned}$$

where m_{iu} and m_{il} are the masses of the upper and lower links of the ith leg, while $\mathbf{I}_{iu}$ and $\mathbf{I}_{il}$ are their inertia tensors.

Taking the first two components of eq.(3.156) and solving for the two unknowns g_{ix} and g_{iy}, one obtains

$$g_{ix} = [-M_{iux} - r_{iu}(F_{iuz}\cos\beta_i - F_{iux}\sin\beta_i)]/l_{i2} \tag{3.158}$$

$$g_{iy} = [-M_{iuy} - r_{iu}(F_{iuz}\cos\beta_i - (F_{iux} - m_{iu}g)\sin\beta_i)]/l_{i2} \tag{3.159}$$

Substituting eqs.(3.158) and (3.159) into equation (3.155), one obtains the forces $\mathbf{f}$.

In order to compute the generalized input forces (here the ith generalized input force is the torque τ_i exerted around the revolute joint connecting the leg to the base of the manipulator), one must first find the constraint forces in the joint connecting the two links of the leg. This can be achieved by applying Newton's equation to the upper link, i.e.,

$$\mathbf{Q}_{iu}(\mathbf{d}_i - \mathbf{g}_i - \mathbf{f}_i) + \mathbf{w}_{iu} = m_{iu}\mathbf{a}_{iu}, \quad i = 1, \ldots, 4 \tag{3.160}$$

where $\mathbf{d}_i$ is the constraint force between the two links of the ith leg.

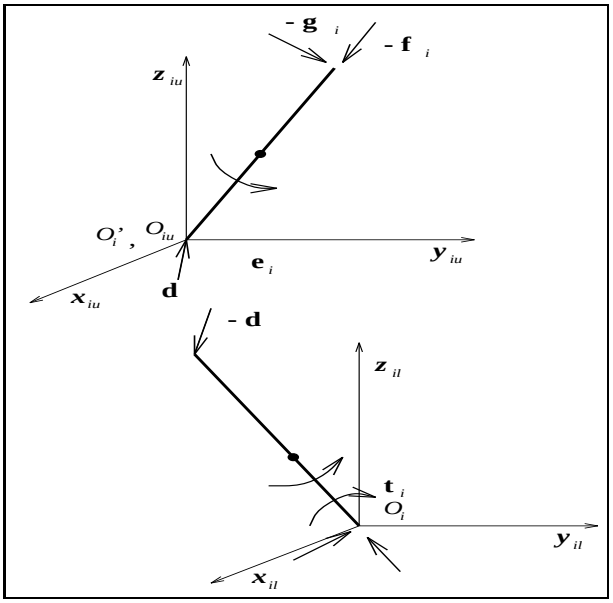

Figure 3.9: The forces acting on the two links of the ith leg for the manipulator with revolute actuators.

From eq.(3.160), one obtains

$$\mathbf{d}_i = \begin{bmatrix} g_{ix} - F_{iux}\cos\alpha_i\cos\beta_i + F_{iuy}\sin\alpha_i - (F_{iuz} - m_{iu}g)\cos\alpha_i\sin\beta_i \\ g_{iy} - F_{iuy}\cos\alpha_i - F_{iux}\cos\beta_i\sin\alpha_i - (F_{iuz} - m_{iu}g)\sin\alpha_i\sin\beta_i \\ f_i - (F_{iuz} - m_{iu}g)\cos\beta_i + F_{iux}\sin\beta_i \end{bmatrix} \tag{3.161}$$

where $F_{iux}, F_{iuy}, F_{iuz}, M_{iux}, M_{iuy}$ and M_{iuz} are previously defined.

Considering axis y_{il}, the application of Euler's equation relative to this axis on the lower link, one finally obtains the input torque as

$$\tau_i = [\mathbf{Q}_{iu}\mathbf{d}_i \times \mathbf{Q}_{il}\mathbf{l}_{il} - \mathbf{w}_{il} \times \mathbf{Q}_{il}\mathbf{r}_{il} + m_{il}\mathbf{a}_{il} + \frac{\mathrm{d}}{\mathrm{dt}}(\mathbf{Q}_{il}\mathbf{I}_{il}\mathbf{Q}_{il}^T\boldsymbol{\omega}_{il})] \cdot \mathbf{j}_i \tag{3.162}$$

where $\mathbf{j}_i$ is the unit vector associated with the direction of the axis of the ith actuated revolute joint.

An example for the four-degree-of-freedom manipulator with revolute actuators is now given to illustrate the results. It is assumed that the end-effector of the manipulator follows a simple trajectory involving vertical motion along the direction of the $\mathbf{z}$ axis with the other three Cartesian coordinates fixed. The trajectory is described in detail below. The force and torque needed to produce the specified motion are obtained using the procedures presented above. The two approaches lead to identical results and the approach based on the principle of virtual work leads to a faster algorithm.

The parameters used in this example are

$$x_{o1} = -1.5,\ y_{o1} = 1.5,\ x_{o2} = -1.5, y_{o2} = 1.5,\ x_{o3} = -1.5,\ y_{o3} = -1.5$$

$$x_{o4} = -1.5,\ y_{o4} = -1.5,\ x_{o5} = 0.0,\ y_{o5} = 0.0,\ z_{oi} = 0.0 (i = 1, \ldots, 5)$$

$$a_1 = 0.2,\ b_1 = 0.6,\ c_1 = -0.4,\ a_2 = -0.6,\ b_2 = 0.6,\ c_2 = -0.4$$

$$a_3 = -0.6,\ b_3 = -0.6,\ c_3 = -0.4,\ a_4 = 0.2,\ b_4 = -0.6,\ c_4 = -0.4$$

$$a_5 = 0.6,\ b_5 = 0.0,\ c_5 = 0.0,\ l_5 = 1.5,\ l_{i1} = 1.5,\ l_{i2} = 2.5 (i = 1, \ldots, 4)$$

$$m_{iu} = m_{il} = 0.1,\ r_{iu} = 1.2,\ r_{il} = 0.7,\ (i = 1, 2, 3, 4),\ \mathbf{r}_p = \mathbf{0}$$

$$r_5 = 0.5,\ m_p = 1.5,\ m_5 = 0.1,\ K_1 = K_2 = 1$$

$$\gamma_1 = \frac{\pi}{4},\ \gamma_2 = \frac{3\pi}{4},\ \gamma_3 = \frac{5\pi}{4},\ \gamma_4 = \frac{7\pi}{4}$$

$$\mathbf{I}_{iu} = \mathbf{I}_{il} = \mathbf{I}_5 = \begin{bmatrix} 0.1/16 & 0 & 0 \\ 0 & 0.1/16 & 0 \\ 0 & 0 & 0.1/16 \end{bmatrix}, \quad \mathbf{I}_p = \begin{bmatrix} 0.08 & 0 & 0 \\ 0 & 0.08 & 0 \\ 0 & 0 & 0.08 \end{bmatrix}$$

The specified trajectory is

$$x = -1.5, \quad y = 0, \quad z = 1.0 + 0.2 \sin 3t, \quad \phi = 0.01 \tag{3.163}$$

with $K_1 = 1$, $K_2 = 1$ and $K_{i3} = -1, (i = 1, 2, 3, 4)$, the masses are given in tons, the lengths in meters and the angles in radians.

The generalized input forces obtained for the four actuated joints are represented in Figure 3.10.

3.2.2.2 Five-degree-of-freedom manipulator

Similarly, the constraint forces between the 6th leg of this manipulator and the platform as well as the associated coordinate frames are represented in Figure 3.11. Here it is assumed that $\mathbf{g}_6$ and $\mathbf{f}_6$ are normal to and along the direction of the 6th leg OP_6, namely

$$\mathbf{g}_6 = \begin{bmatrix} g_{6x} \\ g_{6y} \\ 0 \end{bmatrix}, \quad \mathbf{f}_6 = \begin{bmatrix} 0 \\ 0 \\ f_6 \end{bmatrix} \tag{3.164}$$

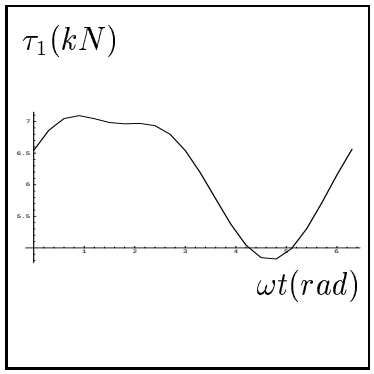

(a) Torque at the actuated joint 1.

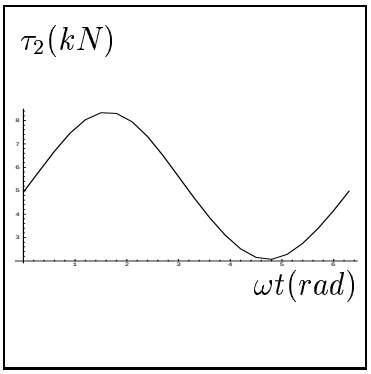

(b) Torque at the actuated joint 2.

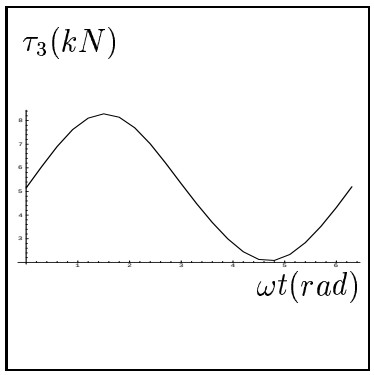

(c) Torque at the actuated joint 3.

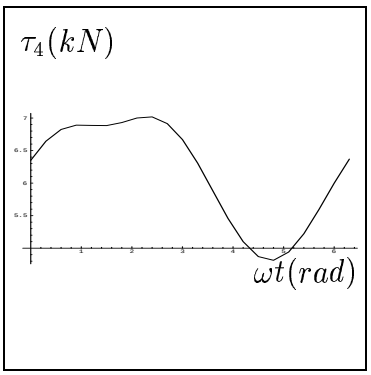

(d) Torque at the actuated joint 4.

Figure 3.10: Generalized force for the spatial four-dof mechanism at the actuated joints 1 to 4.

Moreover, the linear acceleration of the center of mass of the 6th leg can be obtained as follows

$$\mathbf{a}_6 = \dot{\boldsymbol{\omega}}_6 \times \mathbf{Q}_6\mathbf{r}_6 + \boldsymbol{\omega}_6 \times (\boldsymbol{\omega}_6 \times \mathbf{Q}_6\mathbf{r}_6) \tag{3.165}$$

where all the matrices and vectors are as previously defined.

Considering point O, one obtains two elements g_{6x} and g_{6y} of the action force $\mathbf{g}$ by the application of the Euler equation relative to this point. This Euler equation can be written as

$$-\mathbf{Q}_6[\mathbf{g}_6 + \mathbf{f}_6) \times \mathbf{l}_6] + \mathbf{w}_6 \times \mathbf{Q}_6\mathbf{r}_6 = m_6\mathbf{a}_6 \times \mathbf{Q}_6\mathbf{r}_6 + \frac{\mathrm{d}}{\mathrm{dt}}(\mathbf{Q}_6\mathbf{I}_6\mathbf{Q}_6^T\boldsymbol{\omega}_6) \tag{3.166}$$

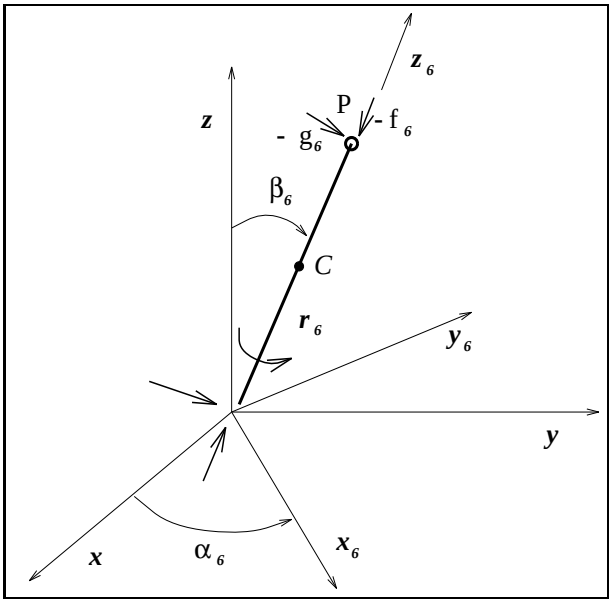

Figure 3.11: The action forces of 6th leg.

where $\mathbf{l}_6 = [0, 0, l_6]^T$ is the vector connecting point O to P_6 and $\mathbf{w}_6 = [0,\ 0,\ m_6 g]^T$ is the weight of the 6th leg, where g is the gravitational acceleration and $\mathbf{I}_6$ is the inertia tensor of the 6th leg with respect to its center of mass.

Substituting eqs.(3.122) and (3.123) into eq.(3.166) and solving the equations, one then obtains g_{6x} and g_{6y}.

Similarly, it is then assumed that forces $\mathbf{g}_i (i = 1, \ldots, 5)$—their determination will be discussed below—are known, and then forces $\mathbf{f}_i (i = 1, \ldots, 6)$ can be determined by the application of the Newton–Euler equations to the platform of the manipulator in the coordinate system of the platform.

Figure 3.12 shows the platform of the manipulator and the forces acting on it. Forces g_{ix} and $g_{iy}\,(i = 1, \ldots, 5)$ are obtained from the ith $(i = 1, \ldots, 5)$ leg as will be shown below. The remaining unknown action forces are only six elements, i.e., $f_i\,(i = 1, \ldots, 6)$. Hence, these unknown forces can be obtained by the application of Newton–Euler equations to the platform of the manipulator, i.e.,

$$\mathbf{Q}_6\mathbf{f}_6 + \mathbf{Q}_i \sum_{i=1}^{5}(\mathbf{f}_i + \mathbf{g}_i) = m_p \mathbf{a}_{O'} \tag{3.167}$$

$$\mathbf{Q}_6\mathbf{f}_6 \times \mathbf{Q}\mathbf{p}_6^{'} + [\mathbf{Q}_i \sum_{i=1}^{5}(\mathbf{f}_i + \mathbf{g}_i)] \times \mathbf{Q}\mathbf{p}_i^{'} = \frac{\mathrm{d}}{\mathrm{dt}}(\mathbf{Q}\mathbf{I}_p\mathbf{Q}^T\boldsymbol{\omega}) \tag{3.168}$$

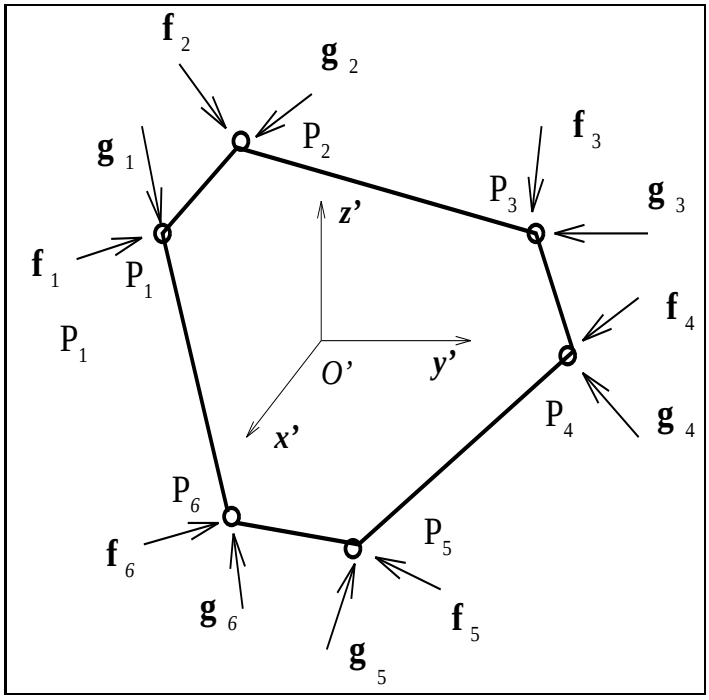

Figure 3.12: The action forces of the platform.

where $\mathbf{a}_{O'}$ is the acceleration of point $O^{'}$ and where it is assumed that the mass center of the platform lies in $O^{'}$ and $\mathbf{I}_p$ is the inertia tensor of the platform body expressed in the local frame, and

$$\mathbf{f}_i = \begin{bmatrix} 0 \\ 0 \\ f_i \end{bmatrix}, \quad \mathbf{a}_{O'} = \begin{bmatrix} \ddot{x} \\ \ddot{y} \\ \ddot{z} \end{bmatrix}, \quad \dot{\boldsymbol{\omega}} = \begin{bmatrix} \dot{\omega}_x \\ \dot{\omega}_y \\ \dot{\omega}_z \end{bmatrix} \tag{3.169}$$

with $i = 1, \ldots, 6$.

Equations (3.167) and (3.168) consist of six scalar equations and six unknowns, which can be written as

$$\mathbf{d}_f = \mathbf{C}_f \mathbf{f} \tag{3.170}$$

where

$$\begin{aligned} \mathbf{f} &= [\, f_1 \quad f_2 \quad f_3 \quad f_4 \quad f_5 \quad f_6 \,]^T \\ \mathbf{d}_f &= [\, d_{fx} \quad d_{fy} \quad d_{fz} \quad d_{mx} \quad d_{my} \quad d_{mz} \,]^T \end{aligned}$$

$$\mathbf{C}_f = \begin{bmatrix} c_f^{11} & c_f^{12} & c_f^{13} & c_f^{14} & c_f^{15} & c_f^{16} \\ c_f^{21} & c_f^{22} & c_f^{23} & c_f^{24} & c_f^{25} & c_f^{26} \\ c_f^{31} & c_f^{32} & c_f^{33} & c_f^{34} & c_f^{35} & c_f^{36} \\ c_f^{41} & c_f^{42} & c_f^{43} & c_f^{44} & c_f^{45} & c_f^{46} \\ c_f^{51} & c_f^{52} & c_f^{53} & c_f^{54} & c_f^{55} & c_f^{56} \\ c_f^{61} & c_f^{62} & c_f^{63} & c_f^{64} & c_f^{65} & c_f^{66} \end{bmatrix}$$

where the elements of vector $\mathbf{d}_f$ and matrix $\mathbf{C}_f$ are obtained from eqs.(3.167) and (3.168). Equation (3.170) is readily solved for vector $\mathbf{f}$. The determination of the forces $\mathbf{g}_i (i = 1, \ldots, 5)$ mentioned above is completed using the same procedure as in the case of the four-dof manipulator. This procedure is therefore not repeated here.

The rest of the procedure is to compute the generalized actuating forces. It is identical to the procedure in the spatial four-dof parallel mechanism.

Therefore, the expression for the computation of the generalized forces of the mechanism can be written as

$$\tau_i = [\mathbf{Q}_{iu}\mathbf{d}_i \times \mathbf{Q}_{il}\mathbf{l}_{il} - \mathbf{w}_{il} \times \mathbf{Q}_{il}\mathbf{r}_{il} + m_{il}\mathbf{a}_{il} + \frac{\mathrm{d}}{\mathrm{dt}}(\mathbf{Q}_{il}\mathbf{I}_{il}\mathbf{Q}_{il}^T\boldsymbol{\omega}_{il})] \cdot \mathbf{j}_i, \quad i = 1, \ldots, 5 \quad (3.171)$$

An example for the five-degree-of-freedom manipulator with revolute actuators is given to illustrate the results. It is assumed that the end-effector of the manipulator follows a simple trajectory involving a vertical motion along the direction of the $\mathbf{z}$ axis with the other four Cartesian fixed coordinates. The trajectory is described in detail below. The force and torque needed to produces the specified motion are obtained by the two approaches.

The parameters used in this example are given as

$$x_{o1} = -2.120,\ y_{o1} = 1.374,\ x_{o2} = -2.380, y_{o2} = 1.224,\ x_{o3} = -2.380,\ y_{o3} = -1.224$$

$$x_{o4} = -2.120,\ y_{o4} = -1.374,\ x_{o5} = 0.0,\ y_{o5} = 0.15$$

$$x_{o6} = 0.0,\ y_{o6} = -0.15,\ z_{oi} = 0.0\,(i = 1, \ldots, 6)$$

$$a_1 = 0.170,\ b_1 = 0.595,\ c_1 = -0.4,\ a_2 = -0.6,\ b_2 = 0.15,\ c_2 = -0.4$$

$$a_3 = -0.6,\ b_3 = -0.15,\ c_3 = -0.4,\ a_4 = 0.170,\ b_4 = -0.595,\ c_4 = -0.4$$

$$a_5 = 0.430,\ b_5 = -0.445,\ c_5 = -0.4,\ a_6 = 0.430,\ b_6 = 0.445,\ c_6 = -0.4$$

$$l_6 = 1.5,\ l_{iu} = 4.5,\ l_{il} = 4.5 (i = 1, \ldots, 5)$$

$$m_{iu} = m_{il} = 0.1,\ r_{iu} = 2.2,\ r_{il} = 1.2,\ (i = 1, \ldots, 5),\ \mathbf{r}_p = \mathbf{0}$$

$$r_6 = 0.5,\ m_p = 1.5,\ m_6 = 0.1,\ K = -1,\ K_{i1} = -1,\ (i = 1, \ldots, 5)$$

$$\mathbf{I}_{iu} = \mathbf{I}_{il} = \mathbf{I}_6 = \begin{bmatrix} 0.1/16 & 0 & 0 \\ 0 & 0.1/16 & 0 \\ 0 & 0 & 0.1/16 \end{bmatrix}, \quad \mathbf{I}_p = \begin{bmatrix} 0.08 & 0 & 0 \\ 0 & 0.08 & 0 \\ 0 & 0 & 0.08 \end{bmatrix}$$

The specified trajectory is

$$x = -1.5, \quad y = 0, \quad z = 1.0 + 0.2 \sin 0.5t, \quad \phi = 0.0, \quad \theta = 0.0 \tag{3.172}$$

The resulting generalized input forces for five actuated joints are represented in Figures 3.13 and 3.14.

3.2.2.3 Six-degree-of-freedom manipulator

Since the Newton-Euler formulation has been applied to the six-dof manipulator by other authors, no derivation is presented here. An example is simply given to illustrate the results. In this example , it is assumed that the end-effector of the manipulator follows a simple trajectory involving a vertical motion along the direction of the **z** axis with the other five Cartesian fixed coordinates. The trajectory is described in detail below. The discussed above torques needed to produce the specified motion are obtained by the two approaches.

The parameters used in this example are given as

$$x_{o1} = -2.120,\ y_{o1} = 1.374,\ x_{o2} = -2.380, y_{o2} = 1.224,\ x_{o3} = -2.380,\ y_{o3} = -1.224$$

$$x_{o4} = -2.120,\ y_{o4} = -1.374,\ x_{o5} = 0.0,\ y_{o5} = 0.15$$

$$x_{o6} = 0.0,\ y_{o6} = -0.15,\ z_{oi} = 0.0\,(i = 1, \ldots, 6)$$

$$a_1 = 0.170,\ b_1 = 0.595,\ c_1 = -0.4,\ a_2 = -0.6,\ b_2 = 0.15,\ c_2 = -0.4$$

$$a_3 = -0.6,\ b_3 = -0.15,\ c_3 = -0.4,\ a_4 = 0.170,\ b_4 = -0.595,\ c_4 = -0.4$$

$$a_5 = 0.430,\ b_5 = -0.445,\ c_5 = -0.4,\ a_6 = 0.430,\ b_6 = 0.445,\ c_6 = -0.4$$

$$l_6 = 1.5,\ l_{iu} = 4.5,\ l_{il} = 4.5 (i = 1, \ldots, 5)$$

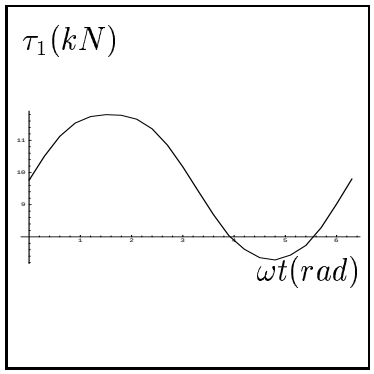

(a) Torque at the actuated joint 1.

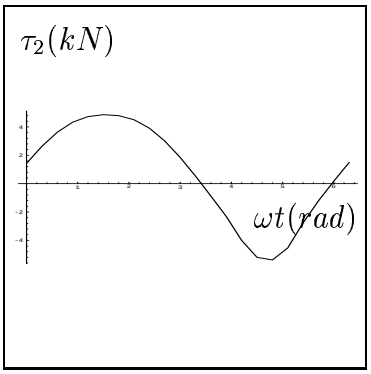

(b) Torque at the actuated joint 2.

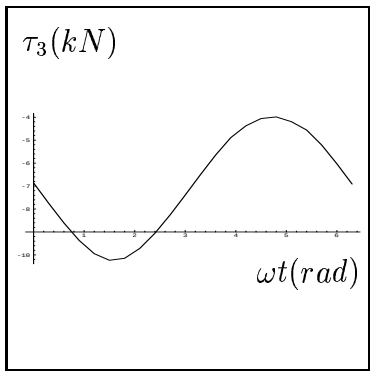

(c) Torque at the actuated joint 3.

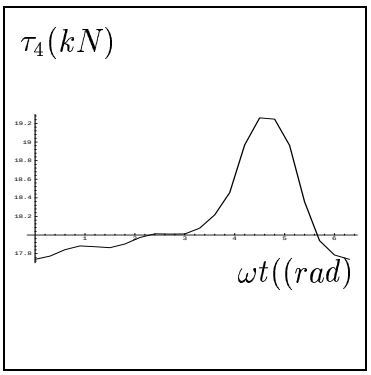

(d) Torque at the actuated joint 4.

Figure 3.13: Generalized force for the spatial five-dof mechanism at the actuated joints 1 to 4.

$$m_{iu} = m_{il} = 0.1,\ r_{iu} = 2.2,\ r_{il} = 1.2,\ (i = 1, \ldots, 5),\ \mathbf{r}_p = \mathbf{0}$$

$$r_6 = 0.5,\ m_p = 1.5,\ m_6 = 0.1,\ K = -1,\ K_{i1} = -1,\ (i = 1, \ldots, 5)$$

$$\mathbf{I}_{iu} = \mathbf{I}_{il} = \mathbf{I}_6 = \begin{bmatrix} 0.1/16 & 0 & 0 \\ 0 & 0.1/16 & 0 \\ 0 & 0 & 0.1/16 \end{bmatrix}, \quad \mathbf{I}_p = \begin{bmatrix} 0.08 & 0 & 0 \\ 0 & 0.08 & 0 \\ 0 & 0 & 0.08 \end{bmatrix}$$

The specified trajectory is

$$x = -1.5, \quad y = 0, \quad z = 1.0 + 0.2 \sin 0.5t$$

$$\phi = 0.0, \quad \theta = 0.0, \quad \psi = 0.0$$

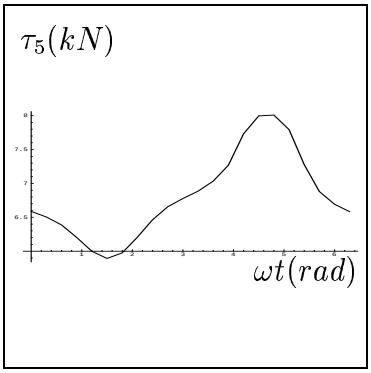

Figure 3.14: Generalized force for the spatial five-dof mechanism at the actuated joint 5.

The resulting generalized input forces for the six actuated joints are represented in Figures 3.15 and 3.16.

3.3 Conclusion

The dynamic analysis of planar and spatial parallel manipulators has been addressed in this chapter. The analysis of the position, velocity and acceleration of these manipulators has been performed. Two different methods for the derivation of the generalized input forces have been presented and each method has its own advantages. Finally, examples have been given for each manipulator in order to illustrate the results. Parallel manipulators are of interest for many applications in robotics and in flight simulation. The dynamic analysis is an important issue for the design and control of the manipulators and can be efficiently handled with the procedures described in this chapter.

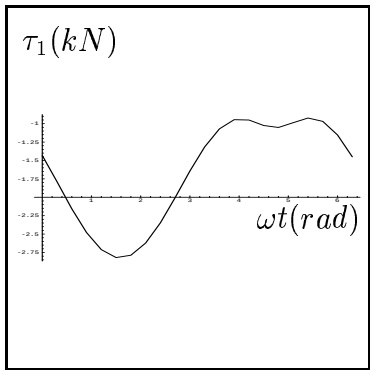

(a) Torque at the actuated joint 1.

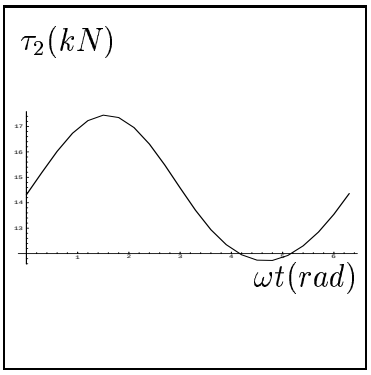

(b) Torque at the actuated joint 2.

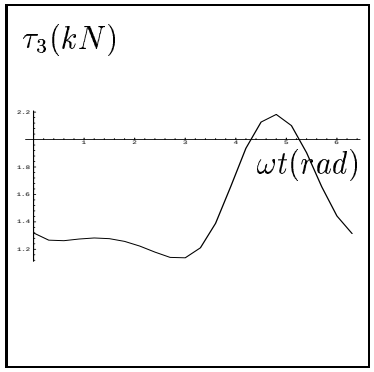

(c) Torque at the actuated joint 3.

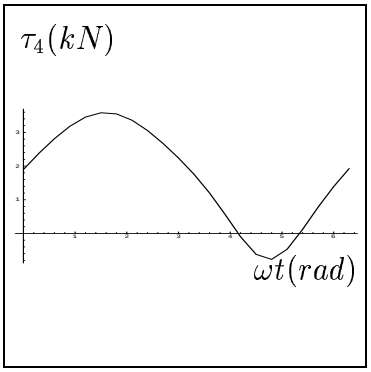

(d) Torque at the actuated joint 4.

Figure 3.15: Generalized force for the spatial six-dof mechanism at the actuated joints 1 to 4.

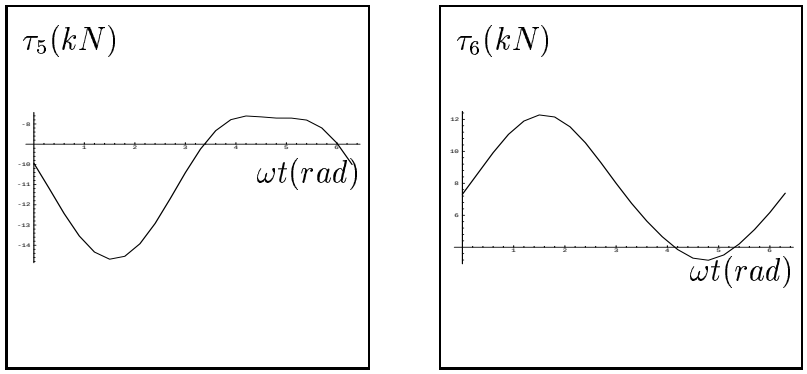

(a) Torque at the actuated joint 5.

(b) Torque at the actuated joint 6.

Figure 3.16: Generalized force for the spatial six-dof mechanism at the actuated joints 5 and 6.

Chapter 4

Static balancing

The static balancing of planar and spatial parallel mechanisms or manipulators with revolute actuators is studied in this chapter. Static balancing is an important issue in the design of parallel manipulators and mechanisms. Indeed, if a mechanism is statically balanced, its actuators will not contribute to supporting the weight of the links in any configuration. Since parallel mechanisms are often used in applications in which large loads are involved, static balancing can lead to significant improvements in the efficiency of the mechanisms. Two static balancing methods, namely, using counterweights and using springs, are used here. The first method leads to mechanisms with a stationary global center of mass while the second approach leads to mechanisms whose total potential energy (including the elastic potential energy stored in the springs as well as the gravitational potential energy) is constant. The position vector of the global center of mass and the total potential energy of the manipulator are first expressed as functions of the position and orientation of the platform as well as the joint coordinates.

Then, the kinematic constraint equations of the mechanism are introduced in order to eliminate some of the dependent variables from the expressions. Finally, conditions for static balancing are derived from the resulting expressions and examples are given in order to illustrate the design methodologies.

4.1 Balancing with counterweights

In this section, the conditions for the static balancing of the mechanisms with counterweights are derived. This is accomplished by specifying that the global center of mass of the mechanism be fixed. This property is useful for applications in which the manipulator or mechanism is required to be statically balanced for all directions. In other words, the resulting manipulator would be statically balanced for any direction of the gravity vector, which is a desirable property for portable systems which may be mounted in different orientations.

4.1.1 Planar parallel manipulators with revolute actuators

4.1.1.1 Two-degree-of-freedom manipulator

This mechanism is represented in Figure 4.1. The black dots represent the center of mass of the links while m_i, l_i, r_i and ψ_i $(i = 1, \ldots, 4)$ are respectively the mass, the length, the distance from the joint to the center of mass and the angle between the link and the line connecting the joint and the center of mass of the ith link. Moreover, it is assumed that the direction of the gravity is along the negative direction of the y axis.

The expression of the global center of mass of the mechanism can be written as

$$M\mathbf{r} = \sum_{i=1}^{4} m_i \mathbf{r}_i \tag{4.1}$$

where M and $\mathbf{r}$ are the total mass and the vector of the global center of mass, while $\mathbf{r}_i$ is the vector of the center of mass of the ith link.

Vectors $\mathbf{r}_i$ can be expressed as functions of the orientation angles of the links, i.e.,

$$\mathbf{r}_1 = \begin{bmatrix} r_1 \cos(\theta_1 + \psi_1) \\ r_1 \sin(\theta_1 + \psi_1) \end{bmatrix}, \quad \mathbf{r}_2 = \begin{bmatrix} l_1 \cos\theta_1 + r_2 \cos(\alpha_1 + \psi_2) \\ l_1 \sin\theta_1 + r_2 \sin(\alpha_1 + \psi_2) \end{bmatrix} \tag{4.2}$$

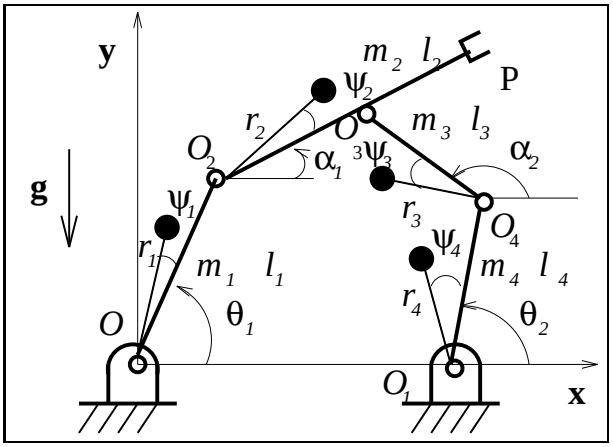

Figure 4.1: Planar two-degree-of-freedom mechanism.

$$\mathbf{r}_3 = \begin{bmatrix} l_4\cos\theta_2 + r_3\cos(\alpha_2+\psi_3) + x_0 \\ l_4\sin\theta_2 + r_3\sin(\alpha_2+\psi_3) + y_0 \end{bmatrix}, \quad \mathbf{r}_4 = \begin{bmatrix} r_4\cos(\theta_2+\psi_4) + x_0 \\ r_4\sin(\theta_2+\psi_4) + y_0 \end{bmatrix} \tag{4.3}$$

where x_0 and y_0 are the position coordinates of point O_1.

The substitution of eqs.(4.2) and (4.3) into eq.(4.1) leads to

$$M\mathbf{r} = \begin{bmatrix} r_x \\ r_y \end{bmatrix} \tag{4.4}$$

where

$$\begin{aligned} r_x &= (m_1r_1\cos\psi_1 + m_2l_1)\cos\theta_1 - m_1r_1\sin\psi_1\sin\theta_1 \\ &\quad (m_4r_4\cos\psi_4 + m_3l_4)\cos\theta_2 - m_4r_4\sin\psi_4\sin\theta_2 \\ &\quad m_2r_2\cos\psi_2\cos\alpha_1 - m_2r_2\sin\psi_2\sin\alpha_1 \\ &\quad m_3r_3\cos\psi_3\cos\alpha_2 - m_3r_3\sin\psi_3\sin\alpha_2 + (m_3+m_4)x_0 \qquad (4.5) \\ r_y &= (m_1r_1\cos\psi_1 + m_2l_1)\sin\theta_1 - m_1r_1\sin\psi_1\cos\theta_1 \\ &\quad (m_4r_4\cos\psi_4 + m_3l_4)\sin\theta_2 - m_4r_4\sin\psi_4\cos\theta_2 \\ &\quad m_2r_2\cos\psi_2\sin\alpha_1 - m_2r_2\sin\psi_2\cos\alpha_1 \\ &\quad m_3r_3\cos\psi_3\sin\alpha_2 - m_3r_3\sin\psi_3\cos\alpha_2 + (m_3+m_4)y_0 \qquad (4.6) \end{aligned}$$

From the closed loop of the mechanism $OO_2O_3O_4O_1$, one can obtain the following constraint equations

$$l_1\cos\theta_1 + l_2\cos\alpha_1 = x_0 + l_3\cos\alpha_2 + l_4\cos\theta_2 \tag{4.7}$$

$$l_1\sin\theta_1 + l_2\sin\alpha_1 = y_0 + l_3\sin\alpha_2 + l_4\sin\theta_2 \tag{4.8}$$

Eliminating $\cos\alpha_2$ and $\sin\alpha_2$ in eq.(4.4) by substitution of eqs.(4.7) and (4.8) into eqs.(4.5) and (4.6), one has

$$\begin{aligned} r_x &= A_1\cos\theta_1 + B_1\sin\theta_1 + A_2\cos\theta_2 + B_2\sin\theta_2 \\ &\quad + A_3\cos\alpha_1 + B_3\sin\alpha_1 + C_x \end{aligned} \tag{4.9}$$

$$\begin{aligned} r_y &= A_1\sin\theta_1 + B_1\cos\theta_1 + A_2\sin\theta_2 + B_2\cos\theta_2 \\ &\quad + A_3\sin\alpha_1 + B_3\cos\alpha_1 + C_y \end{aligned} \tag{4.10}$$

where

$$A_1 = m_1 r_1\cos\psi_1 + \frac{l_1}{l_3} m_3 r_3\cos\psi_3 + m_2 l_1 \tag{4.11}$$

$$B_1 = m_1 r_1\sin\psi_1 + \frac{l_1}{l_3} m_3 r_3\sin\psi_3 \tag{4.12}$$

$$A_2 = m_4 r_4\cos\psi_4 - \frac{l_4}{l_3} m_3 r_3\cos\psi_3 + m_3 l_4 \tag{4.13}$$

$$B_2 = m_4 r_4\sin\psi_4 - \frac{l_4}{l_3} m_3 r_3\sin\psi_3 \tag{4.14}$$

$$A_3 = m_2 r_2\cos\psi_2 + \frac{l_2}{l_3} m_3 r_3\cos\psi_3 + m_3 l_4 \tag{4.15}$$

$$B_3 = m_2 r_2\sin\psi_2 + \frac{l_2}{l_3} m_3 r_3\sin\psi_3 \tag{4.16}$$

and C_x and C_y are constants which are independent from the joint variables, i.e.,

$$\begin{aligned} C_x &= -m_3\frac{r_3}{l_3}(x_0\cos\psi_3 + y_0\sin\psi_3) + (m_3+m_4)x_0 \\ C_y &= -m_3\frac{r_3}{l_3}(y_0\cos\psi_3 + x_0\sin\psi_3) + (m_3+m_4)y_0 \end{aligned} \tag{4.17}$$

In order for the position vector of the global center of mass of the mechanism to be constant, the coefficients of the variables θ_1, θ_2 and α_1 in the above expressions must vanish. Therefore, the conditions for the static balancing of the two-degree-of-freedom manipulator should be

$$A_i = 0, \quad B_i = 0, \quad i = 1, 2, 3 \tag{4.18}$$

An example is now given in order to illustrate the application of the balancing conditions derived above to this type of mechanism.

For the two-dof mechanism, let

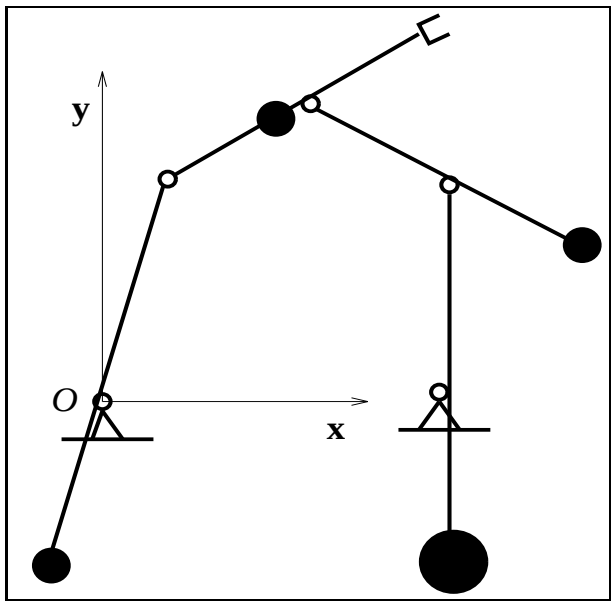

Figure 4.2: Two-degree-of-freedom balanced mechanism with counterweights.

$$m_2 = m_3 = 1,\ l_i = 1\,(i = 1, \ldots, 4)$$

$$\psi_2 = 0,\ \psi_3 = \pi,\ r_2 = r_3 = 0.5$$

$$x_1 = 1.5,\ y_1 = 0$$

where the masses are given in kilograms and the lengths in meters.

From equations (4.18) one obtains

$$m_1 = 1\,(\mathrm{kg}),\ \mathrm{m}_4 = 3\,(\mathrm{kg}),\ \mathrm{r}_1 = \mathrm{r}_2 = 0.5,\ \psi_1 = \psi_4 = \pi$$

The balanced mechanism is represented schematically in Figure 4.2 where the size of the black dots is roughly proportional to the mass of the links. The center of mass of this mechanism will remain fixed for any configuration and hence, the actuators will never contribute to supporting the weight of the links. This mechanism is gravity-compensated for any orientation and magnitude of the gravity vector.

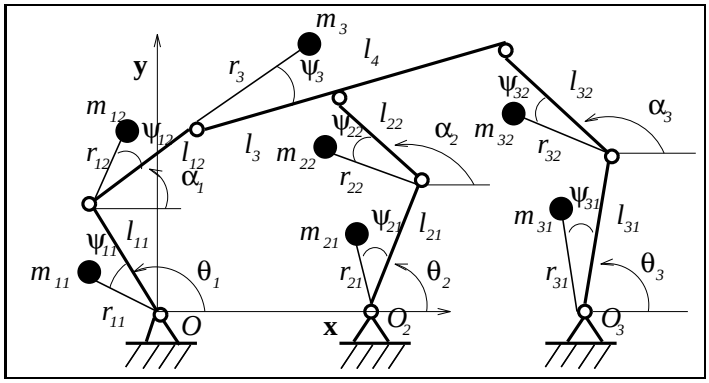

Figure 4.3: Planar three-degree-of-freedom mechanism.

4.1.1.2 Three-degree-of-freedom manipulator

This mechanism is represented in Figure 4.3. Similarly, the black dots represent the center of mass of the links while m_{ij}, l_{ij}, r_{ij} and ψ_{ij} $(i = 1, 2, 3 \quad j = 1, 2)$ are respectively the mass, the length, the distance from the joint to the center of mass and the angle between the link and the line connecting the joint and the center of mass of the jth link of the ith leg.

The expression of the global center of mass of the mechanism can be written as

$$M\mathbf{r} = m_3\mathbf{r}_3 + \sum_{i=1}^{3}(m_{i1}\mathbf{r}_{i1} + m_{i2}\mathbf{r}_{i2}) \tag{4.19}$$

where m_{i1}, m_{i2} , $\mathbf{r}_{i1}$ and $\mathbf{r}_{i2}$ are the mass and the position vector of the center of mass of the two links of the ith leg, m_3 and $\mathbf{r}_3$ are the mass and the position vector of the center of mass of the end-effector and M and $\mathbf{r}$ are the total mass and the position vector of the global center of mass.

Vectors $\mathbf{r}_i$ can be expressed as functions of the orientation angles of the links, i.e.,

$$\mathbf{r}_{i1} = \begin{bmatrix} r_{i1}\cos(\theta_i + \psi_i) + x_{0i} \\ r_{i1}\sin(\theta_i + \psi_i) + y_{0i} \end{bmatrix}, \quad i = 1, 2, 3 \tag{4.20}$$

$$\mathbf{r}_{i2} = \begin{bmatrix} l_{i1}\cos\theta_i + r_{i2}\cos(\alpha_i + \psi_i) + x_{0i} \\ l_{i1}\sin\theta_i + r_{i2}\sin(\alpha_i + \psi_i) + y_{0i} \end{bmatrix}, \quad i = 1, 2, 3 \tag{4.21}$$

$$\mathbf{r}_3 = \begin{bmatrix} l_{11}\cos\theta_1 + l_{12}\cos\alpha_1 + r_3\cos(\phi + \psi_3) + x_{0i} \\ l_{11}\sin\theta_1 + l_{12}\sin\alpha_1 + r_3\sin(\phi + \psi_3) + y_{0i} \end{bmatrix} \tag{4.22}$$

where x_{0i} and y_{0i} with $i = 2, 3$ are the position coordinates of joint O_i.

Substituting eqs.(4.20)–(4.22) into eq.(4.19) leads to

$$M\mathbf{r} = \begin{bmatrix} r_x \\ r_y \end{bmatrix} \tag{4.23}$$

where

$$\begin{aligned} r_x &= [m_{11}r_{11}\cos\psi_{11} + (m_{12}+m_3)l_{11}]\cos\theta_1 + (m_{11}r_{11}\sin\psi_{11})\sin\theta_1 \\ &\quad +(m_{21}r_{21}\cos\psi_{21} + m_{12}l_{21})\cos\theta_2 + (m_{21}r_{21}\sin\psi_{21})\sin\theta_2 \\ &\quad +(m_{31}r_{31}\cos\psi_{31} + m_{32}l_{31})\cos\theta_3 + (m_{31}r_{31}\sin\psi_{31})\sin\theta_3 \\ &\quad +(m_{12}r_{12}\cos\psi_{12} + m_3 l_{12})\cos\alpha_1 + (m_{12}r_{12}\sin\psi_{12})\sin\alpha_1 \\ &\quad +(m_{22}r_{22}\cos\psi_{22})\cos\alpha_2 + (m_{22}r_{22}\sin\psi_{22})\sin\alpha_2 \\ &\quad +(m_{32}r_{32}\cos\psi_{32})\cos\alpha_3 + (m_{32}r_{32}\sin\psi_{32})\sin\alpha_3 + C_x \end{aligned} \tag{4.24}$$

$$\begin{aligned} r_y &= (m_{11}r_{11}\sin\psi_{11})\sin\theta_1 + [m_{11}r_{11}\cos\psi_{11} + (m_{12}+m_3)l_{11}]\cos\theta_1 \\ &\quad +(m_{21}r_{21}\sin\psi_{21})\sin\theta_2 + (m_{21}r_{21}\cos\psi_{21} + m_{12}l_{21})\cos\theta_2 \\ &\quad +(m_{31}r_{31}\sin\psi_{31})\sin\theta_3 + (m_{31}r_{31}\cos\psi_{31} + m_{32}l_{31})\cos\theta_3 \\ &\quad +(m_{12}r_{12}\sin\psi_{12})\sin\alpha_1 + (m_{12}r_{12}\cos\psi_{12} + m_3 l_{12})\cos\alpha_1 \\ &\quad +(m_{22}r_{22}\sin\psi_{22})\sin\alpha_2 + (m_{22}r_{22}\cos\psi_{22})\cos\alpha_2 \\ &\quad +(m_{32}r_{32}\sin\psi_{32})\sin\alpha_3 + (m_{32}r_{32}\cos\psi_{32})\cos\alpha_3 + C_y \end{aligned} \tag{4.25}$$

where C_x and C_y are constant terms.

From the geometric relations of the mechanism (from the closed loops), one can obtain the following kinematic constraint equations

$$x_{01} + l_{11}\cos\theta_1 + l_{12}\cos\alpha_1 + l_3\cos\phi = x_{02} + l_{21}\cos\theta_2 + l_{22}\cos\alpha_2 \tag{4.26}$$

$$y_{01} + l_{11}\sin\theta_1 + l_{12}\sin\alpha_1 + l_3\sin\phi = y_{02} + l_{31}\sin\theta_2 + l_{22}\sin\alpha_2 \tag{4.27}$$

$$x_{01} + l_{11}\cos\theta_1 + l_{12}\cos\alpha_1 + l_4\cos\phi = x_{03} + l_{31}\cos\theta_3 + l_{32}\cos\alpha_3 \tag{4.28}$$

$$y_{01} + l_{11}\sin\theta_1 + l_{12}\sin\alpha_1 + l_4\sin\phi = y_{03} + l_{32}\sin\theta_3 + l_{32}\sin\alpha_3 \tag{4.29}$$

Eliminating $\cos\alpha_2$, $\sin\alpha_2$, $\cos\alpha_3$ and $\sin\alpha_3$ in eq.(4.23) by substitution of eqs.(4.26)–(4.29) into eqs.(4.24) and (4.25), one has

$$\begin{aligned} r_x &= A_1\cos\theta_1 + B_1\sin\theta_1 + A_2\cos\theta_2 + B_2\sin\theta_2 + A_3\cos\theta_3 + B_3\sin\theta_3 \\ &\quad +A_4\cos\alpha_1 + B_4\sin\alpha_1 + A_5\cos\phi + B_5\sin\phi + C_x' \end{aligned} \tag{4.30}$$

$$\begin{aligned} r_y &= A_1\sin\theta_1 + B_1\cos\theta_1 + A_2\sin\theta_2 + B_2\cos\theta_2 + A_3\sin\theta_3 + B_3\cos\theta_3 \\ &\quad +A_4\sin\alpha_1 + B_4\cos\alpha_1 + A_5\sin\phi + B_5\cos\phi + C_y' \end{aligned} \tag{4.31}$$

where

$$\begin{aligned}
A_1 &= m_{11}r_{11}\cos\psi_{11} + (m_{12}+m_3)l_{11} \\
&\quad + \frac{l_{11}}{l_{22}}m_{22}r_{22}\cos\psi_{22} + \frac{l_{11}}{l_{32}}m_{32}r_{32}\cos\psi_{32} && (4.32)\\
B_1 &= m_{11}r_{11}\sin\psi_{11} + \frac{l_{11}}{l_{22}}m_{22}r_{22}\sin\psi_{22} + \frac{l_{11}}{l_{32}}m_{32}r_{32}\sin\psi_{32} && (4.33)\\
A_2 &= m_{21}r_{21}\cos\psi_{21} + m_{22}l_{21} - \frac{l_{21}}{l_{22}}m_{22}r_{22}\cos\psi_{22} && (4.34)\\
B_2 &= m_{21}r_{21}\sin\psi_{21} - \frac{l_{21}}{l_{22}}m_{22}r_{22}\sin\psi_{22} && (4.35)\\
A_3 &= m_{31}r_{31}\cos\psi_{31} + m_{32}l_{31} - \frac{l_{31}}{l_{32}}m_{32}r_{32}\cos\psi_{32} && (4.36)\\
B_3 &= m_{31}r_{31}\sin\psi_{31} - \frac{l_{31}}{l_{32}}m_{32}r_{32}\sin\psi_{32} && (4.37)\\
A_4 &= m_{12}r_{12}\cos\psi_{12} + m_3 l_{12} + \frac{l_{12}}{l_{32}}m_{32}r_{32}\cos\psi_{32} + \frac{l_{12}}{l_{22}}m_{22}r_{22}\cos\psi_{22} && (4.38)\\
B_4 &= m_{12}r_{12}\sin\psi_{12} + \frac{l_{12}}{l_{32}}m_{32}r_{32}\sin\psi_{32} + \frac{l_{12}}{l_{22}}m_{22}r_{22}\sin\psi_{22} && (4.39)\\
A_5 &= m_3 r_3\cos\psi_3 + \frac{l_4}{l_{32}}m_{32}r_{32}\cos\psi_{32} + \frac{l_3}{l_{22}}m_{22}r_{22}\cos\psi_{22} && (4.40)\\
B_5 &= m_3 r_3\sin\psi_3 + \frac{l_4}{l_{32}}m_{32}r_{32}\sin\psi_{32} + \frac{l_3}{l_{22}}m_{22}r_{22}\sin\psi_{22} && (4.41)
\end{aligned}$$

and where C_x' and C_y' are constant terms which can be written as

$$\begin{aligned}
C_x &= (m_{21}m_{22} - \frac{1}{l_{22}})x_{01} + (m_{31}m_{32} - \frac{1}{l_{32}})x_{02} - \frac{y_{01}}{l_{22}} - \frac{y_{02}}{l_{32}} \\
C_y &= (m_{21}m_{22} - \frac{1}{l_{22}})y_{01} + (m_{31}m_{32} - \frac{1}{l_{32}})y_{02} - \frac{x_{01}}{l_{22}} - \frac{x_{02}}{l_{32}}
\end{aligned}$$

Similarly to the previous case, in order for the position vector of the global center of mass of the mechanism be constant, the coefficients of variables $\theta_1, \theta_2, \theta_3, \phi$ and α_1 in the above expressions must vanish. Therefore, the conditions for the static balancing of the three-degree-of-freedom mechanism should be

$$A_i = 0, \quad B_i = 0, \quad i = 1, \ldots, 5 \tag{4.42}$$

An example is now given to illustrate the results derived above.

For the three-dof mechanism, let

$$m_3 = 1,\ m_{i1} = m_{i2} = 1\ (i = 2, 3)$$

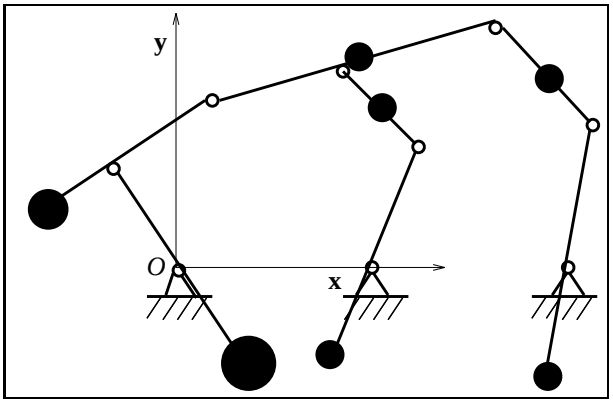

Figure 4.4: Three-degree-of-freedom balanced mechanism with counterweights.

$$l_3 = 0.6,\ l_4 = 1.2,\ l_{i1} = l_{i2} = 1 (i = 1, 2, 3)$$

$$r_{21} = r_{22} = r_{31} = r_{32} = 0.5,\ r_3 = 0.6,\ \psi_{22} = \psi_{32} = 0$$

$$x_0 = 0, x_{02} = 1.5,\ x_{03} = 3,\ y_0 = y_{02} = y_{03} = 0$$

where the masses are given in kilograms and the lengths in meters.

From equations (4.42) one obtains

$$m_{11} = 5\,(\mathrm{kg}),\ \mathrm{m}_{12} = 3\,(\mathrm{kg}),\ \mathrm{r}_{11} = \mathrm{r}_{12} = 0.5$$

$$\psi_{11} = \psi_{12} = \psi_{21} = \psi_{31} = \pi,\ \psi_3 = 0$$

The balanced mechanism is represented schematically in Figure 4.4.

4.1.2 Spatial parallel manipulators with revolute actuators

The conditions for the static balancing of spatial parallel mechanisms will now be derived using counterweights.

Static balancing using counterweights consists in ensuring that the global center of mass of the mechanism remains fixed for any configuration of the mechanism. In other words, the resulting manipulator would be statically balanced for any direction of the gravity vector — and hence the weight of the mechanism does not have any effect on the actuators —, which is a desirable property for portable systems which may be mounted in different orientations.

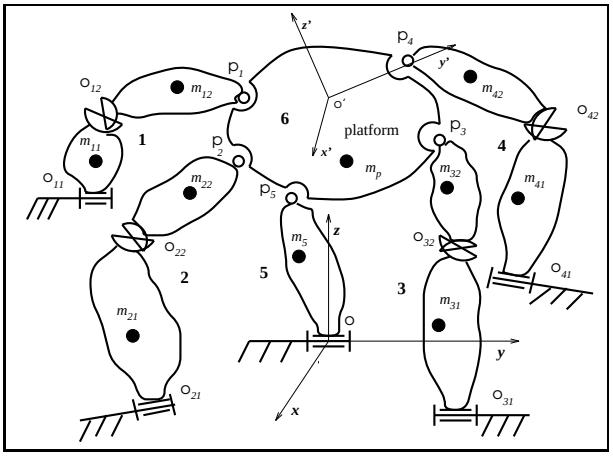

Figure 4.5: Geometric representation of the spatial four-degree-of-freedom system with revolute actuators.

4.1.2.1 Four-degree-of-freedom manipulator

The spatial four-dof parallel mechanism is represented in Figure 4.5. A reference coordinate frame attached to each link must first be defined.

The coordinate frame of the base, designated as the $O - x, y, z$ frame is fixed to the base with its Z-axis pointing vertically upward. Similarly, the moving coordinate frame $O^{'} - x^{'}, y^{'}, z^{'}$ is attached to the platform, as represented in Figure 4.5.

The Cartesian coordinates of the platform are given by the position of point O' with respect to the fixed frame, noted $\mathbf{p} = [x,\ y,\ z]^T$ and the orientation of the platform (the orientation of frame $O' - x'y'z'$ with respect to the fixed frame), represented by matrix $\mathbf{Q}$, which can be written as

$$\mathbf{Q} = \begin{bmatrix} q_{11} & q_{12} & q_{13} \\ q_{21} & q_{22} & q_{23} \\ q_{31} & q_{32} & q_{33} \end{bmatrix} \tag{4.43}$$

where the entries can be expressed as functions of Euler angles, quadratic invariants, linear invariants or any other representation.

Finally, the coordinates of point P_i (Figure 4.5) relative to the moving coordinate frame of the platform are noted (a_i, b_i, c_i) with $i = 1, \ldots, 5$.

One can write

$$\mathbf{p}_i = \mathbf{p}_5 + \mathbf{Q}(\mathbf{p}_i^{'} - \mathbf{p}_5^{'}), \quad i = 1, \ldots, 4 \tag{4.44}$$

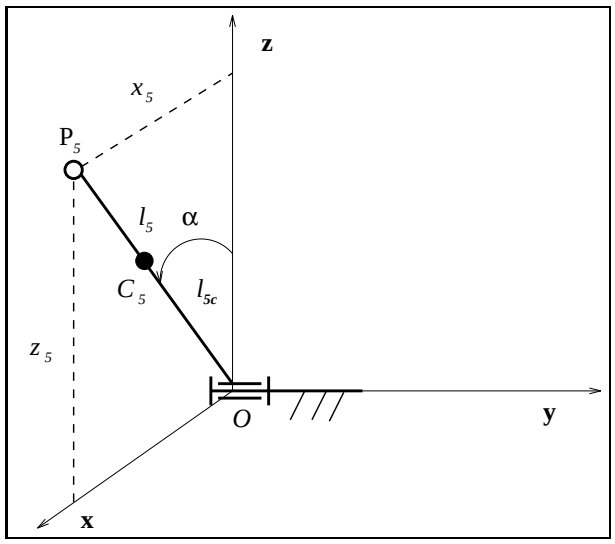

Figure 4.6: Geometry of the fifth leg.

where $\mathbf{p}_i (i = 1, \ldots, 4)$ is the position vector of point P_i expressed in the fixed coordinate frame, $\mathbf{p}_i^{'}$ is the position vector of point P_i expressed in the moving coordinate frame, and

$$\mathbf{p}_i = \begin{bmatrix} x_i \\ y_i \\ z_i \end{bmatrix}, \quad \mathbf{p}_i^{'} = \begin{bmatrix} a_i \\ b_i \\ c_i \end{bmatrix} \tag{4.45}$$

Vector $\mathbf{p}_5$ is the position vector of point P_5 expressed in the fixed coordinate frame, as represented in Figure 4.6 and can be expressed as

$$\mathbf{p}_5 = \begin{bmatrix} l_5 \sin\alpha \\ 0 \\ l_5 \cos\alpha \end{bmatrix} \tag{4.46}$$

If it is assumed that the center of mass of the 5th leg is located on the line connecting point O and P_5, one can compute the position vector of the center of mass of the 5th leg, as represented in Figure 4.6, i.e.,

$$\mathbf{r}_5 \;=\; \mathbf{p}_5(\frac{l_{5c}}{l_5}) \tag{4.47}$$

where $\mathbf{r}_5$ is the position vector of the center of mass of the 5th leg and l_5 is the length of the leg and l_{5c} is the distance from O to C_5.

The two links of the ith leg of the mechanism are represented schematically in Figure 4.7. A reference frame noted $O_{i1} - x_i, y_i, z_i$ is attached to the first link of the

leg. Point O_{i1} is located at the center of the first revolute joint. The coordinates of point O_{i1} expressed in the base coordinate frame are (x_{io}, y_{io}, z_{io}), where $i = 1, \ldots, 4$. Moreover, the unit vectors defined in the direction of axes x_i, y_i and z_i are noted $\mathbf{x}_{i1}, \mathbf{y}_{i1}$ and $\mathbf{z}_{i1}$, respectively.

Vector $\mathbf{z}_{i1}$ is defined along the axis directed from point O_{i1} toward point O_{i2} while vector $\mathbf{x}_{i1}$ is defined along the direction of the first revolute joint axis. Finally, vector $\mathbf{y}_{i1}$ is defined as

$$\mathbf{y}_{i1} = \frac{\mathbf{z}_{i1} \times \mathbf{x}_{i1}}{|\mathbf{z}_{i1} \times \mathbf{x}_{i1}|}, \quad i = 1, \ldots, 4 \tag{4.48}$$

Also, points C_{il} and C_{iu} denote respectively the center of mass of the lower and upper link of each leg.

Let θ_i be the joint variable associated with the first revolute joint of the ith leg and γ_i be the angle between the positive direction of the $\mathbf{x}$ axis of the base coordinate frame and the coordinate axis $\mathbf{x}_{i1}$, where it is assumed that vector $\mathbf{x}_{i1}$ is contained in the xy plane of the fixed reference frame (Figure 4.7). One can write the rotation matrix giving the orientation of frame $O_{i1} - x_i, y_i, z_i$ with respect to the reference frame attached to the base as

$$\mathbf{Q}_{il} = \begin{bmatrix} \cos\gamma_i & -\sin\gamma_i \cos\theta_i & \sin\gamma_i \sin\theta_i \\ \sin\gamma_i & \cos\gamma_i \cos\theta_i & -\cos\gamma_i \sin\theta_i \\ 0 & \sin\theta_i & \cos\theta_i \end{bmatrix}, \quad i = 1, \ldots, 4 \tag{4.49}$$

Moreover, it is assumed that the center of mass of the second link of the ith leg lies on line $O_{i2}P_i$, as represented in Figure 4.7. One can then write

$$\mathbf{p}_{i1} = \mathbf{r}_{io} + \mathbf{Q}_{i1}\mathbf{l}_{il}, \quad i = 1, \ldots, 4 \tag{4.50}$$

where $\mathbf{p}_{i1}$ and $\mathbf{r}_{io}$ are respectively the position vectors of points O_{i2} and O_{i1} expressed in the base coordinate frame, as represented in Figure 4.7, while $\mathbf{l}_{il}$ is the vector pointing from O_{i1} to O_{i2} and expressed in the local coordinate frame, and

$$\mathbf{r}_{io} = \begin{bmatrix} x_{io} \\ y_{io} \\ z_{io} \end{bmatrix}, \quad \mathbf{p}_{i1} = \begin{bmatrix} x_{i1} \\ y_{i1} \\ z_{i1} \end{bmatrix}, \quad \mathbf{l}_{il} = \begin{bmatrix} 0 \\ 0 \\ l_{il} \end{bmatrix}, \quad i = 1, \ldots, 4 \tag{4.51}$$

where l_{il} is the distance from O_{i1} to O_{i2}.

Eq.(4.50) can be written in component form as

$$x_{i1} = x_{io} + l_{i1} \sin\gamma_i \sin\theta_i, \quad i = 1, \ldots, 4 \tag{4.52}$$

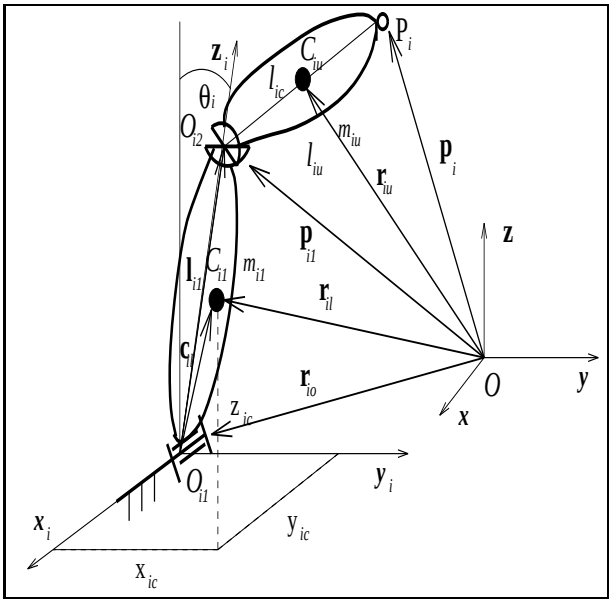

Figure 4.7: Geometry of the ith leg.

$$y_{i1} = y_{io} - l_{i1}\cos\gamma_i \sin\theta_i, \quad i = 1, \ldots, 4 \tag{4.53}$$

$$z_{i1} = z_{io} + l_{i1}\cos\theta_i, \quad i = 1, \ldots, 4 \tag{4.54}$$

Then, one can compute the position vector of the center of mass of the second link of the ith leg from the position vectors of points O_{i2} and P_i as

$$\mathbf{r}_{iu} = \mathbf{p}_i - \frac{l_{ic}}{l_{iu}}(\mathbf{p}_i - \mathbf{p}_{i1}), \quad i = 1, \ldots, 4 \tag{4.55}$$

where $\mathbf{r}_{iu}$ is the position vector of the center of mass of the upper link of the ith leg and where l_{iu} and l_{ic} are respectively the distance from O_{i2} to P_i and from O_{i2} to C_{iu}. Moreover, position vector $\mathbf{p}_i$ can be expressed as a function of the position and orientation of the platform, i.e.,

$$\mathbf{p}_i = \mathbf{p} + \mathbf{Q}\mathbf{p}_i^{'}, \quad i = 1, \ldots, 4 \tag{4.56}$$

where

$$\mathbf{p} = \begin{bmatrix} x \\ y \\ z \end{bmatrix}, \quad \mathbf{p}_i^{'} = \begin{bmatrix} a_i \\ b_i \\ c_i \end{bmatrix}, \quad i = 1, \ldots, 4 \tag{4.57}$$

With all the above definition, the global center of mass of the manipulator can be written as

$$M\mathbf{r} = m_p\mathbf{r}_p + m_5\mathbf{r}_5 + \sum_{i=1}^{4}(m_{il}\mathbf{r}_{il} + m_{iu}\mathbf{r}_{iu}) \tag{4.58}$$

where M is the total mass of all moving links of the mechanism, m_p, m_5, m_{iu} and m_{il} are respectively the masses of the platform, of the special 5th leg, of the upper link and lower link of the ith leg, and

$$M = m_p + m_5 + \sum_{i=1}^{4}(m_{il} + m_{iu}) \tag{4.59}$$

while $\mathbf{r}_p$ and $\mathbf{r}_{il}$ are respectively the position vectors of the center of mass of the platform and of the lower links of the ith leg, namely

$$\mathbf{r}_p = \mathbf{p} + \mathbf{Q}\mathbf{c}_p \tag{4.60}$$

$$\mathbf{r}_{il} = \mathbf{r}_{io} + \mathbf{Q}_{il}\mathbf{c}_{il}, \quad i = 1, \ldots, 4 \tag{4.61}$$

where $\mathbf{c}_p$ and $\mathbf{c}_{il}$ are the position vectors of the center of mass of the platform and the lower link of the ith leg expressed in the local reference frame, and whose components are given as

$$\mathbf{c}_p = \begin{bmatrix} x_p \\ y_p \\ z_p \end{bmatrix}, \quad \mathbf{c}_{il} = \begin{bmatrix} x_{ic} \\ y_{ic} \\ z_{ic} \end{bmatrix}, \quad i = 1, \ldots, 4 \tag{4.62}$$

Substituting eqs.(4.47), (4.55), (4.60) and (4.61) into eq.(4.58), one then obtains

$$M\mathbf{r} = \begin{bmatrix} r_x \\ r_y \\ r_z \end{bmatrix} \tag{4.63}$$

where

$$\begin{aligned} r_x &= \sum_{i=1}^{4}(D_i \sin\gamma_i \sin\theta_i - D_{i+4} \sin\gamma_i \cos\theta_i) \\ &\quad + D_9 q_{11} + D_{10} q_{12} + D_{11} q_{13} + D_{12} \sin\alpha + D_{xo} \end{aligned} \tag{4.64}$$

$$\begin{aligned} r_y &= \sum_{i=1}^{4}(D_{i+4} \cos\gamma_i \cos\theta_i - D_i \cos\gamma_i \sin\theta_i) \\ &\quad + D_9 q_{11} + D_{10} q_{12} + D_{11} q_{13} + D_{yo} \end{aligned} \tag{4.65}$$

$$\begin{aligned} r_z &= \sum_{i=1}^{4}(D_i \cos\theta_i + D_{i+4} \sin\theta_i) \\ &\quad + D_9 q_{11} + D_{10} q_{12} + D_{11} q_{13} + D_{12} \cos\alpha + D_{zo} \end{aligned} \tag{4.66}$$

where D_{xo}, D_{yo} and D_{zo} are constant quantities, and

$$D_i = m_{il} z_{ic} + \frac{l_{il}}{l_{iu}} l_{ic} m_{iu}, \quad i = 1, \ldots, 4$$

$$
\begin{aligned}
D_{i+4} &= m_{il} y_{ic}, \quad i = 1, \ldots, 4 \\
D_9 &= m_p(x_p - a_5) + \sum_{i=1}^{4} \frac{l_{iu} - l_{ic}}{l_{iu}} m_{iu}(a_i - a_5) \\
D_{10} &= m_p(y_p - b_5) + \sum_{i=1}^{4} \frac{l_{iu} - l_{ic}}{l_{iu}} m_{iu}(b_i - a_5) \\
D_{11} &= m_p(z_p - c_5) + \sum_{i=1}^{4} \frac{l_{iu} - l_{ic}}{l_{iu}} m_{iu}(c_i - a_5) \\
D_{12} &= [l_{5c} m_5 + l_5(m_p + \sum_{i=1}^{4} \frac{l_{iu} - l_{ic}}{l_{iu}} m_{iu})]
\end{aligned}
$$

It is clear that when the coefficients of the joint and Cartesian variables in the expressions of r_x, r_y and r_z vanish, the global center of mass of the manipulator will be fixed. Hence, one obtains the conditions for static balancing as follows

$$D_i = 0, \quad i = 1, \ldots, 12 \tag{4.67}$$

An example is now given in order to illustrate the application of the balancing conditions, derived above, to this type of mechanism.

For the 4-dof manipulator with revolute actuators studied here, let

$$m_p = 10,\ m_{il} = m_{iu} = 0.1\,(i = 1, \ldots, 4)$$

$$a_1 = -0.5,\ ,b_1 = -0.5,\ c_1 = -0.3,\ a_2 = 0.5,\ ,b_2 = -0.5,\ c_2 = -0.3$$

$$a_3 = 0.5,\ b_3 = 0.5,\ c_3 = -0.3,\ a_4 = -0.5,\ b_4 = 0.5,\ c_4 = -0.3$$

$$a_5 = 0,\ b_5 = 0,\ c_5 = 0,\ l_5 = 1.0,\ l_{iu} = 0.5$$

$$l_{iu} = l_{il} = 0.5,\ l_{il} = l_{iu} = 1.0\,(i = 1, \ldots, 4)$$

$$x_{1o} = -1.5,\ y_{1o} = -1.5,\ z_{1o} = 0,\ x_{2o} = 1.5,\ y_{2o} = -1.5,\ z_{2o} = 0$$

$$x_{3o} = 1.5,\ y_{3o} = 1.5,\ z_{3o} = 0,\ x_{4o} = -1.5,\ y_{4o} = 1.5,\ z_{4o} = 0$$

$$\gamma_1 = -\frac{\pi}{4},\ \gamma_2 = \frac{\pi}{4},\ \gamma_3 = \frac{3\pi}{4},\ \gamma_4 = \frac{5\pi}{4}$$

where the masses are given in kilograms and the lengths in meters.

From equations (4.67) one obtains

$$y_{ic} = 0,\ z_{ic} = -0.5\,(i = 1, \ldots, 4)$$

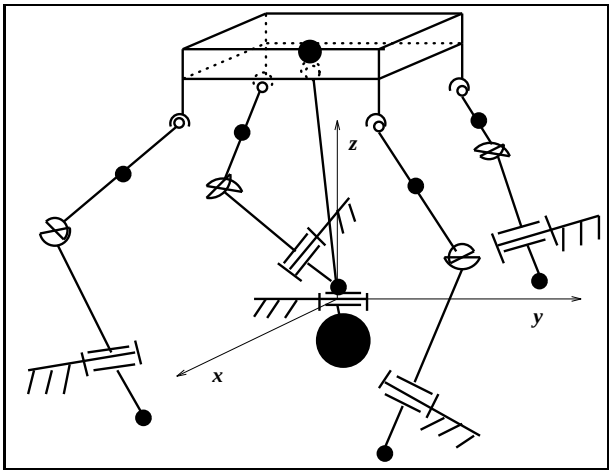

Figure 4.8: Four-degree-of-freedom balanced mechanism with revolute actuators using counterweights.

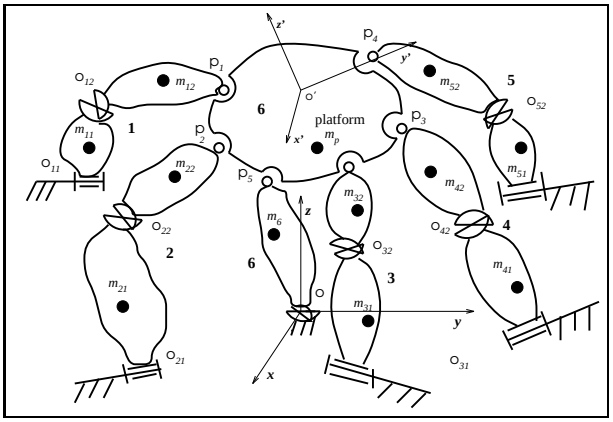

Figure 4.9: Geometric representation of the spatial five-degree-of-freedom mechanism with revolute actuated joints.

$$x_p = 0,\ y_p = 0,\ z_p = 12\,(\mathrm{cm}),\ \mathrm{l_{5c}} = -50\,(\mathrm{cm}),\ \mathrm{m_5} = 24\,(\mathrm{kg})$$

The balanced mechanism is represented schematically in Figure 4.8.

4.1.2.2 Five-degree-of-freedom manipulator

The spatial five-dof parallel mechanism is represented schematically in Figure 4.9.

For this mechanism, the coordinate frames attached to the two links of the identical actuated legs and to the platform are the same as the ones defined in the case of spatial four-dof parallel mechanism. Hence, one can write

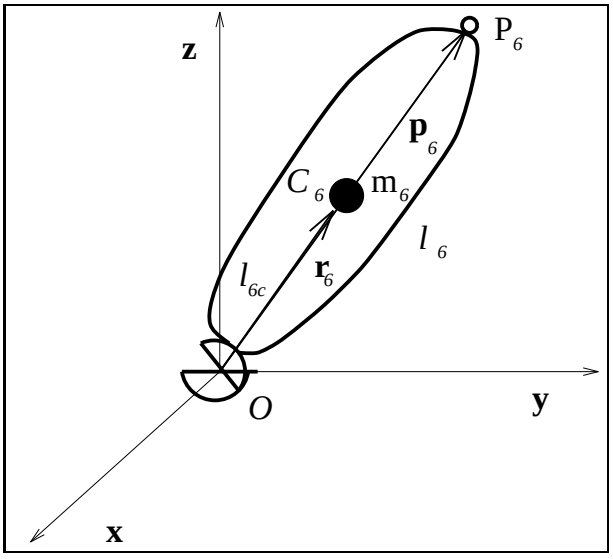

Figure 4.10: Geometry of the sixth leg.

$$\mathbf{p}_i = \mathbf{p} + \mathbf{Q}\mathbf{p}_i^{'}, \quad i = 1, \ldots, 6 \tag{4.68}$$

where $\mathbf{p}_i$ and $\mathbf{p}_i^{'}$ $(i = 1, \ldots, 6)$ are the position vector of point P_i expressed in the fixed coordinate frame and the moving coordinate frame respectively, and

$$\mathbf{p} = \begin{bmatrix} x \\ y \\ z \end{bmatrix}, \quad \mathbf{p}_i = \begin{bmatrix} x_i \\ y_i \\ z_i \end{bmatrix}, \quad \mathbf{p}_i^{'} = \begin{bmatrix} a_i \\ b_i \\ c_i \end{bmatrix}, \quad i = 1, \ldots, 6 \tag{4.69}$$

One can compute the position vector of the center of mass of the 6th leg, namely, the position vector of point C_6, as represented in Figure 4.10.

$$\mathbf{r}_6 \;\; = \;\; \mathbf{p}_6(\frac{l_{6c}}{l_6}) \tag{4.70}$$

where $\mathbf{r}_6$ is the position vector of the center of mass of the 6th leg.

Similarly to the previous case, the position vector of the center of mass of the second link of the ith leg can be determined from the position vectors of points O_{i2} and P_i as

$$\mathbf{r}_{iu} = \mathbf{p}_i - \frac{l_{ic}}{l_{iu}}(\mathbf{p}_i - \mathbf{p}_{i1}), \quad i = 1, \ldots, 5 \tag{4.71}$$

where $\mathbf{r}_{iu}$, l_{iu} and l_{ic} are as previously defined.

Then, the global center of mass of the manipulator can be expressed as

$$M\mathbf{r} = m_p\mathbf{r}_p + m_6\mathbf{r}_6 + \sum_{i=1}^{5}(m_{il}\mathbf{r}_{il} + m_{iu}\mathbf{r}_{iu}) \tag{4.72}$$

where M is the total mass of all moving links of the mechanism, m_p, m_6, m_{iu} and m_{il} are respectively the masses of the platform, of the special sixth leg, of the upper link and lower link of the ith leg, and

$$M = m_p + m_6 + \sum_{i=1}^{5}(m_{il} + m_{iu}) \tag{4.73}$$

while $\mathbf{r}_p$ and $\mathbf{r}_{il}$ are respectively the position vectors of the center of mass of the platform and of the lower links of the ith leg, namely

$$\mathbf{r}_p = \mathbf{p} + \mathbf{Q}\mathbf{c}_p \tag{4.74}$$

$$\mathbf{r}_{il} = \mathbf{r}_{io} + \mathbf{Q}_{il}\mathbf{c}_{il}, \quad i = 1, \ldots, 6 \tag{4.75}$$

where $\mathbf{c}_p$ and $\mathbf{c}_{il}$ are the position vectors of the center of mass of the platform and the first link of the ith leg expressed in the local reference frame, and whose components are given as

$$\mathbf{c}_p = \begin{bmatrix} x_p \\ y_p \\ z_p \end{bmatrix}, \quad \mathbf{c}_{il} = \begin{bmatrix} x_{ic} \\ y_{ic} \\ z_{ic} \end{bmatrix}, \quad i = 1, \ldots, 6 \tag{4.76}$$

Substituting eqs.(4.70) (4.71), (4.74) and (4.75) into eq.(4.72), one then obtains

$$M\mathbf{r} = \begin{bmatrix} r_x \\ r_y \\ r_z \end{bmatrix} \tag{4.77}$$

where

$$\begin{aligned} r_x &= \sum_{i=1}^{5}(D_i \sin\gamma_i \sin\theta_i - D_{i+5} \sin\gamma_i \cos\theta_i) \\ &\quad + D_{11}x + D_{12}q_{11} + D_{13}q_{12} + D_{14}q_{13} \end{aligned} \tag{4.78}$$

$$\begin{aligned} r_y &= \sum_{i=1}^{4}(D_{i+4} \cos\gamma_i \cos\theta_i - D_i \cos\gamma_i \sin\theta_i) \\ &\quad + D_{11}y + D_{12}q_{21} + D_{13}q_{22} + D_{14}q_{23} \end{aligned} \tag{4.79}$$

$$\begin{aligned} r_z &= \sum_{i=1}^{4}(D_i \cos\theta_i + D_{i+4} \sin\theta_i) \\ &\quad + D_{11}y + D_{12}q_{31} + D_{13}q_{32} + D_{14}q_{33} \end{aligned} \tag{4.80}$$

where D_{xo}, D_{yo} and D_{zo} are constant quantities, and

$$D_i = m_{il}z_{ic} + \frac{l_{il}}{l_{iu}}l_{ic}m_{iu}, \quad i = 1, \ldots, 5$$

$$
\begin{aligned}
D_{i+4} &= m_{il} y_{ic}, \quad i = 1, \ldots, 5 \\
D_{11} &= m_p + m_6 \frac{l_{6c}}{l_6} + \sum_{i=1}^{5} m_{iu}(1 - \frac{l_{ic}}{l_{iu}}) \\
D_{12} &= m_p x_p + m_6 a_6 \frac{l_{6c}}{l_6} + \sum_{i=1}^{5} m_{iu} a_i (1 - \frac{l_{ic}}{l_{iu}}) \\
D_{13} &= m_p y_p + m_6 b_6 \frac{l_{6c}}{l_6} + \sum_{i=1}^{5} m_{iu} b_i (1 - \frac{l_{ic}}{l_{iu}}) \\
D_{14} &= m_p z_p + m_6 c_6 \frac{l_{6c}}{l_6} + \sum_{i=1}^{5} m_{iu} c_i (1 - \frac{l_{ic}}{l_{iu}})
\end{aligned}
$$

Similarly, when the coefficients of the variables such as $D_i (i = 1, \ldots, 12)$ vanish, the global center of mass of the manipulator will be fixed. Thereby, one obtains the conditions for static balancing as follows

$$D_i = 0, \quad i = 1, \ldots, 14 \tag{4.81}$$

An example is now given in order to illustrate the application of the balancing conditions derived above to this type of mechanism.

For the 5-dof manipulator with revolute actuators, let

$$m_p = 10,\ l_{iu} = l_{il} = 1\ (i = 1, \ldots, 6)$$

$$a_1 = -0.5,\ ,b_1 = -0.5,\ c_1 = -0.3,\ a_2 = 0.5,\ ,b_2 = -0.5,\ c_2 = -0.3$$

$$a_3 = 0.5,\ b_3 = 0.5,\ c_3 = -0.3,\ a_4 = -0.5,\ b_4 = 0.5,\ c_4 = -0.3$$

$$a_5 = 0.5,\ b_5 = 0,\ c_5 = -0.3,\ a_6 = 0,\ b_6 = 0,\ c_6 = -0.3$$

$$x_{1o} = -1.5,\ y_{1o} = -1.5,\ z_{1o} = 0,\ x_{2o} = 1.5,\ y_{2o} = -1.5,\ z_{2o} = 0$$

$$x_{3o} = 1.5,\ y_{3o} = 1.5,\ z_{3o} = 0,\ x_{4o} = -1.5,\ y_{4o} = 1.5,\ z_{4o} = 0$$

$$x_{5o} = 1.5,\ y_{5o} = 0,\ z_{5o} = 0,\ x_{6o} = 0,\ y_{6o} = 0,\ z_{6o} = 0$$

$$\gamma_1 = -\frac{\pi}{4},\ \gamma_2 = \frac{\pi}{4},\ \gamma_3 = \frac{3\pi}{4},\ \gamma_4 = -\frac{\pi}{4},\ \gamma_5 = \frac{\pi}{4}$$

$$y_{ic} = 0,\ z_{ic} = -0.5,\ x_p = 0$$

where the masses are given in kilograms and the lengths in meters.

From equations (4.81) one obtains

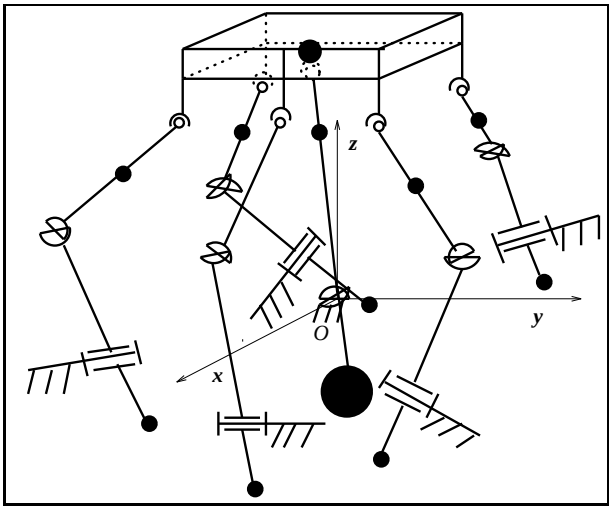

Figure 4.11: Five-degree-of-freedom balanced mechanism with revolute actuators using counterweights.

$$m_{iu} = 4\,(\mathrm{kg}),\ \mathrm{m_{il}} = 13\,(\mathrm{kg})\ (\mathrm{i} = 1, \ldots, 6)$$

$$y_p = 0,\ z_p = 30\,(\mathrm{cm})$$

The balanced mechanism is represented schematically in Figure 4.11.

4.1.2.3 Six-degree-of-freedom manipulator

The spatial six-dof parallel mechanism is represented schematically in Figure 4.12.

The coordinate frame attached to the platform and the two links of the actuated leg are the same as the ones defined for the spatial four-dof parallel mechanism.

With all the definitions of the vectors given for the case of the spatial four-dof parallel mechanism, one has

$$\mathbf{r}_{iu} = \mathbf{p}_i - \frac{l_{ic}}{l_{iu}}(\mathbf{p}_i - \mathbf{p}_{i1}), \quad i = 1, \ldots, 6 \tag{4.82}$$

where $\mathbf{r}_{iu}$ is the position vector of the center of mass of the upper link of the ith leg. and where l_{iu}, l_{ic} are as previously defined.

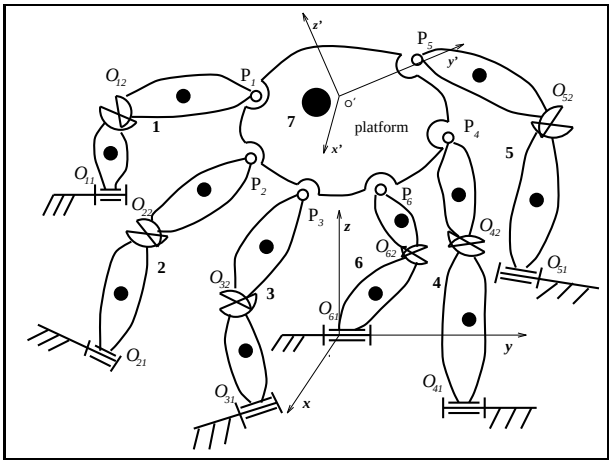

Figure 4.12: Spatial six-degree-of-freedom parallel mechanism with revolute actuators.

Then, the global center of mass of the mechanism, noted $\mathbf{r}$ can be written as

$$M\mathbf{r} = m_p\mathbf{r}_p + \sum_{i=1}^{6}(m_{il}\mathbf{r}_{il} + m_{iu}\mathbf{r}_{iu}) \tag{4.83}$$

where M is the total mass of all moving links of the mechanism, m_p, m_{iu} and m_{il} are respectively the masses of the platform, the upper link and lower link of the ith leg, and

$$M = m_p + \sum_{i=1}^{6}(m_{il} + m_{iu}) \tag{4.84}$$

while $\mathbf{r}_p$ and $\mathbf{r}_{il}$ are respectively the position vectors of the center of mass of the platform of the mechanism and of the center of mass of the lower link of the ith leg, namely

$$\mathbf{r}_p = \mathbf{p} + \mathbf{Q}\mathbf{c}_p \tag{4.85}$$

$$\mathbf{r}_{il} = \mathbf{r}_{io} + \mathbf{Q}_{il}\mathbf{c}_{il}, \quad i = 1, \ldots, 6 \tag{4.86}$$

where $\mathbf{c}_p$ and $\mathbf{c}_{il}$ are the position vectors of the center of mass of the platform and of the lower links expressed in the local reference frame, and whose components are given as

$$\mathbf{c}_p = \begin{bmatrix} x_p \\ y_p \\ z_p \end{bmatrix}; \quad \mathbf{c}_{il} = \begin{bmatrix} x_{ic} \\ y_{ic} \\ z_{ic} \end{bmatrix}, \quad i = 1, \ldots, 6 \tag{4.87}$$

Substituting eqs.(4.82), (4.85) and (4.86) into eq.(4.83), one then obtains

$$M\mathbf{r} = \begin{bmatrix} r_x \\ r_y \\ r_z \end{bmatrix} \tag{4.88}$$

where

$$\begin{aligned} r_x &= \sum_{i=1}^{6}(D_i \sin\gamma_i \sin\theta_i - D_{i+6} \sin\gamma_i \cos\theta_i) \\ &\quad + D_{13}x + D_{14}q_{11} + D_{15}q_{12} + D_{16}q_{13} + D_{xo} \qquad (4.89) \\ r_y &= \sum_{i=1}^{6}(D_{i+6} \cos\gamma_i \cos\theta_i - D_i \cos\gamma_i \sin\theta_i) \\ &\quad + D_{13}y + D_{14}q_{21} + D_{15}q_{22} + D_{16}q_{23} + D_{yo} \qquad (4.90) \\ r_z &= \sum_{i=1}^{6}(D_i \cos\theta_i + D_{i+6} \sin\theta_i) \\ &\quad + D_{13}z + D_{14}q_{31} + D_{15}q_{32} + D_{16}q_{33} + D_{zo} \qquad (4.91) \end{aligned}$$

where D_{xo}, D_{yo} and D_{zo} are constant coefficients, and where

$$\begin{aligned} D_i &= m_{il}z_{ic} + \frac{l_{il}}{l_{iu}} l_{ic} m_{iu}, \quad i = 1, \ldots, 6 \\ D_{i+6} &= m_{il}y_{ic}, \quad i = 1, \ldots, 6 \\ D_{13} &= m_p + \sum_{i=1}^{6} m_{iu}(1 - \frac{l_{ic}}{l_{iu}}) \\ D_{14} &= m_p x_p + \sum_{i=1}^{6} m_{iu} a_i (1 - \frac{l_{ic}}{l_{iu}}) \\ D_{15} &= m_p y_p + \sum_{i=1}^{6} m_{iu} b_i (1 - \frac{l_{ic}}{l_{iu}}) \\ D_{16} &= m_p z_p + \sum_{i=1}^{6} m_{iu} c_i (1 - \frac{l_{ic}}{l_{iu}}) \end{aligned}$$

If the coefficients of the joint and Cartesian variables in eqs.(4.89)-(4.91) vanish, the global center of mass of the manipulator will be fixed. Therefore, one obtains the conditions for static balancing as follows

$$D_i = 0, \quad i = 1, \ldots, 16 \qquad (4.92)$$

An example is now given in order to illustrate the application of the balancing conditions to the type of mechanism described above. For this mechanism, let

$$m_p = 12,\ l_{iu} = l_{il} = 1\ (i = 1, \ldots, 6)$$

$$a_1 = -0.5,\ ,b_1 = -0.5,\ c_1 = -0.3,\ a_2 = 0.5,\ ,b_2 = -0.5,\ c_2 = -0.3$$

$$a_3 = 0.5,\ b_3 = 0.5,\ c_3 = -0.3,\ a_4 = -0.5,\ b_4 = 0.5,\ c_4 = -0.3$$

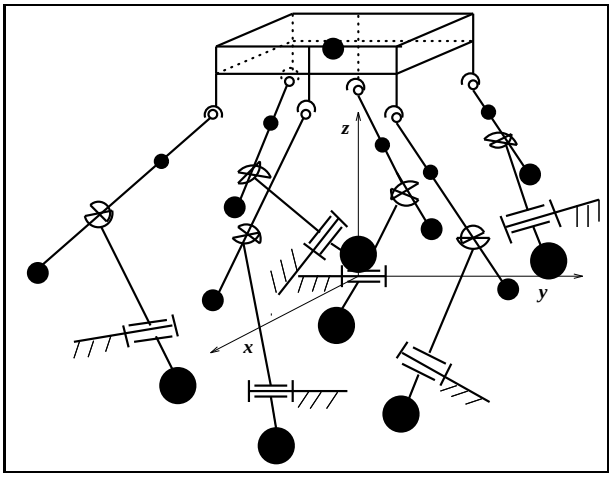

Figure 4.13: Complete balancing using counterweights.

$$a_5 = 0.5,\ b_5 = 0.0,\ c_3 = -0.3,\ a_6 = -0.5,\ b_6 = 0.0,\ c_6 = -0.3$$

$$x_{1o} = -1.5,\ y_{1o} = -1.5,\ z_{1o} = 0,\ x_{2o} = 1.5,\ y_{2o} = -1.5,\ z_{2o} = 0$$

$$x_{3o} = 1.5,\ y_{3o} = 1.5,\ z_{3o} = 0,\ x_{4o} = -1.5,\ y_{4o} = 1.5,\ z_{4o} = 0$$

$$x_{5o} = 1.5,\ y_{5o} = 0,\ z_{5o} = 0,\ x_{6o} = -1.5,\ y_{6o} = 0,\ z_{6o} = 0$$

$$\gamma_1 = \frac{\pi}{6},\ \gamma_2 = -\frac{\pi}{6},\ \gamma_3 = \frac{5\pi}{6},\ \gamma_4 = \frac{3\pi}{6},\ \gamma_5 = \frac{9\pi}{6},\ \gamma_6 = \frac{7\pi}{6}$$

$$y_{ic} = 0,\ \ z_{ic} = -0.5$$

where the masses are given in kilograms and the lengths in meters.

From eqs.(4.92), one obtains

$$z_{6c} = -0.5,\ \ m_{iu} = 4\,(\mathrm{kg}),\ \ m_{il} = 13\,(\mathrm{kg})\ (i = 1, \ldots, 6)$$

$$x_p = 0\,(\mathrm{m}),\ \ y_p = 0,\ \ z_p = 0.3\,(\mathrm{m})$$

The balanced manipulator is represented schematically in Figure 4.13.

As can be realized from the figure, large counterweights are necessary to balance the mechanism.

4.2 Balancing with springs

In this section, the planar and spatial parallel mechanisms or manipulators will be statically balanced using springs. Static balancing using springs consists in ensuring that the total potential energy of the mechanism is kept constant, which means that the weight of the mechanism does not have any effect on the actuators. Moreover, using this approach, the weight of the whole mechanism can be balanced with a much smaller total mass than when using counterweights. This approach may be more appropriate for applications in which large counterweights would be impractical. However, it should be noted that the mechanisms obtained with this approach will be balanced for only one direction and magnitude of the gravity vector.

4.2.1 Planar parallel manipulators with revolute actuators

In order to use springs to balance the manipulator, a special architecture (similar to what was used in [54]) is proposed for the legs. As represented in Figure 4.14, a parallelogram four-bar linkage is used instead of the first link of the ith leg. This enables the attachment of a spring to the upper link of the leg and to a support which is maintained vertically. A spring is also attached to the parallelogram. The upper link of the leg is then mounted on a revolute joint with a horizontal axis. The new architecture is kinematically equivalent to the previous one. However, the new architecture now allows the use of springs for the static balancing of the mechanism. Moreover, it is pointed out that the global center of mass of the parallelogram and the center of mass of the replaced first link of the ith leg can be handled similarly.

4.2.1.1 Two-degree-of-freedom manipulator

The expression of the total potential energy of the mechanism can then be written as

$$\mathrm{V} = \mathrm{V}_w + \mathrm{V}_s \tag{4.93}$$

where V_w and V_s are respectively the the gravitational potential energy of the mechanism and the elastic potential energy stored in the springs. Theses quantities can be

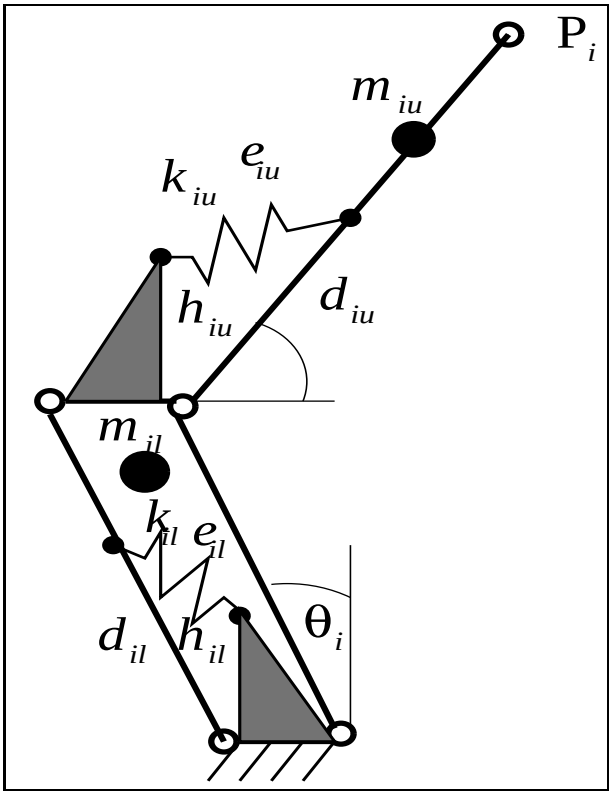

Figure 4.14: Geometry and kinematic architecture of the ith leg.

written, for this mechanism as

$$\mathrm{V}_w = r_y g \tag{4.94}$$

$$\mathrm{V}_s = \sum_{i=1}^{2} \frac{1}{2}(k_{il} e_{il}^2 + k_{iu} e_{iu}^2) \tag{4.95}$$

where r_y is defined in eq.(4.6), g is the gravitational acceleration, k_{il} is the stiffness of the lower spring of the ith leg, e_{il} is the length of the lower spring of the ith leg, k_{iu} is the stiffness of the upper spring of the ith leg and e_{iu} is its length. It is assumed here that the undeformed length of the spring is equal to zero in order to obtain complete balancing [54]. As shown in [54], this condition can easily be met in a practical design using, for instance, cables and pulleys.

Using the law of cosines, the effective length of the springs can be written as

$$e_{il} = \sqrt{h_{il}^2 + d_{il}^2 - 2h_{il}d_{il}\sin\theta_i}, \quad i = 1, 2 \tag{4.96}$$

$$e_{iu} = \sqrt{h_{iu}^2 + d_{iu}^2 - 2h_{iu}d_{iu}\sin\alpha_i}, \quad i = 1, 2 \tag{4.97}$$

where h_{il} and d_{il} are the distances from the revolute joint located at O_{i1} to the attachment points of the lower spring (Figure 4.14) while h_{iu} and d_{iu} are the same distances for the upper spring.

Moreover, from eq.(4.8) one can obtain

$$\sin\alpha_2 = \frac{1}{l_3}(l_1 \sin\theta_1 + l_2 \sin\alpha_1 - l_4 \sin\theta_2 - y_0) \tag{4.98}$$

Substituting eqs.(4.96)–(4.98) into eqs.(4.94) and (4.95) and then substituting the latter equations into eq.(4.93), one obtains

$$\begin{aligned} \mathrm{V} \;=\; & (A_1 g - 2k_{1l}h_{1l}d_{1l} - 2k_{2u}h_{2u}d_{2u})\sin\theta_1 + B_1 g\cos\theta_1 \\ & (A_2 g - 2k_{2l}h_{2l}d_{2l} + 2k_{2u}h_{2u}d_{2u})\sin\theta_2 + B_2 g\cos\theta_2 \\ & (A_3 g - 2k_{1u}h_{1u}d_{1u} - 2k_{2u}h_{2u}d_{2u})\sin\alpha_1 + B_3 g\cos\alpha_1 + D_c \end{aligned} \tag{4.99}$$

From eq.(4.99) one can finally obtain the conditions for the static balancing of the manipulator with springs as follows

$$A_1 g - 2k_{1l}h_{1l}d_{1l} - 2k_{2u}h_{2u}d_{2u} = 0 \tag{4.100}$$

$$B_1 = 0 \tag{4.101}$$

$$A_2 g - 2k_{2l}h_{2l}d_{2l} + 2k_{2u}h_{2u}d_{2u} = 0 \tag{4.102}$$

$$B_2 = 0 \tag{4.103}$$

$$A_3 g - 2k_{1u}h_{1u}d_{1u} - 2k_{2u}h_{2u}d_{2u} = 0 \tag{4.104}$$

$$B_3 = 0 \tag{4.105}$$

where A_i and B_i $(i = 1, 2, 3)$ have been defined in eqs.(4.11)–(4.16).

An example is now given in order to illustrate the application of the balancing conditions derived above.

For the two-dof mechanism, let

$$m_1 = m_2 = m_3 = m_4 = 1,\ l_i = 1\ (i = 1, \ldots, 4)$$

$$\psi_i = 0\ (i = 1, \ldots, 4),\ d_{1u} = d_{2u} = 0.5$$

$$h_{1l} = h_{2l} = h_{1u} = h_{2u} = 0.5,\ r_i = 0.5\ (i = 1, \ldots, 4)$$

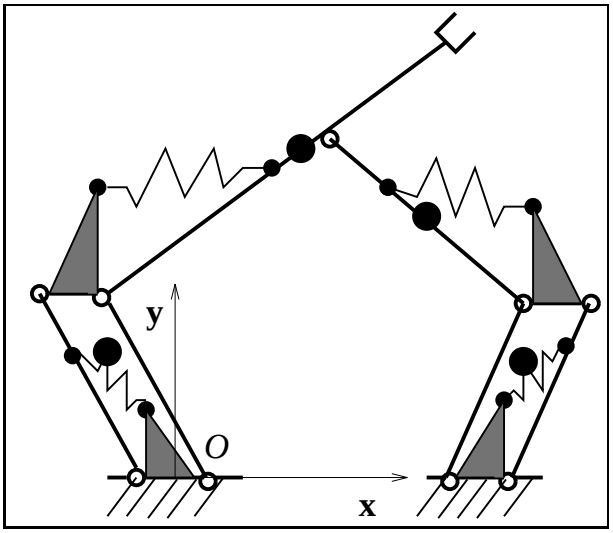

Figure 4.15: Planar two-degree-of-freedom balanced mechanism with springs.

$$x_1 = 1.5,\ y_1 = 0$$

where the masses are given in kilograms and the lengths in meters.

From eqs.(4.100)–(4.105), one obtains

$$d_{1l} = d_{2l} = 0.5$$

$$k_{1l} = k_{1u} = 29\text{N/m},\ k_{2l} = 21\text{N/m},\ k_{2u} = 10\text{N/m},$$

The balanced mechanism is represented schematically in Figure 4.15.

4.2.1.2 Three-degree-of-freedom manipulator

Similarly, the expression of the total potential energy of the planar three-degree-of-freedom manipulator can also be written as

$$\mathrm{V} = \mathrm{V}_w + \mathrm{V}_s \tag{4.106}$$

where V_w and V_s are respectively the gravitational potential energy of the mechanism and the elastic potential energy stored in the springs. These quantities can be written, for this mechanism as

$$\mathrm{V}_w = r_y g \tag{4.107}$$

$$\mathrm{V}_s = \sum_{i=1}^{3} \frac{1}{2}(k_{il} e_{il}^2 + k_{iu} e_{iu}^2) \tag{4.108}$$

where r_y is defined in eq.(4.25).

Using the law of cosines, the length of the springs can be written as

$$e_{il} = \sqrt{h_{il}^2 + d_{il}^2 - 2h_{il}d_{il}\sin\theta_i}, \quad i = 1,2,3 \tag{4.109}$$

$$e_{iu} = \sqrt{h_{iu}^2 + d_{iu}^2 - 2h_{iu}d_{iu}\sin\alpha_i}, \quad i = 1,2,3 \tag{4.110}$$

where h_{il} and d_{il} are the distances from the revolute joint located at O_{i1} to the attachment points of the lower spring (Figure 4.14) while h_{iu} and d_{iu} are the same distances for the upper spring.

Moreover, from eqs.(4.27) and (4.29) one has

$$\sin\alpha_2 = \frac{1}{l_{22}}(l_{11}\sin\theta_1 + l_{12}\sin\alpha_1 + l_3\sin\phi - l_{31}\sin\theta_2 - y_{01}) \tag{4.111}$$

$$\sin\alpha_3 = \frac{1}{l_{32}}(l_{11}\sin\theta_1 + l_{12}\sin\alpha_1 + l_4\sin\phi - l_{31}\sin\theta_3 - y_{02}) \tag{4.112}$$

Substituting eqs.(4.109)–(4.112) into eqs.(4.107) and (4.108) and then substituting the latter equations into eq.(4.106), one can obtain

$$\begin{aligned} \mathrm{V} = {} & (A_1 - 2k_{1l}h_{1l}d_{1l} - 2\frac{l_{11}}{l_{22}}h_{2u}d_{2u} - 2\frac{l_{11}}{l_{32}}h_{3u}d_{3u})\sin\theta_1 + B_1\cos\theta_1 \\ & (A_2 - 2k_{2l}h_{2l}d_{2l} + 2\frac{l_{31}}{l_{22}}h_{2u}d_{2u})\sin\theta_2 + B_2\cos\theta_2 \\ & (A_3 - 2k_{3l}h_{3l}d_{3l} + 2\frac{l_{31}}{l_{32}}h_{3u}d_{3u})\sin\theta_3 + B_3\cos\theta_3 \\ & (A_4 - 2k_{1u}h_{1u}d_{1u} - 2\frac{l_{12}}{l_{22}}h_{2u}d_{2u} - 2\frac{l_{12}}{l_{32}}h_{3u}d_{3u})\sin\alpha_1 + B_4\cos\alpha_1 \\ & (A_5 - \frac{l_3}{l_{22}}h_{2u}d_{2u} - 2\frac{l_4}{l_{32}}h_{3u}d_{3u})\sin\phi + B_5\cos\phi + D_y \end{aligned} \tag{4.113}$$

From eq.(4.113) one can finally obtain the conditions for the static balancing of the manipulator with springs as follows

$$A_1 g - 2k_{1l}h_{1l}d_{1l} - 2\frac{l_{11}}{l_{22}}k_{2u}h_{2u}d_{2u} - 2\frac{l_{11}}{l_{32}}k_{3u}h_{3u}d_{3u} = 0 \tag{4.114}$$

$$B_1 = 0 \tag{4.115}$$

$$A_2 g - 2k_{2l}h_{2l}d_{2l} + 2\frac{l_{31}}{l_{22}}k_{2u}h_{2u}d_{2u} = 0 \tag{4.116}$$

$$B_2 = 0 \tag{4.117}$$

$$A_3 g - 2k_{3l}h_{3l}d_{3l} + 2\frac{l_{31}}{l_{32}}k_{3u}h_{3u}d_{3u} = 0 \tag{4.118}$$

$$B_3 = 0 \quad (4.119)$$

$$A_4 g - 2k_{1u}h_{1u}d_{1u} - 2\frac{l_{12}}{l_{22}}k_{2u}h_{2u}d_{2u} - 2\frac{l_{12}}{l_{32}}k_{3u}h_{3u}d_{3u} = 0 \quad (4.120)$$

$$B_4 = 0 \quad (4.121)$$

$$A_5 g - \frac{l_3}{l_{22}}k_{2u}h_{2u}d_{2u} - 2\frac{l_4}{l_{32}}k_{3u}h_{3u}d_{3u} = 0 \quad (4.122)$$

$$B_5 = 0 \quad (4.123)$$

Similarly to the previous case, an example is now given to illustrate the results derived above.

For the three-dof mechanism, let

$$m_3 = m_{i1} = m_{i2} = 1\,(i = 1, 2, 3)$$

$$h_{il} = h_{iu} = 0.5\,(i = 1, 2, 3), d_{2u} = d_{3u} = 0.5$$

$$l_3 = 0.6,\ l_4 = 1.2,\ l_{i1} = l_{i2} = 1\,(i = 1, 2, 3)$$

$$r_{i1} = r_{i2} = 0.5,\ r_3 = 0.6,\ \psi_{i1} = \psi_{i2} = 0\,(i = 1, 2, 3)$$

$$x_{01} = 1.5,\ x_{02} = 3,\ y_{01} = y_{02} = 0$$

where the masses are given in kilograms and the lengths in meters.

From eqs.(4.114)–(4.123) one obtains

$$k_{iu} = 10\text{N/m},\ k_{il} = 50\text{N/m}\,(i = 1, 2, 3)$$

$$d_{il} = 0.5\,(i = 1, 2, 3) d_{1u} = 0.5$$

The balanced mechanism is represented schematically in Figure 4.16.

4.2.2 Spatial parallel manipulators with revolute actuators

4.2.2.1 Four-degree-of-freedom manipulator

Similarly to what was obtained for the planar manipulators, the expression of the total potential energy of this spatial manipulator can be written as

$$\mathrm{V} = \mathrm{V}_w + \mathrm{V}_s \quad (4.124)$$

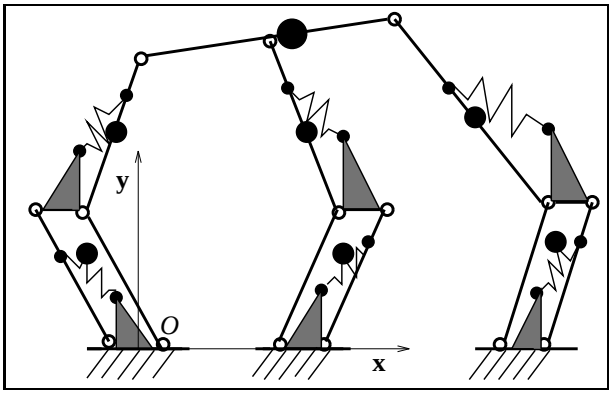

Figure 4.16: Planar three-degree-of-freedom balanced mechanism with springs.

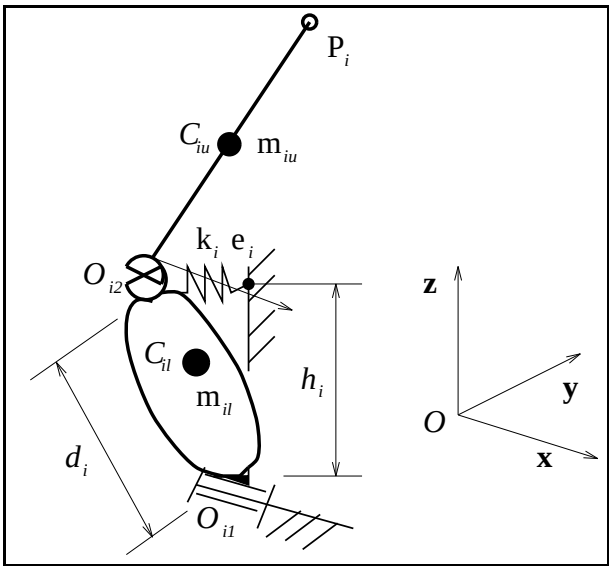

Figure 4.17: Architecture and geometry of the ith leg.

where V_w and V_s are respectively the the gravitational potential energy of the manipulator and the elastic potential energy stored in the springs. These quantities can be expressed as

$$\mathrm{V}_w = r_z g \tag{4.125}$$

$$\mathrm{V}_s = \frac{1}{2}\sum_{j=1}^{5} k_j e_j^2 \tag{4.126}$$

where r_z is defined in eq.(4.66) k_j is the stiffness of the jth spring, e_j is its length and other quantities are as previously defined.

For this type of manipulator, a spring can be used in each revolute joint connecting the ith leg to the base of the manipulator, where $i = 1, \ldots, 5$. This is represented

in Figure 4.17 where the geometric parameters are defined. Therefore, the potential energy stored in the spring attached to the ith leg can be written as

$$\mathrm{V}_{si} = \frac{1}{2} k_i e_i^2 \tag{4.127}$$

where, from the law of cosines

$$e_i = \sqrt{h_i^2 + d_i^2 - 2h_i d_i \cos\theta_i}, \quad i = 1, \ldots, 4 \tag{4.128}$$

and

$$e_5 = \sqrt{h_5^2 + d_5^2 - 2h_5 d_5 \cos\alpha} \tag{4.129}$$

Substituting eqs.(4.125) and (4.126) into eq.(4.124) leads to

$$\begin{aligned} \mathrm{V} &= \sum_{i=1}^{4} [(D_i - 2k_i h_i d_i)\cos\theta_i + D_{i+4}\cos\theta_i) + D_9 q_{11} + D_{10} q_{12} + D_{11} q_{13} \\ &\quad + (D_{12} - 2k_5 h_5 d_5)\cos\alpha + \frac{1}{2} k(h^2 + d^2) + \frac{1}{2}\sum_{i=1}^{4} k_i (h_i^2 + d_i^2) + D_{zo} \end{aligned} \tag{4.130}$$

From eq.(4.130) one can finally obtain the conditions for the static balancing of the manipulator when springs are used as follows

$$D_i - 2k_i h_i d_i = 0, \quad i = 1, \ldots, 4 \tag{4.131}$$

$$D_{i+4} = 0, \quad i = 1, \ldots, 4 \tag{4.132}$$

$$D_{12} - 2k_5 h_5 d_5 = 0 \tag{4.133}$$

where coefficients $D_i, i = 1, \ldots, 12$ are the ones used in eq.(4.67).

An example is now given in order to illustrate the application of the balancing conditions derived above to this type of mechanism with springs.

For the 4-dof manipulator with revolute actuators, let

$$m_p = 10,\ m_5 = 0.15,\ m_{il} = m_{iu} = 0.1\ (i = 1, \ldots, 4)$$

$$a_1 = -0.5,\ ,b_1 = -0.5,\ c_1 = -0.3,\ a_2 = 0.5,\ ,b_2 = -0.5,\ c_2 = -0.3$$

$$a_3 = 0.5,\ b_3 = 0.5,\ c_3 = -0.3,\ a_4 = -0.5,\ b_4 = 0.5,\ c_4 = -0.3$$

$$a_5 = 0,\ b_5 = 0,\ c_5 = 0,\ l_5 = 1.0,\ l_{iu} = 0.5\ (i = 1, \ldots, 4)$$

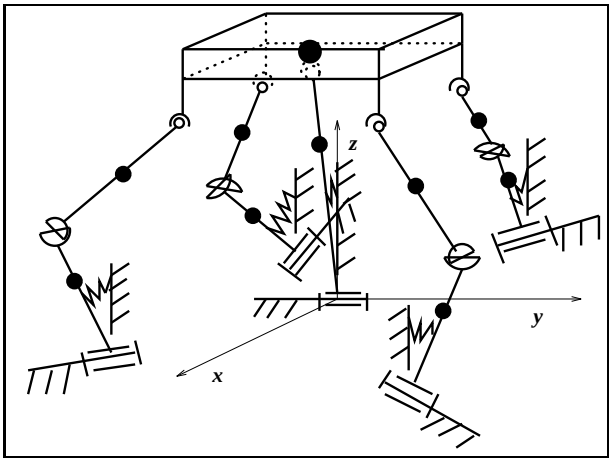

Figure 4.18: Four-degree-of-freedom balanced mechanism with revolute actuators using springs.

$$l_{iu} = l_{il} = 0.5,\ l_{il} = l_{iu} = 1.0\, z_{ic} = 0.5\, (i = 1, \ldots, 4)$$

$$l_{5c} = 0.5,\ m_5 = 1,\ h_i = 0.5,\ d_i = 0.5,\ (i = 1, \ldots, 4)$$

$$x_{1o} = -1.5,\ y_{1o} = -1.5,\ z_{1o} = 0,\ x_{2o} = 1.5,\ y_{2o} = -1.5,\ z_{2o} = 0$$

$$x_{3o} = 1.5,\ y_{3o} = 1.5,\ z_{3o} = 0,\ x_{4o} = -1.5,\ y_{4o} = 1.5,\ z_{4o} = 0$$

$$\gamma_1 = -\frac{\pi}{4},\ \gamma_2 = \frac{\pi}{4},\ \gamma_3 = \frac{3\pi}{4},\ \gamma_4 = \frac{5\pi}{4}$$

where the masses are given in kilograms and the lengths in meters.

From equations (4.131)–(4.133) one obtains

$$y_{ic} = 0,\ k_i = 0.02\,\mathrm{kg/cm} (i = 1, \ldots, 4)$$

$$x_p = 0,\ y_p = 0,\ z_p = 12\,\mathrm{cm}$$

$$k_5 = 0.23\,\mathrm{ton/cm}$$

The balanced mechanism is represented schematically in Figure 4.18.

4.2.2.2 Five-degree-of-freedom manipulator

Similarly to the previous case, the expression of the total potential energy of the manipulator can be written as

$$\mathrm{V} = \mathrm{V}_w + \mathrm{V}_s \tag{4.134}$$

where V_w and V_s are respectively the gravitational potential energy of the manipulator and the elastic potential energy stored in the springs, which can be expressed as

$$V_w = r_z g \tag{4.135}$$

$$V_s = \frac{1}{2}\sum_{j=1}^{6} k_j e_j^2 \tag{4.136}$$

where r_z is defined in eq.(4.80) and other quantities are as previously defined. As in the previous case, a spring is attached to each of the links mounted on the base, as illustrated in Figure 4.17.

From the law of cosines, one still has

$$e_i = \sqrt{h_i^2 + d_i^2 - 2h_i d_i \cos\theta}, \quad i = 1, \ldots, 5 \tag{4.137}$$

and

$$e_6 = \sqrt{h_6^2 + d_6^2 - 2h_6 d_6 \cos\alpha} \tag{4.138}$$

Substituting eqs.(4.135) and (4.136) into eq.(4.134) leads to

$$\begin{aligned} V = & \sum_{i=1}^{5}[(D_i - 2k_i h_i d_i)\cos\theta_i + D_{i+5}\cos\theta_i) \\ & +(D_{11} - 2k_6\frac{h_6 d_6}{l_6})z \\ & +(D_{12} - 2k_6 a_6\frac{h_6 d_6}{l_6})q_{31} \\ & +(D_{13} - 2k_6 b_6\frac{h_6 d_6}{l_6})q_{32} \\ & +(D_{14} - 2k_6 c_6\frac{h_6 d_6}{l_6})q_{33} \\ & +\frac{1}{2}k(h_6^2 + d_6^2) + \frac{1}{2}\sum_{i=1}^{5} k_i(h_i^2 + d_i^2) + D_{zo} \end{aligned} \tag{4.139}$$

From eq.(4.139) one can finally obtain the conditions for the static balancing of the manipulator when springs are used as follows

$$D_i - 2k_i h_i d_i = 0, \quad i = 1, \ldots, 5 \tag{4.140}$$

$$D_{i+5} = 0, \quad i = 1, \ldots, 5 \tag{4.141}$$

$$D_{11} - 2k_6\frac{h_6 d_6}{l_6} = 0 \tag{4.142}$$

$$D_{12} - 2k_6 a_6\frac{h_6 d_6}{l_6} = 0 \tag{4.143}$$

$$D_{13} - 2k_6 b_6 \frac{h_6 d_6}{l_6} = 0 \quad (4.144)$$

$$D_{14} - 2k_6 c_6 \frac{h_6 d_6}{l_6} = 0 \quad (4.145)$$

where coefficients D_i, $i = 1, \ldots, 14$ are the ones used in eq.(4.81).

An example is now given in order to illustrate the application of the balancing conditions derived above to this type of mechanism with springs.

For the 5-dof manipulator with revolute actuators, let

$$m_p = 10,\ m_6 = 1,\ m_{il} = m_{iu} = 1\ (i = 1, \ldots, 5)$$

$$a_1 = -0.5,\ ,b_1 = -0.5,\ c_1 = -0.3,\ a_2 = 0.5,\ ,b_2 = -0.5,\ c_2 = -0.3$$

$$a_3 = 0.5,\ b_3 = 0.5,\ c_3 = -0.3,\ a_4 = -0.5,\ b_4 = 0.5,\ c_4 = -0.3$$

$$a_5 = 0.5,\ b_5 = 0,\ c_5 = -0.3,\ a_6 = 0,\ b_6 = 0,\ c_6 = 0,\ l_6 = 1.0,\ h_6 = 0.5,\ d_6 = 0.5$$

$$l_{il} = l_{iu} = 1.0\, z_{ic} = l_{ic} = 0.5\ (i = 1, \ldots, 5)$$

$$l_{5c} = 0.5,\ m_5 = 1,\ h_i = 0.5,\ d_i = 0.5,\ (i = 1, \ldots, 5)$$

$$x_{1o} = -1.5,\ y_{1o} = -1.5,\ z_{1o} = 0,\ x_{2o} = 1.5,\ y_{2o} = -1.5,\ z_{2o} = 0$$

$$x_{3o} = 1.5,\ y_{3o} = 1.5,\ z_{3o} = 0,\ x_{4o} = -1.5,\ y_{4o} = 1.5,\ z_{4o} = 0$$

$$x_{5o} = 1.5,\ y_{5o} = 0,\ z_{5o} = 0,\ x_{6o} = 0,\ y_{6o} = 0,\ z_{6o} = 0$$

$$\gamma_1 = -\frac{\pi}{4},\ \gamma_2 = \frac{\pi}{4},\ \gamma_3 = \frac{3\pi}{4},\ \gamma_4 = \frac{5\pi}{4}$$

where the masses are given in kilograms and the lengths in meters.

From equations (4.140)–(4.145) one obtains

$$y_{ic} = 0,\ k_i = 2\,\mathrm{N/cm} (i = 1, \ldots, 5)$$

$$x_p = 2.5\,(\mathrm{cm}),\ \mathrm{y_p} = 0,\ \mathrm{z_p} = 33\,\mathrm{cm}$$

$$k_6 = 26\,\mathrm{N/cm}$$

The balanced mechanism is represented schematically in Figure 4.19.

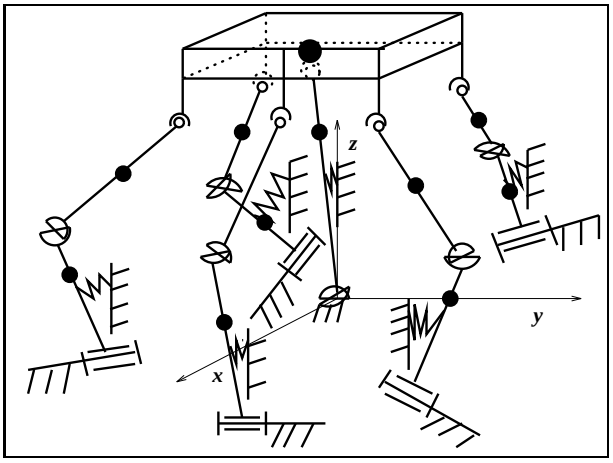

Figure 4.19: Five-degree-of-freedom balanced mechanism with revolute actuators using springs.

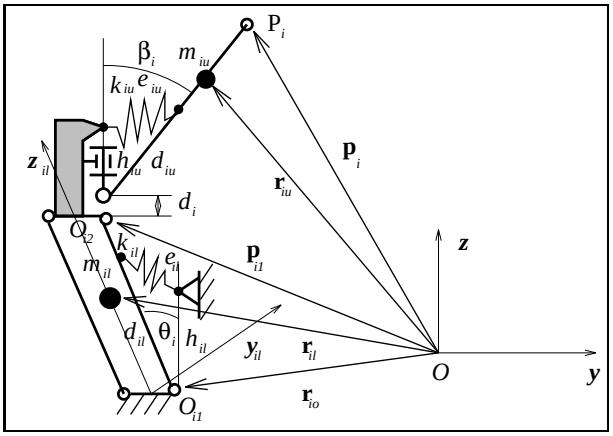

Figure 4.20: Geometry and kinematic architecture of the ith leg.

4.2.2.3 Six-degree-of-freedom manipulator

In order to use springs to balance the manipulator, a special architecture of the leg similar to what was used in the case of static balancing of planar parallel mechanism using springs (Figure 4.14) is proposed for the legs. As represented in Figure 4.20, a parallelogram four-bar linkage is used instead of the first link of the ith leg. The upper link of the leg is then mounted on a revolute joint with a horizontal axis which is in turn mounted on a revolute joint with a vertical axis. The latter two joint form a Hooke joint. This new architecture is equivalent to the original one.

Using the new architecture of the leg, the expression of the total potential energy of the mechanism can then be written as

$$\mathrm{V} = \mathrm{V}_w + \mathrm{V}_s \tag{4.146}$$

where V_w and V_s are respectively the gravitational potential energy and the elastic potential energy stored in the springs. Theses quantities can be written, for this mechanism as

$$\mathrm{V}_w = r_z g + D_c \tag{4.147}$$

$$\mathrm{V}_s = \sum_{i=1}^{6} \frac{1}{2}(k_{il} e_{il}^2 + k_{iu} e_{iu}^2) \tag{4.148}$$

where r_z is defined in eq.(4.91) and D_c is a constant which arises from the distance d_i, which increases the gravitational potential energy. This constant can be written as $D_c = m_p g d_1 + \sum_{i=1}^{6}(m_i g d_i)$. Again, g is the gravitational acceleration, k_{il} is the stiffness of the lower spring of the ith leg, e_{il} is the length of the lower spring of the ith leg, k_{iu} is the stiffness of the upper spring of the ith leg and e_{iu} is its length. It is also assumed here that the undeformed length of the springs is equal to zero in order to obtain complete balancing [54].

Using the law of cosines, the length of the springs can be written as

$$e_{il} = \sqrt{h_{il}^2 + d_{il}^2 - 2h_{il}d_{il}\cos\theta_i}, \quad i = 1, \ldots, 6 \tag{4.149}$$

$$e_{iu} = \sqrt{h_{iu}^2 + d_{iu}^2 - 2h_{iu}d_{iu}\cos\beta_i}, \quad i = 1, \ldots, 6 \tag{4.150}$$

where h_{il} and d_{il} are the distances from the revolute joint located at O_{i1} to the attachment points of the lower spring (Figure 4.20) while h_{iu} and d_{iu} are the same distances

for the upper spring. $\cos\beta_i$ can be expressed as a function of angle θ_i as well as the position and orientation of the platform, i.e.,

$$\cos\beta_i = \frac{z_i - z_{i1}}{l_{iu}} \tag{4.151}$$

and where z_i and z_{i1} are respectively the third components of the position vectors $\mathbf{p}_i$ and $\mathbf{p}_{i1}$.

Substituting eqs.(4.147), (4.148) and (4.149)–(4.151) into eq.(4.146), one then obtains

$$\begin{aligned} \mathrm{V} \;=\; & \sum_{i=1}^{6}[(D_i g - 2k_{il}h_{il}d_{il} - 2k_{iu}h_{iu}d_{iu}\frac{l_{il}}{l_{iu}})\cos\theta_i + D_{i+6}g\sin\theta_i] \\ & +(D_{13}g - 2\sum_{i=1}^{6}\frac{k_{iu}h_{iu}d_{iu}}{l_{iu}})z + (D_{14}g - 2\sum_{i=1}^{6}\frac{k_{iu}h_{iu}d_{iu}}{l_{iu}})q_{31} + (D_{15}g - 2\sum_{i=1}^{6}\frac{k_{iu}h_{iu}d_{iu}}{l_{iu}})q_{32} \\ & +(D_{16}g - 2\sum_{i=1}^{6}\frac{k_{iu}h_{iu}d_{iu}}{l_{iu}})q_{33} + \frac{1}{2}\sum_{i=1}^{6}[k_{il}(h_{il}^2 + d_{il}^2) + k_{iu}(h_{i2}^2 + d_{i2}^2)] \\ & -\sum_{i=1}^{6}2\frac{k_{iu}h_{i2}d_{i2}}{l_{iu}} + D_{zo}g + D_c \end{aligned} \tag{4.152}$$

From eq.(4.152) one can finally obtain the conditions for the static balancing of the manipulator with springs as follows

$$D_i g - 2k_{il}h_{il}d_{il} - 2\frac{l_{il}}{l_{iu}}k_{iu}h_{iu}d_{iu} = 0, \quad i = 1,\ldots,6 \tag{4.153}$$

$$D_{i+6}g = 0, \quad i = 1,\ldots,6 \tag{4.154}$$

$$D_{13}g - 2\sum_{i=1}^{6}\frac{k_{iu}h_{iu}d_{iu}}{l_{iu}} = 0 \tag{4.155}$$

$$D_{14}g - 2\sum_{i=1}^{6}\frac{k_{iu}h_{iu}d_{iu}}{l_{iu}} = 0 \tag{4.156}$$

$$D_{15}g - 2\sum_{i=1}^{6}\frac{k_{iu}h_{iu}d_{iu}}{l_{iu}} = 0 \tag{4.157}$$

$$D_{16}g - 2\sum_{i=1}^{6}\frac{k_{iu}h_{iu}d_{iu}}{l_{iu}} = 0 \tag{4.158}$$

where coefficients D_i are the ones used in eq.(4.81).

An example is now given in order to illustrate the application of the balancing conditions to this type of mechanism.

For the 6-dof manipulator with revolute actuators presented above, let

$$m_p = 12,\ m_{iu} = m_{il} = 1.0,\ l_{il} = l_{iu} = 1.0 (i = 1, \ldots, 6)$$

$$a_1 = -0.5,\ ,b_1 = -0.5,\ c_1 = -0.3,\ a_2 = 0.5,\ ,b_2 = -0.5,\ c_2 = -0.3$$

$$a_3 = 0.5,\ b_3 = 0.5,\ c_3 = -0.3,\ a_4 = -0.5,\ b_4 = 0.5,\ c_4 = -0.3$$

$$a_5 = 1.0,\ b_5 = 0,\ c_5 = -0.3,\ a_6 = -1.0,\ b_6 = 0,\ c_6 = -0.3$$

$$h_{il} = h_{iu} = 0.5,\ d_{il} = d_{lu} = 0.5,\ z_{ic} = l_{ic} = 0.5\ (i = 1, \ldots, 6)$$

$$x_{1o} = -1.5,\ y_{1o} = -1.5,\ z_{1o} = 0,\ x_{2o} = 1.5,\ y_{2o} = -1.5,\ z_{2o} = 0$$

$$x_{3o} = 1.5,\ y_{3o} = 1.5,\ z_{3o} = 0,\ x_{4o} = -1.5,\ y_{4o} = 1.5,\ z_{4o} = 0$$

$$x_{5o} = 1.5,\ y_{5o} = 0,\ z_{5o} = 0,\ x_{6o} = -1.5,\ y_{6o} = 0,\ z_{6o} = 0$$

$$\gamma_1 = \frac{\pi}{6},\ \gamma_2 = -\frac{\pi}{6},\ \gamma_3 = \frac{5\pi}{6},\ \gamma_4 = \frac{3\pi}{6},\ \gamma_5 = \frac{9\pi}{6},\ \gamma_6 = \frac{7\pi}{6}$$

$$y_{ic} = 0\ (i = 1, \ldots, 5)\ z_{ic} = l_{ic} = 0.5\,\mathrm{m}\ (i = 1, \ldots, 6)$$

where the masses are given in kilograms and the lengths in meters.

From eqs.(4.153)–(4.158) one obtains

$$y_{6c} = 0,\ k_{iu} = 300\,\mathrm{N/m},\ k_{il} = 620\,\mathrm{N/m}\ (i = 1, \ldots, 6)$$

$$x_p = 0\,(\mathrm{m}),\ y_p = 0,\ z_p = 0.45\,(\mathrm{m})$$

The balanced mechanism is represented schematically in Figure 4.21. Since each leg of the mechanism has an identical architecture, only one leg is represented in the figure.

As can be clearly seen from the figure, the use of springs has allowed one to eliminate the counterweights. However, the resulting mechanism will be statically balanced if and only if the gravity vector is aligned with the negative direction of the **z** axis of the fixed reference frame and if its magnitude is maintained.

An alternative achitecture is now introduced for this type of manipulator. In the new architecture, each of the legs is mounted on a passive revolute joint having a vertical axis of rotation, as shown in Figure 4.22. The leg itself is a planar mechanism with a parallelogram $ABCD$, a distal link CP_i and a spherical joint at point P_i. Additionally,

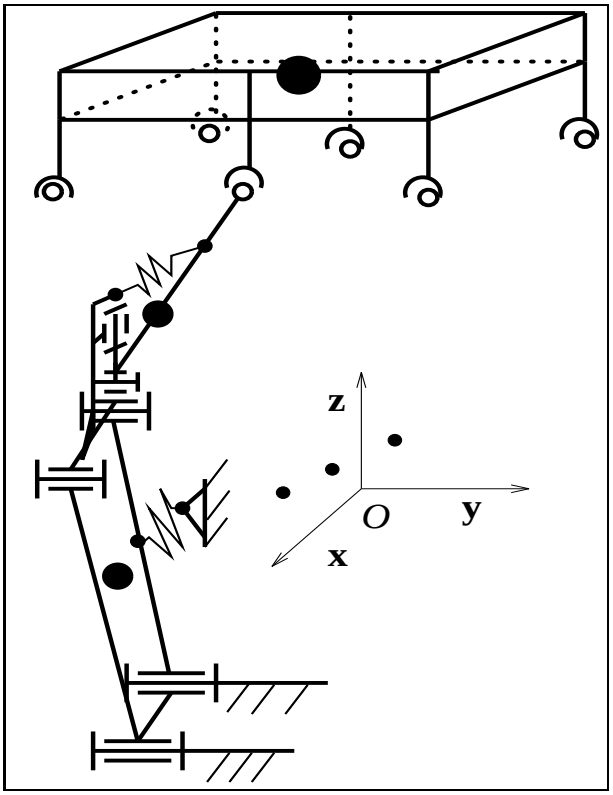

Figure 4.21: Balanced mechanism with springs.

a second parallelogram mechanism $BEFC$ is introduced in the leg, as represented in Figure 4.22. The second parallelogram mechanism is used to actuate the link CP thereby improving the mechanical advantage. Link BE is the actuated link. although this achitecture is more complex than the previous one, it may have design advantages.

The potential energy of the springs used in the manipulator can be written as

$$\mathrm{V}_s = \sum_{i=1}^{6} \frac{1}{2}(k_{il} e_{il}^2 + k_{iu} e_{iu}^2) \tag{4.159}$$

where

$$e_{i1} = \sqrt{h_{il}^2 + d_{il}^2 - 2h_{il} d_{il} \sin\phi_i} \tag{4.160}$$

$$e_{i2} = \sqrt{h_{iu}^2 + d_{iu}^2 - 2h_{iu} d_{iu} \sin\theta_i} \tag{4.161}$$

where ϕ_i and θ_i are respectively the angles between links BC and BE and the coordinate axis $\mathbf{x}_i$.

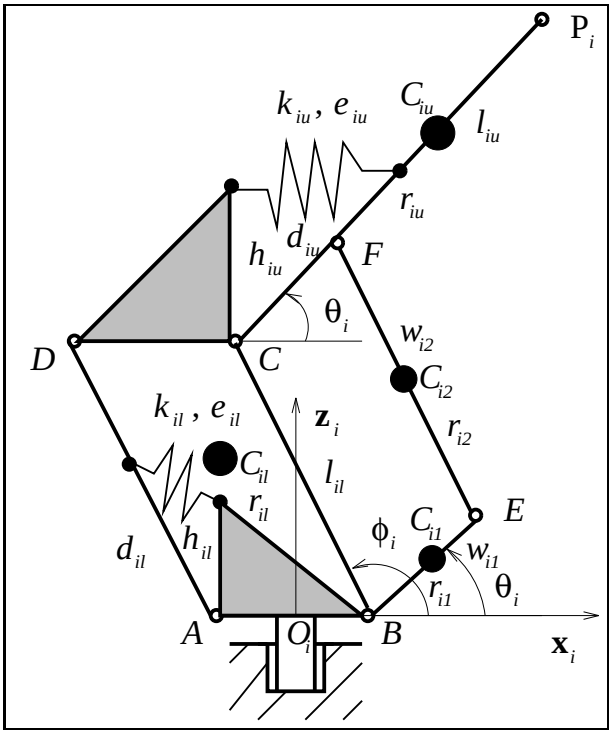

Figure 4.22: Alternative architecture of leg for the 6-dof parallel mechanism with revolute actuators.

The gravitational potential energy of the manipulator can be expressed as

$$\begin{aligned} \mathrm{V}_w &= m_p g(l_{il}\sin\phi_i + l_{iu}\sin\theta_1 + (x_p - a_1)q_{31} + (y_p - b_1)q_{32} + (z_p - C_1)q_{33}) \\ &\quad + \sum_{i=1}^{6}[m_{il}gr_{il}\sin\phi_i + m_{i1}gr_{i1}\sin\theta_i + m_{iu}g(l_{il}\sin\phi_i + r_{iu}\sin\theta_i) \\ &\quad + m_{i2}g(w_{i1}\sin\theta_i + r_{i2}\sin\phi_i)] \end{aligned} \tag{4.162}$$

where w_{i1} and w_{i2} are respectively the lengths of links BE and EF, m_{i1} and m_{i2} are their corresponding masses, and r_{i1} and r_{i2} are the distances of the centers of mass C_{i1} and C_{i2} of the two links to points B and E.

Since the manipulator consists of five independent kinematic closed loops, one can write

$$\begin{aligned} z_{1o} + l_{1l}\sin\phi_1 + l_{1u}\sin\theta_1 &= z_{io} + l_{il}\sin\phi_i + l_{iu}\sin\theta_i + (a_1 - a_i)q_{31} \\ &\quad + (b_1 - b_i)q_{32} + (c_1 - c_i)q_{33}, \quad i = 2,\ldots,6 \end{aligned} \tag{4.163}$$

From eq.(4.163) one has

$$\sin\phi_i = \frac{1}{l_{il}}(z_{1o} + l_{1l}\sin\phi_1 + l_{1u}\sin\theta_1 - z_{io} - l_{iu}\sin\theta_i$$

$$-(a_1 - a_i)q_{31} - (b_1 - b_i)q_{32} - (c_1 - c_i)q_{33}), \quad i = 2, \ldots, 6 \quad (4.164)$$

Substituting eq.(4.164) into eqs.(4.159) and (4.162), one then obtains the total potential energy of this type of manipulator as

$$V = V_w + V_s = \sum_{i=2}^{6} D_i \sin\theta_i + D_7 \sin\phi_1 + D_8 q_{31} + D_9 q_{32} + D_{10} q_{33} \quad (4.165)$$

where

$$\begin{aligned}
D_1 &= m_p g l_{1u} + w_{11} m_{12} g + m_{1u} g r_{1u} + l_{1u} g \sum_{i=2}^{6} m_{iu} \\
&\quad - k_{1u} d_{1u} h_{1u} - l_{1u} \sum_{i=2}^{6} \frac{1}{l_{iu}} k_{il} h_{il} d_{il} \\
&\quad + l_{1u} g \sum_{i=2}^{6} \frac{1}{l_{il}} (m_{i1} r_{i1} + m_{i2} r_{i2} + m_{il} r_{il}) \\
D_i &= m_{iu} g r_{iu} + m_{i2} g w_{i1} - m_{iu} g l_{iu} - k_{iu} h_{iu} d_{iu} \\
&\quad + \frac{l_{iu}}{l_{il}} (k_{il} h_{il} d_{il} - m_{il} g r_{il} - m_{i1} g r_{i1} - m_{i2} g r_{i2}), \quad i = 2, \ldots, 6 \\
D_7 &= m_p g l_{1l} + l_{1l} g \sum_{i=1}^{6} m_{iu} - l_{1l} \sum_{i=1}^{6} \frac{1}{l_{il}} k_{il} h_{il} d_{il} \\
&\quad + l_{1l} g \sum_{i=1}^{6} \frac{1}{l_{il}} (m_{il} r_{il} + m_{i1} r_{i1} + m_{i2} r_{i2}) \\
D_8 &= m_p g (x_p - a_1) + \sum_{i=2}^{6} \frac{a_{1i}}{l_{il}} k_{il} h_{il} d_{il} \\
&\quad - g \sum_{i=2}^{6} a_{1i} [m_{iu} + \frac{1}{l_{il}} (m_{il} r_{il} + m_{i1} r_{i1} + m_{i2} r_{i2})] \\
D_9 &= m_p g (y_p - b_1) + \sum_{i=2}^{6} \frac{b_{1i}}{l_{il}} k_{il} h_{il} d_{il} \\
&\quad - g \sum_{i=2}^{6} b_{1i} [m_{iu} + \frac{1}{l_{il}} (m_{il} r_{il} + m_{i1} r_{i1} + m_{i2} r_{i2})] \\
D_{10} &= m_p g (z_p - c_1) + \sum_{i=2}^{6} \frac{c_{1i}}{l_{il}} k_{il} h_{il} d_{il} \\
&\quad - g \sum_{i=2}^{6} c_{1i} [m_{iu} + \frac{1}{l_{il}} (m_{il} r_{il} + m_{i1} m_{i1} + r_{i2} r_{i2})]
\end{aligned}$$

and where $a_{1i} = a_1 - a_i$, $b_{1i} = b_1 - b_i$, $c_{1i} = c_1 - c_i$.

Similarly to the previous cases, if the coefficients of the configuration variables in eq.(4.165), i.e., $D_i (i = 1, \ldots, 10)$ vanish, the total potential energy will be constant.

Therefore, the conditions for the static balancing for this type of manipulator are

$$D_i = 0, \quad i = 1, \ldots, 10 \tag{4.166}$$

An example is now given in order to illustrate the application of the balancing conditions to this type of mechanism.

For the alternative 6-dof manipulator presented above, let

$$m_p = 12,\ m_{iu} = m_{il} = 1.0,\ m_{i1} = 0.2,\ m_{i2} = 1.0,\ w_{i1} = 0.2 (i = 1, \ldots, 6)$$

$$a_1 = -0.5,\ , b_1 = -0.5,\ c_1 = -0.3,\ a_2 = 0.5,\ , b_2 = -0.5,\ c_2 = -0.3$$

$$a_3 = 0.5,\ b_3 = 0.5,\ c_3 = -0.3,\ a_4 = -0.5,\ b_4 = 0.5,\ c_4 = -0.3$$

$$a_5 = 1.0,\ b_5 = 0,\ c_5 = -0.3,\ a_6 = -1.0,\ b_6 = 0,\ c_6 = -0.3$$

$$h_{il} = h_{iu} = 0.5,\ d_{il} = d_{lu} = 0.5 (i = 1, \ldots, 6)$$

$$x_{1o} = -1.5,\ y_{1o} = -1.5,\ z_{1o} = 0,\ x_{2o} = 1.5,\ y_{2o} = -1.5,\ z_{2o} = 0$$

$$x_{3o} = 1.5,\ y_{3o} = 1.5,\ z_{3o} = 0,\ x_{4o} = -1.5,\ y_{4o} = 1.5,\ z_{4o} = 0$$

$$x_{5o} = 1.5,\ y_{5o} = 0,\ z_{5o} = 0,\ x_{6o} = -1.5,\ y_{6o} = 0,\ z_{6o} = 0$$

$$\gamma_1 = \frac{\pi}{6},\ \gamma_2 = -\frac{\pi}{6},\ \gamma_3 = \frac{5\pi}{6}$$

$$\gamma_4 = \frac{3\pi}{6},\ \gamma_5 = \frac{9\pi}{6},\ \gamma_6 = \frac{7\pi}{6}$$

where the masses are given in kilograms and the lengths in meters.

From eqs.(4.166) one obtains

$$r_{il} = r_{i2} = 0.5\,\mathrm{m},\ r_{i1} = 0.01\,\mathrm{m} (i = 1, \ldots, 6)$$

$$l_{il} = w_{i2} = 1.0\,\mathrm{m},\ l_{i1} = 0.2\,\mathrm{m} (i = 1, \ldots, 6)$$

$$k_{iu} = 140.8\,\mathrm{N/m},\ k_{il} = 160.8\,\mathrm{N/m}\,(i = 1, \ldots, 6)$$

$$x_p = 0\,\mathrm{m},\ y_p = 0,\ z_p = 0.3\,\mathrm{m}$$

The balanced mechanism is represented schematically in Figure 4.23. Similarily to the previous case, since each leg of the mechanism has an identical architecture, only one leg is represented in the figure.

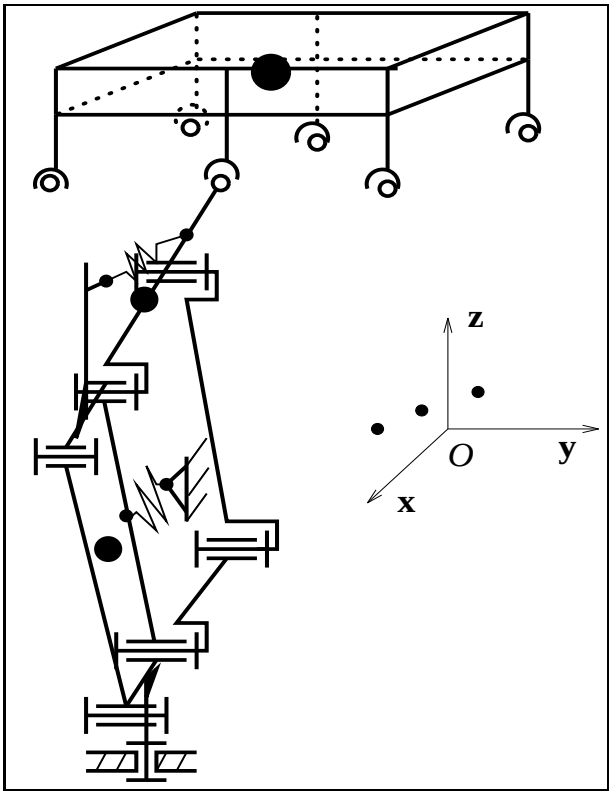

Figure 4.23: Balanced mechanism with springs.

4.3 Conclusion

The static balancing of planar and spatial parallel mechanisms or manipulators has been addressed in this chapter. Two static balancing approaches, namely, with counterweights and with springs, have been introduced. The expressions of the position vector of the global center of mass and of the potential energy of the mechanism have been derived. The kinematic constraint equations of the mechanism have then been used to eliminate some dependent variables from these expressions. The sets of equations of static balancing have finally been obtained from the resulting expressions. Examples have also been given in order to illustrate the results.

It has been shown that the planar and spatial parallel mechanisms presented in the chapter can be statically balanced by the two approaches discussed above. Each approach is suitable to different applications. The static balancing of planar and spatial parallel mechanisms is of great interest, especially in applications where the moving masses are large since it leads to a substantial reduction of the actuator torques. The

conditions derived here can be used directly to design balanced systems.

Conclusion

The kinematic analysis, dynamic analysis and static balancing of planar two- and three-degree-of-freedom as well as spatial four-, five- and six-degree-of-freedom parallel mechanisms or manipulators have been addressed in the thesis.

After having described the architecture of each of the mechanisms, the inverse kinematics has been computed for each of them and a new general algorithm for the determination of the boundary of the workspace of parallel mechanisms or manipulators has been proposed. This algorithm has then been used to obtain the workspace of the planar and spatial mechanisms studied in the thesis. It has been shown that this algorithm is general and can be applied to any type of parallel mechanism or manipulator. The velocity equations of the mechanisms have then been derived using two approaches, namely, the *algebraic formulation* and the *vector formulation*. The latter is a new approach which provides an equation of the velocity relations between the joint velocities and the angular velocities of the moving links of the mechanism. The velocity equations obtained using the two approaches have been used for the determination of the singularity loci and the velocity equation obtained using the new approach leads to a faster computational algorithm for the determination of the singularity loci.

The kinematic optimization of planar and spatial parallel mechanisms or manipulators with reduced degrees of freedom has also been discussed in this thesis. The Generalized Reduced Gradient method of optimization has been used and led to a fast

converging algorithm. The optimum design of the parallel mechanisms is useful for their applications where the dependent Cartesian coordinates are required to follow some prescribed trajectories as closely as possible.

The dynamic analysis of planar and spatial parallel mechanisms or manipulators has been addressed in this thesis. To this end, the analysis of the position, velocity and acceleration of these manipulators has been performed. Two different methods for the derivation of the generalized input forces have been presented. The first approach is a new approach based on the principle of virtual work. It has been verified that this approach is efficient and leads to a faster algorithm for the determination of the generalized input forces, which is useful for the control of a manipulator. The second approach has been used for the dynamic analysis of parallel mechanisms or manipulators by several researchers. It is suitable for the purpose of the design and simulation of a manipulator. It has been used here mainly to verify the results obtained with the new approach. Finally, examples have been given in order to illustrate the results. The dynamic analysis is an important issue for the design and control of the manipulators and can be efficiently handled with the procedures described in this thesis.

The static balancing of planar and spatial parallel mechanisms has also been addressed in this thesis. Two static balancing approaches, namely, with counterweights and with springs have been used. To this end, the expressions of the position vectors of the global center of mass and the potential energy of the mechanisms have been derived. The sets of equations of static balancing have finally been obtained from these expressions. Examples have been given in order to illustrate the results. The examples are provided for illustrative purposes only. Indeed, it is clear, from the equations, that infinitely many statically balanced mechanisms exist, for each of the architectures studied here. Moreover, it is also found, by inspection of the equations, that balancing is always possible for any given value of the geometric parameters. This is an interesting result since it allows the kinematic design of a mechanism to be completed using any criterion and the balancing to be performed *a posteriori*.

It has been clearly shown that the types of planar and spatial parallel mechanisms studied here can be statically balanced using either one of the two approaches presented in this paper. Each approach has its own advantages and is suitable to different applications. In all cases, the mechanisms obtained are perfectly balanced, i.e., no

torque is required at the actuators to maintain the mechanism in static equilibrium for any configuration. Static balancing of parallel mechanisms is of great interest and can be used in the design of mechanisms for robotics, flight simulators and several other applications involving large loads or the simulation of free-floating conditions.

In the kinematic and dynamic analysis of mechanisms, although several types of spatial parallel mechanisms with specified architectures have been studied here, the structure for these mechanisms is not unique. There exist other structure arrangements for these mechanisms, for instance, exchanging the Hooke joint connecting the moving links and the revolute joint attached to the base of the ith leg. The algorithms presented in the thesis for the determination of the workspace and singularity loci as well as for the derivation of the generalized actuator forces can be applied to other spatial parallel mechanisms with different structures. Moreover, if the deformations of the links are considered, considering the links of the mechanisms as flexible bodies, the results obtained from the kinematic and dynamic analysis should be more accurate.

The static balancing of the parallel mechanisms or manipulators using counterweights and springs have been presented in this thesis. However, how to build the practical balanced system, especially, the arrangement of the counterweights and springs, will be worth further studying. It would also be useful for some applications to consider the dynamic balancing of parallel mechanisms.

Bibliography

[1] Angeles, J. and Bernier, A., 1987, 'A general method of four-bar linkage mobility analysis', *ASME Journal of Mechanisms, Transmissions and Automation in Design*, Vol. 109, No. 2, pp. 197–203.

[2] Asada, H. and Youcef-Toumi, K., 1987, 'Analysis and design of a direct-drive arm with a five-bar-link parallel drive mechanism', *ASME Journal of Dynamic Systems, Measurements, and Control*, Vol. 106, No. 3, pp. 225–230.

[3] Agrawal, S. K., 1990, 'Rate kinematics of in-parallel manipulator systems', *Proceedings of the IEEE International conference on Robotics and Automation*, Vol. 1 pp. 104–109.

[4] Bajpai, A. and Roth, B., 1986, 'Workspace and mobility of a closed-loop manipulator', *The International Journal of Robotics Research*, Vol. 5, No. 2, pp. 131–142.

[5] Blajer, W. Schiehlen, W. and Schirm, W., 1993, 'Dynamic analysis of constrained multibody systems using inverse kinematics', *Mechanism and Machine Theory*, Vol. 28, No. 3, pp. 397–405.

[6] Bagci, C., 1979, 'Shaking force balancing of planar linkages with force transmission irregularities using balancing idler loops', *Mechanism and Machine Theory*, Vol. 14, No. 4, pp. 267–284.

[7] Bagci, C., 1983, 'Complete balancing of space mechanisms–shaking force balancing', *ASME Journal of Mechanisms, Transmissions, and Automation in Design*, Vol. 105, No. 12, pp. 609–616.

[8] Benea, R., 1996, 'Contribution à l'étude des robots pleinement parallèles de type 6R-RR-S', Ph.D. Thesis, Université de Savoie, France.

[9] Craver, W.M., 1989, 'Structural analysis and design of a three-degree-of-freedom robotic shoulder module', Master Thesis, The University of Texas at Austin.

[10] Do, W. Q. D. and Yang, D. C. H., 1988, 'Inverse dynamic analysis and simulation of a platform type of robot', *Journal of Robotic Systems*, Vol. 5, No. 3, pp. 209–227.

[11] Fichter, E. F., 1986, 'A Stewart platform-based manipulator: general theory and practical construction', *The International Journal of Robotics Research*, Vol. 5, No. 2, pp. 157–182.

[12] Freudenstein, F., 1955, 'Approximate synthesis of four-bar linkages', *Transactions of the ASME*, Vol. 77, pp. 853–861.

[13] Gosselin, C., 1990, 'Determination of the workspace of 6-DOF parallel manipulators', *ASME Journal of Mechanical Design*, Vol. 112, No. 3, pp. 331–336.

[14] Gosselin, C., 1996, 'Parallel computational algorithms for the kinematics and dynamics of planar and spatial parallel manipulators', *ASME Journal of Dynamic Systems, Measurement and Control*, Vol. 118, No. 1, pp. 22–28.

[15] Gosselin, C. and Angeles, J., 1988, 'The optimum kinematic design of a planar three-degree-of-freedom parallel manipulator', *ASME Journal of Mechanisms, Transmissions and Automation in Design*, Vol. 110, No. 1, pp. 35–41.

[16] Gosselin, C. and Angeles, J., 1990, 'Singularity analysis of closed-loop kinematic chains', *IEEE Transactions on Robotics and Automation*, Vol. 6, No. 3, pp. 281–290.

[17] Gosselin, C. and Hamel J. F., 1994, 'The agile eye: a high-performance three-degree-of-freedom camera-orienting device', Proceedings of the *IEEE International Conference on Robotics and Automation*, pp. 781–786, San Diego.

[18] Gosselin, C, Perreault, L. and Vaillancourt, c., 1995, 'Simulation and Computer-Aided Kinematic Design of Three-Degree-of-Freedom Spherical Parallel Manipulator,' *Journal of Robotic Systems*, Vol. 12, Nu. 12, pp. 857–869.

[19] Gosselin, C. and Wang, J., 1995, 'Singularity loci of planar parallel manipulators', *Proceedings of the Ninth World Congress on the Theory of Machines and Mechanisms*, Milano, Italy, Vol. 2, pp. 1973–1976.

[20] Gosselin, C. and Wang, J., 1997, 'Singularity loci of planar parallel manipulators with revolute actuators', *Journal of Robotics and Autonomous Systems*, Vol. 21, pp. 377–398.

[21] Gosselin, C. and Wang, J., 1997, 'Static balancing of spatial six-degree-of-freedom parallel mechanisms with revolute actuators', *Submitted to Journal of Robotic Systems.*

[22] Guglielmetti, P., 1994, 'Model-based control of fast parallel robots: a global approach in operational space', Ph.D. thesis, EPFL, Lausanne.

[23] Gao, F., 1991, 'Complete shaking force and shaking moment balancing of 17 types of eight-bar linkages only with revolute pairs', *Mechanism and Machine Theory*, Vol. 26, No. 2, pp. 179–206.

[24] Hunt, K.H., 1978, *Kinematic geometry of mechanisms*, Oxford University Press, Cambridge.

[25] Hunt, K.H., 1983, 'Structural kinematics of in-parallel-actuated robot arms', *ASME Journal of Mechanisms, Transmissions and Automation in Design*, Vol. 105, No. 4, pp. 705–712.

[26] Hervé, J.M., 1986, 'Device for counter-balancing the forces due to gravity in a robot arm', United States Patent 4,620,829, May.

[27] Husty, M. and Zsombor-Murray, P., 1994, 'A special type of singular Stewart-Gough platform', *Proceedings of Recent Advances on Robot Kinematics (ARK)*, pp. 449–458, Ljubljana.

[28] Karger, A. and Husty, M., 1996, "On self-motions of a class of parallel manipulators," *Proceedings of Recent Advances in Robot Kinematics (ARK)*, pp. 339–348, Portoroz.

[29] Karger, A. and Husty, M., 1997, "Singularities and self-motions of Stewart-Gough platforms," *Proceedings of Computational Methods in Mechanisms, NATO Advanced Study Institute*, Varna, Bulgaria, pp. 279–288.

[30] Kumar, V., 1990, 'Instantaneous kinematics of parallel-chain robotic mechanisms', *21st ASME Mechanisms Conference*, pp. 279–287.

[31] Kazerooni, H. and Kim, S., 1988, 'A new architecture for direct drive robots', *Proceedings of the IEEE Int. Conference on Robotics and Automation*, Philadelphia, pp. 442–445.

[32] Liu, Z. and Angeles, J., 1992, 'Least-Square optimization of planar and spherical four-bar function generator under mobility constraints', *ASME Journal of Mechanical Design*, June, Vol. 114, pp. 569–580.

[33] Lang, S., 1984, 'Algebra', *Addison-Wesley Publishing Company Inc., Menlo Park, California*, Second edition.

[34] Luh, J. Y. S. and Zheng Y. F., 1985, 'Computation of input generalized forces for robots with closed kinematic chain mechanisms', *IEEE Journal of Robotics and automation*, June, No. 2, pp. 95–103.

[35] Lowen, G.G. Tepper, F.R. and Berkof, R.S. 1983, 'Balancing of linkages – an update', *Mechanism and Machine Theory*, Vol. 18, No. 3, pp. 213–220.

[36] Lee, K. M. and Shah, D. K., 1988, 'Dynamic analysis of a three-degree-of-freedom in-parallel actuated manipulator', *IEEE Journal of Robotics and Automation*, Vol. 4, No. 3, pp. 361–367.

[37] Merlet, J.-P., 1987, 'Force-feedback control of parallel manipulators', Proceedings of the *IEEE International Conference on Robotics and Automation*, Vol. 3, pp. 1484–1489.

[38] Merlet, J.-P., 1988, 'Parallel manipulators, part I: theory, design, kinematics, dynamics and control', *Technical report No. 646 INRIA, France.*

[39] Merlet, J.-P., 1989, 'Singular configurations of parallel manipulators and Grassmann geometry', *The International Journal of Robotics Research*, Vol. 8, No. 5, pp. 45–56.

[40] Merlet, J.P. Gosselin, C. and Mouly, N., 1996, 'Workspaces of planar parallel manipulators', *Mechanism and Machine Theory* Vol. 33, No. 1, pp. 7–20.

[41] Mayer St-Onge, B. and Gosselin, C., 1996, 'Singularity analysis and representation of spatial six-degree-of-freedom parallel manipulators', *Proceedings of the 5th International Symposium on Advances in Robot Kinematics (ARK)*, Portorož-Bernardin, Slovenia, June 22-26.

[42] Nathan, R.H., 1985, 'A constant force generation mechanism', *ASME Journal of Mechanisms, Transmissions, and Automation in Design*, Vol. 107, No. 4, pp. 508–512.

[43] Pierrot, F., 1990, C. Reynaud and A. Fournier, 'Delta: a simple and efficient parallel robot', *Robotica*, Vol. 8, pp. 105–109.

[44] Premkumar, P. and Kramer, S., 1990, 'Synthesis of multi-loop spatial mechanisms by iterative analysis: the RSSR-SS path generator', *ASME Journal of Mechanical Design*, Vol. 112, No. 2 pp. 69–78.

[45] Sinatra, R. and Angeles, J., 1995, 'A new tool in the teaching of planar mechanism and machine theory', *Proceedings of the Ninth World Congress on the Theory of Machines and Mechanisms*, Milano, Italy, Vol. 4, pp. 3181–3186.

[46] Sefrioui, J. and Gosselin, C., 1993, 'Singularity analysis and representation of planar parallel manipulators', *Journal of Robotics and Autonomous System*, Vol. 10, pp. 209–224.

[47] Sefrioui, J. and Gosselin, C., 1995, 'On the quadratic nature of the singularity curves of planar three-degree-of-freedom parallel manipulators', *Mechanism and Machine Theory*, Vol. 30, No. 4, pp. 533–551.

[48] Stewart, D., 1965, 'A platform with six degrees of freedom', *Proceedings of the Institution of Mechanical Engineers*, Vol. 180, No. 5, pp. 371–378.

[49] Sugimoto, K., 1987, 'Kinematic and dynamic analysis of parallel manipulators by means of motor algebra', *Journal of Mechanisms, Transmissions, and Automation in Design*, Vol. 109, No. 1, pp. 3–7.

[50] Sugimoto, K., Duffy, J. and Hunt, K. H., 1982, 'Special configurations of spatial mechanisms and robot arms', *Mechanism and Machine Theory*, Vol. 17, No. 2, pp. 119–132.

[51] Stevenson, E. N. Jr., 1973, 'Balancing of machines', *ASME Journal of Engineering for Industry*, Vol. 95, No. 2, pp. 650–656.

[52] Smith, M. R., 1975, 'Optimal balancing of planar multi-bar linkages', *Proceedings of the 5th World Congress on the Theory of Machines and Mechanisms*, New-Castle-Upon-Tyne, pp. 142–149.

[53] Streit, D.A. and Gilmore, B.J., 1989, 'Perfect spring equilibrators for rotatable bodies', *ASME Journal of Mechanisms, Transmissions, and Automation in Design*, Vol. 111, No. 4, pp. 451–458.

[54] Streit, D.A. and Shin, E., 1990, 'Equilibrators for planar linkages', *Proceedings of the ASME Mechanisms Conference*, Chicago, Vol. DE-25, pp. 21–28.

[55] Shi, X. and Fenton, R. G., 1992, 'Structural instabilities in platform-type parallel manipulators due to singular configurations', *Proceedings of the ASME Mechanisms Conference on Robotics, Spatial Mechanisms and Mechanical Systems*, Chicago, Vol. 45, pp. 347–352.

[56] Ulrich, N. and Kumar, V., 1991, 'Passive mechanical gravity compensation for robot manipulators', Proceedings of the *IEEE International Conference on Robotics and Automation*, Sacramento, pp. 1536–1541.

[57] Walsh, G.J., Streit, D.A. and Gilmore, B.J., 1991, 'Spatial spring equilibrator theory', *Mechanism and Machine Theory*, Vol. 26, No. 2, pp. 155–170.

[58] Wang, J. and Gosselin, C., 1996, 'Kinematic analysis and singularity loci of spatial four-degree-of-freedom parallel manipulators' *Proceedings of the 1996 ASME Mechanisms Conference*, Irvine, California, USA.

[59] Wang, J. and Gosselin, C., 1997, 'Dynamic analysis of spatial four-degree-of-freedom parallel manipulators' *1997 ASME Design Automation Conference*, Sacramento, California.

[60] Wang, J. and Gosselin, C., 1996, 'Kinematic analysis and singularity representation of spatial five-degree-of-freedom parallel mechanisms' *Journal of Robotic Systems* Vol. 14, No.12, pp. 851–869.

[61] Wang, J. and Gosselin, C., 1997, 'Kinematic analysis and singularity loci of spatial four-degree-of-freedom parallel manipulators' *Submitted to ASME Journal of Mechanical Design.*

[62] Wang, J. and Gosselin, C., 1997, 'Static balancing of spatial three-degree-of-freedom parallel mechanisms' *Submitted to Mechanism and Machine Theory.*

[63] Wang, Z. and Xie, B., 1991, 'Solution of nonlinear equations using the generalized reduced gradient method', *Chinese Journal of Computer*, Vol. 6, No. 1, pp. 26–39.

[64] Ye, Z. and Smith, M.R., 1994, 'Complete balancing of planar linkages by an equivalence method', *Mechanism and Machine Theory*, Vol. 29, No. 5, pp. 701–712.

[65] Yang, D. C. H. and Lee, T. W., 1984, 'Feasibility study of a platform type of robotic manipulators from a kinematic viewpoint', *ASME Journal of Mechanisms, Transmissions, and Automation in Design*, Vol. 106, No. 2, pp. 191–198.

[66] Zlatanov, D., Fenton, R. G. and Benhabib, B., 1994, 'Singularity analysis of mechanisms and robots via a motion-space model of the instantaneous kinematics', *Proceedings of the IEEE International Conference on Robotics and Automation*, Vol. 1, pp. 980–991.

Appendix A

Polynomial formulation of the singularity loci of planar parallel manipulator

As explained in Chapter 2, eqs.(2.78) and (2.85) are the expressions describing the singularity loci of the two- and three-degree-of-freedom manipulators, respectively. Since these expressions contain some square roots—when they are expressed as functions of the Cartesian coordinates— it is difficult to extract from them the information about the characteristics of the singularity locus. In this appendix, the polynomial expressions of the singularity loci of the manipulators will be found. Polynomial expressions are useful since they can provide some insight into the locus and they may lead to alternative numerical solutions.

A.1 Two-degree-of-freedom manipulator

Solving eq.(2.1) (with $i = 1$) and (2.78) for $\cos\alpha_1$ and $\sin\alpha_1$, one obtains

$$\cos\alpha_1 = \frac{c_1\cos\alpha_2}{a_1\cos\alpha_2 + b_1\sin\alpha_2} \tag{A.1}$$

$$\sin\alpha_1 = \frac{c_1\sin\alpha_2}{a_1\cos\alpha_2 + b_1\sin\alpha_2} \tag{A.2}$$

Substituting eqs.(A.1) and (A.2) into $\sin^2\alpha_1 + \cos^2\alpha_1 = 1$ then leads to the following relation

$$a_1\cos\alpha_2 + b_1\sin\alpha_2 = Sc_1 \tag{A.3}$$

where $S = \pm 1$ denotes the type of singularity. When $S = -1$, links l_3 and l_4 are aligned whereas when $S = +1$, they are folded.

Then, letting $i = 2$ in eq.(2.1), the substitution of eqs. (A.1) and (A.2) into eq.(2.1) leads to

$$a_2\cos\alpha_2 + b_2\sin\alpha_2 = c_2 \tag{A.4}$$

From eqs.(A.3) and (A.4), one obtains

$$\cos\alpha_2 = \frac{Sc_1b_2 - c_2b_1}{a_1b_2 - a_2b_1} \tag{A.5}$$

$$\sin\alpha_2 = \frac{c_2a_1 + Sc_1a_2}{a_1b_2 - a_2b_1} \tag{A.6}$$

By squaring both sides of eqs.(A.5) and (A.6) and adding, one then obtains the polynomial expression of the singularity loci of this manipulator, which can be written as

$$(Sc_1b_2 - c_2b_1)^2 + (c_2a_1 + Sc_1a_2)^2 - (a_1b_2 - a_2b_1)^2 = 0 \tag{A.7}$$

The latter expression, eq.(A.7) is a polynomial of degree 6 in x and y where mixed terms are present. The curves representing the singularity loci in the Cartesian space are therefore of degree 6. The detailed expression is rather complex and is not given here because of space limitation but it can be obtained from the author upon request.

A.2 Three-degree-of-freedom manipulator

Similarly, for the three-degree-of-freedom manipulator, one can rewrite eq.(2.85) as

$$a_0\cos\alpha_1 + b_0\sin\alpha_1 = 0 \tag{A.8}$$

where

$$\begin{aligned} a_0 &= l_4 \sin\phi \sin\alpha_2 \cos\alpha_3 - l_4 \cos\phi \sin\alpha_2 \sin\alpha_3 \\ &\quad + l_3 \cos\phi \sin\alpha_2 \sin\alpha_3 - l_3 \sin\phi \cos\alpha_2 \sin\alpha_3 \\ b_0 &= l_4 \cos\phi \cos\alpha_2 \sin\alpha_3 - l_4 \sin\phi \cos\alpha_2 \cos\alpha_3 \\ &\quad + l_3 \sin\phi \cos\alpha_2 \cos\alpha_3 - l_3 \cos\phi \sin\alpha_2 \cos\alpha_3 \end{aligned}$$

Letting $i = 1$, eq.(2.14) can be rewritten as

$$a_1 \cos\alpha_1 + b_1 \sin\alpha_1 = c_1 \tag{A.9}$$

Solving eqs.(A.8) and (A.9) for $\cos\alpha_1$ and $\sin\alpha_1$ and then substituting the results into equation $\sin^2\alpha_1 + \cos^2\alpha_1 = 1$, one obtains an equation involving only α_2 and α_3, i.e.,

$$(a_1 b_0 - b_1 a_0)^2 - c_1^2(a_0^2 + b_0^2) = 0 \tag{A.10}$$

Eq.(A.10) can be rewritten as

$$C_{c2} \cos^2\alpha_2 + C_{cs} \cos\alpha_2 \sin\alpha_2 + C_{s2} \sin^2\alpha_2 = 0 \tag{A.11}$$

where coefficients C_{c2}, C_{cs} and C_{s2} are functions of $\cos\alpha_3$ and $\sin\alpha_3$.

Letting $i = 2$ in eq.(2.14), one obtains the second equation involving α_2, i.e.,

$$a_2 \cos\alpha_2 + b_2 \sin\alpha_2 = c_2 \tag{A.12}$$

Eliminating $\sin\alpha_2$ from eqs.(A.11) and (A.12), one then obtains

$$D_2 \cos^2\alpha_3 + D_1 \cos\alpha_3 + D_0 = 0 \tag{A.13}$$

$$E_2 \cos^2\alpha_3 + E_1 \cos\alpha_3 + E_0 = 0 \tag{A.14}$$

where

$$\begin{aligned} D_0 &= (c_2^2 C_{s2})/b_2^2 \\ D_1 &= (b_2 c_2 C_{cs} - 2a_2 c_2 C_{s2})/b_2^2 \\ D_2 &= (a_2^2 C_{s2} + b_2^2 C_{c2} - a_2 b_2 C_{cs})/b_2^2 \\ E_0 &= c_2^2 - b_2^2 \\ E_1 &= -2a_2 c_2 \\ E_2 &= a_2^2 + b_2^2 \end{aligned}$$

Using the resultant [33] on eqs.(A.13) and (A.14) to eliminate α_2, one obtains

$$\begin{aligned} &C_{c4}\cos^4\alpha_3 + C_{c3s1}\cos^3\alpha_3\sin\alpha_3 + C_{c2s2}\cos^2\alpha_3\sin^2\alpha_3 \\ &+C_{c1s3}\cos\alpha_3\sin^3\alpha_3 + C_{s4}\sin^4\alpha_3 = 0 \end{aligned} \tag{A.15}$$

where coefficients $C_{c4}, C_{c3s1}, C_{c2s2}, C_{c1s3}$ and C_{s4} are functions of x, y and ϕ.

Similarily, letting $i = 3$ in eq.(2.14) one obtains the equation involving α_3, i.e.,

$$a_3\cos\alpha_3 + b_3\sin\alpha_3 = c_3 \tag{A.16}$$

Eliminating $\sin\alpha_3$ from eqs.(A.15) and (A.16) then leads to

$$F_4\cos^4\alpha_3 + F_3\cos^3\alpha_3 + F_2\cos^2\alpha_3 + F_1\cos\alpha_3 + F_0 = 0 \tag{A.17}$$

$$G_2\cos^2\alpha_3 + G_1\cos\alpha_3 + G_0 = 0 \tag{A.18}$$

where

$$\begin{aligned} F_0 &= (c_3^4 C_{s4})/b_3^4 \\ F_1 &= -(4a_3c_3^3 Cs4)/b_3^4 \\ F_2 &= (b_3c_3^2 C_{c2s2} + 6a_3^2c_3^2 C_{s4})/b_3^4 \\ F_3 &= (b_3^3c_3 C_{c3s1} - 4a_3^2c_3 C_{s4} - 2a_3b_3c_3 C_{c2s2})/b_3^4 \\ F_4 &= (a_3^4 C_{s4} + b_3^4 C_{c4} + b_3^4 C_{c1s3} - a_3b_3^3 C_{c3s1} + a_3^2b_3 C_{c2s2})/b_3^4 \\ G_0 &= c_3^2 - b_3^2 \\ G_1 &= -2a_3c_3 \\ G_2 &= a_3^2 + b_3^2 \end{aligned}$$

Using the resultant once again on eqs.(A.17) and (A.18), one obtains the expression describing the singularity locus of this manipulator. The expression is a polynomial in x and y in which the highest degree of y is 64 while the highest degree of x is 48. Therefore, the curves representing the singularity loci in the Cartesian space are of a very high degree. This result is in contrast with the results obtained in [47] for manipulators with prismatic actuators, which lead to quadratic singularity loci. Moreover, the reason for the difference in degree between x and y is the assumption on the geometry (fixed pivots are assumed to be aligned on the x axis).

Appendix B

General expressions of $\det(\mathbf{A}^*)$ for planar parallel manipulators

For the two-degree-of-freedom manipulator, one has

$$\begin{aligned}\det(\mathbf{A}^*) &= \frac{l_3 l_4}{(a_1^2+b_1^2)(a_2^2+b_2^2)}(((a_2b_1-a_1b_2)c_1c_2)\\ &\quad +(a_1a_2+b_1b_2)c_2K_1\sqrt{\delta_1}\\ &\quad -(a_1a_2+b_1b_2)c_1K_2\sqrt{\delta_2}\\ &\quad +(a_2b_1-a_1b_2)K_1K_2\sqrt{\delta_1}\sqrt{\delta_2}) \qquad \text{(B.1)}\end{aligned}$$

For the three-degree-of-freedom manipulator, one has

$$\begin{aligned}\det(\mathbf{A}^*) &= N(D_0+D_1\sqrt{\delta_1}+D_2\sqrt{\delta_2}+D_3\sqrt{\delta_3}+D_4\sqrt{\delta_1}\sqrt{\delta_2}\\ &\quad +D_5\sqrt{\delta_1}\sqrt{\delta_3}+D_6\sqrt{\delta_2}\sqrt{\delta_3}+D_7\sqrt{\delta_1}\sqrt{\delta_2}\sqrt{\delta_3}) \qquad \text{(B.2)}\end{aligned}$$

where

$$
\begin{aligned}
N &= \frac{l_2^3}{(a_1^2+b_1^2)(a_2^2+b_2^2)(a_3^2+b_3^2)} \\
D_0 &= (c_1c_2c_3(((a_1b_3-a_3b_1)b_2l_3+(a_2b_1-a_1b_2)b_3l_4)\cos\phi \\
&\quad +((a_3b_1-a_1b_3)a_2l_3+(a_1b_2-a_2b_1)a_3l_4)\sin\phi) \\
D_1 &= (c_2c_3(((b_1b_3-a_1a_3)b_2l_3+(b_1b_2+a_1a_2)b_3l_4)\cos\phi \\
&\quad +((a_1a_3-b_1b_3)a_2l_3-(b_1b_2+a_1a_2)a_3l_4)\sin\phi)K_1 \\
D_2 &= (c_1c_3(((a_1b_3-a_3b_1)a_2l_3-(a_1a_2+b_1b_2)b_3l_4)\cos\phi \\
&\quad +((a_1b_3-a_3b_1)b_2l_3+(a_1a_2-b_1b_2)a_3l_4)\sin\phi)K_2 \\
D_3 &= (c_1c_2(((a_1a_3+b_1b_3)b_2l_3+(a_2b_1-a_1b_2)a_3l_4)\cos\phi \\
&\quad +(-(a_1a_3+b_1b_3)a_2l_3+(a_2b_1-a_1b_2)b_3l_4)\sin\phi)K_3 \\
D_4 &= (c_3((-(a_1a_3+b_1b_3)a_2l_3+(a_2b_1-a_1b_2)b_3l_4)\cos\phi \\
&\quad +(-(a_1a_3+b_1b_3)b_2l_3+(a_1b_2-a_2b_1)a_3l_4)\sin\phi)K_1K_2 \\
D_5 &= (c_2(((a_1b_3-a_3b_1)b_2l_3+(a_1a_2+b_1b_2)a_3l_4)\cos\phi \\
&\quad +((a_1b_3-a_3b_1)a_2l_3+(a_1a_2+b_1b_2)b_3l_4)\sin\phi)K_1K_3 \\
D_6 &= (c_1(((a_1a_3+b_1b_3)a_2l_3-(a_1a_2+b_1b_2)a_3l_4)\cos\phi \\
&\quad +((a_1a_3+b_1b_3)b_2l_3-(a_1a_2+b_1b_2)b_3l_4)\sin\phi)K_2K_3 \\
D_7 &= (((a_1b_3-a_3b_1)a_2l_3+(a_2b_1-a_1b_2)a_3l_4)\cos\phi \\
&\quad +((a_1b_3-a_3b_1)b_2l_3+(a_2b_1-a_1b_2)b_3l_4)\sin\phi)K_1K_2K_3
\end{aligned}
$$

Appendix C

Simplification of Jacobian matrix

The original Jacobian matrix of the four-degree-of-freedom manipulator can be written as

$$\mathbf{J}_{rv} = \begin{bmatrix} \mathbf{S}_1 & 0 & 0 & 0 & \mathbf{V}_1 & \mathbf{C} \\ 0 & \mathbf{S}_2 & 0 & 0 & \mathbf{V}_2 & \mathbf{C} \\ 0 & 0 & \mathbf{S}_3 & 0 & \mathbf{V}_3 & \mathbf{C} \\ 0 & 0 & 0 & \mathbf{S}_4 & \mathbf{V}_4 & \mathbf{C} \end{bmatrix}$$

and its determinant can actually be written as

$$\det(\mathbf{J}_{rv}) = \begin{vmatrix} l_{12y} & l_{12z}c_1 & 0 & 0 & 0 & 0 & 0 & 0 & 0 & -v_{1z} & v_{1y} & v_{5z} \\ -l_{12x} & l_{12z}s_1 & 0 & 0 & 0 & 0 & 0 & 0 & v_{1z} & 0 & -v_{1x} & 0 \\ 0 & sc_1 & 0 & 0 & 0 & 0 & 0 & 0 & -v_{1y} & v_{1x} & 0 & -v_{5x} \\ 0 & 0 & l_{22y} & l_{22z}c_2 & 0 & 0 & 0 & 0 & 0 & -v_{2z} & v_{2y} & v_{5z} \\ 0 & 0 & -l_{22x} & l_{22z}s_2 & 0 & 0 & 0 & 0 & v_{2z} & 0 & -v_{2x} & 0 \\ 0 & 0 & 0 & sc_2 & 0 & 0 & 0 & 0 & -v_{2y} & v_{2x} & 0 & -v_{5x} \\ 0 & 0 & 0 & 0 & l_{32y} & l_{32z}c_3 & 0 & 0 & 0 & -v_{3z} & v_{3y} & v_{5z} \\ 0 & 0 & 0 & 0 & -l_{32x} & l_{32z}s_3 & 0 & 0 & v_{3z} & 0 & -v_{3x} & 0 \\ 0 & 0 & 0 & 0 & 0 & sc_3 & 0 & 0 & -v_{3y} & v_{3x} & 0 & -v_{5x} \\ 0 & 0 & 0 & 0 & 0 & 0 & l_{42y} & l_{42z}c_4 & 0 & -v_{4z} & v_{4y} & v_{5z} \\ 0 & 0 & 0 & 0 & 0 & 0 & -l_{42x} & l_{42z}s_4 & v_{4z} & 0 & -v_{4x} & 0 \\ 0 & 0 & 0 & 0 & 0 & 0 & 0 & sc_4 & -v_{4y} & v_{4x} & 0 & -v_{5x} \end{vmatrix}$$

where $sc_i = -(l_{i2y}s_i + l_{i2x}c_i)$, $(i = 1, \ldots, 4)$, and

$$s_i = \sin(\alpha_i)$$
$$c_i = \cos(\alpha_i)$$
$$i = 1, 2, 3, 4$$

(i) multipling the first row of this matrix by l_{12x}/l_{12y} and adding to the second row, one obtains (it is assumed that $l_{12y} \neq 0$ and $l_{12x} \neq 0$)

$$\begin{vmatrix}
l_{12y} & l_{12z}c_1 & 0 & 0 & 0 & 0 & 0 & 0 & 0 & -v_{1z} & v_{1y} & v_{5z} \\
0 & \frac{-sc_1 l_{12z}}{l_{12y}} & 0 & 0 & 0 & 0 & 0 & 0 & v_{1z} & \frac{-v_{1z}l_{12x}}{l_{12y}} & -v_{1x} + v_{1y}\frac{l_{12x}}{l_{12y}} & v_{5z}\frac{l_{12x}}{l_{12y}} \\
0 & sc_1 & 0 & 0 & 0 & 0 & 0 & 0 & -v_{1y} & v_{1x} & 0 & -v_{5x} \\
0 & 0 & l_{22y} & l_{22z}c_2 & 0 & 0 & 0 & 0 & 0 & -v_{2z} & v_{2y} & v_{5z} \\
0 & 0 & -l_{22x} & l_{22z}s_2 & 0 & 0 & 0 & 0 & v_{2z} & 0 & -v_{2x} & 0 \\
0 & 0 & 0 & sc_2 & 0 & 0 & 0 & 0 & -v_{2y} & v_{2x} & 0 & -v_{5x} \\
0 & 0 & 0 & 0 & l_{32y} & l_{32z}c_3 & 0 & 0 & 0 & -v_{3z} & v_{3y} & v_{5z} \\
0 & 0 & 0 & 0 & -l_{32x} & l_{32z}s_3 & 0 & 0 & v_{3z} & 0 & -v_{3x} & 0 \\
0 & 0 & 0 & 0 & 0 & sc_3 & 0 & 0 & -v_{3y} & v_{3x} & 0 & -v_{5x} \\
0 & 0 & 0 & 0 & 0 & 0 & l_{42y} & l_{42z}c_4 & 0 & -v_{4z} & v_{4y} & v_{5z} \\
0 & 0 & 0 & 0 & 0 & 0 & -l_{42x} & l_{42z}s_4 & v_{4z} & 0 & -v_{4x} & 0 \\
0 & 0 & 0 & 0 & 0 & 0 & 0 & sc_4 & -v_{4y} & v_{4x} & 0 & -v_{5x}
\end{vmatrix}$$

(ii) multipling the second row of this matrix by l_{12y}/l_{12z} and adding to the third row leads to (it is assumed that $l_{12z} \neq 0$)

$$\begin{vmatrix}
l_{12y} & l_{12z}c_1 & 0 & 0 & 0 & 0 & 0 & 0 & 0 & -v_{1z} & v_{1y} & v_{5z} \\
0 & -sc_1\frac{l_{12z}}{l_{12y}} & 0 & 0 & 0 & 0 & 0 & 0 & v_{1z} & -v_{1z}\frac{l_{12x}}{l_{12y}} & -v_{1x} + v_{1y}\frac{l_{12x}}{l_{12y}} & v_{5z}\frac{l_{12x}}{l_{12y}} \\
0 & 0 & 0 & 0 & 0 & 0 & 0 & 0 & \frac{j_{11}}{l_{12z}} & \frac{j_{12}}{l_{12z}} & \frac{j_{13}}{l_{12z}} & \frac{j_{14}}{l_{12z}} \\
0 & 0 & l_{22y} & l_{22z}c_2 & 0 & 0 & 0 & 0 & 0 & -v_{2z} & v_{2y} & v_{5z} \\
0 & 0 & -l_{22x} & l_{22z}s_2 & 0 & 0 & 0 & 0 & v_{2z} & 0 & -v_{2x} & 0 \\
0 & 0 & 0 & sc_2 & 0 & 0 & 0 & 0 & -v_{2y} & v_{2x} & 0 & -v_{5x} \\
0 & 0 & 0 & 0 & l_{32y} & l_{32z}c_3 & 0 & 0 & 0 & -v_{3z} & v_{3y} & v_{5z} \\
0 & 0 & 0 & 0 & -l_{32x} & l_{32z}s_3 & 0 & 0 & v_{3z} & 0 & -v_{3x} & 0 \\
0 & 0 & 0 & 0 & 0 & sc_3 & 0 & 0 & -v_{3y} & v_{3x} & 0 & -v_{5x} \\
0 & 0 & 0 & 0 & 0 & 0 & l_{42y} & l_{42z}c_4 & 0 & -v_{4z} & v_{4y} & v_{5z} \\
0 & 0 & 0 & 0 & 0 & 0 & -l_{42x} & l_{42z}s_4 & v_{4z} & 0 & -v_{4x} & 0 \\
0 & 0 & 0 & 0 & 0 & 0 & 0 & sc_4 & -v_{4y} & v_{4x} & 0 & -v_{5x}
\end{vmatrix}$$

where

$$\begin{aligned}
j_{11} &= v_{1z}l_{12y} - v_{1y}l_{12z} \\
j_{12} &= v_{1x}l_{12z} - v_{1z}l_{12z} \\
j_{13} &= v_{1y}l_{12x} - v_{1x}l_{12y} \\
j_{14} &= v_{5z}l_{12x} - v_{5x}l_{12z}
\end{aligned}$$

(iii) multipling the first column of this matrix by $l_{12z}c_1/l_{12y}$ and adding to the second column and then factoring l_{12y} from the first column, $(l_{12y}s_1 + l_{12x}c_1)(l_{12z}/l_{12y})$ from the second column and $1/l_{12z}$ from the third row of the matrix, one finally obtains

$$D_{01}\begin{vmatrix}
1 & 0 & 0 & 0 & 0 & 0 & 0 & 0 & 0 & -v_{1z} & v_{1y} & v_{5z} \\
0 & 1 & 0 & 0 & 0 & 0 & 0 & 0 & v_{1z} & -v_{1z}\frac{l_{12x}}{l_{12y}} & -v_{1x}+v_{1y}\frac{l_{12x}}{l_{12y}} & v_{5z}\frac{l_{12x}}{l_{12y}} \\
0 & 0 & 0 & 0 & 0 & 0 & 0 & 0 & j_{11} & j_{12} & j_{13} & j_{14} \\
0 & 0 & l_{22y} & l_{22z}c_2 & 0 & 0 & 0 & 0 & 0 & -v_{2z} & v_{2y} & v_{5z} \\
0 & 0 & -l_{22x} & l_{22z}s_2 & 0 & 0 & 0 & 0 & v_{2z} & 0 & -v_{2x} & 0 \\
0 & 0 & 0 & sc_2 & 0 & 0 & 0 & 0 & -v_{2y} & v_{2x} & 0 & -v_{5x} \\
0 & 0 & 0 & 0 & l_{32y} & l_{32z}c_3 & 0 & 0 & 0 & -v_{3z} & v_{3y} & v_{5z} \\
0 & 0 & 0 & 0 & -l_{32x} & l_{32z}s_3 & 0 & 0 & v_{3z} & 0 & -v_{3x} & 0 \\
0 & 0 & 0 & 0 & 0 & sc_3 & 0 & 0 & -v_{3y} & v_{3x} & 0 & -v_{5x} \\
0 & 0 & 0 & 0 & 0 & 0 & l_{42y} & l_{42z}c_4 & 0 & -v_{4z} & v_{4y} & v_{5z} \\
0 & 0 & 0 & 0 & 0 & 0 & -l_{42x} & l_{42z}s_4 & v_{4z} & 0 & -v_{4x} & 0 \\
0 & 0 & 0 & 0 & 0 & 0 & 0 & sc_4 & -v_{4y} & v_{4x} & 0 & -v_{5x}
\end{vmatrix}$$

where

$$D_{01} = l_{12y}s_1 + l_{12x}c_1$$

Using similar operations in the other rows and columns and then exchanging some rows of the matrix, one can obtain

$$\det(\mathbf{J}_p) = D_0\begin{vmatrix}
1 & 0 & 0 & 0 & 0 & 0 & 0 & 0 & 0 & -v_{1z} & v_{1y} & v_{5z} \\
0 & 1 & 0 & 0 & 0 & 0 & 0 & 0 & v_{1z} & -v_{1z}\frac{l_{12x}}{l_{12y}} & -v_{1x}+v_{1y}\frac{l_{12x}}{l_{12y}} & v_{5z}\frac{l_{12x}}{l_{12y}} \\
0 & 0 & 1 & 0 & 0 & 0 & 0 & 0 & 0 & -v_{2z} & v_{2y} & v_{5z} \\
0 & 0 & 0 & 1 & 0 & 0 & 0 & 0 & v_{2z} & -v_{2z}\frac{l_{22x}}{l_{22y}} & -v_{2x}+v_{2y}\frac{l_{22x}}{l_{22y}} & v_{5z}\frac{l_{22x}}{l_{22y}} \\
0 & 0 & 0 & 0 & 1 & 0 & 0 & 0 & 0 & -v_{3z} & v_{3y} & v_{5z} \\
0 & 0 & 0 & 0 & 0 & 1 & 0 & 0 & v_{3z} & -v_{3z}\frac{l_{32x}}{l_{32y}} & -v_{3x}+v_{3y}\frac{l_{32x}}{l_{32y}} & v_{5z}\frac{l_{32x}}{l_{32y}} \\
0 & 0 & 0 & 0 & 0 & 0 & 1 & 0 & 0 & -v_{4z} & v_{4y} & v_{5z} \\
0 & 0 & 0 & 0 & 0 & 0 & 0 & 1 & v_{4z} & -v_{4z}\frac{l_{42x}}{l_{42y}} & -v_{4x}+v_{4y}\frac{l_{42x}}{l_{42y}} & v_{5z}\frac{l_{42x}}{l_{42y}} \\
0 & 0 & 0 & 0 & 0 & 0 & 0 & 0 & j_{11} & j_{12} & j_{13} & j_{14} \\
0 & 0 & 0 & 0 & 0 & 0 & 0 & 0 & j_{21} & j_{22} & j_{23} & j_{24} \\
0 & 0 & 0 & 0 & 0 & 0 & 0 & 0 & j_{31} & j_{32} & j_{33} & j_{34} \\
0 & 0 & 0 & 0 & 0 & 0 & 0 & 0 & j_{41} & j_{42} & j_{43} & j_{44}
\end{vmatrix}$$

where $l_{ix} \neq 0, l_{iy} \neq 0$ and $l_{iz} \neq 0 (i = 1, 2, 3, 4)$.

which can be written in another form

$$\det(\mathbf{J}_p) = D_0\begin{vmatrix} \mathbf{E} & \mathbf{D} \\ \mathbf{0} & \mathbf{J} \end{vmatrix} \tag{C.1}$$

where $\mathbf{E}$ is the 8 by 8 identity matrix, $\mathbf{0}$ the 4 by 8 zero matrix, $\mathbf{D}$ the 8 by 4 matrix and $\mathbf{J}$ the reduced 4 by 4 matrix.

$$D_0 = D_{01}D_{02}D_{03}D_{04}$$

and

$$\begin{aligned} D_{0i} &= l_{iy}s_i + l_{ix}c_i \\ j_{i1} &= v_{iz}l_{iy} - v_{iy}l_{iz} \\ j_{i2} &= v_{ix}l_{iz} - v_{iz}l_{iz} \\ j_{i3} &= v_{iy}l_{ix} - v_{ix}l_{iy} \\ j_{i4} &= v_{5z}l_{ix} - v_{5x}l_{iz} \\ i &= 1, 2, 3, 4 \end{aligned}$$

Finally, one obtains

$$\det(\mathbf{J}_p) = D_0 \det(\mathbf{J})$$

Appendix D

Expressions associated with the elements of the matrix $\mathbf{C}_f$ and vector $\mathbf{d}_f$

The detailed expressions of the elements of $\mathbf{C}_f$ and $\mathbf{d}_f$ can be written as:

$$
\begin{aligned}
c_f^{11} &= q_{31}\cos\alpha_1\cos\beta_1 - q_{32}\sin\alpha_1 + q_{33}\cos\alpha_1\sin\beta_1 \\
c_f^{12} &= q_{31}\cos\alpha_2\cos\beta_2 - q_{32}\sin\alpha_2 + q_{33}\cos\alpha_2\sin\beta_2 \\
c_f^{13} &= q_{31}\cos\alpha_3\cos\beta_3 - q_{32}\sin\alpha_3 + q_{33}\cos\alpha_3\sin\beta_3 \\
c_f^{14} &= q_{31}\cos\alpha_4\cos\beta_4 - q_{32}\sin\alpha_4 + q_{33}\cos\alpha_4\sin\beta_4 \\
c_f^{15} &= q_{31}
\end{aligned}
$$

$$
\begin{aligned}
c_f^{16} &= q_{21} \\
c_f^{21} &= q_{32}\cos\alpha_1 + q_{31}\cos\beta_1\sin\alpha_1 + q_{33}\sin\alpha_1\sin\beta_1 \\
c_f^{22} &= q_{32}\cos\alpha_2 + q_{31}\cos\beta_2\sin\alpha_2 + q_{33}\sin\alpha_2\sin\beta_2 \\
c_f^{23} &= q_{32}\cos\alpha_3 + q_{31}\cos\beta_3\sin\alpha_3 + q_{33}\sin\alpha_3\sin\beta_3 \\
c_f^{24} &= q_{32}\cos\alpha_4 + q_{31}\cos\beta_4\sin\alpha_4 + q_{33}\sin\alpha_4\sin\beta_4 \\
c_f^{25} &= q_{32} \\
c_f^{26} &= q_{22} \\
c_f^{31} &= q_{33}\cos\beta_1 - q_{31}\sin\beta_1 \\
c_f^{32} &= q_{33}\cos\beta_2 - q_{31}\sin\beta_2 \\
c_f^{33} &= q_{33}\cos\beta_3 - q_{31}\sin\beta_3 \\
c_f^{34} &= q_{33}\cos\beta_4 - q_{31}\sin\beta_4 \\
c_f^{35} &= q_{33} \\
c_f^{36} &= q_{23} \\
d_{fx} &= g_{1x}(q_{11}\cos\alpha_1\cos\beta_1 - q_{12}\sin\alpha_1 + q_{13}\cos\alpha_1\sin\beta_1) \\
&\quad + g_{1y}(q_{21}\cos\alpha_1\cos\beta_1 - q_{22}\sin\alpha_1 + q_{23}\cos\alpha_1\sin\beta_1) \\
&\quad + g_{2x}(q_{11}\cos\alpha_2\cos\beta_2 - q_{12}\sin\alpha_2 + q_{13}\cos\alpha_2\sin\beta_2) \\
&\quad + g_{2y}(q_{21}\cos\alpha_2\cos\beta_2 - q_{22}\sin\alpha_2 + q_{23}\cos\alpha_2\sin\beta_2) \\
&\quad + g_{3x}(q_{11}\cos\alpha_3\cos\beta_3 - q_{12}\sin\alpha_3 + q_{13}\cos\alpha_3\sin\beta_3) \\
&\quad + g_{3y}(q_{21}\cos\alpha_3\cos\beta_3 - q_{22}\sin\alpha_3 + q_{23}\cos\alpha_3\sin\beta_3) \\
&\quad + g_{4x}(q_{11}\cos\alpha_4\cos\beta_4 - q_{12}\sin\alpha_4 + q_{13}\cos\alpha_4\sin\beta_4) \\
&\quad + g_{4y}(q_{21}\cos\alpha_4\cos\beta_4 - q_{22}\sin\alpha_4 + q_{23}\cos\alpha_4\sin\beta_4) + g_{5x}q_{11} \\
d_{fy} &= g_{1x}(q_{12}\cos\alpha_1 + q_{11}\cos\beta_1\sin\alpha_1 + q_{13}\sin\alpha_1\sin\beta_1) \\
&\quad + g_{1y}(q_{22}\cos\alpha_1 + q_{21}\cos\beta_1\sin\alpha_1 + q_{23}\sin\alpha_1\sin\beta_1) \\
&\quad + g_{2x}(q_{12}\cos\alpha_2 + q_{11}\cos\beta_2\sin\alpha_2 + q_{13}\sin\alpha_2\sin\beta_2) \\
&\quad + g_{2y}(q_{22}\cos\alpha_2 + q_{21}\cos\beta_2\sin\alpha_2 + q_{23}\sin\alpha_2\sin\beta_2) \\
&\quad + g_{3x}(q_{12}\cos\alpha_3 + q_{11}\cos\beta_3\sin\alpha_3 + q_{13}\sin\alpha_3\sin\beta_3) \\
&\quad + g_{3y}(q_{22}\cos\alpha_3 + q_{21}\cos\beta_3\sin\alpha_3 + q_{23}\sin\alpha_3\sin\beta_3) \\
&\quad + g_{4x}(q_{12}\cos\alpha_4 + q_{11}\cos\beta_4\sin\alpha_4 + q_{13}\sin\alpha_4\sin\beta_4) \\
&\quad + g_{4y}(q_{22}\cos\alpha_4 + q_{21}\cos\beta_4\sin\alpha_4 + q_{23}\sin\alpha_4\sin\beta_4) + g_{5x}q_{12}
\end{aligned}
$$

$$
\begin{aligned}
d_{fz} \;=\; & g_{1x}(q_{13}\cos\beta_1 - q_{11}\sin\beta_1 + g_{1y}(q_{23}\cos\beta_1 - q_{21}\sin\beta_1) \\
& + g_{2x}(q_{13}\cos\beta_2 - q_{11}\sin\beta_2) + g_{2y}(q_{23}\cos\beta_2 - q_{21}\sin\beta_2) \\
& + g_{3x}(q_{13}\cos\beta_3 - q_{11}\sin\beta_3) + g_{3y}(q_{23}\cos\beta_3 - q_{21}\sin\beta_3) \\
& + g_{4x}(q_{13}\cos\beta_4 - q_{11}\sin\beta_4) + g_{4y}(q_{23}\cos\beta_4 - q_{21}\sin\beta_4) + g_{5x}q_{13}
\end{aligned}
$$